11-19-2021

Optimizing Vaccine Supply Chains with Drones in Less-Developed Regions: Multimodal Vaccine Distribution in Vanuatu

Deng Pan
University of Missouri-St. Louis, dpkq8@mail.umsl.edu

Optimizing Vaccine Supply Chains with Drones in Less-Developed Regions: Multimodal Vaccine Distribution in Vanuatu

Deng Pan

M.S., Statistics, University of Toledo, 2014
B.A, Administrative Management, Capital University of Economics and Business, 2008

A Dissertation Submitted to The Graduate School at the University of Missouri-St. Louis
in partial fulfillment of the requirements for the degree
Doctor of Philosophy in
Business Administration with an emphasis in Logistics & Supply Chain Management

December
2021

Advisory Committee

James F. Campbell, Chairperson, Ph.D.
Haitao Li, Ph.D.
Shakiba Enayati, Ph.D.
Donald C. Sweeney, Ph.D.
Andrea C. Hupman, Ph.D.

Acknowledgment

I would like to acknowledge the generous support of the Association for Supply Chain Management for funding this research. It has allowed me to focus on my dissertation research without worrying about financial burdens.

I would also like to express my most profound appreciation to my dissertation chair Dr. James Campbell and my dissertation committee member Dr. Haitao Li for not only their invaluable advice and guidance on my dissertation, my other research projects, and classes they taught, but also for their encouragement, patience, and opportunities they provided throughout the entire duration of my Ph.D. study. I am deeply moved by their dedication to helping students succeed and am grateful to the significant amount of time they invested in me.

I am grateful to my dissertation committee member Dr. Shakiba Enayati. Her rigorous research attitude and especially her sincere help on modeling and coding for my dissertation have inspired me. I am also grateful to my dissertation committee member Dr. Donald Sweeny for his continuous support and care for my dissertation, my other research projects, and the classes he taught me from an early stage in my Ph.D. study. Finally, I would like to thank my dissertation committee member Dr. Andrea Hupman for her valuable suggestions for my dissertation and the class materials she shared that helped me greatly when I taught Business Statistics.

Abstract

In recent years, many less-developed countries (LDCs) have been exploring new opportunities provided by drones, such as the capability to deliver items with minimal infrastructure, fast speed, and relatively low cost, especially for high value-added products such as lifesaving medical products and vaccines. This dissertation optimizes the delivery network and operations for routine childhood vaccines in LDCs. It analyzes two important problems using mathematical programming, with an application in the South Pacific nation of Vanuatu. The first problem is to optimize the nation-wide multi-modal vaccine supply chain with drones to deliver vaccines from the national depot to all health zones in an LDC. The second problem is to optimize vaccine delivery using drones within a single health zone while considering the synchronization of drone deliveries with health worker outreach trips to remote clinics. Both problems consider a cold chain time limit to ensure vaccine viability. The two research problems together provide a holistic solution at the strategic and operational levels for the vaccine supply chain network in LDCs. Results from the first problem show that drones can reduce cost and delivery time simultaneously by replacing expensive and/or slow modes. The use of large drones is shown to save up to 60% of the delivery cost and the use of small drones is shown to save up to 43% of the delivery cost. The research highlights the tradeoff between delivery cost and service, with tighter cold chain limits providing faster delivery to health zones at the expense of added cost. Results from the second problem show that adding drones to delivery plans can save up to 40% of the delivery cost and improve the service time simultaneously by resupplying vaccines when the cold chain and payload limit of health workers are reached. This research contributes to both literature and practice. It develops

innovative methodologies to model drone paths with relay stations and to optimize synchronized multi-stop drone trips with health worker trips. The models are tested with real-world data for an island nation (Vanuatu), which provides data for a geographic setting new to the literature on drone delivery and vaccine distribution.

Table of Contents

List of Figures

List of Tables

1. Introduction

1.1.Background and motivation

The use of drones has the potential to save the lives of children in less-developed countries (LDCs) by increasing the efficiency of the vaccine supply chain. According to the World Health Organization (WHO), in 2017, children in LDCs were 14 times more likely to die before the age of five than children in developed countries (WHO, 2017). About 70% of these deaths could be prevented with access to simple, affordable healthcare interventions, such as vaccination (WHO, 2011a). The vaccination rate of children in LDCs was 80% in 2016 (Gavi, 2017), compared to around 95% in developed countries. The coverage remains low mainly due to the following factors.

1. Transportation is difficult due to poor or non-existent transport infrastructure (e.g., roads), especially in wet seasons, and there is a need to reach remote locations that may be accessible only by footpaths or boats.

2. It is difficult to maintain the "cold chain" that is required for most types of vaccines, both in transit and in storage, due to limited or no refrigeration or electricity, or a lack of fuel and generators, and the long transit times due to the lack of effective transport infrastructure (WHO, 2012; Kaufmann et al., 2011). The cold chain refers to the requirement that vaccines remain below a specified temperature to stay viable.

3. Supply chain planning in these regions is usually poor, with healthcare (including medical supplies and vaccine inventories) often organized along political administrative lines, rather than using principles of good supply chain management. For example, healthcare products may be delivered from the national capital (the location of

the national depot) to provincial capitals, and then to lower administrative districts, and finally to patients in the field.

As a result of these difficulties, in many LDCs the vaccine supply chain is costly, the coverage is low, and the wastage rate is high (Rao et al., 2017).

There is a pressing need to overcome the transport and logistics challenges in order to deliver vaccines to the children in need. Many non-governmental organizations (NGOs) have been striving to raise public awareness of the importance of improving the vaccination rate, as immunization is one of the world's most successful and cost-effective health interventions. In 2012, the "Decade of Vaccines Collaboration" led by the Bill and Melinda Gates Foundation, the Global Alliance for Vaccines and Immunization (Gavi), the United Nations International Children's Emergency Fund (UNICEF), United States National Institute of Allergies and Infectious Diseases, and WHO developed the Global Vaccine Action Plan with a goal to prevent millions of deaths by 2020 for people in all communities (WHO, 2011b). In 2015, the United Nations (UN) announced a goal to end "preventable deaths of newborns and children under five years of age and achieve universal health coverage including affordable and essential medicines and vaccines *for all* " as one of its 17 Sustainable Development Goals for the year 2030 (The United Nations, 2015). In June 2019, the Gavi board released a new five-year strategy with a core focus on reaching "zero-dose" children and missed communities, and also providing support for countries that were never eligible for Gavi support (Gavi, 2019).

Unmanned Aerial Vehicles (UAVs), colloquially known as "drones", are pilotless aerial vehicles that recently have been attracting a lot of attention in the public health sector globally. There are now several examples of drones being used for regular medical

deliveries, as well as increasing cases of drone flight tests for delivery of medical supplies. Based on the items being delivered, these cases can be divided into two groups: (i) delivery of perishable biological supplies such as blood, vaccines, organs, and patient samples in LDCs, and (ii) delivery of lightweight unperishable medical products, such as medicines and automated external defibrillators (AEDs) in developed countries. The most prominent example of drone use for healthcare is the regular blood delivery program, since October 2016, in Rwanda by Zipline. Zipline has been delivering medicines, vaccines, and blood products, such as whole blood, fresh frozen plasma, and platelets, from two warehouses in Rwanda that cover the entire country with fixed-wing drones at speeds of over 100 km/h. Zipline also has been delivering vaccines, drugs, and blood from four warehouses in Ghana since 2019. As of July 12, 2021, Zipline has provided 25 million people with quick access to urgent medicines, made a total of 161,407 deliveries, and flown over 11 million miles (Zipline, 2021). The average time from health workers placing an order by a text message to receiving the order is 30 minutes, compared to 2.5 hours for truck delivery on average (McNabb, 2019, Spires, 2019). During the 2020 Covid pandemic, the US Federal Aviation Administration (FAA) granted an emergency waiver that enabled Zipline to deliver medical supplies and personal protective equipment to medical facilities in North Carolina (Ackerman, 2020). Since March 2021, Zipline has being delivering Covid-19 vaccines to Ghana after they added ultra-low temperature freezers to their distribution centers (Peters, 2021;Vincent, 2021). Zipline planned to deliver Covid-19 vaccines to Nigeria later in 2021(Munoz, 2021).

Other examples of drone delivery in LDCs include vaccine delivery in the rugged mountainous terrain of Vanuatu with Wingcopter and Swoop Aero (UNICEF, 2018),

blood samples delivery in Madagascar with Vayu (Stony Brook University News, 2016), HIV samples delivery testing in Malawi with Matternet (Phillips et al., 2016), medicine and patient samples delivery tests in the Dominican Republic and Peruvian Amazon with WeRobotics (WeRobotics, 2019), medical supplies delivery tests in Lake Victoria, Tanzania, with Wingcopter and DHL (Karuri, 2019), tuberculosis (TB) samples transport between a hospital and a health clinic in Papua New Guinea as a joint effort between Médecins Sans Frontières (MSF) and Matternet (Meier and Soesilo, 2016), routine drone delivery of medical products and return trips with lab samples and reports in Republic of Congo since December 2020 with Swoop Aero (VillageReach, 2021a), and TB samples and Covid-19 samples delivery in Mozambique since October 2020 by Swoop Aero, which also validated that drone transportation does not compromise the quality of lab samples (VillageReach, 2021b).

An example of drone delivery for healthcare in developed countries is the delivery of AEDs to cardiac arrest patients by a team at Karolinska Institute in Stockholm, Sweden (Claesson et al., 2016; Fredman, 2018). While this dissertation focuses on drone delivery for healthcare products, especially vaccines, in LDCs, drones have several other use cases in public health. Due to the ability of drones to gather real-time high-resolution temporal and spatial data cost-effectively, drones are used to track disease spread and detect health hazards (Rosser et al. 2018). For example, camera-carrying drones are used in Malaysia to map out the areas affected by a type of malaria parasite (Palermo, 2014). Researchers in the US have tested using drones with nucleic acid analysis modules to detect the Ebola virus (Priye et al., 2016).

Drones have the potential to deliver vaccines more efficiently and effectively compared with the use of manned vehicles, such as 4-wheel drive trucks or motorcycles, in LDCs where roads are in poor condition or nonexistent. The fast speed of drones could decrease the transport time, so it is more likely that the vaccines will be delivered without violating the cold chain requirement. Drones with vertical takeoff and landing (VTOL) capability, or using tethers or parachutes to deliver products without landing, are also flexible in where they can deliver, because these drones can reach remote areas more easily without the need for a large landing field. These types of drones are usually small to medium sized single or multi-copter drones or small fixed wing drones. Large fixed-wing drones, which are akin to small airplanes and use a runway that is shorter than runways for piloted airplanes can also be used. These drones often have faster speeds than single or multi-copter drones (Chapman, 2016). Drone deliveries are relatively low cost compared to many traditional modes of transportation, such as trucks and airplanes. Large fixed-wing drones are usually more expensive than small to medium sized single or multi-copter drones, but they often have a much larger payload capacity, so they can lower the cost by combining trips, compared to drones with smaller payload.

1.2.My research: vaccine supply chain optimization in LDCs

The goal of my dissertation research is to develop mathematical models to optimize the vaccine supply chain with drones as a new mode of transportation for LDCs. Due to the recent drone tests in Vanuatu, my models are applied and tested with data from this country.

Vaccines are usually distributed along administrative lines in LDCs, and vaccine supply chains often consist of four to five tiers starting from the national vaccine depot,

then to provincial vaccine storage locations, then to regional district vaccine storage locations, and then to local health centers, and then sometimes to remote villages through outreach campaigns (Lee et al., 2015; Kaufmann et al, 2011). For the highest-level tiers, there may be scheduled airline (or bus or boat) service and truck transport is also often available, although roads may be limited in certain times of the year (e.g., due to flooding). For the lower tiers of the supply chain, health workers often have to travel to pick up vaccines from the next higher tier, carrying them in cold boxes and using a combination of trucks, motorcycles, boats, buses, oxcarts, etc., and even walking, especially for the outreach activities. A cold box in a vaccine delivery setting is an approved insulated container that can be filled with icepacks (or cold water) to keep vaccines cool for a short period of time. Drones, depending on their type and capability, allow various benefits to be achieved in vaccine supply chains in LDCs. For example, large fixed-wing drones that have high payloads and long ranges (e.g., 500 km) can skip a couple of tiers in the vaccine logistics network to reduce vaccine inventory, transportation, and facility cost. Small drones, such as those that can carry a few kilograms and travel 20-40 km, and with VTOL capability, can deliver a small amount of vaccines quickly to hard-to-reach remote clinics on a regular basis or when needed to reduce the inventory cost and wastage rate. Moreover, using drones to deliver vaccines can free up health workers to spend more time on patient care.

In my dissertation, I develop optimization models for vaccine supply chain networks with drones and other available modes of transportation. To reflect real-world settings, the models use a single national vaccine depot (e.g., in the capital city) that serves as the origin for vaccines in the country. To administer health care, the country is

divided into non-overlapping health zones, where each health zone has one designated vaccine distribution center (DC), and includes several clinics distributed across the health zone that provide vaccinations to children (along with other health care). The clinics are denoted as either “permanent”, if they are permanently staffed with health workers that are authorized to immunize children and have cold chain capabilities (i.e., refrigeration), or “temporary”, if they are only temporarily staffed by authorized health workers who make periodic scheduled visits to provide vaccinations and other health care (i.e., outreach activities).

Considering the large difference in the scale of the geographical distance between the two vaccine distribution phases (i.e., from the national depot to DCs across the country, and from DCs to clinics in the same health zone), and to allow flexibility in modeling parts of the supply chain (e.g., with certain locations fixed), I divide the vaccine distribution problem into two parts: (i) a national-level problem to transport vaccines from the national depot to the DCs in each health zone, and (ii) a local distribution problem within a health zone to transport vaccines from a DC to the permanent and temporary clinics.

In the first problem, this research designs a country-wide multi-modal vaccine supply chain network model from the national depot to vaccine DCs for all local health zones with the lowest possible cost, while satisfying the vaccination demand for all targeted children and the cold chain requirements. The first model decides the location of the DCs in the health zones, and the optimal flow of vaccines that are transported by drones and other available modes of transportation, such as scheduled airlines, boats, and trucks. The model also determines the location of drone bases for launching and

recovering drones that are used for vaccine deliveries between the national depot and the DCs. The model also decides where to locate relay stations that can recharge drones (e.g., replace the batteries of drones, or refuel drones) to extend the range of drones. The problem for vaccine distribution in the entire nation is modeled as a multi-modal network flow problem with decisions on vaccine flows, and the locations of DCs, drone bases, and drone relay stations.

In the second problem, this research optimizes vaccine distribution with the option of drone delivery within a single health zone from the local DC(s) to the permanent and temporary clinics within the health zone. For this second problem, vaccines may travel with the healthcare worker (either carried in a cold box while walking or traveling on a boat or a truck), or if a drone is used for vaccine delivery, then the vaccines would travel separately from the healthcare workers. This separate travel requires the synchronization of the drone deliveries with the healthcare worker travel to the clinics using available local modes of transportation (including walking). Generally, healthcare workers need to be at the drone delivery site prior to the vaccine delivery to ensure the vaccines are safely received and to prevent any pilferage or damage. The problem for vaccine distribution within a single health zone is modeled as a variant of the multi-depot synchronized traveling salesman problem with lowest possible traveling cost, where healthcare workers are treated as "vehicles" that can travel on routes visiting several vaccination sites before returning to their home base.

To simplify the discussion, I refer the first problem/model as the *national research problem/model* or P1 and the second problem/model as the *local research problem/model* or P2 in the following. In the dissertation research, the locations of the

national depot and all local permanent and temporary clinics are given, and the locations of the DCs are to be selected from a discrete set of candidate DC locations. Several types of drones are considered in the research for the two problems, as they require drones with different performance characteristics. Two fixed-wing drones are modeled for the national problem that designs the country-wide vaccine distribution network. Small drones (rotor-copter or hybrid designs) are modeled for the local problem that designs distribution for a single health zone. Sensitivity analyses are conducted to examine the influence of changes in the levels of demand and other key modeling parameters on the optimal model solutions. Combining the two problems provides a holistic solution for the in-country vaccine supply chain design with the goals of directly reducing the total cost, and indirectly increasing the vaccination rate, reducing the vaccine wastage rate, and ultimately saving children's lives.

1.3.Real world application

Vanuatu provides an ideal application for this research because the government of Vanuatu has worked with UNICEF on a drone delivery test project on three islands (Ministry of Health Vanuatu, 2018). I have been in contact with several individuals involved in the Vanuatu drone project and they have provided a variety of data for vaccine delivery in Vanuatu.

Vanuatu is a Y-shaped archipelagic country in the South Pacific with 83 relatively small islands that runs about 1300 km from north to south as shown in Figure 1.1. There are six provinces in the country. There are 65 inhabited islands with a total population of about 300,000, and about 20 islands have airstrips (often grass). Many islands do not have established roads, so vaccine delivery is often accomplished by boat and walking.

Currently, vaccines from outside of the country arrive and are stored at the national depot at the capital city Port Vila in Vanuatu. (The inbound vaccine supply chain to Port Vila is not considered in my research, as it is outside Vanuatu.) Then vaccines are distributed through the in-country health system which consists of four levels: 6 provincial hospitals, 38 health centers, 113 dispensaries, and 243 aid posts (Brown and Gilbert, 2012; WorldBank, 2018). Vaccines are shipped from the national depot by airplane in bulk with temperature loggers in WHO-approved insulated cold boxes to the six provincial hospital pharmacies (Graves, 2018), from where they are transported to health centers and dispensaries (which could be DCs) in each health zone by combinations of boats, trucks, and airplanes. Vaccines are transported to aid posts by combinations of boats and walking through outreach activities (Ministry of Health Vanuatu, 2018). The national depot and provincial hospital pharmacies have cold chain facilities such as electric refrigerators. Health centers and some dispensaries are equipped with solar refrigerators. All aid posts do not have refrigerators. The lack of qualified health workers in some dispensaries, and in all aid posts, is an important issue, as currently, 37% of health facilities in Vanuatu do not have health workers, cold chain capability or both (Gustiana, 2018). Health facilities with refrigeration allow health workers to transport vaccines in cold boxes with ice packs on boats, trucks where available, or by foot to reach remote sites to administer vaccines to children. Vanuatu is currently divided into 48 health zones, where large islands may include several health zones, and many small neighboring islands may collectively form a health zone.

Due to various levels of development in the health system in different health zones, the staffing and cold chain capabilities at various health facilities are not the same,

e.g., not all health zones have health centers and not all dispensaries have permanent health workers. A *permanent clinic* is a health facility that is both staffed by permanent health workers and equipped with cold chain facilities. A *temporary clinic* is a health facility that requires outreach activities to be served by health workers from a permanent clinic. Therefore, for my research applied to the vaccine supply chain of Vanuatu, all health centers and most dispensaries are permanent clinics (some dispensaries are not staffed with permanent health workers) (Ministry of Health Vanuatu, 2018), and all aid posts and the dispensaries that are not staffed with permanent health workers are temporary clinics. Thus, in each health zone in Vanuatu, there are several permanent clinics and some temporary clinics, and each permanent clinic is responsible for several temporary clinics nearby. Vaccinations can be performed at the permanent clinics and the temporary clinics. Local villagers travel with their children to a designated vaccination site (e.g., the nearest permanent or temporary clinic) to get their children vaccinated based on a prearranged schedule. How people with their children travel to vaccination sites are not considered in my research.

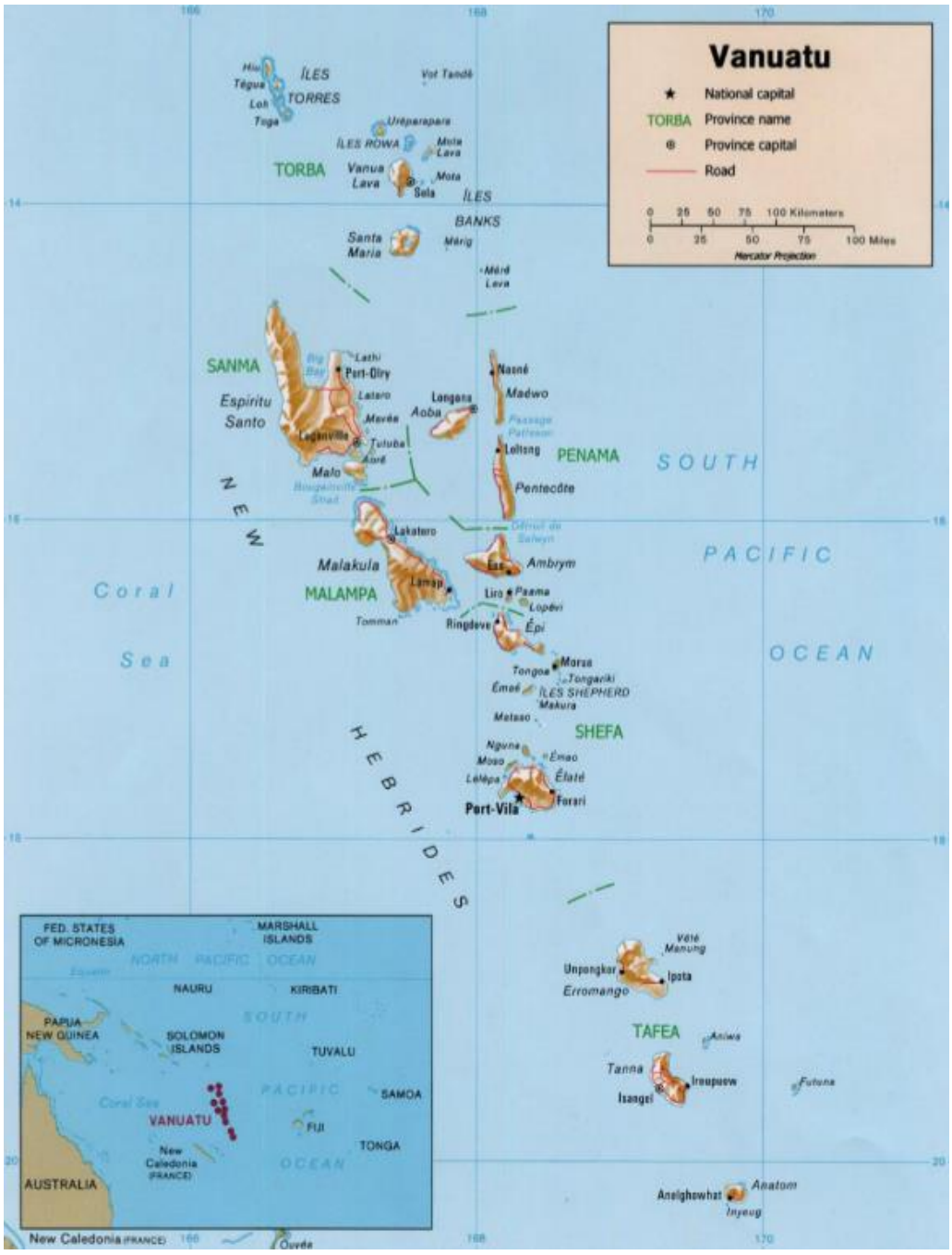

Figure 1.1 Map of Vanuatu
Source: Roadmap for the transition from analogue to digital terrestrial television in Vanuatu March 2014

Vanuatu provides the practical setting for my research, but the models and solutions from my research can be adapted and applied to many other places, including

the other thirteen less developed Pacific Island countries (UNICEF, 2019) where 1.2 million children and youth need efficient vaccination service. The models can also be modified and applied to evaluate drone delivery of vaccines and healthcare products in other LDCs, especially countries with limited transport infrastructure in Africa, Asia, and South America.

1.4.Dissertation structure

The remainder of the dissertation is presented in five sections. Section 2 provides a review of the relevant literature with regards to the global healthcare supply chain and delivery problem with drones, and identifies the research gaps that motivate this research. Section 3 presents details regarding the data, mathematical formulations, and computational studies and analyses for the first research problem of national-level vaccine distribution. Section 4 provides the mathematical formulations and illustrations of the results for the second research problem of local vaccine delivery within one health zone. Section 5 summarizes the two research problems and describes the connections between them, identifies practical implications and the limitations of the modeling, and provides some directions for the future research.

2. Literature Review

The literature review is organized in two parts. Section 2.1 summarizes the issues and literature regarding global health supply chains. Section 2.2 presents the relevant literature with regards to facility location and delivery problems with drones.

2.1.Global healthcare supply chain

This section is structured as follows: Section 2.1.1 provides an introduction to key issues in global healthcare. Section 2.1.2 provides a summary of managerial issues and challenges in vaccine supply chains in LDCs. Section 2.1.3 focuses on supply chain network design in global healthcare. Relevant vehicle routing problems in global healthcare are summarized in Section 2.1.4. Note that this subsection is limited to papers without the use of drones; reviews for vaccine delivery problems with drones are in Section 2.2.

2.1.1. Introduction

In the US, "global healthcare" is often used to refer to public healthcare in less developed or developing countries/regions. In the literature, "less-developed countries," "developing countries," and "low- or middle-income countries" are often viewed as the same in a broader sense, and I use "LDC" in the dissertation to refer to these settings. LDCs face a set of different and more severe healthcare challenges and issues compared to more developed regions. LDCs, especially in remote regions, often lack reliable infrastructure for transportation and power systems. Healthcare supply chains in LDCs are often organized along inefficient hierarchical administrative or political lines, instead of by the principles of supply chain management and optimization (Zaffran et al. 2013).

Some populations in LDCs live in hard-to-reach and isolated regions that need health care workers to serve them through outreach campaigns, which can involve long, slow and arduous travel.

Healthcare can be broken down into two categories: reactive healthcare and preventive healthcare. My dissertation focuses on improving preventive healthcare supply chains, specifically, supply chains for routine vaccination in LDCs. The research does not consider vaccine supply chains for epidemic emergency outbreaks and bioterror where the demand, time, quantity, and type are uncertain. It is worth noting that the models in the research are not designed to be applied to the Covid-19 vaccine delivery operations. Both the research problems in this dissertation stem from regular immunization planning in a fixed period such as once a month or once a week as part of a long-term ongoing program, so the demand for vaccines can be estimated based on the number of targeted people. Further, uncertainty is not considered in either model in this dissertation. Note that with Covid-19 vaccines, there are (so far) at most two doses per vaccine (administered at different time intervals), and the demand appears to be very uncertain.

LDCs usually receive vaccines from developed countries where they are manufactured. Typically, the vaccine strains, the number of vaccine doses per vial, and the packaging of vaccines are decided outside of the LDC (by the manufacturer or provider, such as an NGO). My dissertation only considers the in-country vaccine distribution processes after vaccines are received by the country. According to Kaufmann et al. (2011), even though there is a need to improve the synchronization of the overall supply chain from the beginning with manufacturing to the final vaccine administration, the in-country emphasis is more urgent and critical. For vaccine supply chain issues in

vaccine production, allocation, and choosing the right type of vaccines, interested readers are referred to Duijzer et al. (2018).

2.1.2. Issues and challenges in global healthcare

Some of the top issues for developing and operating vaccine supply chains are common issues for general supply chains, such as supply chain coordination, inventory management, and shipment visibility (Privett and Gonsalvez, 2014). Kaufmann et al. (2011) argues that key challenges and issues include inaccurate demand forecasting and uncoordinated financing and procurement processes. One of the most critical issues of vaccine supply chains in LDCs is poorly designed and executed supply chain systems that often delay and limit the impact that vaccines have on population health (Rao et al. 2017). More investments in improving vaccine supply chain design, rather than improving the vaccine products themselves, are critical for gaining the health benefit from vaccines (Zaffran et al. 2013). It is common to see four to five tiers in LDC vaccine supply chains including the national level, a provincial level, regional levels, districts, and local healthcare centers (Kaufmann et al. 2011; Aina et al. 2017; Brown et al. 2014; VillageReach, 2017; VillageReach, 2018; Chen at al. 2014). Complex multi-tier supply chains increase the risk of inefficient vaccine delivery and cold chain failure, both in transit and in inventory (Kaufmann et al., 2011).

Most vaccines must be kept in cold storage or they will lose potency (Kaufmann et al. 2011, WHO 2015). However, developing countries face severe cold chain capacity constraints for vaccines in both transport and storage, as well as unopened vial wastage due to issues such as accidental freezing, expiry, etc. (Zaffran et al. 2013, Lee et al. 2012). In some countries, 50% of all vaccine doses are wasted either before or after a vial

is opened (Zaffran et al. 2013). According to Privett and Gonsalvez (2014), the cold chain in vaccine supply chains is often measured twice a day at best, which is not enough to prevent cold chain failure. Condition monitoring technology (e.g., Vaccine Vial Monitors (VVMs) and FreezeWatch^{TM} tags) now allows better tracking of whether a vaccine has been exposed to temperature extremes that may cause damage. However, the benefit from these tools in LDCs is limited due to human resource and training issues (Privett and Gonsalvez, 2014). Lin, Zhao, and Benjamin (2020) proposed models to study the decision of a distributor of vaccines on choosing a cold chain or non-cold chain for vaccine distribution under the situation that stingy distributors will use a non-cold chain to distribute vaccines with the hope that patients will never be infected (hence never discover ineffective vaccines) and to study how the retailer's inspection at the end of transportation affects the distributor's original decision.

Lee et al. (2012) discuss the benefits of converting vaccines to thermostable formulations, which do not degrade under heat or excessive cold. The authors developed a detailed discrete-event simulation model of the Niger vaccine supply chain utilizing the HERMES (Highly Extensible Resource for Modeling Supply Chains) framework. The model includes the type, make, model, age, and the specific capacity of every cold room, refrigerator, and freezer in the Niger supply chain. The results of the study show that making pentavalent vaccines thermostable not only increased their own vaccine availability from 87% to 97%, but also increased availability for the non-thermostable EPI (Expanded Program on Immunization from WHO) vaccines to over 93% since more cold storage was freed up for non-thermostable vaccines.

Stockouts caused by improper stock management and insufficient cold chains is another important issue in vaccine supply chains in LDCs (VillageReach, 2017; VillageReach, 2018). Vaccine stockouts lasting one month or longer occur in one of three countries globally, and about 89% of these national stockouts reduced vaccine availability at the service delivery level (Rao et al. 2017). Poor data quality also makes the situation worse. For example, reported vaccine coverage rates were above 100 percent in nearly 25 percent of districts and also reported administered vaccines were above the total amount of stock received in Zambia (VillageReach, 2017). Many LDCs faced severe strain when new vaccines were introduced to their already fragile and inefficient vaccine supply chains (Zaffran et al., 2013).

2.1.3. Supply chain network design in global healthcare

Supply chain network design (SCND), from an operations research (OR) point of view, is the discipline used to determine the optimal location of facilities and the product flow through the facilities in a multi-tier supply chain network (Autry et al., 2013). Yang et al. (2021) developed a vaccine network design mixed integer linear programming (MILP) model with facility location decision on transshipment nodes between the national center and clinics for low- and middle-income countries. The authors designed a algorithm that disaggregates and consolidates the problem to solve the large MILP model efficiently. The algorithm was tested with numerical experiments with the data from EPI networks in four countries in sub-Saharan Africa. The results show that the overall savings is roughly between 6% to 27%, and the algorithm generated solutions that are within 0.5% of the optimality gap. The model assumes all vehicles and vaccine storage rooms are equipped with cold chain facilities, so the authors did not model the cold chain

requirement explicitly as my research does. The model also assumes fixed locations for the clinics that are the final destinations of vaccines, which is different than in my research that includes facility location decisions for the DCs, as well as for drone bases and relay stations.

Some studies such as Rahman and Smith (2000) and Smith et al. (2009) developed location models or location-allocation models for health service in developing countries, but none of them take temperature control, which is an indispensable element in the vaccine supply chain, into consideration. Rahman and Smith (2000) summarized literature that uses location-allocation models designed to find a set of optimal sites for health facilities and simultaneously assign demands to the facilities in healthcare in developing countries. Most papers developed the location-allocation models as a *p*-median problem, set covering problem or maximum coverage location problem. The location-allocation models designed for health services such as treatments for diseases often assume there are limited resources, and they seek to maximize the population that can be covered by the health facilities.

Other relevant literature for vaccine SCND includes Chen et al. (2014), which presented a linear programming (LP) model for multi-period vaccine distribution in developing countries without considering facility location decisions. Chen et al. (2014) applied the model to Niger's vaccine distribution network. There are four tiers in Niger's vaccine distribution network: the national store, regional stores, district stores, and clinics. The primary objective is to maximize the number of fully immunized children (FIC), and a secondary objective is to maximize partially vaccinated children. The results showed that the average FIC percentage increased to 93.18% by adding cold room

capacities as recommended in Niger's 2011-2015 Comprehensive Multiple Year Plan. Another analysis showed the FIC percentages were not significantly decreased after removing the entire regional level (the second tier) in the vaccine distribution network, so removing the regional tier can save costs without degrading the performance of the vaccine distribution network.

Lemmens et al. (2016) provided a literature review on model-based supply chain network design and tried to identify whether existing literature was able to address the key issues of vaccine supply chains. The paper explained why vaccines are different from other medical or pharmaceutical products. However, the paper mainly focused on the literature with regard to manufacturing, storage, uncertainty, and performance metrics, and not on distribution. The authors concluded that the existing SCND literature was not sufficient to model the typical complexities of vaccine supply chains.

Besides the mathematical programming models for vaccine SCND reviewed above, Brown et al. (2014) developed a HERMES simulation model to explore the impact on cost and vaccine availability of three vaccine supply chain redesign options in Benin. The research was motivated by the goal to accommodate new vaccines without straining Benin's vaccine supply chain. Prior to the study, the vaccine supply chain in Benin had four tiers. The national depot delivered vaccines in cold trucks to some of the tier 2 depots, while others picked up vaccines from the national depot using 4-wheel drive trucks. The tier three depots picked up vaccines from tier 2 using 4-wheel drive trucks, while tier 4 health posts used motorbikes to pick up vaccines from tier 3. The first redesign option reduced 80 tier 3 locations to 34. The other two redesign options reduced the supply chain to three tiers by removing tier 3. The third option also expanded tier 2

from 7 to 14 regional depots and added multi-stop delivery routes from tier 1 to tier 2 (i.e., serving three regional depots on one route). For each option, additional experiments replaced point-to-point motorcycle trips (i.e., a single stop trip) with 4-wheel drive truck routes that served multiple health posts on a trip. The results showed the benefits of replacing the point-to-point motorcycle trips with truck routes at the lowest level, and of removing tier 3 to increase vaccine availability from 93% to 96% and decrease logistics cost per dose from $0.26 to $0.25.

In addition to the OR research, several studies are relevant to my vaccine SCND model. Aina et al. (2017) conducted a review of a new direct vaccine delivery program in Kano, the largest state in northern Nigeria. The vaccine distribution system prior to redesign had four tiers. The redesigned distribution system eliminated the 44 stores in tier 3 and used 6 regional depots in tier 2. Another change was to outsource the distribution of vaccines for 4 of the 6 regional depots in tier 2. The main conclusion of this paper is that there are direct vaccine delivery benefits with fewer tiers between the supply points (i.e., the national depot) and local clinics serving the population.

Two case studies (VillageReach, 2017; VillageReach, 2018) for the vaccine supply chains in Zambia and in Equateur Province in the Democratic Republic of Congo (DRC), respectively, reflected some common issues with regard to vaccine distribution in LDCs. Both countries have four tiers in their vaccine supply chain: the national store, provincial stores, district stores, and local health clinics. Health workers in clinics usually travel long distances (54 km in Zambia or 100 km in DRC on average) to pick up vaccines monthly from district stores. Further, these trips are often slow, using boat, oxcart, public transportation, or walking. In Zambia, staff in health facilities spend more

than 100,000 hours annually on vaccine pickup activities which greatly reduced their time for patient care. Stock-outs caused by improper stock management and insufficient cold chains is another important issue that prevents children from getting vaccines. These reports also summarized the improvements in these two countries as results of EPI and initiatives led by VillageReach. Direct delivery by skipping a tier and transporting vaccines with multi-stop tours instead of back-and-forth trips benefited the two countries significantly. For example, in Zambia, the cost per dose was reduced 9% and total travel time of health workers was reduced by 94%. In DRC's Equateur Province, the total vaccine supply chain cost was reduced by 34% and monthly consumption of vaccine doses increased by 22%.

There has been large surge in publications related to Covid-19 vaccine supply chains since the pandemic started in 2020. However, as far as I aware, there is only one paper by Mehdi et al. (2020) that developed a Covid-19 vaccine network model for less-developed countries, as the rest of the publications are not focusing on less developed countries (Shretta, Hupert, Osewe and White, 2021), and often only discuss the challenges and propose strategies for Covid-19 supply chains in the future conceptually (Otuto and Chinenye, 2021). Further, many of the papers focus on different aspects of Covid-19 vaccine supply chains, such as reverse logistics and waste management (e.g., Shadkam, 2021). Mehdi et al. (2020) developed a MILP model for equitable Covid-19 vaccine distribution in developing countries by considering a multi-period location-inventory problem. The model maximized the minimum delivery-to-demand ratio while considering five types of vaccines that needs specific refrigeration levels for cold, very cold, and ultra-cold temperature requirements. The vaccines are supplied from multiple

manufacturers. The model also incorporates the possibility of storage for future periods that might face a shortage. The model is validated with data from India and simulated data. The population is divided into eight groups. The result shows how many doses of Covid-19 vaccines the Indian government could purchase with a certain amount of budget for each type of vaccines.

2.1.4. Vehicle routing problems in global healthcare

This section reviews the studies that are relevant to vehicle routing problems (VRPs) in healthcare settings based on whether the study considered synchronization of vehicles. There is a large body of research on vehicle scheduling and routing problems in the healthcare sector focused on home health care (HHC), mainly designed for the aging populations in developed countries. For survey papers, see Fikar and Hirsch (2017) and Cissé et al. (2017). Unfortunately, no publications address HHC vehicle routing problems in LDCs. HHC routing and scheduling problems usually involve the following aspects:

1. Route and assign caregivers to patients or vice versa. Some papers also take preferences (i.e., preferred caregivers by patients or vice versa) into consideration.
2. Match caregivers' skills and patients' requirements.
3. Model the time of events, including arrival times, departure times, and durations in patients' homes taking into account time windows, driving, caretaking, and lunch breaks.

4. Schedule the synchronized services (obeying temporal constraints) for activities that need more than one caregiver or for services with precedence relationships.

I review literature about VRPs without synchronization first.

Two papers that consider problems especially relevant to my research are the traveling therapist scheduling problem (TThSP) in Bard et al. (2014) and the mobile facility routing problem (MFRP) in Halper and Raghavan (2011). Bard et al. (2014) developed a mixed integer linear programming (MILP) model for the traveling therapist scheduling problem that seeks to route therapists from different starting locations to treat patients with fixed time windows over a five-day planning horizon. Therapists may be full-time or part-time and have different wage rates and working hours. The model includes lunch breaks, overtime and driving reimbursement. The objective is to minimize the total cost that includes the travel cost, service cost, and driving reimbursement and overtime pay for therapists over the five-day planning horizon. Patient preferences for specific therapists can also be taken into account. The TThSP is a multi-depot vehicle scheduling problem (there is no "routing" since the patients' time window and service duration are fixed). Two solution methods were developed: one was based on a Branch and Price and Cut (B&P&C) algorithm, and the other used a two-phase rolling horizon heuristic methodology. In the two-phase rolling horizon heuristic, phase one decomposed the problem into 30 minute time periods and iteratively solved for a 4-hour segment of the day. The rolling horizon approach extended the 4-hour period across the entire day to produce a daily schedule. In phase two, the daily schedules were "re-optimized" by considering the entire 5-day week, but solved for each single day, with the other four

days fixed. The model and solution methods were tested with data from a company in the U.S. Midwest. The B&P&C algorithm can solve only small instances with five therapists. The rolling horizon heuristic solved instances with up to 20 therapists and 650 patient visits, with solution gaps that were at most 2%. Results showed that including lunch breaks and overtime greatly increased the model complexity and solutions times.

Halper and Raghavan (2011) developed the mobile facility routing problem (MFRP) which seeks to create routes for a fleet of homogeneous mobile service facilities to maximize the demand served by the mobile facilities during a continuous time planning horizon. Mobile facilities could provide cell phone services, vaccinations and medical services, postal services, etc. For example, a mobile vaccination or medical clinic could travel to various locations from which it might serve (treat) the population in nearby villages, where the demand at each event point (village) may vary over time. In the MFRP, the facility can provide service only when stationary, and there is a discrete set of potential locations where the facility can stop to provide service. The MFRP aims to maximize the demands served by the mobile facilities, where the demand served depends on the arrival and departure time at each location. Demand for service is generated at discrete points (in space) as rates that vary over time. The MFRP is first formulated as an infinite-dimensional mixed integer program, because of the continuous nature of time. The authors provide an optimal polynomial algorithm for the problem with a single mobile facility. Because the problem with multiple facilities is not polynomially solvable, the authors developed two routing heuristics that rely on iterative use of the algorithm for the single facility problem. A sequential and an insertion routing heuristic are used to generate routes, followed by a local search improvement procedure.

The solution methods were tested using simulated data sets. The results showed the sequential routing heuristic typically outperforms the insertion heuristic. The authors also calculated lower bounds for the MFRP by fixing facility locations and by discretizing time.

The purpose of reviewing publications on the VRP with synchronization constraints is for the local problem (i.e., delivery from local DCs to vaccination sites) which involves the synchronization of activities between drones (carrying vaccines) and healthcare workers at vaccination sites. Synchronized VRPs typically address various types of synchronization of visits of two vehicles at a customer location. For my research, the healthcare worker can be viewed as one "vehicle" and the travel of vaccines can be viewed as occurring in a second vehicle. If the healthcare worker carries the vaccines, then the two "vehicles" travel together, but if the vaccines travel by drone and the healthcare worker travels by foot, then the two vehicles have separate routes. To provide vaccinations at a clinic, both the healthcare worker and the vaccines must be in the same place at the same time; hence the need for synchronization.

The following papers by Bredstrom and Ronnqvist (2008), Rasmussen et al. (2012), Redjem et al. (2012), and Labadie et al. (2014) represent this body of literature that is relevant to the synchronization in the local vaccine delivery research problem. There is no published study about VRPs with synchronization designed for vaccine delivery in LDCs.

Redjem et al. (2012) developed a MILP model for a home healthcare caregiver routing and scheduling problem, modeled as a VRP with time windows and synchronization for some visits. In this problem, each caregiver departs from the health

care service center, visits a set of preassigned customers, and returns to the center. Each patient can be visited multiple times a day within a predefined time window by different caregivers, and some patients need synchronized visits by specified caregivers. Synchronized visits are limited to two caregivers with identical starting times, although a caregiver that arrives early may wait for the second caregiver. Synchronized visits are also assumed to have the same duration. The problem is to determine each caregiver's tour and timing under two objectives: to minimize the total travel and waiting time of caregivers; and to minimize the total completion time of all visits. The MILP model was tested on two scenarios for 4 caregivers and 15 patients with 4 patients needing synchronized visits. The first scenario assumed all patients live near each other, and the second scenario assumed patients live in two different regions, separated by 40-60 minutes of travel. Results showed that solutions within 4% of the optimal solution could be achieved in 20 minutes of CPU time. The result also showed that the objective function of minimizing the total sum of travel time and waiting time was more efficient.

Labadie et al. (2014) proposed a mixed integer linear programming model to solve the vehicle routing problem with time windows and a synchronization constraint for the home health care system. The objective is to minimize the total travel cost. Some customers require more than one service at the same time, and the synchronized services are required to have the same start time and the same work duration. Each vehicle could provide a type of service. The model determines the routes for each vehicle, and the arrival time, start time, and wait time for each service. The paper provides a constructive heuristic and an iterated local search metaheuristic to solve the problem. The authors also proposed a definition for a vehicle routing problem with synchronized constraints

(VRPS), that is a vehicle routing problem where there exists at least one vertex requiring simultaneous visits of vehicles (simultaneous synchronization), or successive visits resulting from precedence constraints (precedence synchronization).

Bredstrom and Ronnqvist (2008) developed a MILP for a vehicle routing and scheduling problem with time window and synchronization constraints (VRSPTW). The problem can be applied in homecare staff scheduling where two distinct vehicles may be used to visit the same "customer" (node) at either the same time or with a specified precedence order. The objective function is a weighted sum of the total preference for a particular vehicle to visit a particular customer, the total travel time, and the maximal difference in work duration among vehicles (a fairness measure). An optimization-based heuristic was developed and tested against a MILP model. Simulated data based on problems from the literature were used for the numerical experiments. The results showed that the proposed heuristic can find very good, and often optimal, solutions in only a few minutes (faster than solving the MILP directly) for problems with 20 customers and 4 vehicles. Different time window sizes were tested for larger instances with up to 80 visits and 16 vehicles, and the result showed that feasible solutions were easier to find with wider time windows for synchronized visits.

Rasmussen et al. (2012) developed a MILP for a multi-depot home care crew scheduling problem with temporal dependencies. The formulation is very similar to the formulation in Bredstrom and Ronnqvist (2008). The objective contains three parts with varying weights: minimizing the travel cost, maximizing home caregiver-visit preference, and minimizing uncovered visits. Each patient has a group of preferred home care givers. A visit is either scheduled in a daily operation under restrictions or marked as uncovered

rather than to be rescheduled or canceled. Uncovered visits will be dealt with by manual planners appropriately. Five types of temporal dependencies between two care givers for a patient were defined (synchronization, overlap, minimum difference, maximum difference, and min+max difference). The authors developed a branch-and-price algorithm. The paper modeled the types as generalized preference constraints in the MILP formulation using a parameter to represent the difference of the start time between the two home care givers visiting the same patient (i.e., not modeling the five types specifically), and enforced the temporal dependencies through the branching. A visit clustering approach was introduced based on the generalized reference constraint.

Drexl (2012) provided a detailed review of VRPs with multiple synchronization constraints. The author categories this body of literature into five groups, and my local research problem falls into the "Operation synchronization" group. "Offset" was defined as the time difference between one vehicle's start time of a specific operation and another vehicle's start time of another specific operation. When the offset is zero, the two vehicles start the operation at the same time, and when the offset is greater than zero, there is a precedence relationship between the two operations. In my local delivery problem, the offset is with regard to the arrival time of a health worker and the arrival time of a drone. The type of "offset" required in the local vaccine delivery model depends on the vaccine delivery policy in the health zone in Vanuatu. Health workers could arrive first at a vaccination site before the vaccines so as to prepare for the administration of vaccines and perform other patient care. Alternatively, healthcare workers and a drone could arrive at the site at the same time based on the "just-in-time" delivery principle.

2.1.5. Research gap

This section provided an overview of problems and models in healthcare in LDCs in the literature without use of drones. My first research problem to optimize the vaccine distribution network from the national depot to DCs in local health zones with multiple modes of transportation for all targeted populations in LDCs, is different than the optimization models in the existing literature in the following three ways.

First, as stated above, the national research model optimizes the vaccine flow and vaccine DCs simultaneously; however, none of the existing literature determines network flows and facility locations simultaneously for LDCs. Second, the literature that models health facility locations for developing countries (e.g., Smith et al. (2009)) does not consider all targeted populations; instead, they assume the heath facilities can only cover a percentage of the targeted population due to limited resources. The national vaccine distribution model is designed to serve all targeted populations. Third, none of the optimization models in the literature incorporate multiple modes of transportation or several types of drones. The resources of transportation infrastructure in LDCs are not evenly distributed. In most cases, there are international airports in the capital cities and a few important cities, some established roads in higher-level administrative areas, and poor or non-existent road networks in other areas. Incorporating multiple modes of transportation allows the model to find the best combinations of vehicles that are most suitable for the existing situation in a certain country to transport vaccines throughout the entire network.

My second research problem to optimize the vaccine delivery network in a single health zone with the option of drones is a variant of the synchronized traveling salesman

problems (TSPs) with multiple depots. The differences between this model and the optimization models in the existing literature about VRPs and TSPs in healthcare are summarized in the following three points. First, none of the studies specifically model vaccine deliveries. Vaccines are different than many healthcare products and services due to their perishability and limited shelf life. Second, none of the studies on VRPs and TSPs with synchronization synchronize two "vehicles" from different depots. Third, none of the studies incorporate multiple transport modes including drones into the routing network.

2.2.Facility location and delivery problems with drones

This section is structured as follows: Section 2.2.1 provides an introduction for the section. Section 2.2.2 summarizes relevant publications with regards to facility location and delivery models with only drone transportation. Section 2.2.3 reviews literature regarding facility location and delivery models with truck and drone transportation. Section 2.2.4 identifies the research gaps.

2.2.1. Introduction

The number of studies on the use of drones in supply chain management is rapidly increasing. The studies related to facility location and delivery problems with drones are reviewed in this section. Studies that are not directly related to supply chain network design with product flow and facility location, and problems for last-mile delivery such as variants of traveling salesmen problems and vehicle routing problems are not included in this section. For example, the following topics are not included in this section: material handling with drones in an indoor manufacturing environment setting (e.g., Khosiawan and Nielsen, 2016), deliveries using ground-based drones (e.g., Boysen et al., 2018),

mapping, disaster surveillance, and search and rescue operations using drones in humanitarian settings (Sandvik and Lohne, 2014), and regulatory and ethical issues about drone delivery (e.g., Rao et al, 2016). For related problems such as drone path or trajectory planning and drone arc routing, see Coutinho et al. (2018). For drone delivery using continuous approximation methods, see Carlsson and Song (2017), Choi and Schonfeld (2017), Campbell et al. (2018), and Zhang (2021) .

The feasibility of using drones to deliver healthcare products, especially perishable and biological products (e.g., vaccine and blood samples), is examined in Thiels et al. (2015) and Amukele et al. (2017). Thiels et al. (2015) provided a conceptual evaluation of the feasibility and risk of medical product delivery (blood, gauze, and defibrillators) by drones in the US. Amukele et al. (2017) tested whether drones can be used to transport chemistry and hematology samples that need to be stored at a controlled temperature over long distances. The results showed that long drone flights of biological samples are feasible but require strict temperature control to ensure the quality of the samples. The above papers demonstrate that using drones to deliver healthcare products, especially vaccines, may be practical and safe without damaging the potency of the products.

Nyaaba and Ayamga (2021) review literature related to evaluating using drones for medical items delivery from the socio-technical perspective, and provide implications for African countries' adoption in delivering medical supplies with drones. The authors found that the majority of medical products delivered by drone in the literature are blood, AEDs, drugs, vaccines, and lab test samples. The results indicate that implementation of medical drones might revolutionize the healthcare logistics systems in Africa, as drones

can help Africa to leapfrog in technology adoption and replace slow and expensive transportation vehicles such as trucks. But because the initial investment for medical drone systems is high, the adoption of medical drone delivery should be a long-term goal that recognizes the need to offset the initial cost by reaping the long-term benefits, such as timely delivery, especially in an emergency setting, and saving lives.

The relevant research for drone delivery and facility location problems can be grouped into two categories: problems that use drones as the sole transportation mode, and problems that use drones with other transportation modes (typically trucks). This section is organized in these two categories. For a survey paper on drone operations planning optimization, see Otto et al. (2018).

2.2.2. Facility location and delivery models with drone only

This section reviews the studies related to facility location and delivery models with only drone transport. Phillips et al. (2016) compared the cost of using drones or motorcycles to transport lab samples, such as early infant diagnosis DBS (dried blood spot) and VL (viral load) samples for testing HIV between health clinics and laboratories in Malawi. Note that this paper is put in this section since lab samples are transported with only drones or with only motorcycles, not both. Four scenarios were considered based on whether the vehicles (drones or motorcycles) perform routes (visit multiple clinics) or use direct delivery, and whether the transportation was for only DBS samples or both DBS and VL samples. Costs considered include the costs of the vehicle, fuel, maintenance, vehicle insurance, battery, charger, landing device, and labor (which includes training costs, per diem costs for transporting samples, and salaries). The results

showed that drones were cost-efficient for deliveries that didn't exceed the payload capacity compared to motorcycles for the same delivery missions.

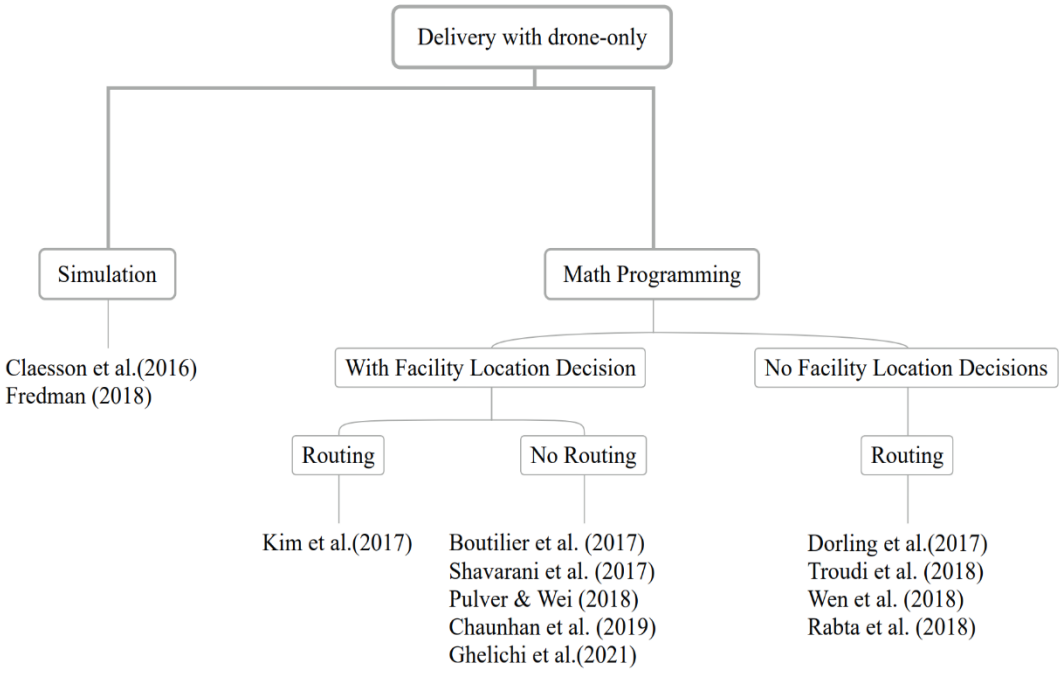

Figure 2.1 Classification of Operations Research literature for delivery with drone-only transportation

The academic studies with regards to drone delivery models in operations research (OR) that are relevant to my research are organized as in Figure 2.1. The majority of these publications use mathematical programming to model drone-only delivery. Under the category of math programming, the literature is grouped into two categories based on whether or not the study modeled facility location decisions for drone delivery. The publications are reviewed based on the categories shown in Figure 2.1.

Haidari et al. (2016) is the only paper I found that addressed drone delivery of vaccines. Haidari et al. (2016) used the HERMES (Highly Extensible Resource for Modeling Event-driven Supply Chains) simulation software to evaluate the efficiency of

the vaccine supply chain in a province (Gaza) in Mozambique with drones versus the traditional three-tiered land transport system (TMLTS). Key metrics were vaccine availability (the percentage of people receiving vaccines out of the number of people arriving at health centers for vaccines) and the cost per dose administered (annual total vaccine logistics costs, including storage, transport, building costs, and labor divided by the annual vaccine doses administered). Two scenarios were compared. In the first scenario, drones deliver vaccines from 3 district drone hubs to health centers on an as-needed basis in southern Gaza. Northern Gaza used the original delivery system (no drones) because the low population density would require a large number of hubs to supply a small number of health centers. In the second scenario, the delivery distances were restricted to be less than or equal to 75 km, which is the maximal flight range of the drones considered for use, for both TMLTS and the drone delivery network. The simulation results showed that implementing drones improved vaccine availability by 2% (from 94% to 96%), and reduced costs by $0.08 per dose administered ($0.41 to $0.33). The improvement in availability is because drones can deliver more frequently to health centers that don't have sufficient storage capacity for monthly supply by TMLTS. The cost was reduced because the savings in lower transport cost per day and labor cost offset the added hub infrastructure costs. The authors conducted a sensitivity analysis for the second scenario to examine how the logistics cost savings per dose administered are affected by six factors: road speed, the vaccination population (i.e., newborns in this model), road distance, distribution of newborns, seasonality for impassable roads, and introduction of new vaccines. The first three factors impact the cost savings the most. The results showed that as the road speed decreased from the baseline 59 km/h to 5 km/h, the

cost savings increased from $0.1 to $0.21. As the number of newborns changed from 720 to 180, the cost savings increased from $0.05 to $0.16. As the road distance increased from 39 km to 154 km, the cost savings increased from $0.06 to $0.14.

Claesson et al. (2016) and Fredman (2018) both explored the feasibility of using drones to transport Automated External Defibrillators (AEDs) to patients with out-of-hospital-cardiac-arrest (OHCA), rather than relying on ambulance trips to deliver the AEDs. The goal was to improve the survival rate of patients by making AEDs available faster. Both studies included test flights of drones in rural areas and used Geographic Information System (GIS)-simulated analysis for both urban and rural areas to determine suitable locations for basing drones using historical data for Stockholm County, Sweden. The results showed that drones could reduce the response time especially in rural areas (i.e., AEDs arrive 1.5 minutes earlier in urban areas and 19 minutes earlier in rural areas).

In terms of the application areas, the literature on delivery and facility location problems with drones using mathematical programming models can be divided into three categories: AED delivery with drones (Boutilier et al. 2017 and Pulver and Wei 2018); drone delivery in disaster relief and emergency settings (Chauhan et al. 2019, Rabta et al. 2018, Dorling et al. 2017, and Wen et al. 2016); and drone delivery in urban settings or developed countries (Kim et al. 2017, Shavarani et al. 2018, and Troudi et al. 2018).

Kim et al. (2017) presented two hierarchical models for drone-aided healthcare item delivery and pickup in rural areas. The goal was to use drones to free home caregivers for more important activities. The first model is a set covering-based facility location binary linear programming (BLP) model developed as the strategic tool to determine the optimal drone base locations. The model minimizes the initial investment

of opening drone bases and ensures that each patient is covered by at least one drone base. Using the solution from this location model as input, the second model is a delivery and pickup multi-depot vehicle routing problem to determine the minimal number of drones needed at each drone base and the drone routes for delivery and pickup activities. The objective is to minimize the total operating cost (i.e., each type of drone has a fixed operating cost per flight) of drones under constraints on drone flight time and capacity. Drones can visit a patient with both pickup and delivery needs at the same time. The paper used data from two counties in Texas, with 9 candidate drone bases and 40 customers in computational experiments. Preprocessing and partitioning are used to speed solutions, along with Lagrangian Relaxation, and gaps of 5% between the upper and lower bounds were allowed. The paper also presented a cost-benefit analysis as a decision tool for stakeholders.

Boutilier et al. (2017) presented a BIP model and a queuing model for designing a drone network to deliver defibrillators to individuals suffering from a cardiac arrest. A goal was to locate enough drone bases to provide fast delivery and good coverage of the region for potential cardiac victims. The BIP model located the minimum number of drone bases that would improve the response time over the historical level (from ambulance delivery) by a specified amount (one, two or three minutes). Following the location of drone bases, a queueing model was developed to determine how many drones to base at each location to ensure 99% availability of a drone. This depended on the demand (number of cardiac events) and the drone "service" time (for the delivery of a defibrillator and return) in the region served by the base. Takeoff and landing time were assumed to be 10 seconds and the drone flying speed was assumed to be 100 km/hr. The

two models were tested using data from 8 regions in the Toronto area. Results from treating the 8 regions separately showed that 81 drone bases with 100 drones are needed to provide deliveries 3 minutes faster than historical response times. The 90th percentile of the defibrillator arrival time was reduced by about 6.75 minutes in the most urban areas, and by about 10.5 minutes in the most rural areas. An integrated drone network to serve the 8 regions as one unified region achieved similar performance with 39.5% fewer bases and 30% fewer drones.

Pulver and Wei (2018) proposed a MILP model for a backup coverage location problem to locate drone bases for defibrillator delivery in an urban region. They modeled the benefits of primary coverage, where a point is covered if the distance to the drone base is within the drone's flight range, as well as backup coverage by a second (or third or more) drone base that may be farther, but still within the drone's flight range. Two objectives are to maximize the total amount of primary coverage (% of the population covered) and total amount of backup coverage. The two objective functions can be combined in one objective function as a weighted sum (i.e., the sum of the two weights is 1). By varying the number of drones in the system, the model can determine the best locations to maximize a weighted sum of primary and backup coverage. The population covered for a fixed drone base was determined using GIS tools with historical data on cardiac arrests in census blocks. The goal was to achieve 90% coverage with a 1 minute response time. The model was tested using data for Salt Lake County, Utah. The MILP was solved to find optimal drone bases and the associated coverage with the number of drones varying from 1 to 75, and with different weights in the objective function. The results showed that when maximizing only the primary coverage, 56 drones and drone

bases were needed to give primary coverage of 90%, with 19.5% backup coverage. When maximizing only the backup coverage, using 75 drones provided primary coverage of only 84% (not reaching the desired 90% level), but backup coverage was 75.9% (as the objective encouraged multiple coverage over covering more demand, but only with one drone).

Chauhan et al. (2019) presented a BLP formulation for the Maximum Coverage Facility Location Problem with Drones. One of the goals of this paper was to test whether drones can be used in time-sensitive settings such as for blood, medicine or food delivery after a natural disaster. The mathematical formulation is designed to locate a fixed number of capacitated drone facilities in a service region, allocate drones to each open facility, and assign demand points to drones. Each drone can make multiple direct (origin-to-destination) trips from its base to demand points until the battery runs out of power without recharging. The objective function is to maximize the coverage of the demand in the service region under drone energy and facility capacity (weight) constraints. The model explicitly considered drone battery capacity as a function of the demand served by a drone, the mass of a drone and its battery, the round-trip distance from the drone base facility, the power transfer efficiency of the battery and the lift-to-drag ratio. A greedy heuristic and three-stage heuristic (3SH) were developed to solve the problem. The mathematical formulation and the heuristic solution methods were tested using data from the Portland Metropolitan Area. The results showed that the Gurobi solver could find optimal solutions in 2 hours when there were at least 20 drone facilities and 60 available drones, and the coverage of demand was 93.8%. A sensitivity analysis

on battery capacity was conducted and the result showed that full coverage can be achieved with about a 165% increase in the battery capacity.

Shavarani et al. (2018) developed a mixed integer non-linear programming model for a drone facility location and delivery problem. In this problem, several drone launching stations and recharging station are selected from predefined candidate locations, and a drone will depart from a launching station and perform a single delivery to a customer. Depending on the distance, a drone might stop at one or more refueling stations in between. Demands in the model are uniformly distributed on customer location arcs in the graph and arise based on a Poisson distribution. The objective is to minimize the total cost that includes the construction costs of drone launching sites and refueling sites, the purchase cost of drones, and the traveling cost for drone deliveries. A genetic algorithm improved by a local search method was developed for the model. The heuristic method was applied in San Francisco with a population of around 850 thousand, and 2 launching stations and 22 recharging stations were selected among 110 drone facility candidates. Assuming the drone working duration is 8 hours per day, then 54,345 drones are needed to serve customers in San Francisco based on 0.12 deliveries per day per person in the US. The total annual cost is $298.5 million to cover San Francisco for the first year. If drone speed increased from 80 km/h to 100 km/h, then the cost would decrease to $255.0 million. If drones are able to work 16 hours per day and fly at a speed of 100 km/h, then the number of drones required decreased to 7000.

Ghelichi et al. (2021) developed a mixed integer optimization model to locate drone recharging stations and to deliver medical items from urban providers (e.g., drugstores) to rural clinics with a fleet of drones. Each provider has a fleet of drones, and

a drone will depart from a provider, stop at one or more recharging stations selected by the model, visit a clinic and return to the provider in each trip. The model also assigns clinics to providers and schedules and sequences each trip to ensure the completion time to visit all clinics is minimized through a novel timeslot formulation. In this research, the authors consider the scenario that locates the recharging station on existing structures with electricity such as billboards and traffic lights. The model is applied to a case study with data from Louisville, KY, USA. The results show a minimal number of charging stations is required to ensure the timely delivery to all rural and suburban clinics in Louisville. The study also indicates that more charging station will be needed if more drones are allowed to avoid congestion at the charging stations.

The above six papers which address facility location and delivery problems with drones are most similar to my national level research problem. However, four out of five papers, all except Shavarani et al. (2018) and Ghelichi et al. (2021), aim to maximize coverage for the facility location part of the problem. As stated in Section 2.1.5, my first research problem is to optimize the vaccine supply chain with drones in LDCs *for all* the demand (targeted children) and not just for a percentage of these children. Shavarani et al. (2018) designed a system for drone delivery in urban settings on a daily operational level, which is very different than a strategic facility location and network flow model across a large region (the entire country), as in my research. The model developed in Ghelichi et al. (2021) is for developed countries where there are street lights and billboards with stable electricity supplies. Also, the authors claim the model is designed for medical products delivery, but they do not consider the cold chain time limitation which is a critical factor for vaccine supply chain design.

Rabta et al. (2018) presented a straightforward MILP model for last-mile drone delivery of humanitarian products such as water purification tablets or other small light-weight items while considering the energy consumption and the payload limit of drones, as well as the use of existing recharging stations for drones. The objective is to minimize the total traveling distance of the drone. The decision variables are the number of times a drone travels between two locations, the beginning energy level of a drone for a leg of a route, and the number of packages a drone carries at the beginning of a leg of a route. The model was used to solve a few small instances with one depot, one recharging station, and five demand points, with limits on the energy level and drone payload capacity. The results showed the maximum energy level of the drone affected the frequency of the recharging station usage (i.e., the recharging station wasn't used when the maximum energy level was large, and vice versa).

Dorling et al. (2017) proposed two MILP models to solve two multi-trip VRPs for drone delivery problems in emergency response scenarios. One model minimizes the total costs (cost of drones and energy) subject to the time limit, while the other model minimizes the makespan (total time for all deliveries) subject to a budget constraint. The authors also develop and validate a linear model for drone energy consumption to use in the MILP formulations. Problems with up to eight customers are solved optimally in 19 minutes. A simulated annealing heuristic is developed to solve larger instances and problems with up to 500 customers are solved in about 9 minutes. The results show that allowing drones to be reused (perform more than one route) can save costs significantly. For example, if the delivery time limit (i.e., max drone route time) is 60 minutes, then reusing drones can save 87% compared to not reusing drones.

Troudi et al. (2018) developed a MILP model for last-mile urban delivery using drones. The model is essentially a capacitated VRP with time windows that takes energy consumption into consideration. The model assumes each drone can perform several tours and will be fully charged for each tour. Three objectives are considered: minimizing the total travel distance, minimizing the number of drones used, and minimizing the total number of batteries needed by minimizing the total number of tours (the paper assumed one tour uses one battery by default). The authors examined the impact of the length of time windows on the total travel distance, the total number of drones, and the energy consumption by minimizing the three objectives respectively with 5 to 10 customer instances. The time window was varied between 0.1 to 0.5 hours. The results showed that the number of batteries used decreased as the length of the time window increased. The travel distance and energy consumption decreased at first as the length of time window increased, then stabilized for the rest, which represented the minimal distance and energy consumption respectively.

Wen et al. (2016) developed a BLP model for a drone routing problem designed for blood delivery in an emergency setting. In this problem, each drone carries blood and a heating or cooling agent (water) to keep the blood between 2°-10° C. The drones perform multiple deliveries under a payload constraint that considers the combined weight of the blood and water. Two objectives are considered: (i) minimize the total travel distance, and (ii) minimize the total number of drones. The weight of water needed for a visit can be determined by the mathematical model of heat conduction that consists of two differential equations which involve the travel time, the weight of blood carried (i.e., demand), several parameters about the temperatures of water, blood, and the

environment, several parameters about heat conductance among water, blood, the container, and the environment, and parameters about heat capacities of blood and water. A decomposition-based multi-objective evolutionary algorithm and a local search method were developed to solve this problem, and nine instances were generated based on different proportions between water and blood. The experimental results showed that the proposed algorithm outperformed two other algorithms by 3%.

2.2.3. Facility location and delivery models with truck and drone

This section reviews the studies related to facility location and delivery models with truck and drone. These studies are classified in Figure 2.2. The literature is first grouped into two categories based on whether or not the research modeled facility location decisions for deliveries with drone and truck. The majority of these studies did not consider facility location decisions for drone delivery. Under this subcategory, the studies are further divided into two groups based on whether drones and trucks operate in tandem (often trucks carry drones) or independently. Under the category of "truck carries drone", the studies are classified into two groups based on whether or not trucks make deliveries. For the "trucks deliver" category, studies are grouped based on the different numbers of drones and trucks. The publications are reviewed based on the categories shown in Figure 2.2.

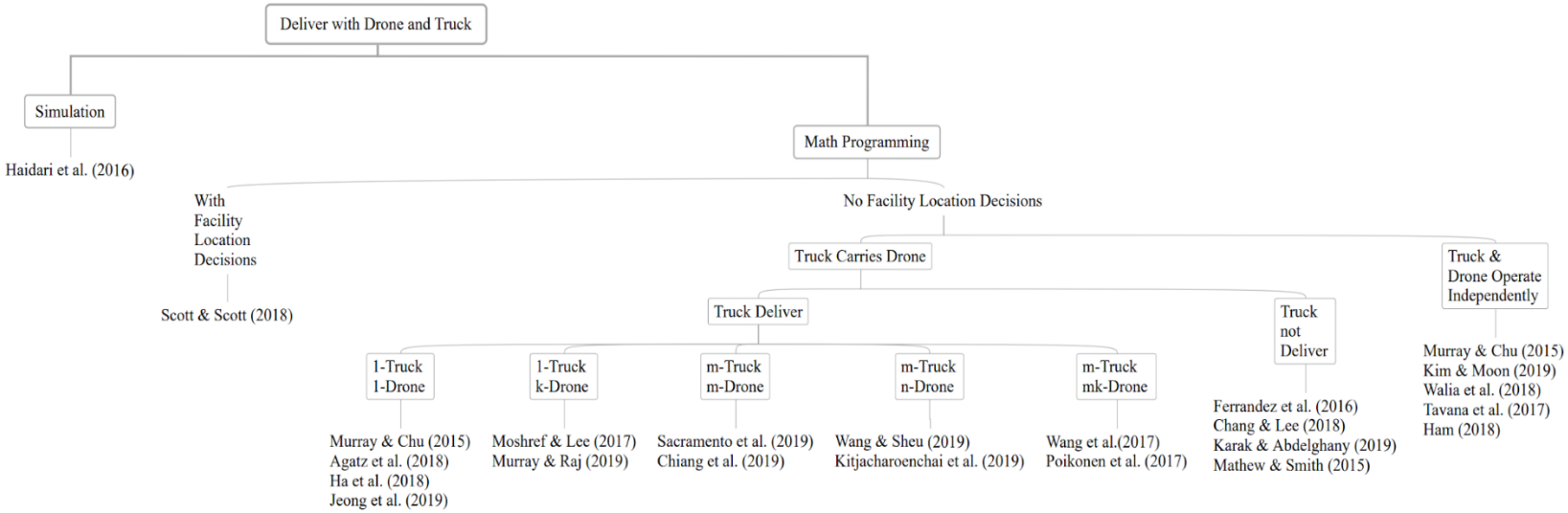

Figure 2.2 Classification of literature for delivery with drone and truck transportation

Since road conditions are often poor (or roads are non-existent in many places) in most LDCs, the majority of literature on delivery problems using both trucks and drones is designed for countries or urban areas with well-established road networks. Only the model developed by Walia et al. (2018) is for medical product delivery in LDCs. Walia et al. (2018) presented a BLP model for a three-level hierarchical medical distribution network with trucks and drones. The model assumes trucks are always used for distribution from the national store (the first tier) to the regional stores (the second tier), and the model will choose either trucks or drones for each arc from a regional store to a health center (the third tier) based on which mode generated the smaller cost for that arc and subject to a road condition constraint for trucks and an environmental risk (due to weather) constraint, a payload constraint, and a flight range constraint for drones. The model assumed that the cost per mile for trucks and the cost per pound for drones exponentially increase as a road condition parameter and an environmental risk parameter increase. The objective is to minimize the transportation cost for the entire network. The model was tested on the medicine supply chain in Tanzania. The results simply showed that the model worked and can provide guidance on the right mode of transportation to use from the economical perspective for the deliveries between the second and third-tier based on the weather, road condition, and drone payload and flight range limitations.

Scott and Scott (2019) claimed their model is for delivery of medical products such as blood or defibrillators in humanitarian settings. The authors developed a nonlinear programming model for a continuous space drone facility location and delivery problem. There is a depot to be located from which trucks depart to carry products to several drone bases (to be located), and drones are used to serve nearby customers with

back and forth trips. The location of the depot and drone bases are the only decision variables. Two models are developed. The first one is to minimize the total weighted delivery time over all truck trips and drone trips to serve all customers. The second model is to minimize the maximum weighted travel time from the depot to a customer to prevent unacceptably long delivery times to a customer that can result from the first model. A weight is the number of packages to be delivered to a customer location. Both models take into consideration a drone flight distance limit per trip and a budget constraint for the total truck and drone delivery cost. A small numerical example with nine customer locations and three drone bases is solved with the two models, and sensitivity analyses are conducted to show how changes in the budget and drone flight distance limit affect the two objective function values. The results showed that the two objective functions first decreased as the budget increased, and then remained flat for greater increases. The two objective functions decreased rather linearly as the drone flight distance limit increased from 50 miles to 70 miles, and the second objective function has a flatter slope than the first objective function against the distance limit.

Tavana et al. (2017) developed a MILP model to compare a traditional truck-based cross-docking delivery system with a direct shipping system by drones where products can be delivered to end customers directly from suppliers without going through the intermediate cross-docking step that trucks use. The model minimized the total delivery cost and completion time simultaneously. A multi-objective epsilon-constraint method was used to solve the model. The results showed that the total cost decreased as drones started to be used for direct shipping, and also delivery times decreased as fewer trucks were sent through the cross-dock.

Inspired by truck and drone tandem delivery pilot projects, a large body of studies on delivery with both trucks and drones in an urban setting rapidly emerged. As shown in the left branch in Figure 2.2, research can be divided into many clusters based on the collaboration level between the truck and drone, whether trucks serve customers or not, and the number of trucks and drones in the problem. Some papers also aimed to find in what situations it is best to use trucks or drones independently, such as Murray and Chu (2015), Kim and Moon (2019), Walia et al. (2018), and Tavana et al. (2017).

Murray and Chu (2015) developed two MILP models for two truck-drone tandem problems: the flying sidekick TSP (FSTSP), which is reviewed separately, and the parallel drone scheduling TSP (PDSTSP). In PDSTSP, drones can serve customers near the depot with demands that fit on a drone (e.g., lightweight packages) through back and forth trips independently, and the truck can serve customers throughout the region using a TSP tour. The model decides the assignment of drones to customers. The objective is to minimize the arrival time of the last vehicle at the depot. The solution approach solves a parallel machine scheduling problem for drone-to-customer assignments and then the routing component for the customers not served by a drone. The MILP model for PDSTSP was able to get optimal solutions for small test instances with 10 customers using Gurobi. Several solution approaches were presented with different combinations of three TSP methods for the truck tour (i.e., integer programming, a savings heuristic to remove customers from the TSP tour, and a nearest neighbor heuristic) and two parallel machines scheduling methods for drone deliveries (i.e., IP and longest processing time (LPT)). These were tested against the optimal MILP solutions from Gurobi. The results showed that the combination of a savings heuristic and LPT was the best for the 20

customer instances with a 3.9% gap and a CPU time of 0.008 seconds. Sensitivity analysis with regards to the drone speed and flight endurance were examined for PDSTSP. The results showed that drone speed is more important than endurance in terms of time savings.

Ham (2018) proposed a constraint programming (CP) approach to solve the parallel drone scheduling traveling salesman problem with delivery and pick-up ($PDSTSP^{+DP}$). Different than the PDSTSP proposed by Murray and Chu (2015), Ham incorporates drone drop and pick-up activities. After a drone completes a delivery, the drone can either travel back to the depot for the next delivery or fly directly to a destination for a pickup. A customer may need pickup at their location for returning an item, hence this paper addresses a reverse logistics problem. The paper presents two CP models. The first one is for a single depot, and the second one allows drones and trucks to stop at a different depot for pickup and serve the customers near that depot. This problem is modeled as an unrelated parallel machine scheduling with sequence-dependent setups (the sequence of customer visits), precedence-relations (for drop-pickup), and reentrant. Reentrant happens when a customer will receive multiple packages during a scheduling horizon. The objective is to minimize the maximum completion time over all tasks. The author chose minimizing makespan as the objective because it is directly related to the working hours of truck drivers and depots. The paper assumes the recharging time of the drone can be neglected.

Kim and Moon (2019) presented a TSP with a given drone station (TSP-DS) which is an extension of PDSTSP in Murray and Chu (2015). In PDSTSP, only customers that are close to the DC can be served by drones, however, Kim and Moon

argued that, in many cases, the DC is far away from the city center where the majority of customers are located, so in this case, many customers cannot be served by drones. Hence, TSP-DS allows a drone station that houses drones and recharging facilities (but not commodities), to be located near customers. In TSP-DS, a truck departs from the DC carrying packages for both truck customers and drone customers. Then truck travels through a TSP tour while delivering packages to truck customers that are not in the flight range of drones, and during the TSP tour the truck visits the drone station and drops off the packages to be delivered by a drone. This "activates" the drone station and then the truck and drones operate independently. Drones make single deliveries from the drone station, recharge, and serve the next customer. The authors showed that TSP-DS is more effective than PDSTSP when a majority of customers are located far from the DC, so TSP-DS can be used to overcome the range limits of drone facility problems.

Different than in the above five studies where trucks and drones operate independently, trucks and drones work in tandem in the following studies. The motivation for the research on problems where the truck carries drones is to use the trucks to extend the drone's range and to take advantage of the drone's fast speed, minimal needs for transportation infrastructure, and eco-friendliness. Among these papers, Ferrandez et al. (2016), Chang and Lee (2018), and Karak and Abdelghany (2019) modeled the situation when drones are the only transportation vehicles that serve customers (i.e. trucks do not make deliveries).

Ferrandez et al. (2016) presented a new truck-drone tandem delivery scenario where a delivery area is divided into clusters of customer locations, where the centroid of each cluster can be a stop location for the truck and then drones serve customers in the

cluster on out-and-back deliveries while the truck is stopped at the centroid. The truck can deliver to the customer located at the truck stop. The authors use the K-means algorithm (MacQueen, 1967) to find the optimal number of clusters and truck stops, and then a genetic algorithm to solve the truck routing problem as a traveling salesman problem. The objective is to minimize the total delivery time composed of the truck's traveling time and the sum of the drone's average delivery time in each cluster. The authors also performed a total energy requirement analysis of the tandem system as a function of the number of truck stops. The authors found the speed of drones should be at least twice the speed of the truck to significantly reduce the route time. The result also showed that multiple drones per truck can contribute to savings in both energy and time.

Chang and Lee (2018) considered a truck and drone tandem delivery scenario very similar to the one in Ferrandez et al. (2016). The authors tried to shorten the total delivery time by shifting the truck stop serving each cluster closer to the depot to reduce the truck travel time. The authors solved this by first using a K-means clustering algorithm to group delivery locations within the drone's flight range. Next, a TSP truck tour through the center point of each cluster and the depot was developed to minimize the truck's travel time. Last, a nonlinear programming model was used to shift the center of clusters towards the depot to reduce the total delivery time composed of the total travel time of the truck, the maximum drone flight time in each cluster and a service time for each cluster. The longest flight time was used for the travel time of drones in each cluster, rather than the total or average flight time as in Ferrandez et al. (2016). Results showed that shifting the truck stop locations reduced the delivery time by about 4.73% for problems with 100 delivery locations.

Karak and Abdelghany (2019) proposed a mixed integer linear programming model for a hybrid vehicle-drone routing problem (HVDRP) for the "mothership pick-up and delivery system". The mothership system is different from FSTSP in the following aspects. First, only drones serve the customers and the vehicle serves as a mobile depot for drones and only visits pre-defined stations. Second, each vehicle carries a "swarm" of drones that can be dispatched simultaneously. Third, a drone can return to the same location where it departs. This dispatch-wait-collect tactic allows drones to remain within sight for safety consideration. Fourth, a drone can visit multiple customers. The objective is to minimize the total vehicle and drone routing cost while serving all customers. The authors extended the classic savings heuristic to solve the HVDRP and compared the performance to two other heuristics. The first heuristic is a vehicle-driven heuristic where the iterative process begins with an initial vehicle route to visit all nodes, and then multi-stop drone routes are constructed based on the largest savings from moving nodes from the vehicle route to the drone route; the process ends when no node can be eliminated from the vehicle route. The second heuristic is a drone-driven heuristic that reverses the process of the vehicle-driven heuristic by constructing the drone multi-stop routes first. The authors also perform sensitivity analysis on the number of drones carried by the vehicle and the trade-off between flight range and drone load capacity. All numerical experiments were tested using a common grid network with randomly generated demand. A maximum flight range of 7 miles and drone capacity of 10 lbs. are used, based on UPS drone delivery field experiments in 2017.

Mathew and Smith (2015) developed a path planning model for a truck-drone delivery problem with one drone per truck. In this problem, the truck departs from the

warehouse and travels through a set of arcs representing streets (on a gridded graph) while carrying the drone, and the drone performs a single delivery task while the truck stops at a street vertex. The truck can either wait for the drone or drive to the next street vertex to collect the drone. The model optimizes the paths traveled by a truck and a drone by minimizing total fuel consumption and total time respectively. The authors developed a second model without the truck by replacing street vertexes with warehouses, so the drone can stop and reload and recharge at the warehouses rather than at the truck. A reduction to the generalized TSP method was used to solve the problems. Computational results showed that this truck and drone tandem problem saved 35% in total travel time compared to truck-only delivery.

Murray and Chu (2015) is the first published academic paper that models the truck-carries-drone tandem delivery problem and this is coined the Flying Sidekick Traveling Salesmen Problem (FSTSP). In FSTSP, a truck carrying a drone departs from the depot and visits a set of customers, and the drone can depart from the truck and perform a single delivery to a customer that can be served by drone (e.g., due to low package weight) and the drone then returns to the truck or the depot. The drone can also depart from the depot independent of the truck to make a delivery. The launch time and recovery time of the drone at the truck are modeled explicitly. The truck and the drone must be synchronized at the launch and recover locations for each drone's sortie. The objective is to minimize the arrival time of the last vehicle at the depot. A MILP formulation is presented along with several solution heuristics. The authors used Gurobi to solve the MILP and limited the run time to 30 minutes for test instances with 10 customers, so there was no guarantee that the results were optimal. A proposed FSTSP

heuristic framework is built on repeatedly solving TSPs. Four TSP solution approaches, including IP, a savings method heuristic, a nearest neighbor heuristic and a "sweep" heuristic were investigated and compared to the Gurobi solution.

There is another group of related papers that developed models for the "TSP with drone" (TSPD), a problem presented by Agatz et al. (2018). TSPD is essentially FSTSP with a different objective function. The objective of TSPD is to minimize the total traveling cost of serving all customers. Agatz et al. (2018) proposed a BLP formulation for TSPD and developed a theoretical analysis for the heuristics to solve larger instances of TSPD. The theoretical analysis proved that the maximum gain from truck and drone tandem delivery is of factor $1+\alpha$, where α is the ratio of drone speed to truck speed. The truck and drone tandem tour is composed of a sequence of "operations", where each operation begins and ends at a "combined node" where the truck and drone are together. In between these, the route includes at most one node which is served by the drone and one or more nodes served by the truck. (A truck can also launch, wait for, and recover the drone at the same node, in which case the start node is the end node.) The formulation ensures that each node is covered by at least one operation. A route-first and cluster-second procedure was developed. In the route-first step, an optimal TSP tour and a minimum spanning tree (MST) heuristic were constructed for the initial TSP tour. In the cluster-second step, an exact partitioning heuristic and a greedy partitioning heuristic were developed to partition the TSP tour into a truck subtour and a drone subtour. Four local search heuristics were used to improve the initial TSP tour. The BLP can be solved by the Concorde TSP solver to optimality with 10 nodes within 38.7 seconds, though it takes more than 2 hours for 12 nodes. The results of numerical experiments with 10

nodes and $\alpha = 2$ showed that the best heuristic gave an average optimality gap of 4.6% and achieved 16 out of 30 optimal instances. The total travel distance of the drone is roughly twice that of the truck in the heuristic solutions. The authors also showed that the savings of truck-and-drone tandem delivery over truck-only delivery increased as the drone flight endurance increased to an extent with the larger instances (20, 50, 100 nodes). For 100 nodes instances, savings of almost 30% can be achieved.

Ha et al. (2018) developed a MILP model for TSPD that takes into consideration the waiting time of a truck and a drone for each other at the drone recovery locations based on the FSTSP model of Murray and Chu (2015). The authors modeled waiting time by introducing the departure time at each location and the waiting time at the drone recovery location for the truck and the drone (there is only arrival time in Murray and Chu (2015)). The objective function is to minimize the operating cost including the travel cost of the two vehicles and the penalty cost due to waiting. The proposed MILP model can solve the problem with at most 10 nodes within an hour. A greedy randomized adaptive search procedure (GRASP) and a TSP with local search (TSP-LS) adapted from the heuristics in Murray and Chu (2015) were developed for larger instances. For both 50 customer and 100 customer instances, TSP-LS performed better in terms of run time with average solution times of 0.15 and 1.79 seconds respectively, and GRASP performed better in terms of the objective values (i.e., cost) with an average cost of about 75% of the TSP solution where only a truck is used. In all instances, the waiting time of the truck was much longer than that of the drone. In the 50 and 100 customer instances, the maximal waiting times were 6-7 minutes for drones and 113-175 minutes for trucks. The larger waiting times for trucks were due to the truck transport rate being 25 times more

expensive than the transport rate for a drone, so solutions tended to choose drones more for far customer locations thereby producing some long truck waits.

Jeong et al. (2019) extended the FSTSP from Murray and Chu (2015) by considering a drone's flight restrictions in certain areas and during certain times, as well as a limit on flight duration that is affected by a drone's energy demand and payload weight. The authors presented the FSTSP-energy consumption and no-fly zone (FSTSP-ECNZ) problem and proposed a MILP formulation for the problem. The paper estimated the possible flight duration using energy expenditures of drones that are dependent on the weight of the drone, including payload. The paper also suggested a detour method to avoid the time-dependent no-fly zones. The objective is to minimize the arrival time of the last returning vehicle at the depot. The authors developed a Two-Phase Construction and Search Algorithm. The first phase was an evolutionary-based algorithm that generated the initial truck-only tour, the second phase used a constructive algorithm to assign customers to a drone, and the third phase used search operators including 2-opt, swap, insertion, and cross-over to improve the solution. The authors compared FSTSP-ECNZ and FSTSP with 10 customers, and the results showed that the optimality gap ranged from 0% with 1 no-fly zone and a 2 kg payload, to 22.5% with 3 no-fly zones and a 4 kg payload. This showed that FSTSP-ECNZ, which is more practical than FSTSP, can generate acceptable solutions. The authors also compared solutions to those from four well-known heuristics (genetic algorithm, simulated annealing, partial swarm optimization, and nearest neighbor) with 10 customers, and results showed the superiority of their approach. Large size problems up to 50 customers were also tested.

Moshref-javadi and Lee (2017) developed a MILP model for a 1-truck and k-drone tandem delivery problem. In this problem, the truck departs from the depot while carrying multiple drones to serve customers in a TSP tour. Every time the truck stops at a customer location, it launches drones that serve nearby customers in single delivery back-and-forth trips. The truck waits for all drones to return, and also serves a customer at the stop. The objective is to minimize the total arrival time of the truck and drones at all customer locations. The model decided the truck arcs, drone arcs, waiting time of the truck for drones at truck stops, and the arrival time of the truck and drones at nodes. The formulation was applied in Richmond, VA with 10 nodes. The results showed that the total arrival time can be reduced by 58% and 38% when 3 and 2 drones are used respectively.

Murray and Raj (2019) proposed the multiple flying sidekick traveling salesman problem (mFSTSP) by extending the original FSTSP of Murray and Chu (2015) to incorporate a fleet of heterogeneous drones that have different travel speeds, payload capacities, service time, and flight endurance limitations. Inspired by the energy consumption expression in Dorling et al (2017), the authors developed a function to calculate the flight endurance which depends on payload weight, travel distance with or without a parcel, battery energy consumption, and flight phases. The flight phase is divided into takeoff from the launch point, flying to a customer location, landing, service duration, takeoff from a customer location, flying to a recovery point, landing at a recovery point, and waiting time for the truck. Considering there might not be enough space in a delivery truck to accommodate multiple drones landing or launching simultaneously, the paper also queues and schedules the drones in both the launch and

retrieval phases to avoid mid-air collisions. This means that the truck can only launch or retrieve one drone at a time. The objective in mFSTSP is to minimize the latest time at which either the truck or a drone returns to the depot. The authors solved the MILP formulation optimally for a small problem with eight custom locations. The impacts of the size of the region and the speeds/ranges combinations of drones on the makespan were also tested. Realistic sized problems were tested using a three-phased heuristic solution approach. The paper tested 1600 instances with the combinations of various levels of number of customers, the size of regions, the depot locations, the number of drones per truck, and the speed and flight range. Results show that adding more drones to an existing fleet tends to have diminishing marginal improvements and densely distributed customers tend to benefit the most. The authors also developed two variants of the mFSTSP: one is when the truck (and also driver) is not required at the depot for launch and recovery, and the other is when the driver, but not the truck, is not required at customer locations for launch and recovery. The two variants reflect future automation functions that allow drones to serve customers automatically from the depot and launch and recovery at the truck without the help of the driver at customer locations, respectively. Five cases involving combinations of the two automation systems were tested with two different metrics: the time the last vehicle returns to the depot, and the time the truck returns to the depot. The results indicate that automation at the depot may be more beneficial than automating the truck (removing the driver) at customer locations.

Sacramento et al. (2019) considered an extension of FSTSP by allowing a fleet of homogenous capacitated trucks that each carry a drone to serve customers. The authors define the problem as the vehicle routing problem with drones (VRPD). The main

difference between FSTSP and VRPD, besides the number of trucks in the model are as follows. First, the objective of VRPD is to minimize the total delivery cost incurred by both trucks and drones. The cost of trucks is affected by the fuel price and the fuel consumption rate implicitly in the MILP model. However, the paper did constrain the maximal tour time of trucks. Second, unlike FSTSP, VRPD also considered the service time at each customer location by both trucks and drones. Third, the paper also takes the load capacity (in kg) of trucks into consideration. An adaptive large neighborhood search (ALNS) metaheuristic was developed to solve the VRPD. The initial solution was constructed by three heuristics in sequence: a nearest neighbor heuristic as a construction algorithm for truck tours, an improvement heuristic for truck tours, and a drone addition algorithm. In each iteration, a destroy method and a repair method were used to modify the solution. Test instances are randomly generated using parameters from the academic literature and some published reports. The result showed that ALNS achieved 0% optimality gap with up to 12 customers in at most 82 seconds. Savings from using drones and trucks with ALNS relative to truck-only were calculated, and the results showed 20-30% savings for problems with up to 200 customers. Sensitivity analysis for drone features including the operating cost incurred by drones, endurance, speed, and payload capacity were tested. The results showed there were barely any savings when the drone arc-cost was up to 50% of truck arc-cost (drone arc-cost is α times truck arc-cost for each arc). Savings increased as the endurance increased from 5 minutes to 30 minutes, but there were no significant increased savings for endurance levels beyond 30 minutes. There were large savings even when the speed of drones was relatively low (40 km/h), and the difference among savings for the various speeds of drones ranging from 40 km/h

to 120 km/ph was not obvious. The savings increased from about 10% to 30% as the drone payload increased from 1 kg to very large payloads.

Chiang et al. (2019) proposed a MILP model with two objective functions to solve a Green VRPD problem. One objective function is to minimize the total CO_2 emissions, including the emissions of the petroleum-based ground vehicles and the emissions from power generation facilities for drones (for charging batteries). The other objective function is to minimize the total cost including the fixed cost of the vehicles and the variable routing cost of the vehicles and the drones. There is a fixed cost associated with each vehicle-drone tandem. The variable routing cost (fuel cost) is a function of distance traveled and gross weight that depends on the empty weight of the vehicle, the weight of the payload, and the weight of the drone. A genetic algorithm was developed to solve large-scale problems. The experimental results showed that the use of drones can help save fixed costs by reducing the total delivery time and the number of vehicles required. The use of drones can also save variable costs and reduce carbon emissions.

Wang and Sheu (2019) and Kitjacharoenchai et al. (2019) developed m-truck and n-drone tandem delivery models. The main difference compared to other papers in terms of problem features is that drones do not have to depart and land on the same truck. Wang and Sheu (2019) developed arc-based and path-based MILP formulations for the Vehicle Routing Problem with Drones (VRPD) with drone docking hubs. A drone can depart from the depot, a docking hub, or a truck, perform a single delivery or multiple deliveries, and then land on the depot or a docking hub. Each docking hub serves as a transfer station and landing spot for drones, and also can store and maintain backup

drones. The objective is to minimize the total cost, including the fixed cost of using trucks, and the truck and drone transportation cost. The authors developed a branch-and-price algorithm based on the path-based formulation. Computational results included 20 instances with 8 or 13 customers and 2 docking nodes. Customers were either uniformly distributed or clustered. The branch-and-price algorithm solved all instances to optimality and outperformed the arc-based model. The authors also compared VRPD with the corresponding VRP without drones by converting the docking hub nodes to customer nodes. The results showed that the VRPD saved an average of 20% in cost and on average allowed customers to receive deliveries 5.5 minutes earlier. Sensitivity analysis for drone flight endurance showed that doubling the flight endurance (from 20 minutes to 40 minutes) can reduce the total cost by nearly 10%.

Kitjacharoenchai et al. (2019) developed a MILP formulation to solve a multiple traveling salesman problem with drones (mTSPD). It is an extension of FSTSP and mTSP with multiple homogenous trucks and homogenous drones. A drone is allowed to depart from a truck and return to a different truck or the depot, or depart from the depot and return to a truck or the depot directly, in addition to coordinating with the trucks. The objective is to minimize the arrival time of the last vehicle (a drone or a truck) at the depot. The problem only allows drones to return to a truck at a customer node while the truck is stationary. Just like in the mFSTSP by Murray and Raj (2019), in this paper, multiple drones can be in flight simultaneously, but cannot be launched and retrieved at a truck at the same customer location. The authors solved the problem optimally with 10 nodes within one hour. An adaptive insertion algorithm (ADI) with two phases was used to solve the problem with up to 100 locations. The mTSP tours without drones were

generated in the first phase with three heuristics, respectively, a genetic algorithm (GA), combined K-means clustering with nearest neighbor, and a random cluster algorithm. The second phase used one removal operator and three insertion operators to add drone arcs to the solution. The results showed that the GA gave the minimal makespan and performed the best, so only the GA was used in the second phase. The authors also compared TSP-MILP and FSTSP-MILP with the proposed mTSPD for both MILP and ADI for small instances, and the results showed that the ADI for mTSPD performed very well, such that the "worst" instance had a gap of 1.18% and was obtained within 4 seconds.

Wang et al. (2017) used analytical methods to develop several worst-case theoretical bounds for the Vehicle Routing Problem with Drones (VRPD). The objective is to minimize the maximum duration of routes for both truck-only and truck-drone tandem settings and evaluate the maximum savings in route completion time that can be obtained from using drones. The problem assumes that the payload capacity of drones is 1 unit, each truck can carry multiple drones, there is no delivery service time, and the vehicle (truck or drone) that arrives at the pick-up location first has to wait for the other one. The analysis shows that the worst-case bounds depend on the number of drones per truck and the speed of the drones relative to the speed of the truck. Poikonen (2017) extended several worst-case results from Wang et al. (2017), including explicitly incorporating the limited battery life of drones and using Euclidean distances for drone travel. The paper also defined the min-max Close-Enough VRP (CEVRP) as the problem of minimizing the time required for at least one in a set of trucks to come within some distance of each customer location before returning to the depot. The paper proves that the VRPD is an intermediate problem that connects the VRP and CEVRP.

2.2.4. Research gap

For the national level vaccine SCND problem, Scott and Scott (2019) is the only study that incorporates facility location decisions and drone delivery simultaneously; however, the model chose the depot and drone ports from continuous space and the objective is to minimize the total delivery distance. This approach to the location problem is not a good fit in most LDCs due to the limited infrastructure (and hence a limited set of feasible facility locations), nor in island regions. Vanuatu fits both of these conditions, so a discrete location model is more appropriate where the specified set of feasible facility locations (e.g., those with highly reliable electricity and transport connections) can be identified. Moreover, Scott and Scott (2019) did not optimize the flows in the network or allow multiple modes.

As previously indicated, there is only one paper (Walia et al. 2018) designed for medical product drone delivery in LDCs; however, this paper did not take facility location decisions into consideration. Further, both Walia et al. (2018) and Scott and Scott (2019) limit the mode of transportation in the first tier of the network to truck. By contrast, my national level vaccine SCND problem allows the model to select the best mode of transportation for all arcs (boat, truck, airline, drone).

The majority of the other papers discussed in this section are relevant to my local delivery in a health zone research problem (P2) to some extent, but there are more differences than similarities between these papers and my local delivery problem P2. First, drones and trucks in the models of these papers depart from the same depot, where drones either leave the depot carried by trucks or by themselves, while the two types of vehicles depart from different locations in my local delivery problem. Second, although

most of the truck-carries-drone papers modeled synchronized visits between trucks and drones and my local delivery problem requires a drone to synchronize with a healthcare worker for receiving and administering the vaccine, there are two differences between my local delivery problem and the truck-carries-drone papers: (i) Among all modes of transportation in my local delivery problem (i.e., trucks, drones, boats, and health workers by walking), only health workers might be carried by other modes of transportation, including trucks and boats. Drones are not carried on the other transport modes, so this might require different modeling features; (ii) The purposes of synchronization in my local delivery problem and in the truck-carries-drone literature are different. For the former, synchronization is required at the demand points for deliveries, while for the latter, synchronization is required for the return of the drone to the truck so the demand points are visited by only one of the vehicles.

It is worth noting that my research does not consider stockouts and related inventory uncertainty issues, nor does it consider uncertainty in demand. These are areas of future research.

3. National Vaccine Supply Chain Network Design

The national level vaccine supply chain design problem (P1) is to design a multi-modal multi-tier vaccine supply network for LDCs where vaccines are delivered from a national depot to a set of vaccine DCs serving the local non-overlapping health zones. Vaccines may be transported by a variety of modes, e.g., truck, boat, aircraft, and long-range drones. A novel feature of using drones is the ability to recharge the drone at a "relay station" to extend its range. Vaccines are to be sent monthly to satisfy the demand in the health zones, while maintaining the cold chain requirement and with the lowest possible cost. DC candidates must be health clinics with health workers and cold chain facilities (i.e., permanent clinics). There is a given set of drone base candidates in the network, and the selected drone bases will serve as stations for storing, maintaining, and dispatching the long-range drones that are used in this model for national level delivery. There is a given set of drone relay station candidates in the network, and the selected relay stations allow longer drone paths. A drone base will always include a relay station to ensure all drones dispatched are fully charged. A drone path must start with a drone base (which includes a relay station), and it can include intermediate points along drone flights paths that recharge the drone battery, and it ends with a relay station to ensure drones are fully charged for return trips (return trips are not in the model). The problem description is given in section 3.1. Section 3.2 introduces the research questions for problem P1. Optimization models are developed in section 3.3. Section 3.4 describes the data for Vanuatu used in this section, and is followed by sections 3.5-3.7 that present three case studies. The last section, section 3.8, conducts a sensitivity analysis on key parameters for problem P1.

3.1. Problem description

In the nationwide vaccine supply network design problem with drone, vaccines are delivered by a set of transportation modes from a national depot to selected DCs. This is modeled on a network with a set of nodes representing facilities of various types and arcs representing transportation between facilities. There are four modes of transportation available in this problem: drones, boats, trucks, and airplanes. The use of airplanes may reflect scheduled airline activity or chartered aircraft. Note that a pair of nodes may be connected by several different transportation modes.

We assume that all modes of transportation are always available on their corresponding arcs when needed, and I consider only feasible travel arcs that satisfy the travel range for each mode (e.g., due to a battery limit for drone flights) and the cold chain limit as well. Further, i assume the cold chain is restarted at the end of every boat, truck or airplane arc. This is based on the assumption that the end of every one of these arcs includes facilities with cold chain equipment. Note that in reality some transshipments of vaccines between modes may not have (or need to have) the cold chain restarted (e.g., vaccines may be transshipped directly from an airplane to a truck without storage in a freezer to lower the temperature, or without replacing ice packs) if the trip portion between the permanent storage (e.g., a refrigerator) using several arcs and/or multiple modes is short enough to not violate the cold chain. Detailed modeling of cold chain requirements over multi-arc paths with multiple modes is left for future research. In our model, while I assume the cold chain restarts at the end of every boat, truck or airplane arc, I do not make that assumption for every drone arc. For drone arcs, the cold

chain restarts only at the end of a drone path (where the vaccine either reaches its destination DC, travels further on another mode, or starts a new drone path).

This problem includes three different types of facilities to be located at nodes, and several different facility types may be located at a single node. The facility types are: a local health zone distribution center (DC), a drone base (DB), and a drone relay station (RS). A DC is a facility that is the destination of all vaccines for a particular health zone and exactly one DC is to be selected in each health zone. Each candidate DC is associated with a single health zone and has a demand corresponding to the vaccine demand of that health zone. A DC has permanent staff and permanent cold chain equipment to store vaccines. The DC also serves as the origin for the vaccination outreach program to remote locations in each health zone, which is modeled in the second research problem P2 (analyzed in Chapter 4). A drone base (DB) is a facility that serves as the start of a drone path, where a drone path is a sequence of one or more drone flights by a particular drone. A DB has electricity and cold chain equipment, where the cold chain can be restarted. An RS is a facility for recharging the drone. A relay station may be an automatous drone pad or drone dock that does not have cold chain equipment, and its only function is to recharge the drone. I consider two types of relay stations: “regular” relay stations and remote relay stations. A remote relay station is located at a remote site (e.g., away from staff and other infrastructure), and transfers to and from other transport modes are not allowed at a remote drone relay station; thus a remote RS cannot be the start or end of a drone path. Note that a RS can be co-located with DCs, and every drone base has a RS which allows charging the drone for the first flight on a drone path.

Visiting a RS on a drone path does not restart the cold chain, but I reiterate that a DB and RS coincide at the start of the drone path where the cold chain is restarted.

In our model, drones are dispatched from a DB and can fly through a series of drone relay stations (i.e. on several sequential drone arcs) as long as the total flight time is within the vaccine cold chain time limitation. Thus, each drone path begins at a DB, possibly visits one or more RSs, and then ends at a RS. I assume the drone is fully charged at the beginning of a drone path and on visiting every node along a drone path. Thus, the starting node of a drone path and every intermediate node on a drone path are RSs. The end of every drone path is a RS, which may coincide with a DC or a DB for another drone path. Note that a drone base can be the start of more than one drone path, and because drone paths may intersect or overlap, a particular node that is an RS but not a DB for one drone path, may be a DB (and RS) for a different drone path.

The problem addresses the tactical-level vaccine delivery network design, and the monthly volume of vaccines is usually small compared to typical capacities of airplanes, trucks and boats. Thus, the model assumes all non-drone modes of transportation have capacity large enough to handle the vaccine being sent (i.e. the vehicle capacity does not limit the flow). Therefore, a non-drone arc is only travelled once in the planning horizon, e.g., per month. Two types of drones can be used in problem P1: small fixed wing (SFW) drones and large fixed wing (LFW) drones. Considering the appropriate specifications of drones for flight range and capacity that fit the P1 problem the best, SFW and LFW drones are selected for modeling from the seven types of drones in the toolkit developed by VillageReach based on field experiences with drones in global health settings (VillageReach, 2019).

LFW drones have a capacity similar to a small airplane and SFW drones have a much smaller capacity (10 liters in our base case). To satisfied the demand at each DC, a drone arc for an SFW drone could be travelled more than once per month due to the limited capacity, while a drone arc of an LFW drone is travelled at most once in the planning horizon because the capacity is larger than the demand at DCs.

I refer to a traversal by a drone of a drone arc as a drone trip. I define a drone trip the same as a drone flight which corresponds to one drone arc and is travelled between a takeoff point and a landing point. A drone arc can have more than one drone trip when the liters transported via a drone arc are more than the payload capacity of a drone. For example, if an SFW drone has a capacity of 10 liters, and 30 liters are to be sent on a particular arc by SFW drones, then there are three SFW drone trips on that arc. Our modeling is strategic and does not address the detailed scheduling of multiple drone trips per arc.

To model the cost for drone trips I developed two cost models to accommodate both LFW and SFW drones and to investigate how charging for drone usage differently affects the solution and the use of drones. The first cost model considers the capacity of drones and models drone transportation cost as proportional to the vaccine flow that the drone carries each month. This effectively models fractional drone trips. For example, sending 25 liters per month on a drone with a capacity of 10 liters is modeled as 25/10 = 2.5 drone trips. The second cost model is a fixed charge per month for using the drone on an arc. This models the situation when the amount of vaccine carried does not appreciably affect the cost of operating the drone, as with a very large drone (where the added weight for the vaccine payload may be a small fraction of the total drone weight).

The first drone cost model is suitable for a drone with a smaller capacity relative to the vaccines it carries on a drone arc, while the second model is suitable for a large drone like a small airplane (which might have a capacity of several hundred liters or more). Figure 3.1 shows examples of large and small drones of the type included in LFW and SFW categories.

We also include in our model a fixed cost for drone arcs, for both drone types, to capture the cost to establish a drone arc. This can include the necessary scouting flights for a drone arc to ensure the takeoff and landing/delivery areas and the airspace for the flight are safe and feasible (e.g., avoiding "...unforeseen obstacles such as large trees or challenging terrain…" (Wingcopter 2019)).

a. Example of a large drone LFW

b. Example of a small drone SFW.

Figure 3.1 Examples for LFW and SFW

Solving the national level vaccine distribution problem requires determining (i) the sets of DCs, DB and RS to locate, (ii) the flow of vaccines from the national depot to the DCs, and (iii) the set of transportation arcs to use to carry vaccine using the various modes so that there is one DC in each health zone that receives the vaccine demand for that health zone, the cold chain is not violated, and the total cost is minimized.

3.2. Research questions

Based on the problem described in section 3.1, this dissertation addresses the following eight research questions.

- *R1: how useful are drones in delivering vaccines on a monthly basis in an island country?*
- *R2: how are the non-drone modes affected by the use of drones?*
- *R3: how useful are multi-step drone paths?*
- *R4: how does the use of different drone types affect the use of drones and performance of the delivery network?*
- *R5: how does the cost of drone bases affect the use of drones and performance of the delivery network?*
- *R6: how does the cost of drone relay stations affect the use of drones and performance of the delivery network?*
- *R7: how does the magnitude of demand affect the use of drones and performance of the delivery network?*
- *R8: how does the length of cold chain time limitation affect the use of drones and performance of the delivery network?*

R1 is the most important and fundamental question I answer for problem P1. It is answered by comparing solutions with drones to solutions without drones while holding the remaining problem settings the same. The cost and service performance of the delivery network with drones is compared with the cost and service performance of the

delivery network without drones. I use the transportation cost for the cost performance, and weighted delivery time to a health zone for the service performance. The two drone cost models discussed earlier are used to evaluate the impacts from different drone types.

Research question *R2* is answered by comparing the solutions with drones to solutions without drones as well, however, I look at the cost and performance of the various transport modes for this research question. I evaluate how the usage of each existing mode changes once drones are allowed in the delivery network. I examine in what situation and which mode(s) are replaced, or used more, after adding drones as an additional delivery option.

R3 and *R4* are research questions to help us understand the impact of different drone use and drone types on the performance of the delivery network. *R3* is answered by a case study varying the number of drone steps (the number of drone arcs in a drone path) and the number of drone paths. I examine how varying the number of drone steps and drone paths affects the use of drones and the overall delivery cost and service performance. *R4* is answered by comparing solutions with SFW drones to solutions with LFW drones with regards to cost and service performance of the delivery network.

Questions *R5-R8* are answered by a sensitivity analysis that varies four key parameters: the drone base fixed cost, the relay station fixed cost, the demand magnitude, and the cold chin limit. I evaluate how changes in the value of each key parameter affect the cost and service performance of the delivery system.

3.3. Model formulation

P1 can be formally described as follows. Let $G = (V, E)$ be the supply network graph with the set of nodes V and the set of arcs E. Set V includes the origin node for vaccines (e.g., the national depot) and destination nodes for vaccines that correspond to the set of DC candidates. Let O denote the set with a single element, the origin node for vaccines, and let H denote the set of health zones. Let set G_h be the set of DC candidates in health zone $h \in H$. Set V also includes "intermediate nodes" corresponding to the endpoints of the feasible transportation arcs for all modes. This includes the nodes needed to model drone paths, which are drone base candidates in set U, regular relay station candidates in set $R1$, and remote relay station candidates in set $R2$, where $R1 \cup R2 = R$ Note that $R1 \cap R2 = \emptyset$, $U \cap R2 = \emptyset$ and U is a subset of $R1$. I use italics letters to indicate the transportation modes: airplane (*A*), boat (*B)*, truck (*K*) and drone (*D*). Set *M* is the set of all transportation modes *M* = {*A, B, K, D*}. The top panel of Table 3.1 shows the sets used in the model.

Let E refer to the collection of feasible arcs corresponding to all transportation modes in M, denoted by $a = (i, j, m)$, where $i, j \in V$ and $m \in M$. An arc is feasible if it satisfies the vehicle range (travel distance) limit and the cold chain limit. Also, recall that no non-drone arcs connect to the remote relay stations. To identify feasible arcs, I devise a pre-processing procedure using the cold chain time limit λ_{max} (e.g., 8 hours) and the transportation mode range limit δ_{max} (e.g., 150 km for a SFW drone). I assume that only the drone has a range limit, and other modes have an unlimited traveling range. Each arc $a = (i, j, m) \in E$ has an associated travel time t_a and travel distance k_a. Note that two arcs connecting the same pair of nodes may have a different travel distance, as, for

example, the truck driving distance may be (much) longer than the airplane flying distance. Thus, every feasible drone arc $a = (i, j, D) \in E$ is such that $t_a \leq \lambda_{max}$ and $k_a \leq \delta_{max}$, and every non-drone arc $a = (i, j, m) \in E | m \neq D$ is such that $t_a \leq \lambda_{max}$

The monthly vaccine demand of health zone $h \in H$ is denoted as d_h. To satisfy demand d_h, $h \in H$, the vaccines are shipped from the origin node to the destination DC along a path consisting of a sequence of arcs of possibly different travel modes that starts at the origin in set O and ends at a selected DC candidate in a health zone. For example, a path 0→1→2→3→4→5 may use all four modes in the five arcs: (0, 1, *A*), (1, 2, *B*), (2, 3, *K*), (3, 4, *D*), and (4, 5, *D*), where node 0 is the national depot and node 5 is the selected DC candidate in a health zone A. The vaccine path above includes a drone portion 3→4→5 consisting of two arcs. A "drone path" is a sequence of drone arcs flown by a single drone, which satisfies the cold chain. For each drone path, the start node is a drone base and all nodes on the path are assumed to be relay stations to allow the drone to begin each arc in the path fully charged. The last node in a drone path is a relay station to allow the drone to be fully charged for the return trip, which may retrace the outbound trip or may shortcut some portions if feasible. Planning of the return trips is not considered in this model. I let n be an exogenous index for the drone paths, $n \in P$, where P is the set of indices. Let N be the largest index in $P = \{1, 2, \dots, N\}$, so N is the largest number of drone paths allowed in a solution. Although the maximum number of drone paths is limited by N, the set of drone paths actually used in a solution is not prespecified, but a result of the optimization. Thus, using different numbers for N might generate different solutions. Small values of N reflect a resource limit. For example, there could be 0, 1, 2, or 3 drone paths formed in a solution when $N = 3$. To define the arcs in each drone path I

use the binary variables p_{ij}^n, which equals 1 if drone path n uses arc (i,j), $i,j \in R$, and 0 otherwise. For each drone path, I also define binary variables $u1_j^n$, which equal 1 if drone path n begins at node j, $j \in U$, and 0 otherwise; and binary variables $u2_j^n$, which equal 1 if drone path n ends at node j, $j \in R$, and 0 otherwise. Note that drone paths may overlap (use the same arc) or be traveled in sequence. For example, $p_{02}^1 = p_{23}^1 = p_{34}^1 = 1$ and $p_{02}^2 = p_{25}^2 = p_{56}^2 = 1$ define two drone paths 0→2→3→4 and 0→2→5→6 that both involve using drones on arc $(0,2)$. In addition, I use Ω to denote the maximal number of sequential drone arcs allowed in a drone path in a solution. For example, if $\Omega = 2$, then a drone path can have at most 2 sequential drone arcs, so a drone path like 0→2→3→4 would not be allowed. Thus, the parameter Ω allows control over the length of drone paths. However, note that multiple drone paths can occur in sequence, as for example with two drone paths 0→2→3 and 3→4→5 with nodes 0 and 3 as the DBs (the need for two such drone paths could be that the cold chain limitation can be extended by adding a DB at node 3, so the demand at node 5 can be fulfilled). Those two paths together reflect one or more drones flying from 0→2→3→4→5, but because it is two drone paths there are two DBs at nodes 0 and 3. The maximum of drone arcs in a drone path is $|R| - 1$.

Let f_a be a continuous variable to track the vaccine flow in liters on arc $a = (i,j,m) \in E$. Let cap be the drone capacity (e.g., 10 liters) in liters, which is used in the first drone cost model. If the volume of vaccines carried on a drone arc exceeds the drone capacity cap, then the drone arc may be flown more than once in the time period. The first cost model captures the lower bound of drone trips using f_a/cap, $a = (i,j,D) \in E$. I reiterate that I assume all non-drone modes of transportation (e.g., *A, B, K*) have unlimited capacity. Thus, all non-drone modes make at most one traversal of an arc. Let

c_a denote the cost of arc $a \in E$. (Arc costs may be given data, or I can calculate the arc costs by multiplying the arc travel distance k_a by the variable cost rate $e_m, m \in M$ (e.g., dollar per km) for the appropriate transportation mode.) Thus the first drone cost model for arc a is $c_a \times f_a/cap$. In the second drone cost model, the cost for arc a is just c_a; thus it is independent of the volume of vaccine the drone carries. Let c' be the fixed drone arc cost to establish a safe drone arc.

The following defines the remaining parameters and decision variables in this model. Let g_i be the monthly fixed cost of operating DC $i \in G_h, h \in H$ (e.g., \$200 per month), m_i be the monthly fixed cost of operating drone base $i \in U$ (e.g., \$50 per month), and h_i be the monthly fixed cost of operating relay station $i \in R$ (e.g., \$10 per month). Let y_i be the binary variable to track if DC $i \in G_h, h \in H$ is open, so $y_i = 1$ if DC i is open, and 0 otherwise. Let r_i be the binary variable to track if a relay station $i \in R$ is open, so $r_i = 1$ if RS i is open, and 0 otherwise. Let u_i be the binary variable to track if a drone base $i \in U$ is open, so $u_i = 1$ if DB i is open, and 0 otherwise. Let x_a be the binary variable to denote if an arc $a = (i, j, m) \in E$ is selected, so $x_a = 1$ if arc a is used in the solution. Continuous variable fd_{ij}^n captures the flow of vaccines by drone on arc (i, j), $i, j \in R$ in path $n \in P$. Let b_n be the binary variable to denote if path $n \in P$ is formed in a feasible solution, so $b_n = 1$ if drone path n is used in the solution. Finally, continuous variable $w_j^n, j \in R, n \in P$ and continuous number Γ are used in the MTZ subtour elimination constraints. Table 3.1 lists sets, parameters, and decision variables in this model.

Sets	
H	Set of health zones
G_h	Set of DC candidates in health zone $h \in H$
O	Set of a single vaccine origin node
$R1$	Set of regular relay station candidate nodes
$R2$	Set of remote relay station candidate nodes
R	Set of relay station candidate nodes, $R = R1 \cup R2$
U	Set of drone base candidate nodes
P	Set of indices for the drone paths, where $P = \{1, 2, \dots, N\}$
M	Set of transportation modes.
Parameters	
g_i	Monthly fixed cost of operating DC $i \in G_h, h \in H$
m_i	Monthly fixed cost of operating drone base $i \in U$
h_i	Monthly fixed cost of operating relay station $i \in R1 \cup R2$
d_h	Monthly vaccine demand required by health zone $h \in H$
λ_{max}	Cold chain time limitation for vaccines
t_a	Travel time of arc $a = (i, j, m) \in E$
c_a	Variable cost of arc $a = (i, j, m) \in E$
c'	Fixed cost of drone arc $a = (i, j, D) \in E$
cap	Drone payload
N	Number of drone paths allowed in the model, $\|P\| = N$
Ω	Maximum number of drone arcs in a drone path (integer)
Γ	Continuous number used in MTZ subtour elimination
Decision Variables	
y_i	Binary variable, 1 if DC $i \in G_h, h \in H$ is open, 0 otherwise
r_i	Binary variable, 1 if relay station $i \in R$ is open, 0 otherwise
u_i	Binary variable, 1 if drone base $i \in U$ is open, 0 otherwise
$u1_j^n$	Binary variable, 1 if drone path n begins at node j, $n \in P, j \in U$, 0 otherwise
$u2_j^n$	Binary variable, 1 if drone path n ends at node j, $n \in P, j \in R1$, 0 otherwise
x_a	Binary variable, 1 if arc $a = (i, j, m) \in E$ is selected, 0 otherwise
f_a	Continuous variable for the flow of vaccines on arc $a = (i, j, m) \in E$

fd_{ij}^n	Continuous variable for the flow of vaccines of drone arc (i,j) on path $n \in P, i,j \in R$
p_{ij}^n	Binary variable, 1 if drone path n includes arc (i,j), $n \in P, i,j \in R$, 0 otherwise
b_n	Binary variable, 1 if path $n \in P$ is formed in a feasible solution
w_j^n	Continuous variable to label node $j \in R$ on path $n \in P$ in MTZ subtour elimination

Table 3.1 Summary of notations in P1

The goal is to determine (i) the set of DCs, drone bases, and relay stations to open, (ii) the flow of vaccines on each arc, and (iii) the set of transportation arcs, so that each health zone has a DC, the cold chain is never violated, and the total facility cost and transportation cost are minimized. I present the mixed-integer linear programming (MILP) formulation with the first drone cost model, denoted P1-C1, as follows:

P1-C1

Minimize:

$$\sum_{i\in G_h, h\in H} g_i y_i + \sum_{i\in U} m_i u_i + \sum_{i\in R} h_i r_i + \sum_{a=(i,j,m)\in E | m\neq D} c_a x_a + \sum_{a=(i,j,D)\in E} (c_a f_a / cap + c' x_a) \quad 3.1$$

Subject to:

$$\sum_{m\in\mathbb{M}} \sum_{a=(i,j,m)\in E} f_a - \sum_{m\in\mathbb{M}} \sum_{a=(k,i,m)\in E} f_a = -d_h y_i, \forall h \in H, \forall i \in G_h \quad 3.2$$

$$\sum_{m\in\mathbb{M}} \sum_{a=(i,j,m)\in E} f_a - \sum_{m\in\mathbb{M}} \sum_{a=(k,i,m)\in E} f_a = 0, \forall i \in V/O \cup \bigcup_{h\in H} G_h \quad 3.3$$

$$\sum_{i\in G_h} y_i = 1, \forall h \in H \quad 3.4$$

$$f_a \leq x_a \cdot \sum_{h\in H} d_h, \forall a \in E \quad 3.5$$

$$\sum_{n\in P} p_{ij}^n \geq x_a, \forall i,j \in R, \forall a = (i,j,D) \in E \quad 3.6$$

$\sum_{n\in P} p_{ij}^n \leq N x_a, \forall i,j \in R, \forall a = (i,j,D) \in E$ 3.7

$\sum_{n\in P} b_n \leq N$ 3.8

$2p_{ij}^n \leq r_i + r_j, \forall i,j \in R, \forall n \in P$ 3.9

$\sum_{i\in R} p_{ji}^n - \sum_{i\in R} p_{ij}^n \leq u1_j^n, \forall j \in U, \forall n \in P$ 3.10

$-\sum_{i\in R} p_{ji}^n + \sum_{i\in R} p_{ij}^n \leq u2_j^n, \forall j \in R1, \forall n \in P$ 3.11

$\sum_{i\in R} p_{ji}^n - \sum_{i\in R} p_{ij}^n = 0, \forall j \in R2, \forall n \in P$ 3.12

$u1_j^n \leq u_j, \forall j \in U, \forall n \in P$ 3.13

$b_n = \sum_{j\in U} u1_j^n, \forall n \in P$ 3.14

$b_n = \sum_{j\in R1} u2_j^n, \forall n \in P$ 3.15

$\sum_{i\in R}\sum_{j\in R} p_{ij}^n \geq b_n, \forall n \in P$ 3.16

$p_{ij}^n \leq b_n, \forall i,j \in R, \forall n \in P$ 3.17

$u1_j^n \leq \sum_{i\in R} p_{ji}^n, \forall j \in U, \forall n \in P$ 3.18

$u2_j^n \leq \sum_{i\in R} p_{ij}^n, \forall j \in R1, \forall n \in P$ 3.19

$b_n \leq b_{n-1}, \forall n \in P, n \neq 1$ 3.20

$\sum_{j\in R} p_{ij}^n \leq 1, \forall i \in R, \forall n \in P$ 3.21

$\sum_{i\in R}\sum_{j\in R} p_{ij}^n \leq \Omega, \forall n \in P$ 3.22

$w_i^n - w_j^n + \Gamma\, p_{ij}^n \leq \Gamma - 1, \forall i,j \in R, \forall n \in P$ 3.23

$f_a = \sum_{n\in P} fd_{ij}^n, \forall a = (i,j,D) \in E, \forall i,j \in R$ 3.24

$$fd_{ij}^{n} \le p_{ij}^{n} \cdot \sum_{h \in H} d_h \,, \forall i,j \in R, \forall n \in P \quad 3.25$$

$$\sum_{a=(i,j,D) \in E, i,j \in R} t_a p_{ij}^{n} \le \lambda_{max}, \forall n \in P \quad 3.26$$

$$y_i \in \{0,1\}, \forall i \in G_h, \forall h \in H \quad 3.27$$

$$x_a \in \{0,1\}, \forall a = (i,j,m) \in E \quad 3.28$$

$$f_a \ge 0, \forall a = (i,j,m) \in E \quad 3.29$$

$$r_i \in \{0,1\}, \forall i \in R \quad 3.30$$

$$u_i \in \{0,1\}, \forall i \in U \quad 3.31$$

$$u1_i^{n} \in \{0,1\}, \forall i \in U, \forall n \in P \quad 3.32$$

$$u2_i^{n} \in \{0,1\}, \forall i \in R1, \forall n \in P \quad 3.33$$

$$fd_{ij}^{n} \ge 0, \forall i,j \in R, \forall n \in P \quad 3.34$$

$$p_{ij}^{n} \in \{0,1\}, \forall i,j \in R, \forall n \in P \quad 3.35$$

$$b_n \in \{0,1\}, \forall n \in P \quad 3.36$$

$$w_i^{n} \ge 0, \forall i \in R, \forall n \in P \quad 3.37$$

The model with the second type of drone cost, denoted **P1-C2**, has the same constraints as above, so the mixed-integer linear programming (MILP) formulation with the second drone cost model is:

P1-C2

Minimize:

$$\sum_{i\in G_h, h\in H} g_i y_i + \sum_{i\in U} m_i u_i + \sum_{i\in R} h_i r_i + \sum_{a=(i,j,m)\in E} c_a x_a + \sum_{a=(i,j,D)\in E} c' x_a \qquad 3.38$$

Subject to:

Constraints 3.2 – 3.37

The objective function 3.1 in P1-C1 minimizes the total monthly costs consisting of five components. The first term is the total monthly cost of opening and operating DCs. The second term is the total monthly cost of opening and operating drone bases. The third term is the total monthly cost of opening and operating drone relay stations. The fourth term is the total monthly transportation cost for airplane, truck, and boat. The fifth term is the total monthly transportation variable cost for drones, based on a possibly fractional number of drone trips on an arc (from the flow divided by the drone capacity). The last term is the fixed cost to establish the drone arcs. The objective function 3.38 in P1-C2 replaces the total monthly drone transportation cost based on flows, with a fixed charge corresponding to sending at most one drone flight per arc. Recall that objective 3.1 and P1-C1 are appropriate for settings where the drone flow on an arc may exceed the drone capacity, while objective 3.38 and P1-C2 are appropriate for settings where the drone transportation cost does not depend significantly on the payload of vaccines. I now describe the constraints in the model.

Constraint 3.2 conserves the vaccine flow for DC candidates. It ensures the demand for each health zone is satisfied in the selected DC of its health zone. Constraint 3.3 conserves the vaccine flows for intermediate nodes in the network that do not have a

demand. Constraint 3.4 ensures one DC is open for each health zone. Constraint 3.5 ensures there is no vaccine flow on arc a if arc a is not selected. $\sum_{h \in H} d_h$ is an upper bound of the arc flow on any arc.

Constraint 3.6 ensures that if a drone arc is selected, then the drone arc is on at least one drone path. In other words, there is at least one drone flight on the drone arc. Constraint 3.7 ensures that there is no drone flight on a drone arc if the drone arc is not selected. If the drone arc is selected, then there are at most N drone paths that use that drone arc. Constraint 3.8 ensures the total number of drone paths in the solution is not more than the maximum number of drone paths allowed.

Constraint 3.9 ensures two end nodes of a drone arc are open as relay stations if the drone arc is selected. Constraint 3.10 ensures a node on a drone path is open as a drone base on that drone path if there are more outgoing drone arcs than incoming drone arcs to the node. Constraint 3.11 identifies a node on a drone path as the end node of the path if there are more incoming drone arcs than outgoing drone arcs from the node. Constraint 3.12 conserves the number of drone flight arcs at a remote relay station on a drone path. Thus a drone path cannot start or end at a remote RS. Constraint 3.13 ensures a node is open as a drone base if the node is open as a drone base on any drone path. Constraint 3.14 ensures there is only one start node on a drone path. Constraint 3.15 ensures there is only one end node on a drone path. Constraint 3.16 ensures a drone path contains at least one drone flight arc. Constraint 3.17 ensures if a drone path does not exist, then no drone flight arc is on that drone path. Constraint 3.18 ensures no node is selected as a drone base for drone paths that are not used. Constraint 3.19 ensures no node is identified as an end node of a drone path for drone paths that are not used.

Constraint 3.20 ensures drone paths used in a solution are formed in order. For example, if drone path 3 exists in a solution, then so must drone paths 1 and 2. Constraint 3.21 ensures that a drone path is a sequence of drone arcs and not another topology (e.g., like a tree). Constraint 3.22 limits the number of drone arcs on a drone path. Constraint 3.23 is the MTZ subtour elimination constraint for the drone paths.

Constraint 3.24 ensures the flow of vaccines carried on a drone arc is the sum of the flow of vaccines carried on all drone paths that use that arc. Constraint 3.25 links the drone arc binary variable to the drone arc flow variables for each path. This is a "big-M" constraint where the maximum flow is just the sum of demand for all health zones. Constraint 3.26 ensures the total travel time of a drone path is within the cold chain time limitation. Constraints 3.27 - 3.37 specify the domains for all the decision variables.

3.3.1. Service measures

To supplement the cost objective I also include a service measure of liter-hours in the model. The total liter-hours in a solution is given as follows:

$$\sum_{a=(i,j,m)\in E} f_a t_a.$$

The weighted average time for vaccines to reach a health zone can then be calculated as the average liter-hours per health zone divided by the average demand (liters) per health zone:

$$\frac{\sum_{a=(i,j,m)\in E} f_a t_a/|H|}{\sum_{h\in H} d_h/|H|} = \frac{\sum_{a=(i,j,m)\in E} f_a t_a}{\sum_{h\in H} d_h}.$$

Note that the denominator is a constant, the total demand of all health zones, so the service really is reflected in the total liter-hours of a solution.

Model P1-S optimizes the overall service by replacing the cost objective with minimizing the average time to reach a health zone:

P1-S

Minimize:

$$\frac{1}{\sum_{h\in H} d_h} \sum_{a=(i,j,m)\in E} f_a t_a \qquad 3.39$$

Subject to:

Constraints 3.2 – 3.37

We can also introduce service into the P1-C1 and P1-C2 models by adding a constraint on the average time to reach a health zone:

$$\frac{1}{\sum_{h\in H} d_h} \sum_{a=(i,j,m)\in E} f_a t_a \leq L \qquad 3.40$$

where L is the maximum allowable average time to reach a health zone. The value of L can be varied to control the service level. For example, if a solution with the average time to reach a health zone to be at most 6 hours is needed, then $L = 6$.

3.3.2. Additional constraints to reduce computational time

Several constraints are added to the model to speed up the computational time by limiting the number of arcs in the model. These constraints do not affect the optimal solutions.

$$M \sum_{a=(i,j,m)\in E|m\neq D, i\in V/O} f_a \geq \sum_{a=(i,j,m)\in E|m\neq D, i\in V/O} x_a \,, \forall j \in V/O, \forall m \in \mathbb{M} \quad 3.41$$

$$M \sum_{a=(i,j,m)\in E|m\neq D, j\in V/O} f_a \geq \sum_{a=(i,j,m)\in E|m\neq D, j\in V/O} x_a \,, \forall i \in V/O, \forall m \in \mathbb{M} \quad 3.42$$

$$\sum_{a=(i,j,m)\in E|m\neq D, j\in V/O} x_a \leq 1 \,, \forall j \in V/O, \forall m \in \mathbb{M} \quad 3.43$$

M is a large number. Constraint 3.41 ensures if there is no flow into node j on a boat, truck or plane, then there is no active arc for that mode into node j. Constraint 3.42 ensures if there is no flow out of node i on a boat, truck or plane, then there is no active arc for that mode out of node i. Constraint 3.43 ensures that there is at most one incoming arc allowed into a node j for each mode. Considering such a limitation is possible as there is no capacity limitation for non-drone modes. To minimize the cost, the model would select only one arc for a given mode to come into a node.

3.3.3. Performance measurement

To evaluate the networks and help answer the research questions for problem P1, I developed 8 groups of performance metrics. These are:

1. cost metrics,
2. liter-hour metrics,
3. liter-km metrics,
4. time metrics,
5. distance metrics,
6. liter metrics,

7. network metrics, and

8. computational performance metrics.

Metrics 2 to 6 are used to evaluate different aspects of service for the solutions. To capture the performance of each transportation mode, I break down each metric group (except the network metrics) based on the four modes, so there are 5 metrics for metric groups 1 to 6 respectively, with the first 4 metrics as the individual metrics for each mode and the last one as the total (aggregate) for all modes. Metric 8 is used to evaluate the computational efficiency. The metrics are described in detail below.

1. Cost metrics

1.1. Cost metric for drone

Since I developed two cost models that capture different methods to charge for drone transportation, the cost metrics for drones are different in the two cost models:

1.1.1. Cost metric for drones with model P1-C1: $\sum_{i\in U} m_i u_i + \sum_{i\in R} h_i r_i + \sum_{a=(i,j,D)\in E}(\frac{c_a f_a}{cap} + c' x_a)$

1.1.2. Cost metric for drones with model P1-C2: $\sum_{i\in U} m_i u_i + \sum_{i\in R} h_i r_i + \sum_{a=(i,j,D)\in E}(c_a + c')x_a$

These two cost metrics for drones are the summation of cost terms related to drones, which include the total DB cost, the total RS cost, the total drone transportation variable cost, and the total drone arc fixed cost. The cost in 1.1.1. charges drones in terms of the volume of vaccines carried by drone, while the cost in 1.1.2. charges drones based on the total drone arcs selected in the model.

Since the two cost models do not affect non-drone cost terms, there is one cost metric for each non-drone mode:

1.2. Cost metric for non-drone mode m': $\sum_{a=(i,j,m)\in E|m=m'} c_a x_a$, $\forall m' \in \mathbb{M}$

1.3. Cost metric for all modes, or transportation cost metric:

1.3.1. Transportation cost metric in model P1-C1: 1.1.1+$\sum_{a=(i,j,m)\in E|m\neq D} c_a x_a$

1.3.2. Transportation cost metric in model P1-C2: 1.1.2+$\sum_{a=(i,j,m)\in E|m\neq D} c_a x_a$

2. Liter-time metrics:

2.1. Liter-time metric for each mode m': $\sum_{a=(i,j,m)\in E|m=m'} t_a f_a$, $\forall m' \in \mathbb{M}$

2.2. Liter-time metric for all modes: $\sum_{a=(i,j,m)\in E} t_a f_a$

3. Liter-distance metrics:

3.1 Liter-distance metric for each mode m': $\sum_{a=(i,j,m)\in E|m=m'} k_a f_a$, $\forall m' \in \mathbb{M}$

3.2. Liter-distance metric for all modes: $\sum_{a=(i,j,m)\in E} k_a f_a$

4. Time metrics:

4.1. Time metric for each mode m': $\sum_{a=(i,j,m)\in E|m=m'} t_a x_a$, $\forall m' \in \mathbb{M}$

4.2. Time metric for all modes: $\sum_{a=(i,j,m)\in E} t_a x_a$

5. Distance metrics:

5.1. Distance metric for each mode m': $\sum_{a=(i,j,m)\in E|m=m'} k_a x_a$, $\forall m' \in \mathbb{M}$

5.2. Distance metric for all modes: $\sum_{a=(i,j,m)\in E} k_a x_a$

6. Liter metrics:

6.1. Liter metric for each mode m': $\sum_{a=(i,j,m)\in E|m=m'} f_a$, $\forall m' \in \mathbb{M}$

6.2. Liter metric for all modes: $\sum_{a=(i,j,m)\in E} f_a$

7. Network metrics:

7.1. # of arcs for each mode m': $\sum_{a=(i,j,m)\in E|m=m'} x_a$, $\forall m' \in \mathbb{M}$

7.2. # of total arcs: $\sum_{a=(i,j,m)\in E} x_a$

7.3. # of DB: $\sum_{i\in U} u_i$

7.4. # of RS: $\sum_{i\in R} r_i$

Notice that in each metric group, the percentage of a specific metric for each mode can be calculated by dividing the value for a particular mode by the total. For example, the percentage of arcs that are drone arcs is $\sum_{a=(i,j,D)\in E} x_a \,/\, \sum_{a=(i,j,m)\in E} x_a$ (from item 7.1 divided by item 7.2).

8. Computational performance metrics:

8.1. CPU time

8.2. Optimality gap

Metrics 8.1 and 8.2 are reported by the optimization solver Gurobi automatically for each run.

3.4. Data for Vanuatu

The data used for problem P1 is a mixture of real-world data and synthetic data, with real-world data used whenever possible. Reasons to use synthetic data include lack of reliable and complete data in LDCs for aspects that relate to my dissertation, and available real-world data might not be appropriate to the situation of the application in this dissertation. As stated earlier, the models in my dissertation are applied using data to represent vaccine delivery in Vanuatu.

There are 107 nodes in the network for problem P1 In Vanuatu. Among these, 91 nodes are DC candidates, where 11 of them are also airports. There is one national

vaccine depot, which is also an airport, and the remaining 15 nodes (of the 107 total) are airports only. Table 3.2 shows the breakdown of the 107 nodes in problem P1.

Node	# of nodes	Nodes
Airport	27	0,9,10,14,19,22,38,41,56,84,88,89,92-106
DC candidates	91	1-91
Depot	1	0
DC candidate & Airport	11	9,10,14,19,22,38,41,56,84,88,89
Total	107	0-106

Table 3.2 Nodes in P1

In this section, I use Tafea, the most southern province of Vanuatu as an example to demonstrate the data used in problem P1 in detail. The depot, node 0 (which is in Shefa Province), is also included as this is the national depot for the vaccines. Figure 3.2 shows a map of Tafea. There are five main islands (Erromango, Aniwa, Tanna, Futuna, and Aneityum) with 8 health zones (denoted TAF01, TAF02a, TAF03a, TAF04a, TAF02b, TAF03b, TAF04b, and TAF04c) and 17 nodes in Tafea Province. Tanna Island has 4 health zones (shown separated by blue lines), with 8 DC candidates (nodes 1-8) and one airport (node 92). The other 4 health zones in Tafea are separate islands (or island groups). Erromongo Island has two DC candidates and the other three health zones have a single DC candidate – plus one other node that is an airport. DC candidate nodes are from node 1 to node 13. The six airports in Tafea are nodes 9, 10, and 92-95, where node 92 is one of the three large airports in Vanuatu, Tanna airport. The three large airports are Port Vila International Airport in Port Vila on Efate Island, Tanna airport (or Whitegrass) on Tanna Island, and Santo-Pekoa International Airport on Espiritu Santo Island. The

large airports have international airlines, and can handle large jet aircraft. The other airports in Vanuatu are small, with many being dirt strips that typically handle small planes for domestic flights, for example with up to 20 passengers.

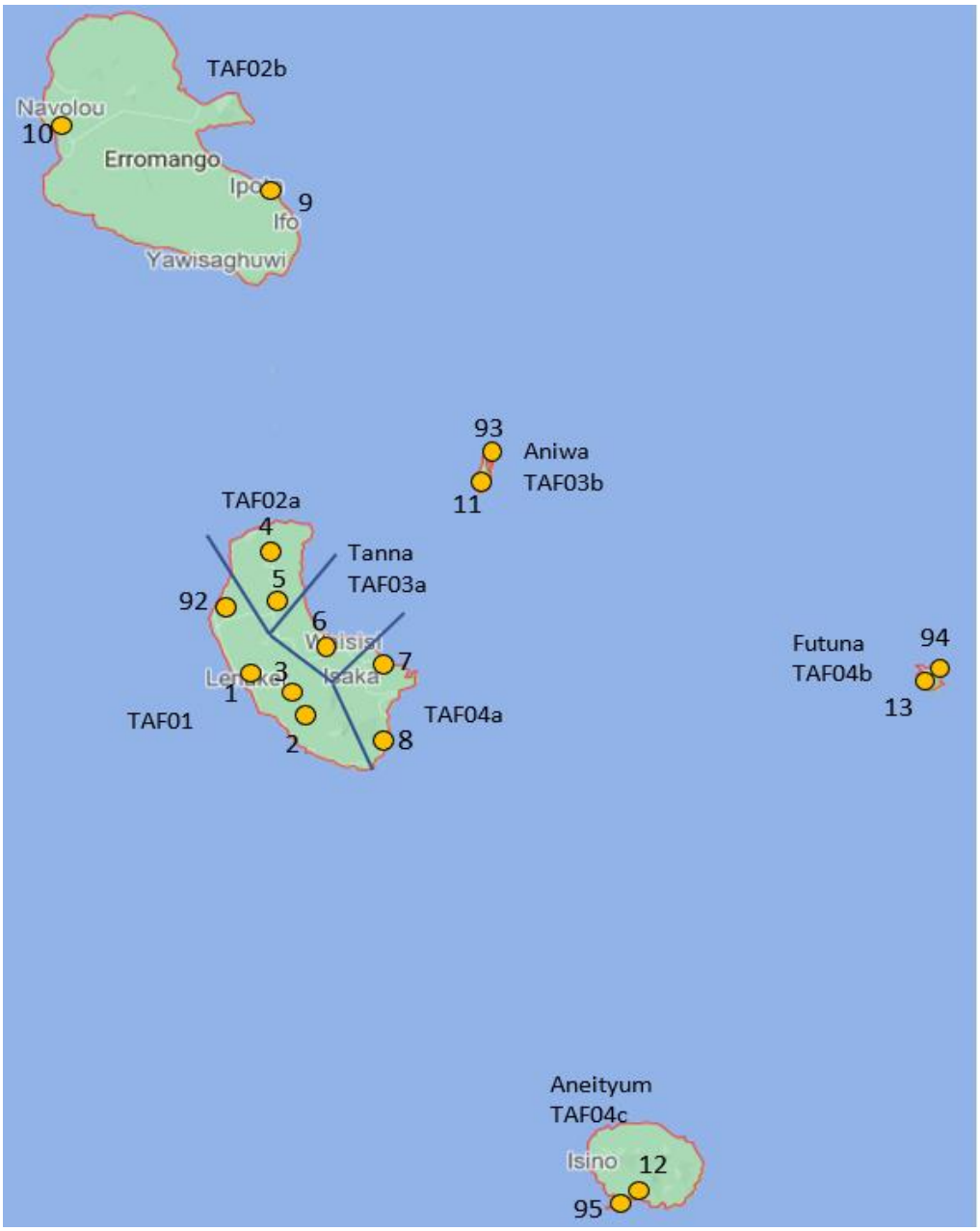

Figure 3.2 Tafea map

3.4.1. Demand and cost of DC candidates

There are 48 health zones (HZs) in Vanuatu, each with 1 to 4 DC candidates. The DC candidates are identified manually from Vanuatu health facility catchment maps

(Vanuatu Ministry of Health, 2011) and verified with the Vanuatu Immunisation Microplanning document (Gustiana, 2018). There are 91 DC candidates in Vanuatu.

A FIC (fully immunized child) is defined as a child less than one year old that receives all types of vaccines required by Ministry of Health (MoH) in the first year of their life. A FIC needs a total of 123.3 cm^3 (i.e., 0.1233 liters) of the nine types of vaccines according to the current MoH Expanded Program on Immunization (EPI) as Figure 3.3 shows. The 0.1233 liters includes the historical wastage rate, the right number of doses of all vaccine types, and necessary diluents of certain types of vaccines. Figure 3.3 shows the volume and weight of vaccine cargo that can serve 50 FICs per month. It includes 4 icepacks and 513.75 cm^3 of vaccines (including dilute vaccines). (To explain the volume of vaccine number "513.75" in Figure 3.4: a FIC needs an average of $\frac{123.3}{12} = 10.275$ cm^3 vaccines per month from Figure 3.3, which is the same as saying that 50 FIC need $50 \times 10.275 = 513.75$ cm^3 of vaccine per month). Thus, the average volume of vaccine and diluent to be delivered for each FIC each month, and that is to be carried in a cold box during transport is $\frac{2513.75}{50} = 50.275$ $cm^3 \approx 0.05$ liter. So the 0.05 liter value is the average volume of vaccines plus icepacks needed for an FIC per month.

Table 3.3 shows the vaccine demands in liters per month for each of the eight health zones in Tafea based on historical records. The monthly demand of a health zone $d_h, h \in H$ in Vanuatu is calculated based on a goal of having all children be fully immunized children (FIC). The demand is then the number of children in each health zone multiplied by 0.05 liters.

Health zone	DC candidates	Island	#FIC	Demand in liter (d_h)
TAF01	1, 2, 3	Tanna	580	29
TAF02a	4, 5		260	13
TAF03a	6		100	5
TAF04a	7, 8		200	10
TAF02b	9, 10	Erromango	60	3
TAF03b	11	Aniwa	40	2
TAF04c	12	Aneityum	80	4
TAF04b	13	Futuna	60	2

Table 3.3 Health zone monthly demand

Type of vaccine	Doses per target	Dose per vial	Wastage rate	Volume per dose (cm3)		Weights per vials (grams)		FIC Volume required (cm3)	FIC Weight (grams)
	Current			Vaccine	Diluents	Vaccine	Diluents		
BCG	1	20	84	1.20	1.10	6.00	2.00	2.30	8.00
DTP-HepB-Hib	3	1	10	17.20		6.00		51.60	18.00
MR	2	10	80	2.40	3.20	7.50	10.00	11.20	35.00
OPV	4	10	30	2.00		7.50		8.00	30.00
HepB	1	10	60	3.50		6.00		3.50	6.00
HepB	1	1	10	16.00		17.50		16.00	17.50
TT	2	10	31	3.10		13.50		6.20	27.00
Td	2	10	31	3.00		13.50		6.00	27.00
IPV	1	1	5	18.50		9.50		18.50	9.50
							Total (per child per year)	123.30	178.00
FIC: Fully Immunized Child									

Figure 3.3 Vaccine required for a FIC
Source: Request for Tender (RFT) Physical Services.
Ministry of Health Vanuatu (2018).

Cargo for a polulation of Children<1 = 50	Volume (cm^3)	Weight (grams)
Small icepack (4 units)	2000	1840
Vaccine + Diluent	513.75	741.667
Total (per monthly shipment)	**2513.75**	**2581.67**

Figure 3.4 Vaccine and icepacks required for 50 FIC
Source: Request for Tender (RFT) Physical Services. Ministry of Health Vanuatu, V. (2018).

For problem P1, I use the same fixed cost for all the DC candidates, as the P1 model in my dissertation is designed to examine the drone usage and performance, and linkages between different DC candidate costs and drone usage is left for future research. However, the P1 model has the capability to allow different DC candidate costs. I was unable to find accurate DC candidate costs for Vanuatu, which is not surprising given that a DC may perform a variety of health-related functions in addition to those associated with vaccination. There is data from the multiyear Expanded Program on Immunization (EPI) plan for the Republic of Senegal (Ministry of Public Health and Prevention, 2012), that may provide a reasonable estimate of the DC candidate cost for Vanuatu. In Senegal, the DC costs reported for buildings, including electricity, water, etc., were \$2136 per year in 2016; thus, I could use g_i =\$178, $\forall i \in G_h, \forall h \in H$ as the monthly cost for each DC candidate. However, since there is one DC selected in each health zone, when the DC costs are the same for all DC candidates, then the total DC cost is a fixed cost that does not affect the optimization. Thus, I use \$0 as the DC fixed cost in the optimization runs. If all DC candidate fixed costs are the same, then for any problem, the DC fixed costs could be added to the model solution as the number of health zones times the fixed cost per DC.

3.4.2. Arc network and data for non-drone modes

It takes two steps to generate arc network data for all non-drone modes of transportation. The first step is to obtain the arc network of all modes of transportation based on the geographic situation and schedules where available (i.e., airline schedules). Instances with different cold chain limitations will have different arc networks, as there will be fewer arcs in the network when the cold chain limitation is shorter. Thus the second step is to eliminate infeasible arcs with a travel time that is longer than the cold chain time used in an instance, i.e., feasible arcs are those where $t_a \leq \lambda_{max}$.

Travel time and cost of airplane arcs:

According to Flight Connections (2021), Air Vanuatu serves 27 domestic airports and there are 78 air routes among the 27 airports as of April 2021. In problem P1, the distance of each air route k_a, $a = (i, j, A) \in E$ is calculated as the product of haversine distance in kilometers and a circuity factor of 1.1. The time of each air route t_a, $a = (i, j, A) \in E$ is then calculated using k_a and the speed of airplanes.

In Vanuatu, large airplanes such as the ATR 72 (a 70-80 passenger turboprop) are used between the three large airports. The remaining airports are served by small airplanes such as de Havilland Canada Twin Otters and Britten-Norman Islanders (CAPA, 2019). According to Annex 05 “Domestic Flight Schedules. Air Vanuatu” in Ministry of Health Vanuatu (2018), the flight time from Port Vila to Santo is 50 minutes, and the distance between these two airports is 272 kilometers from Google Map. Thus, 272 kilometers /(50 minutes/60 minutes)=327 km/hr is a good estimate of the speed of the large airplanes used in Vanuatu. The speed of Islanders and Twin Otters are 271 km/h and 296 km/h, but the actual average flight speed is slower due to additional time the

airplanes require for takeoff and landing. For example, the distance between Port Vila and Ipota Airport on Erromango island is 161 km, with a 50 minute scheduled flight time (Ministry of Health Vanuatu, 2018), so the average speed is 193 km/h. Considering many pairs of the air routes in Vanuatu, 220 km/h is selected as a reasonable estimate of the average speed of small airplanes used in Vanuatu.

The arc cost for airplanes $c_a, a = (i, j, A) \in E$ is calculated as the product of the arc distance k_a and the variable cost per km of an airplane. The airfare of travelling from Port Vila to Valesdir airport is \$76, and the distance is 102 kilometers, so the cost rate is \$0.75/km, which is used in the model as a good estimate for variable cost of transporting vaccines by plane.

Table 3.4 lists t_a and c_a of 9 undirected airplane arcs (i.e., 18 directed airplane arcs) that are used in problem P1 for Tafea to illustrate the airplane arcs in one province.

Airport Node	**Airport Node**	t_a **(minutes)**	c_a **(dollars)**
0	92	43	175.5
0	9	48	132.75
0	10	41	111.75
9	10	10	26.25
9	92	20	54.75
92	93	14	38.25
92	94	32	87.75
92	95	32	87
93	94	22	60.75

Table 3.4 Travel time and cost of airplane arcs for Tafea in P1

Travel time and cost of boat arcs:

By closely examining the geography of Vanuatu with Google Maps, and with careful judgement, 84 out of the 107 nodes in Vanuatu are included in the boat network as these nodes are by the coast, and I believe can serve as ports or landing areas for boat transportation of vaccines. There are 6972 directed boat arcs between the 84 coastal nodes with 38 hours and 3 minutes as the largest travel time (using a speed of 25 km/hr as explained below) between the most northern coastal node 87 in Torba Province and the most southern coastal node 95 in Tafea Province. The number of boat arcs is reduced in the model as the cold chain limitation is less than 38 hours.

The distance of each boat arc is calculated as the product of haversine distance in kilometers $k_a, a = (i, j, B) \in E$ and a circuity factor ranging from 1.2 to 10. The boat travel paths vary greatly depend on the shape of the coast line and other geographic situations between two coastal nodes. The circuity factor of each boat arc is assigned by closely examining the prospective travel route in Google Maps. Thus, two nodes that may not be far apart but are on opposite sides of a long narrow island could have a circuity factor as large as 10. As another example, the circuity factor for a trip between node 1 and node 7 on Tanna Island (See Figure 3.2) is 3 as a boat has to travel along the coast around the southern part of Tanna and that distance is roughly 3 times of the direct distance between node 1 and node 7.

The time of each boat arc $t_a, a = (i, j, B) \in E$ is calculated using the distance k_a and the speed of boat. The available boats in Vanuatu are generally slow vessels, so 25 km/h is a reasonable assumption of the average speed. The arc cost $c_a, a = (i, j, B) \in E$ is the product of the arc distance of each boat arc k_a and the variable cost of boat travel.

According to Vanuatu Travel Guide (Matt, 2021), it costs $70 to travel from Port Vila to Santo by boat, and the distance between them is about 250 km, which gives a rate of approximately $0.3/km. Thus, $0.30/km is used in problem P1 for the variable cost of boat travel. Table 3.5 list t_a and c_a for the 28 undirected boat arcs (i.e., 56 directed boat arcs) that are used in problem P1 for Tafea Province.

According to the Vanuatu Ministry of Health (Ministry of Health Vanuatu, 2018), the cold chain limitation in Vanuatu is 8 hours. This time is determined by the type of cold box and the cooling materials (e.g., ice packs) that travel with the vaccine in Vanuatu. Thus, after 8 hours or less, health workers need to replace the cooling materials carefully if the vaccines need to travel farther in the ice box so that the vaccines remain viable until reaching their final destination (where they may be stored in a refrigerator or used). Since the cold chain method limit in Vanuatu is 8 hours, Table 5 for the boat arcs in Vanuatu includes only arcs that are traveled in 8 hours or less.

Coastal Node	**Coastal Node**	t_a **(minutes)**	c_a **(dollars)**
0	9	466	58.2
0	10	391	48.9
1	7	146	18.3
1	8	67	8.4
1	9	216	27
1	10	259	32.4
1	12	274	34.2
1	92	29	3.6
1	95	276	34.5
7	8	41	5.1
7	9	216	27
7	10	276	34.5
7	12	252	31.5
7	92	125	15.6
7	95	257	32.1
8	9	250	31.2
8	10	307	38.4
8	12	221	27.6
8	92	113	14.1
8	95	223	27.9
9	10	154	19.2
9	12	466	58.2
9	92	194	24.3
9	95	470	58.8
10	92	230	28.8
12	92	302	37.8
12	95	7	0.9
92	95	305	38.1

Table 3.5 Travel time and cost of boat arcs for Tafea in P1

Travel time and cost of truck arcs:

Truck arcs are determined by examining Google Maps and based on data from the Vanuatu Ministry of Health (2011). The distance of a truck arc k_a, $a = (i, j, K) \in E$ is determined by examining Google Maps directly. There 136 directed truck arcs in the network for the country. The time of each truck arc t_a, $a = (i, j, K) \in E$ is calculated using k_a and the speed of truck. I use 50 km/h as the truck speed, which seems a reasonable estimate for truck speed considering the rugged terrain in Vanuatu.

The truck arc cost $c_a, a = (i, j, K) \in E$ is the product of the arc distance of each truck arc k_a and the variable cost of truck. The variable costs of truck is estimated using the average cost of three land vehicles in the toolkit developed by VillageReach (VillageReach, 2019): land cruiser, van, and 4-ton truck. The average cost is $1/km.

Table 3.6 lists t_a and c_a for the 14 undirected truck arcs (i.e., 28 directed truck arcs) that are used in problem P1 for Tafea. Finally, Table 3.7 summarizes the specifications for the non-drone modes.

Truck Node	Truck Node	t_a (minutes)	c_a (dollars)
1	2	16	13
1	3	13	11
1	8	43	36
1	92	13	11
2	3	14	12
2	8	34	28
3	8	41	34
4	5	12	10
4	92	24	20
5	6	22	18
5	92	13	11
6	7	8	7
11	93	4	3
13	94	4	3

Table 3.6 Travel time and cost of truck arcs for Tafea in P1

Non-Drone Mode	Range	Payload	Speed (km/h)	Variable Cost ($/km)	Circuity Factor
Airplane	Unlimited		Large: 327 Small: 220	0.75	1.1
Boat			25	0.3	1.5-10
Truck			50	1	Varies

Table 3.7 Specifications of non-drone modes

3.4.3. Drone data

Travel time and cost of drone arcs:

The large fixed wing (LFW) and small fixed wing (SFW) drones are used separately in the P1 model. Because LFW drones need a runway for takeoff and landing, they are used only between the 27 airports of Vanuatu in the model. For SFW drones, I

assume all nodes except the two large airports in Santo and Tanna allow SFW transportation. Note that small drones are generally restricted from airspace near airports due to the possibility of collisions between drones and low flying aircraft near the airport. Although the 25 "non-large" airports in Vanuatu that are modeled do have scheduled commercial flights, these are not frequent and I assume the SFW drones can be scheduled to operate outside of the times when aircraft are using the airport. (Note that many of these airports are dirt airstrips with very limited infrastructure.) The distance of each drone arc $k_a, a = (i, j, D) \in E$ is calculated as the product of haversine distance in kilometers and a circuity factor of 1.2. The distance of drone arcs in the P1 model needs to be within the drone range, i.e., $k_a \leq drone\ range, a = (i, j, D) \in E$. LFW drones have a range of 500 km with a maximum payload of 230 liters. SFW drones have a range of 150 km with a maximum payload of 10 liters (based on data in VillageReach, 2019). There are 562 directed LFW drone arcs that are less than 500 km, and 4024 directed SFW drone arcs that are less than 150 km in Vanuatu.

The time associated with each drone arc $t_a, a = (i, j, D) \in E$ is calculated using k_a and the speed of the drone. An LFW drone is similar to a small airplane, and I use a speed of 200 km/h for LFW drones. For SFW drones I use a speed of 70 km/h. The drone arc cost $c_a, a = (i, j, D) \in E$ is computed as the product of the arc distance of each drone arc k_a and the variable cost for the drone. According to VillageReach (2019), the variable cost of an LFW drone is \$0.38/km, and the variable cost of an SFW drone is \$0.12/km. Table 3.8 summarizes the specifications of drones used in problem P1.

Drone Type	Range (km)	Payload in liter (cap)	Speed (km/h)	Variable Cost ($/km)	Circuity Factor
LFW	500	230	200	0.38	1.2
SFW	150	10	70	0.12	

Table 3.8 Specifications of drones in P1

Tables 3.9 and 3.10 illustrate the drone arcs for the Tafea Province. Table 3.9 lists t_a and c_a for the 21 undirected LFW arcs (i.e., 42 directed LFW arcs) that are used in the P1 model for Tafea. Table 3.10 (a)-(d) lists t_a and c_a for the 114 undirected SFW arcs (i.e., 228 directed SFW arcs) that are used in the P1 model for Tafea.

LFW Node	LFW Node	t_a (minutes)	c_a (dollars)
0	9	58	73.34
0	10	49	61.56
0	92	77	97.28
0	93	77	97.66
0	94	102	128.82
0	95	115	145.16
9	10	11	14.44
9	92	24	30.40
9	93	19	24.32
9	94	44	56.24
9	95	59	74.10
10	92	29	36.10
10	93	29	37.24
10	94	56	70.30
10	95	66	83.60
92	93	17	21.28
92	94	38	48.64
92	95	38	48.26
93	94	26	33.44
93	95	41	52.06
94	95	34	42.94

Table 3.9 Travel time and cost of LFW in P1

SFW Node	SFW Node	t_a (minutes)	c_a (dollars)
1	2	13	1.8
1	3	9	1.32

1	4	18	2.52
1	5	11	1.56
1	6	15	2.16
1	7	21	2.88
1	8	23	3.24
1	9	77	10.8
1	10	92	12.84
1	11	47	6.6
1	12	98	13.68
1	13	101	14.16
1	93	49	6.84
1	94	104	14.52
1	95	99	13.8
2	3	5	0.72
2	4	27	3.84
2	5	20	2.76
2	6	14	1.92
2	7	15	2.16
2	8	11	1.56
2	9	86	12
2	10	103	14.4
2	11	47	6.6
2	12	85	11.88
2	13	92	12.84
2	93	50	6.96
2	94	94	13.2
2	95	86	12
3	4	22	3.12
3	5	15	2.04
3	6	9	1.32
3	7	13	1.8
3	8	14	1.92

3	9	81	11.28
3	10	99	13.8
3	11	44	6.12
3	12	90	12.6
3	13	93	12.96
3	93	46	6.48
3	94	95	13.32
3	95	91	12.72
4	5	8	1.08
4	6	18	2.52
4	7	23	3.24
4	8	33	4.68
4	9	59	8.28
4	10	76	10.68
4	11	35	4.92
4	12	111	15.6
4	13	99	13.92
4	93	37	5.16
4	94	102	14.28
4	95	112	15.72
5	6	12	1.68
5	7	18	2.52
5	8	27	3.72
5	9	67	9.36
5	10	84	11.76
5	11	38	5.28
5	12	104	14.52
5	13	98	13.68
5	93	39	5.52
5	94	100	14.04
5	95	105	14.76
6	7	7	0.96

6	8	15	2.16
6	9	74	10.32
6	10	93	13.08
6	11	33	4.68
6	12	94	13.2
6	13	87	12.12
6	93	36	5.04
6	94	89	12.48
6	95	95	13.32
7	8	12	1.68
7	9	77	10.8
7	10	99	13.8
7	11	32	4.44
7	12	90	12.6
7	13	81	11.28
7	93	35	4.92
7	94	83	11.64
7	95	91	12.72
8	9	89	12.48
8	10	109	15.24
8	11	43	6
8	12	78	10.92
8	13	81	11.4
8	93	46	6.48
8	94	84	11.76
8	95	80	11.16
9	10	33	4.56
9	11	57	8.04
9	13	125	17.52
9	93	55	7.68
9	94	127	17.76
10	11	86	12

10	93	84	11.76
11	12	112	15.72
11	13	72	10.08
11	93	3	0.48
11	94	74	10.32
11	95	114	15.96
12	13	93	13.08
12	93	116	16.2
12	94	95	13.32
12	95	2	0.24
13	93	73	10.2
13	94	3	0.36
13	95	96	13.44
93	94	75	10.56
93	95	117	16.44
94	95	97	13.56

Table 3.10 Travel time and cost of SFW in P1

There are in total 2017 undirected SFW arcs in P1 that are within the range for SFW drones (i.e., 150 km), and 281 LFW arcs in P1 that are within the range of LFW drones (i.e., 500 km).

While the P1-C1, P1-C2 and P1-S models include both regular and remote drone relay stations, in the computational illustrations for Vanuatu I do not locate remote relay stations. A remote relay station (RS) is defined as a drone RS that is at a remote location far away from people and major facilities (including electricity), and as a remote RS node is related only to drone arcs, remote RS candidates do not coincide with DC candidates or generally airports. Remote RSs are not modeled for Vanuatu, primarily due to the

geography of Vanuatu and the availability of other sites (e.g., DC candidates) as regular RS candidates. If there were to be remote RS in Vanuatu that are strategically located to extend the drone range, then likely locations may be in the sea (it makes sense to locate them between the regular RSs, which are on islands). However, the cost of opening and operating a RS in the sea is uncertain, and could be very expensive, especially for an LDC. However, the idea of a remote RS located on a ship would allow it to be relocated to be strategically positioned at different sites during the month to service different provinces. This concept is beyond the scope of the dissertation and is left for future research.

To estimate the fixed costs for drone arcs, drone bases and relay stations I use data from VillageReach (2019), Shavarani et al. (2019) and JSI Research and Training Institute, Inc., Llamasoft (2019). The fixed costs for drone arcs reflect the activities needed to establish that the desired drone arcs in a province are safe for flights. I assume this is done by a set of drone workers that include one drone operator and three ground staff (Llamasoft,2019). These individuals can determine appropriate takeoff and landing locations and drone flight paths, and then conduct several test flights to verify the drone arc can be reliably flown. From Llamasoft (2019), the monthly cost for a drone operator is \$12,500/12 = \$1041.67 and the monthly cost for three drone staff members is \$6500/12×3 = \$1625. The personnel costs for one province are then \$1041.67+1625 = \$2666.67. I estimate it takes an average of one month to establish the drone arcs for a province in Vanuatu, and I assume this cost can be allocated over 2 years (24 months). This produces a monthly personnel cost to establish drone arcs of \$2666.67/24 = \$111.11. The average number of drone arcs per province is 2298/6 = 344.7, so the

average personnel cost to establish a drone arc is about 32 cents ($111.11/344.7 = $0.322). To include other costs involved in establishing drone arcs, in addition to personal costs, I therefore set the fixed cost of a drone arc c', as $0.4 per drone arc in P1. For details on activities associated with fixed costs for establishing drone arcs, see Ministry of Health Vanuatu (2018) and Wingcopter (2019). I acknowledge that $0.4 is an initial estimation that can be replaced by a more accurate value if data is available.

It is very challenging to estimate the DB and RS fixed costs for SFW and LFW drones for problem P1, as there is very limited publicly available real-world data for these values in LDCs. In the developed world, there are some values reported for fixed costs of drone facilities, but these are generally quite expensive. For example, the drone facility cost ranges from $0.23 million to $1.65 million in San Francisco (Shavarani et al. 2019). There is some data from JSI and LLamasoft (2019) on fixed costs for drone operations in LDCs, but these values range widely and depend on the scale of drone operations, as reflected in the number of drone flights. Table 3.11 shows fixed facility costs for LDCs along with the number of drone flights, number of drones and number of staff.

Drone Type	# of Flights/month	Fixed Cost ($/month)	# of ground Staff	# of Operators
LFW	92	12,500	1	1
SFW	83	6,167	1	1
Hybrid (Small)	13	3,667	1	1
Hybrid (Medium)	18	6,583	1	1

Table 3.11 Drone facility cost for LDCs
Source: Toolkit for Generating Evidence around the Use of Unmanned Aircraft Systems (UAS) for Medical Commodity Delivery. VillageReach. (2019).

The drone fixed facility costs for DB and RS can play a key role in designing the distribution network, with a larger number of drone flights that use a DB or RS resulting in a reduced fixed cost per flight. However, there are not likely to be a very large number of drone flights for vaccine delivery alone in a place with a small population, like Vanuatu, where there are monthly deliveries to 48 health zones. If delivering vaccine to each health zone required two drone flights on average, there would be only about 100 drone flights per month over the six provinces, or about 16 per province per month on average, which is less than one per day in each province. Note that this level of two drone flights per health zone is far less than the levels shown in Table 3.11. (Further, the results in Sections 3.5- 3.7 tend to use a much smaller number of drone flights per DB, even with zero drone base fixed facility costs.) Thus the available data for drone fixed facility costs in LDCs does not seem to fit well with the situation for vaccine delivery alone in Vanuatu. (Note however, that if drones were used for other tasks in addition to vaccine delivery, there might be many more flights per DB; however, the fixed DB costs would then need to be apportioned among the various tasks.) Therefore, in this research to assess the possibilities of using drones in the P1 model, I use a range of values for the DB and RS fixed costs in the computational studies, including low values to show the greatest potential for using drones. Note that the P1 model has fixed facility costs only for the drone mode, as there are no fixed facility costs included for other modes (i.e., for a "truck port", "boat port" or "airport").

3.4.4. Other data and summary of data for Vanuatu

The number of drone paths N and the number of drone arcs in a drone path Ω can affect the optimal solutions, because they constrain the drone networks. For example,

there can be 8 drone paths and with a maximum 5 drone arcs in a drone path in the optimal solution when using $N = 8$, and $\Omega = 5$. However, there can only be at most 3 drone paths and with a maximum of 2 drone arcs per drone path in the optimal solution when using $N = 3$, and $\Omega = 2$ for the same dataset. Large values for parameters N and Ω will make the model computational challenging and take a longer time to solve. Due to this, I designed a case study (in the next Section) to examine how variations of N and Ω affect drone usage and computational time. Different values for parameters N and Ω are used in other computational studies. Detailed discussion about how to select the values for N and Ω is presented in each computational studies' section.

The parameter Γ is used in the subtour elimination constraint 3.23. Γ needs to be at least 2 to allow P1 to generate feasible solutions. Γ also needs be at least as large as the possible largest number of drone nodes in a model, which is Ω +1. For example, if the possible longest drone path contains 6 drone nodes (i.e., $\Omega = 5$), and the path is $i \to j \to k \to h \to g \to f$, then $p_{ij}^n = 1, p_{jk}^n = 1, p_{kh}^n = 1, p_{hg}^n = 1, p_{gf}^n = 1.$ Let's assume $w_i^n = 1, w_j^n = 2, w_k^n = 3, w_h^n = 4, w_g^n = 5, w_f^n = 6.$ To prevent subtours, some arcs cannot be formed, such as $f \to i$, so $p_{fi}^n = 0$. If $\Gamma = 5$, then $w_f^n - w_i^n \leq 4$ from constraint 3.23, however, $w_f^n - w_i^n = 6 - 1 = 5 > 4$, so the model will be infeasible if $\Gamma < \Omega$ +1. I use $\Gamma = \Omega$ +1 in the computational studies.

Table 3.12 lists some fundamental summary data for the six Provinces of Vanuatu. For each province, and collectively, this shows the number of health zones, the amount of demand of vaccines (in liters per month), and the number of DC candidates, airports and nodes in the model.

Province	#HZ	Demand (L)	#DC candidates	#Airport	#Nodes
Torba	6	22	8	4	9
Sanma	9	99	20	1	20
Penama	10	50	18	5	21
Malampa	12	57	24	6	27
Shefa	3	32	8	5	13
Tafea	8	68	13	6	17
Total	**48**	**328**	**91**	**27**	**107**

Table 3.12 Summary of nodes for each province in P1

The next four sections provide computational results of the P1 model. These sections include case studies of interesting situations and a sensitivity analysis, which varies four parameters to evaluate different delivery scenarios and test the drone usage and performance. The four parameters varied are: the DB cost, RS cost, demand, and cold chain time limit. Unless otherwise stated, the parameters for the model are as specified in this section. All the computational results are from solving models using Gurobi 9.1 on an HP Intel Quard-Core i7 with 3.9 Ghz CPU and 64 GB RAM.

3.5. Case Study I: delivery without drones

This section presents optimal solutions for Vanuatu from the P1-C1, P1-C2 and P1-S models without any drones. This is accomplished by simply removing the drone arcs from the input data (which also effectively removes the constraints specific to drones). The first purpose of this case study is to evaluate the level of cost and service performance for vaccine delivery that can be achieved without drones. These results are the baseline for comparison to solutions when drones are allowed to deliver vaccines,

which is Case Study II in Section 3.6. The P1 model is a variant of the network flow problem, which incorporates facility location problems as well, which are NP hard (Krarup and Pruzan, 1983). The model is computationally challenging, especially with the large dataset that covers the entire country of Vanuatu and with all the constraints and variables for modeling longer drone paths. For example, even after running the solver for a week on a problem for the complete Vanuatu data set (all 6 provinces) with SFW drones, when allowing up to 20 paths of length 5, the optimality gap was still at 10%. Hence to generate insights for the whole country, I run the P1 model with drones separately for each province of Vanuatu and then use the aggregation of the cost and other performance metrics to represent service to the whole country. This setting is aligned with the current practice, as noted earlier, where each province receives vaccines direct from the national depot. However, this strategy of aggregating solutions for the provinces has the disadvantage of not finding the best system-wide optimal solution, obtained by running the model for the entire country. In order to sense how large is the difference between a system-wide solution and the aggregated solutions (from adding results for each province), I use Case Study I to examine both options. The design of Case Study I is provided in Section 3.5.1. Section 3.5.2 presents the solutions of Case Study I, and Section 3.5.3 provides the cost and service tradeoff and mode usage analysis.

3.5.1. Design of Case Study I

With the two purposes mentioned above, I designed the following situations for Case Study I.

- Case 1.1: Minimize the total transportation cost without drones for the entire country. (1 run)

- Case 1.2: Minimize the total weighted delivery time without drones for the entire country. (1 run)
- Case 1.3: Minimize the total transportation cost without drones for the entire country while limiting the average delivery time to a HZ to 2 hours. (1 run)
- Case 1.4: Minimize the total transportation cost without drones for the entire country while limiting the average delivery time to a HZ to 5 hours. (1 run)
- Case 1.5: Minimize the total transportation cost without drones for each of the 6 provinces separately, and sum up the performance metrics of the 6 provinces. (6 runs)
- Case 1.6: Minimize the total weighted delivery time without drones for each of the 6 provinces separately, and sum up the performance metrics of the 6 provinces. (6 runs)
- Case 1.7: Minimize the total transportation cost without drones for each of the 6 provinces separately, while limiting the average delivery time to a HZ in Torba to 2.5 hours, and limiting the average delivery time to a HZ in other provinces to 2 hours, and sum up the performance metrics of the 6 provinces. (6 runs) Note that 2 hours is too short for Torba, as it is the farthest province from the national depot, so I use 2.5 hours for Torba instead.
- Case 1.8: Minimize the total transportation cost without drones for each of the 6 provinces separately, while limiting the average delivery time to a HZ to 5 hours, and sum up the performance metrics of the 6 provinces. (6 runs)

- Case 1.9: The baseline case. Minimize the total transportation cost without drones for each of the 6 provinces separately, while forcing use of an airplane to deliver the vaccines from the national depot to each province (i.e., forcing the 1st leg to be an airplane arc), and sum up the performance metrics of the 6 provinces. (6 runs)

As enumerated above, there are in total 34 runs in Case Study I. Cases 1.1 – 1.4 use the data for the entire country, while Case 1.5 – 1.9 use the data for each province separately, so there are 6 separate runs in each case. There are four pairs of cases that can be used to compare the difference of cost and service performance from solving the model once for the entire country versus aggregating solutions from the 6 provinces. These four pairs are Case 1.1 and Case 1.5, Case 1.2 and Case 1.6, Case 1.3 and Case 1.7, and Case 1.4 and Case 1.8, as each pair evaluates the same scenario. Later in this Chapter is the comparison of the situations for the 6 provinces with and without drones. Case 1.1 and Case 1.5 minimize the total transportation cost without drones. Notice here we minimize the total transportation cost, rather than the total cost, soIset the DC fixed costs to zero. There are two reasons to support the decision. First, the DC cost of each DC candidate is the same, as discussed earlier in the data section, so with one DC required in each health zone, the total DC fixed cost is a constant and thus will not affect the solution. Second, the total DC fixed cost is large compared to the remaining cost, so if the DC fixed costs were included, then the solver may terminate with a small optimality gap (say 0.01%) that reflects a much larger optimality gap if the transportation costs alone were considered.

Cases 1.5 and 1.7 both optimize the transportation cost for each of the six provinces separately. When setting up the dataset for each province for both cases, all

available arcs that connect node 0, the depot, and nodes in each province are added to each provincial dataset. However, for Torba, the province farthest away from the depot, no arc between node 0 and nodes in Torba is shorter than 8 hours, the cold chain time limit. To address this, a series of boat arcs is added to the Torba dataset as a route to reach Torba from the depot. The series of boat arcs is 0→99→34→41→40→91.I picked this series of boat arcs because all arcs are within 8 hours and it gives the lowest cost to reach Torba as Case 1.5 and 1.7 both minimize the cost.

Thus, for all models with a cost objective in Case Study I (all but Cases 1.2 and 1.6), the objective function (without drones or DC fixed costs) reduces to

$$\sum_{a=(i,j,m)\in E} c_a x_a \qquad 3.1a$$

where the set E does not include any drone arcs and is for the region of interest (e.g., all of Vanuatu in Case 1.1 and for a single province in each of the six runs for Case 1.5). I call this objective function 3.1a. For Case Study I, I also do not need the constraints related to drones, so only constraints 3.2 to 3.5, and 3.27 and 3.28 are used. Case 1.2 and Case 1.6 minimize the total weighted delivery time, so the objective is to minimize 3.39. I remove the sum of demands (a constant), and minimize

$$\sum_{a=(i,j,m)\in E} f_a t_a \qquad 3.39a$$

The weighted average delivery time to a HZ can then be calculated as in 3.39, after the solution is generated using $\sum_{a=(i,j,m)\in E} f_a t_a \,/\, \sum_{h\in H} d_h$.

Cases 1.3, 1.4, 1.7 and 1.8 minimize the total transportation cost without drones with a limit on the average weighted delivery time to a HZ. These cases minimize 3.1a

with constraints 3.2 to 3.5, and 3.27, 3.28 and 3.40. Note that the set of health zones in constraint 3.40 (used for summing the demand) is for the region of interest (e.g., all of Vanuatu in Case 1.3 and for a single province in each of the six runs for Case 1.6).

Case 1.9 uses the same objective function and constraints as Case 1.5, with an additional constraint that forces delivering the vaccines for the entire province from the national depot (i.e., node 0) to an airport j by airplane:

$$x_a = 1, a = (0, j, A) \in E$$

Case 1.9 is the baseline case, because it mimics the actual operations in Vanuatu where for each province the total demand is first sent from the national depot (in Port Vila) to a provincial storage location (Vanuatu Ministry of Health, 2016). Then the vaccine is distributed from the provincial storage location to the health zones in that province.

In Case Study 1, I use the demand for each health zone, as discussed in section 3.4.1 for d_h and set $\lambda_{max} = 8$, which is the cold chain limitation in Vanuatu.

3.5.2. Solutions of Case Study I

The 34 runs for Case Study I solved using Gurobi 9.1 using an HP Intel Quard-Core i7 with 3.9 Ghz CPU and 64 GB RAM. Since the 34 runs are without drones, they solve to optimality quickly with an average of 51 seconds of CPU time, or 14 seconds in real time. The maximum CPU time was 752 seconds (or 213 seconds in real time).

Cases 1.1, 1.2, 1.5, and 1.6 provide the solutions with the lowest cost and best service, so I show the detailed solutions for these four cases in Figure 3.5, Figure 3.6, Figure 3.7, and Figure 3.8 respectively. Table 3.13 shows the number of boat, plane and

truck arcs in these solutions, as well as the time for the longest paths. We see that the boat mode, which has the lowest cost, is most heavily used in Case 1.1, and is heavily used in Case 1.5, because Case 1.1 and Case 1.5 minimize the transportation cost. Airplane, which is the mode with the highest speed, is most heavily used in Case 1.2, and is heavily used in Case 1.6, because these two cases minimize the delivery time. Case 1.1 and 1.5 still used three airplane arcs, which are the most expensive arcs, to reach nodes 84, 93, and 94, because these three nodes are inland nodes so there is no boat service available. Case 1.5 also uses airplane to reach nodes 56 and 103, because using boat arcs to reach the two nodes from node 0, the depot, is longer than the 8 hours cold chain time limit for any arc. Case 1.2 and Case 1.6 (that minimize time) still use boat and truck arcs which are slower at some places, because there is no faster mode available at those places. Both of the longest paths in terms of time in Cases 1.1 and 1.5 lead to node 87 in Torba. Notice that the time in Case 1.5 is shorter than in Case 1.1 because the path in Case 1.1 has to go through many arcs to serve more DCs between the depot and Torba to minimize the total cost for the entire country. Both of the longest paths in terms of time in Cases 1.2 and 1.6 lead to node 67 in Sanma, and the two paths are the same.

Case	Figure	Number of boat arcs	Number of plane arcs	Number of truck arcs	Time of longest path (hrs)
1.1	3.5	43	3	8	28.2
1.2	3.6	9	23	36	4.4
1.5	3.7	46	5	8	19
1.6	3.8	9	21	38	4.4

Table 3.13 Solutions with the lowest cost and best service

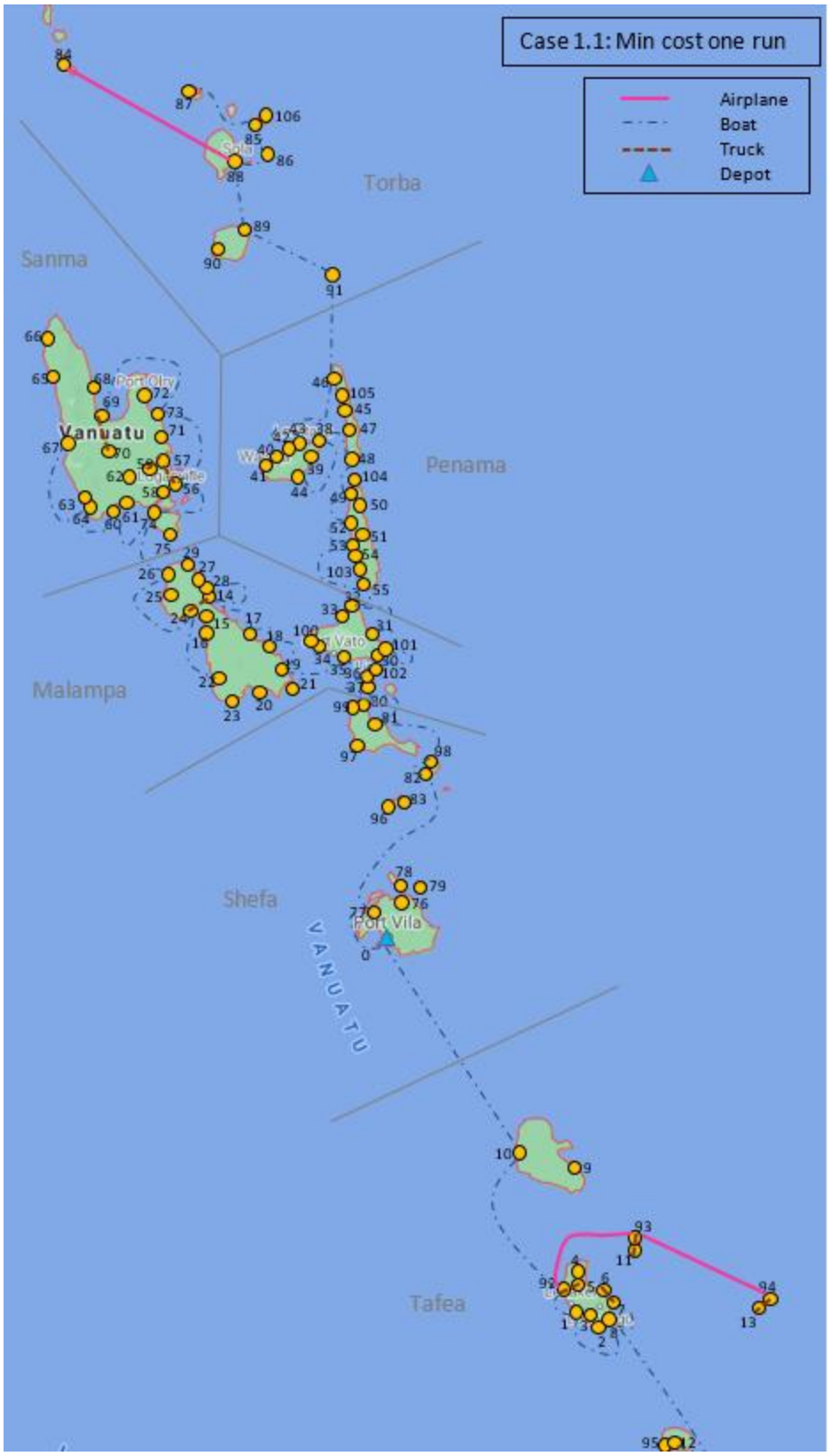

Figure 3.5 Solution map of Case 1.1

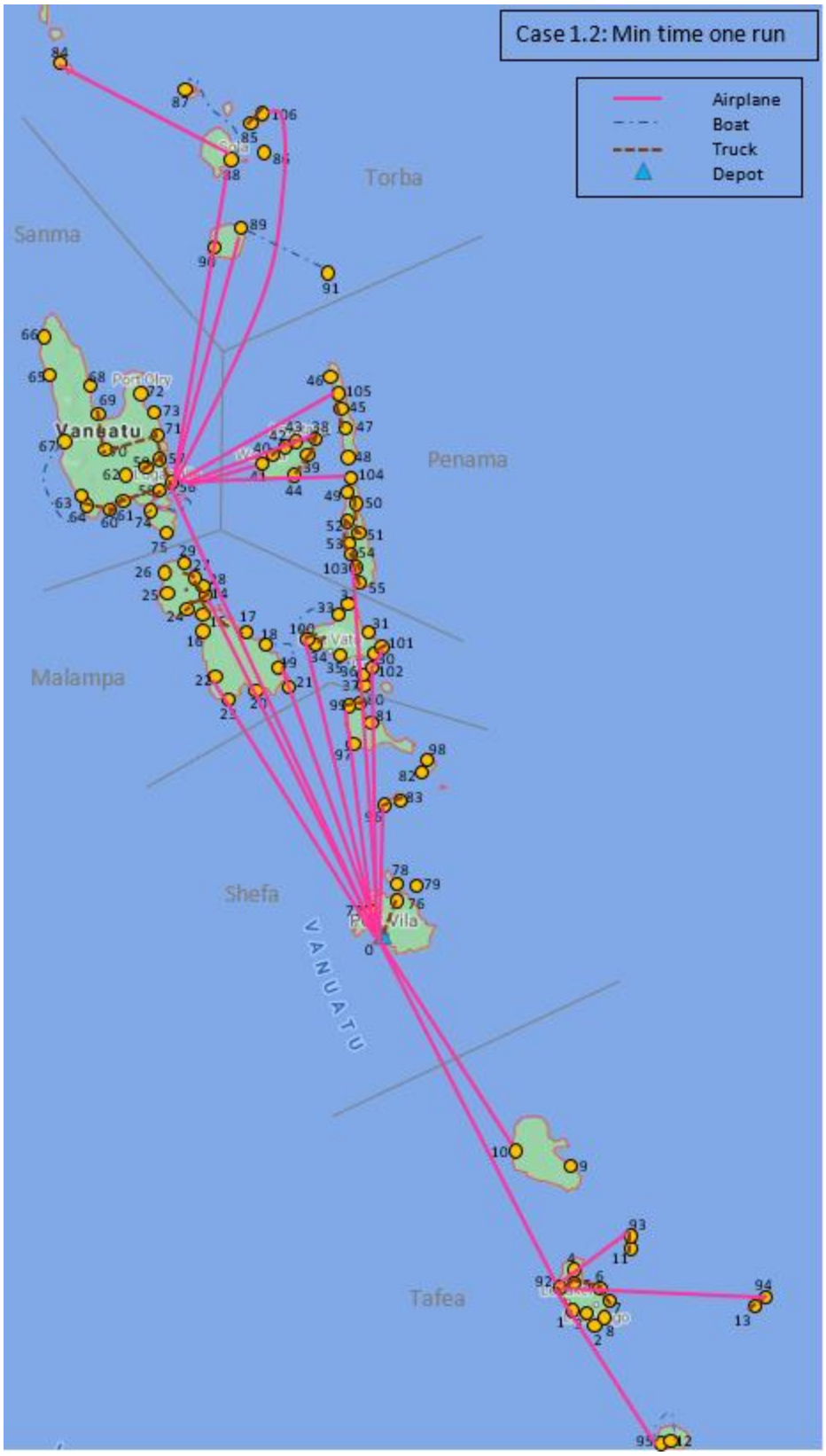

Figure 3.6 Solution map of Case 1.2

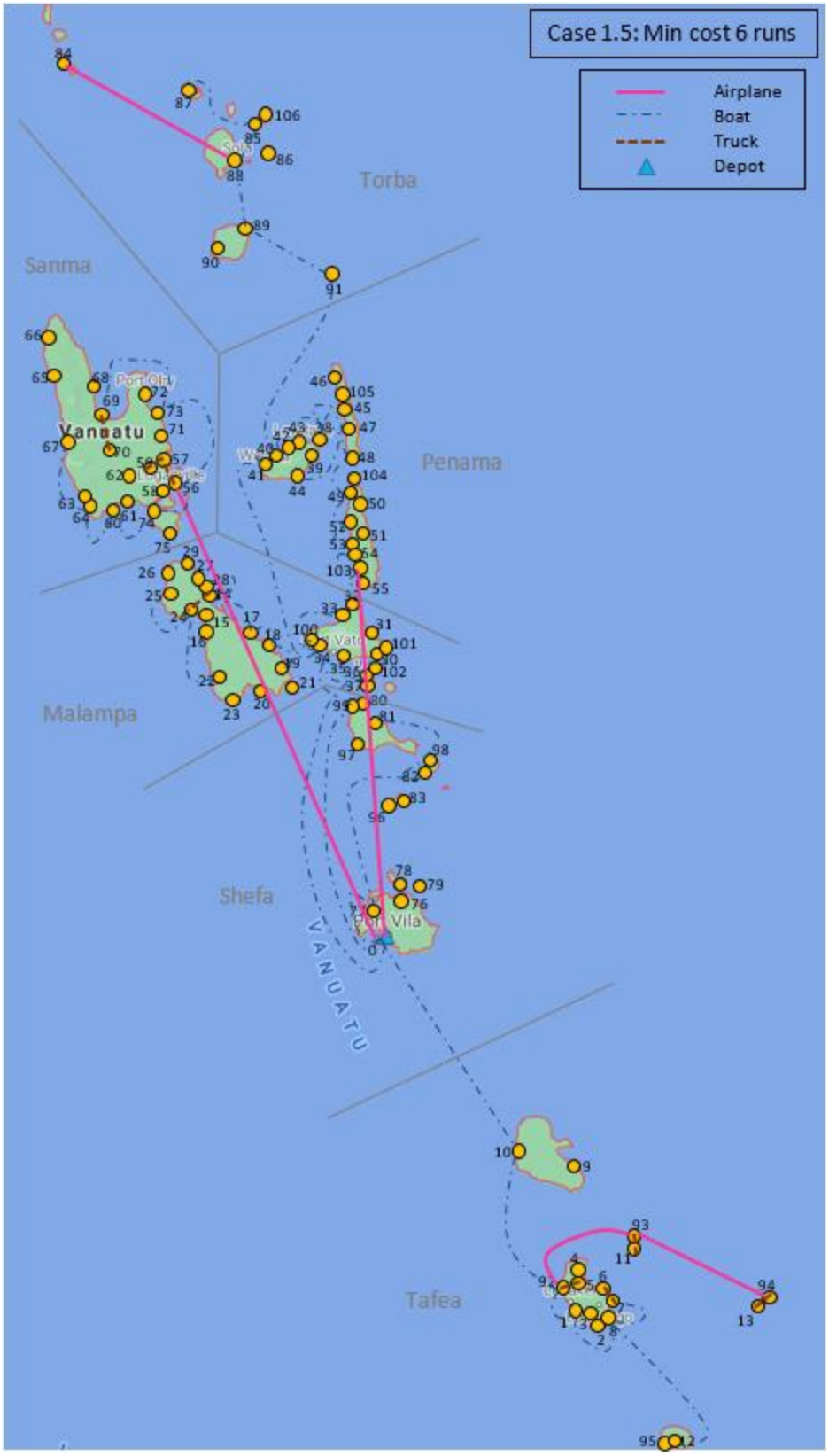

Figure 3.7 Solution map of Case 1.5

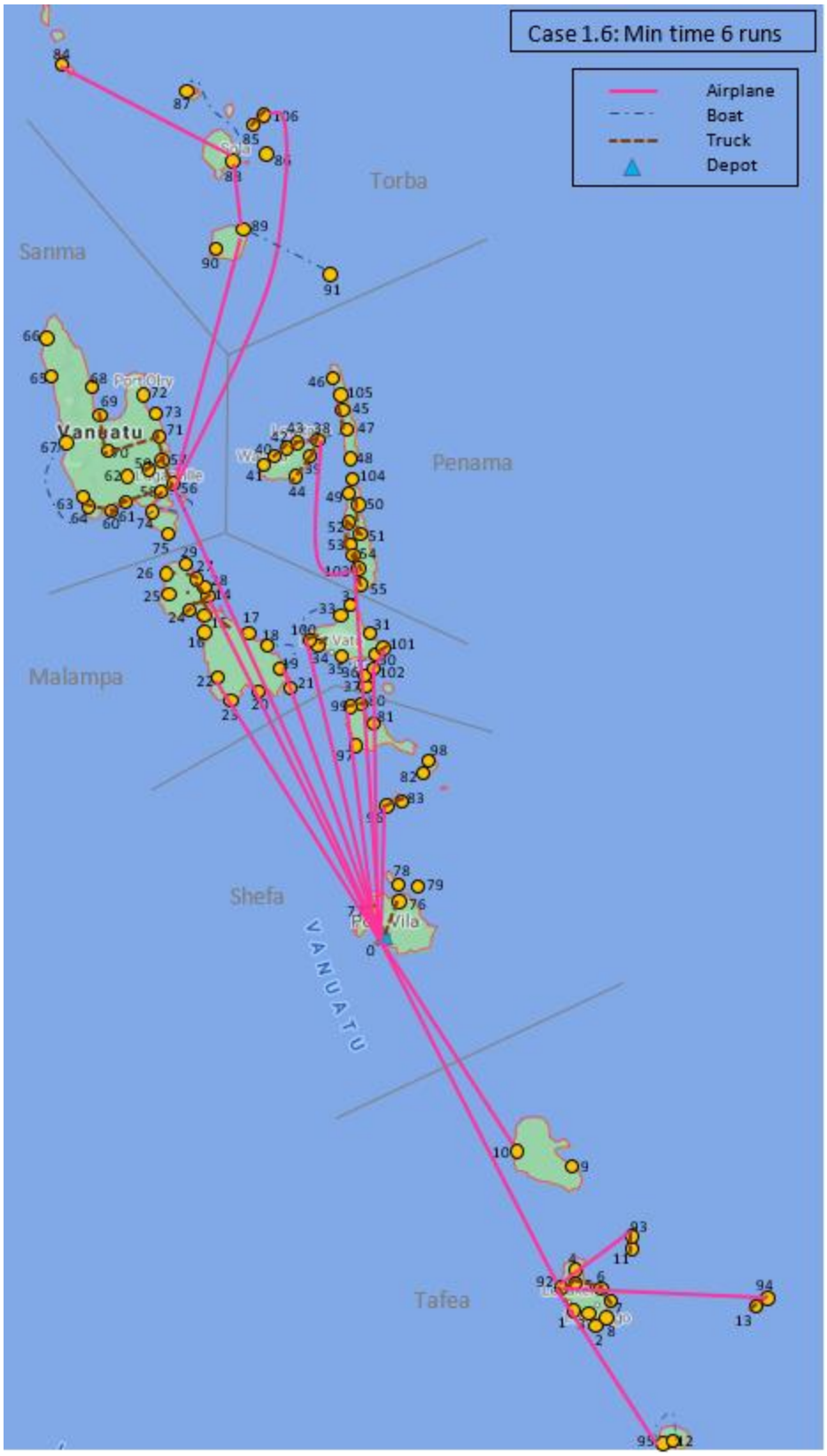

Figure 3.8 Solution map of Case 1.6

Table 3.14 shows the average transportation cost per HZ and the weighted average delivery time to a HZ in each run for the 9 cases for Case Study I. Columns 1-5 list the case number, the objective and special constraint, the area, transportation cost per health zone, and the weighted delivery time to each health zone respectively. The transportation cost/HZ for each area is calculated using the total transportation cost for each area divided by the number of health zones in its corresponding area. The weighted Hr/HZ is a service measure, which is the average time to travel to each health zone in a region, weighted by the demand of each health zone. For example, if a region has 2 health zones, A and B, and if the time to reach A is 2 hours, and the demand is 10 liters, and the time to reach B is 12 hours, and the demand is 1 liter, the weighted average time is $\frac{2*10+12*1}{10+1} = 2.9$ hours. The unweighted average time is 7 hours, which cannot reflect the fact that most vaccines in this region are delivered in a relatively short time, 2 hours.

Notice that the shortest weighted Hr/HZ that can be achieved is 1 hour and 26 minutes in Case 1.2, and the best cost for Vanuatu without drones is $16.61/HZ in Case 1.1. In Case 1.5, notice that the range of the weighted Hr/HZ for different provinces is very large, from 24 hours and 13 minutes to 2 hours and 41 minutes. This is partially caused by the relative distance of each province to the depot, and partially caused by the available modes at certain points and network configuration to minimize the cost. We see the cost and weighted time between the two cases that both minimize the weighted delivery time, Cases 1.2 and 1.6, are very similar. This means that aggregating the solution for the country by solving 6 provinces separately does not affect the service model P1-S as much. Comparing Cases 1.6 and 1.7, we see that enforcing a 2 hour service time limit in Case 1.7 makes the average service time when minimizing cost

almost as good as the service time from minimizing the time (in the P1-S model), but with a lower cost! That is, minimizing cost with a tight service constraint can find solutions with both low cost and fast service. Comparing Cases 1.7 and 1.8, we see how allowing 3 extra hours for delivery in Case 1.8 reduces the cost by 13% (from $40.81 to $35.43). Comparing to Case 1.5, Case 1.9, which forces use of an airplane flight to move the vaccines quickly to each province, improved the service time by more than 4 hours, while increasing the total cost substantially (by 30%). We see that the cost and service time of Cases 1.8 and 1.9 are similar, because the solutions of five provinces, except Tafea, are the same.

Case	**Objective**	**Area**	**Transportation cost ($)/HZ**	**Weighted Hr/HZ**
Case 1.1	Min Cost	*Vanuatu*	*16.62*	*14h 53m*
Case 1.2	Min Time	*Vanuatu*	*67.59*	*1h 26m*
Case 1.3	Min Cost, <2 hr	*Vanuatu*	*31.44*	*2h*
Case 1.4	Min Cost, <5 hr	*Vanuatu*	*21.67*	*5h*
Case 1.5	Min Cost	Torba	50.28	24h 13m
		Sanma	40.46	2h 41m
		Penama	22.95	3h 49m
		Malampa	12.52	11h 33m
		Shefa	17.90	4h 50m
		Tafea	30.68	11h 11m
		Vanuatu	*28.01*	*7h 49m*
Case 1.6	Min Time	Torba	117.07	2h 22m
		Sanma	51.22	1h 45m
		Penama	38.78	1h 47m
		Malampa	68.60	1h 16m

		Shefa	76.75	48m
		Tafea	69.27	1h 4m
		Vanuatu	*65.81*	*1h 29m*
Case 1.7	Min Cost, <2 hr	Torba	86.73	2h 25m
		Sanma	44.88	2h
		Penama	29.56	2h
		Malampa	22.52	1h 59m
		Shefa	35.93	1h 47m
		Tafea	45.14	1h 59m
		Vanuatu	*40.81*	*2h*
Case 1.8	Min Cost, <5 hr	Torba	83.70	3h 28m
		Sanma	40.46	2h 29m
		Penama	22.95	3h 54m
		Malampa	18.94	3h 26m
		Shefa	17.90	4h 50m
		Tafea	40.51	4h 57m
		Vanuatu	*35.43*	*3h 40m*
Case 1.9	Min Cost, 1st leg plane	Torba	83.70	3h 28m
		Sanma	40.46	2h 29m
		Penama	22.95	3h 54m
		Malampa	18.94	3h 26m
		Shefa	17.90	4h 50m
		Tafea	45.94	2h 58m
		Vanuatu	*36.34*	*3h 3m*

Table 3.14 Solutions of cases in Case Study I in P1

3.5.3. Cost and service tradeoff and mode usage analysis

Figure 3.9 shows the cost and service tradeoff for the solutions for Vanuatu, where the blue circles show the system-wide solutions where the input data is for all of

Vanuatu, and the orange squares show the aggregated results from combining the performance from separate solutions for the six provinces (the input data for each of the six solutions is a single province). These points in Figure 3.9 correspond to entries in Italics in Table 3.14 and the labels in Figure 3.9 match the entries in column two of Table 3.14. Both the blue dots and orange squares show the cost and service tradeoff as a higher level of service (i.e., shorter average delivery time) requires a larger cost. Among the system-wide solutions (blue dots), the minimum cost (Case 1.1) is $16.62/HZ with a 14 hours and 53 minutes delivery time per health zone on average. The best delivery time that can be achieved (Case 1.2) is 1 hour and 26 minutes per health zone on average, but with a high cost of $67.59/HZ, which is more than 4 times the minimum cost. Comparing the system-wide “Min Cost” and “Min Cost,<5 hr” solutions (Cases 1.1 and 1.4), the 5-hour time limit decreased the average delivery time by almost 10 hours or 66%, while increasing cost per health zone about 30% ($5.05). To achieve an average delivery time of less than 2 hours (Case 1.3) increases the cost by 89% (vs. Case 1.1).

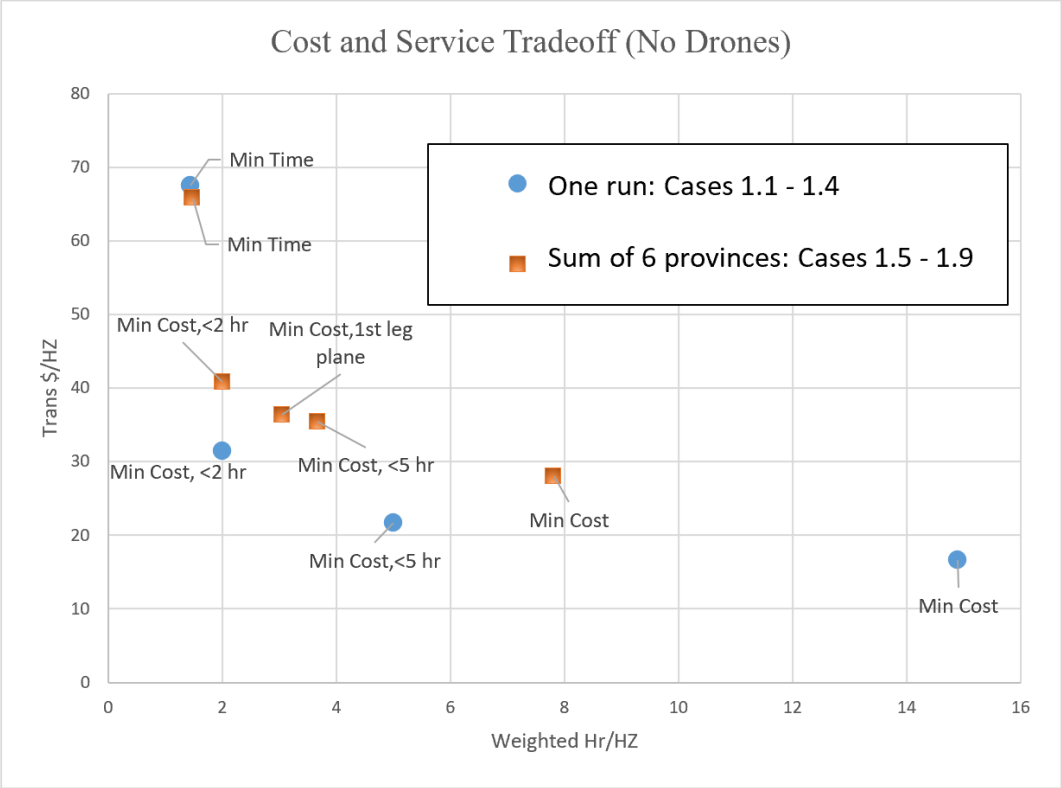

Figure 3.9 Cost and service tradeoff in Case Study I in P1

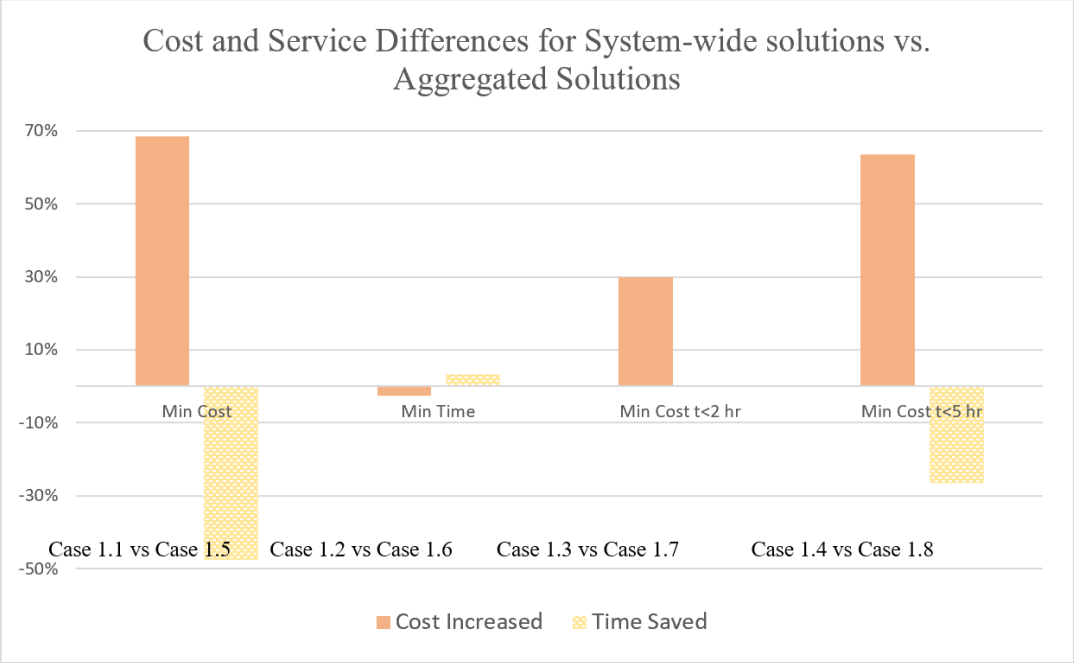

Figure 3.10 Bar chart for 6 runs vs 1 run

The orange squares are above (higher cost) and to the left (shorter average delivery time) of the corresponding blue dots, so running the model separately for each province achieves better delivery times, but with higher transportation cost. This is because arcs between provinces cannot be selected in the cases shown by orange squares, so the lowest cost solution for the whole country cannot be formed. However, the benefit is that the average delivery time decreases, which is as expected, because vaccines are delivered to each province directly without the possibility of vaccines for the farther provinces incurring the time on more circuitous routes to serve the nearer provinces. An interesting observation from the cost and service tradeoff chart is that between the "Min Time" and "Min Cost,<2 hours" cases for both the system-wide and the aggregated solutions (Case 1.2 or 1.6 versus Case 1.3 or 1.7), the "Min Cost,<2 hours" case is a better option as the cost dropped significantly on the vertical axis, and the service time only increased around a half hour. But from a percentage perspective, for example, from Case 1.2 to Case 1.3, the cost dropped 54%, and the service improved 39% which is not a small percentage compared to the cost deduction percentage. On the other hand, Case 1.2 "buys" 0.56 Hr/HZ for $36.15/HZ on average, which equals to $64 per hour of reduction in the average service time. So one could apply the solutions in Case 1.2 assuming it is worth $64 per hour to improve the average service time.

Similarly, between the "Min Cost" and "Min Cost,<5 hours" cases for both the system-wide and the aggregated solutions (Case 1.1 or 1.4 versus Case 1.5 or 1.8), the "Min Cost,<5 hours" case may be a better option as the cost increased relatively little on the vertical axis, but the service time improved significantly on the horizontal axis (a large shift to left), especially for the system-wide solutions. From a percentage

perspective, for example, from Case 1.1 to Case 1.4, the service time improved by 66.4% while cost increased by 30%, which is not a small percentage. On the other hand, Case 1.4 "buys" 9.88 hours for $5.05, which equals to $0.51 per hour of reduction in the average service time. So comparing to the $64 per hour value mentioned above when comparing Case 1.2 with Case 1.3, $0.51 per hour seems reasonable. Thus, the "Min Cost,<5 hours" case may be a better option than the "Min Cost" case because it does not cost too much to improve the service time. But the "Min Time" case may or may not be a better option than the "Min Cost,<2 hours" case because it is expensive for improving the service time.

Figure 3.10 shows the percentage of cost and service differences from comparing the aggregated solutions to the system-wide solutions. Between the two cases that minimize the cost (i.e., Case 1.1 and Case 1.5), the cost from the aggregated solution (orange square in Figure 3.9) costs 69% more than the cost of the system-wide solution (blue dot in Figure 3.9), but with 7 hours and 4 minutes per health zone lower delivery time on average (or -48%). Between the two cases that minimize the time (i.e., Case 1.2 and Case 1.6), the performance measures for the aggregated solution are almost the same as those for the system-wide solution, differing by only 3 minutes (3%) and -$1.78 (-3%).

Between the two cases that minimize the cost while limiting the delivery time to 2 hours (i.e., Case 1.3 and Case 1.7), the aggregated solution costs 30% more than the system-wide solution for the same 2 hour average delivery time. The weighted Hr/HZ for Torba is 2 hours and 55 minutes in Case 1.3 even when the weighted Hr/HZ for all provinces is 2 hours. Case 1.7 on the other hand has a 2 hours weighted Hr/HZ for all

provinces as well, but with a better service time for each province, especially for far away province Torba which has a service time of 2 hours and 25 minutes. Between the two cases that minimize the cost while limiting the delivery time to 5 hours (i.e., Case 1.4 and Case 1.8), the aggregated solution costs 63% more than the system-wide solution, but it does provide a 1 hour and 20 minute faster average delivery time (reducing the average time 27%).

To sum up Cases 1.1 to 1.8, the transportation cost to serve a health zone on average is more expensive in the aggregated solutions where each province is considered separately, but the aggregated solutions often provide faster service, as it is the current practice in Vanuatu (Graves, 2018). As Figure 3.10 shows, the transportation cost increased in 3 out of 4 cases ranging from 69% to 30%, and the cost improved by 3% only in the "Min Time" case when comparing the aggregated case (i.e., Case 1.6) against the system-wide cases (i.e., Case 1.2). The service time on the other hand, improved in 2 out of the 4 cases, ranging from 48% in the "Min Cost" case to 27% in the "Min Cost,<5 hours" case. The service time increased by 3% in the "Min Time" case.

Figure 3.10 shows that system-wide solutions can provide large cost savings (up to 69%) especially when the service level is low as in the "Min Cost" and "Min Cost, <5 hours" cases. In other words, the large cost savings come with the "cost" of worse service, which can be as much as 27% to 48% worse. Another way to look at it is that the benefit of cost savings is offset by the disadvantage of poor service in system-wide cost minimizing solutions. Also, when the service level is high, as in the "Min Time" case, a system-wide solution can improve the service level more compared to the aggregated solution, but with an increased cost. However, the percentage of the improved service

level and the percentage of increased cost are small and similar; in other words, the impact of the aggregated solution when the service level is high is not as significant as the impact of aggregated solution when the service level is low. Note that when the service level is in between the best case (i.e., "Min Time" case) and the worse cases (i.e., "Min Cost" and "Min Cost,<5 hours" cases), which is in the "Min Cost,<2 hours" case, there is a 30% cost savings without deteriorating the service level (i.e., 0%). The above analyses suggest future research could examine the cases between the "Min Cost,<2 hours" case and "Min Cost,<5 hours" case to further explore the cost and service tradeoff.

Case 1.9 shows that using an airplane to deliver to each province provides a solution that improved the delivery time compared to Case 1.5 by 4 hours and 46 minutes, but with a 30% increased cost by using expensive airplanes. Notice that five of the six provinces in Case 1.8 and Case 1.9 that have the same cost and service (not Tafea). The five provinces have the same delivery network for the two cases, which means Case 1.8 uses airplanes as the 1st leg to reach each province without a constraint forcing it to do so. The service time for Tafea in Case 1.8 is slower than in Case 1.9 because a shorter airplane arc 0-10 is used in Case 1.8, while a longer airplane arc 0-92 is used in Case 1.9, which also explains why the cost is more expensive for Tafea in Case 1.9. Both Cases 1.8 and 1.9 use airplanes in Tafea for arcs 92-93 and 93-94. Notice that compared to Case 1.3 (Min Cost, <2 hr), Case 1.9 has worse service and higher cost. Case 1.3 uses 12 truck arcs, 10 airplane arcs, and 33 boat arcs, while Case 1.9 uses 8 truck arcs, 9 airplane arcs, and 39 boat arcs. So the solution of Case 1.9 provides slower delivery time due to the higher percentage of boat arcs used (i.e., 70% vs 60% in Case 1.3), and it is more expensive because vaccines need to be delivered to each province

separately. Hence more arcs are used for the entire country (i.e., 56 arcs) compared to Case 1.3 that optimized the delivery network as a whole and used one fewer arc (i.e., 55 arcs).

Figure 3.11 Mode usage for Cases 1.1-1.8 in Case study I in P1

For Case 1.5 - Case 1.7, it took the longest average time to serve a health zone in Torba province, ranging from 24 hours 13 minutes to 2 hours 22 minutes. Torba is also the most expensive province to serve in all solutions for Cases 1.5-1.9, due to the greater distance from the national depot. From the analyses for Torba, we see that serving places that are far away from the depot requires a fast but expensive mode of transport such as airplanes. Thus, I anticipate that many drone arcs may replace airplane arcs in Case Study II when drones are allowed, since drones are fast, but with lower cost. Another way to serve places far away from the depot without using fast, but expensive modes of transport might be by increasing the cold chain time limitation, for example, by replacing temperature sensitive vaccines with thermostable vaccines (which will be more expensive).

Figure 3.11 shows the breakdown for usage of the three modes for Case 1.1 to Case 1.8. Each of the eight charts includes three bars, where the first bar shows the percentage of each mode used in terms of transportation cost, the second bar shows the percentage of each mode used in terms of transportation time, and the third bar shows the percentage of each mode used in terms of liter-km (combing the amount of vaccine and the distance). Due to the low cost for boat transport, and the higher cost for truck and airplane transport, boat arcs are used heavily for the cost minimizing cases, and airplane and truck arcs are used when minimizing the average delivery time. Among the cost minimizing cases, airplane is used more and boat is used less as the time restriction become tighter. When comparing the relative mode use in each chart in the bars for "Trans Cost" and "Time", note that the boat portion is always smaller in the "Trans Cost" bar than in the "Time" bar. This is a result of boats being the slowest and least expensive

mode. Similarly, the airplane portion is always larger in the "Trans Cost" bar than in the "Time" bar, due to the high cost and fast speed of airplane. Also notice that in all bar charts except Case 1.1, the airplane portion in the "Time" bar is smaller than in the "Liter-distance" bar. This is because airplanes have a large payload capacity and fast speed that allow airplanes to carry a large amount a long distance in a short time. For Case 1.1, airplane is used for three arcs around the edges of Vanuatu, where they carry small amounts on arcs 92-93, 93-94, and 88-84, carrying 4, 2, and 2 liters respectively (see Figure 3.6), which explains why the liter-distance portion of airplane in Case 1.1 is very minimal. The plane use increases and boat use decreases in both the system-wide and aggregate solutions when the service level increases, as shown in the third bar in each chart for liter-distance. Trucks are not used as much compared to airplanes and boats, because (i) there are fewer truck arcs in the network (i.e., 136) compared to boat arcs (i.e., 3616), and (ii) there are more truck arcs compared to airplane arcs (which is 78), but airplanes are faster than trucks and also cost less. Recall that the transportation cost of an airplane arc is \$0.75/km, and it is \$1/km for a truck arc. The speed of regular airplanes is 220 km/hr, and truck speed is 50 km/h. Thus, trucks are only used at places where there is no airplane when the service level is high, and at places where there is no boat when the service level is low. This explains why trucks are used the most in Case 1.2 and Case 1.6 when the service level is the highest.

3.6. Case Study II: delivery with drones

The second case study evaluates performance for vaccine delivery with drones and compares the solutions to those from Case Study I without drones to assess the benefits of adding drones to the vaccine delivery network.

3.6.1. Design of Cases Study II

As mentioned in Case Study I, due to the complexity of the model and the large dataset when drones are available, I run the model separately for each province of Vanuatu in Case Study II. In Case Study II, I evaluate the two drone cost models P1-C1 and P1-C2 with large drones (LFW drones) and small drones (SFW drones). As mentioned in Section 3.1, the drone cost model in P1-C2 is appropriate for large capacity drones that need to fly each drone arc only once in a month, so this cost is used with the LFW drones due to their large payload capacity. The drone cost model in P1-C1 that charges based on the vaccine flow carried by drones (using flow divided by the drone capacity) is used with both the SFW and LFW drones. In Case Study II, I examine the vaccine delivery network when minimizing the transportation cost, minimizing the average delivery time, and minimizing the transportation cost with a service constraint of 5 hours (average delivery time to a health zone is less than 5 hours). I use the 5 hour time limit as this provides balanced solutions that have relatively low cost and good delivery time. Note that a two hour delivery time would be an extreme case for routine vaccine delivery as most vaccines have a substantially longer allowable cold chain time. (Note that for medical products that require a much higher service level, the models could still be used with short time limits.)

To assess the advantage of using drones for vaccine delivery, I examine the following cases in Case Study II:

- Case 2.1: Minimize the total transportation cost with SFW drones using the first drone cost model (in P1-C1) for each of the 6 provinces separately, and sum up the performance metrics of the 6 provinces. (6 runs)

- Case 2.2: Minimize the average weighted delivery time with SFW drones using P1-S for each of the 6 provinces separately, and sum up the performance metrics of the 6 provinces. (6 runs)
- Case 2.3: Minimize the total transportation cost with SFW drones using the first drone cost model (in P1-C1) for each of the 6 provinces separately, while limiting the average delivery time to a HZ to 5 hours, and sum up the performance metrics of the 6 provinces. (6 runs)
- Case 2.4: Minimize the total transportation cost with LFW drones using the first drone cost model (in P1-C1) for each of the 6 provinces separately, and sum up the performance metrics of the 6 provinces. (6 runs)
- Case 2.5: Minimize the average weighted delivery time with LFW drones using P1-S with the first drone cost model for each of the 6 provinces separately, and sum up the performance metrics of the 6 provinces. (6 runs)
- Case 2.6: Minimize the total transportation cost with LFW drones using the first drone cost model (in P1-C1) for each of the 6 provinces separately, while limiting the average delivery time to a HZ to 5 hours, and sum up the performance metrics of the 6 provinces. (6 runs)
- Case 2.7: Minimize the total transportation cost with LFW drones using the second drone cost model (in P1-C2) for each of the 6 provinces separately, and sum up the performance metrics of the 6 provinces. (6 runs)
- Case 2.8: Minimize the total transportation cost with LFW drones using the second drone cost model (in P1-C2) for each of the 6 provinces separately, while

limiting the average delivery time to a HZ to 5 hours, and sum up the performance metrics of the 6 provinces. (6 runs)

There are 48 runs in Case Study II. Cases 2.1, 2.4 and 2.7 are compared with Case 1.5 in Case Study I as they all minimize the total transportation cost with no limit on average delivery time. Cases 2.2 and 2.5 are compared with Case 1.6 in Case Study I as they all minimize the average delivery time. Cases 2.3, 2.6 and 2.8 are compared with Case 1.8 in Case Study I as they all minimize the total transportation cost with the average weighted delivery time to a health zone limited to be less than 5 hours. Comparison of the results for Case Study I and II provides the information to address research question *R1*: *How useful are drones in delivering vaccines on a monthly basis in an island country?* Results for Case Study II provide the information to address research questions *R2: How are the non-drone transportation modes affected by the use of drones?* and *R4: How does the use of different drone types affect the use of drones and system performance?*

In Case Study II, I use the same values for demand and the cold chain limit as in Case Study I for a fair comparison. Thus, the demand for each health zone $d_h$is from Section 3.4.1, and the cold chain limit $\lambda_{max} = 8$ hours. For the fixed facility costs for the drones, with SFW drones I use \$3/month as the DB cost and \$1.5/month as the RS cost; and for LFW drones I use \$10/month as the DB cost and \$5/month as the RS cost. In Case Study II, for each province I allow at most seven drone paths in each province ($N = 7$) and two drone arcs per drone path ($\Omega = 2$). These values provide a reasonable computational time for the 48 runs and they allow the model to generate good solutions that reflect the benefit of using drones. Longer drone paths ($\Omega > 2$) could provide better

performance, but with the added complexity in the drone operations. In the results that follow, 5 out of the 48 runs used the maximum number of drone paths, i.e., 7; and 16 out of the 48 runs used the maximum number of drone arcs per path, i.e., 2.

3.6.2. Solutions of Case Study II

Optimal solutions were generated for the 48 runs using the P1-C1, P1-C2 and P1-S models with Gurobi 9.1 on an HP Intel Quard-Core i7 with 3.9 Ghz CPU and 64 GB RAM. The average solution time for a run was 1229 CPU seconds (or 322 seconds in real time), with a range from 0.05 CPU seconds (0.03 seconds in real time) to 23,137 CPU seconds (5996 seconds in real time). All runs reached optimality with a zero gap.

To compare results from Case Study II to the detailed solution maps in Case Study I, detailed solution maps are shown in Figure 3.12 to Figure 3.16 for Cases 2.1, 2.2, 2.4, 2.5, and 2.7. Results of Case Study II and Case Study I are compared for the three conditions: “Min Cost”, “Min Time”, and “Min Cost, <5hrs”, and Table 3.15 lists average transportation cost per health zone and the average weighted delivery time to a health zone for each case in Case Study II and also for the corresponding cases in Case Study I (i.e., Cases 1.5, 1.6 and 1.8). Column 1 shows the condition, and Column 2 indicates the case number. Colum 3 shows the drone type and the MIP model solved, where P1-ND indicates the P1 model without drones. Columns 4 and 5 show the transportation cost and average time to a health zone, respectively.

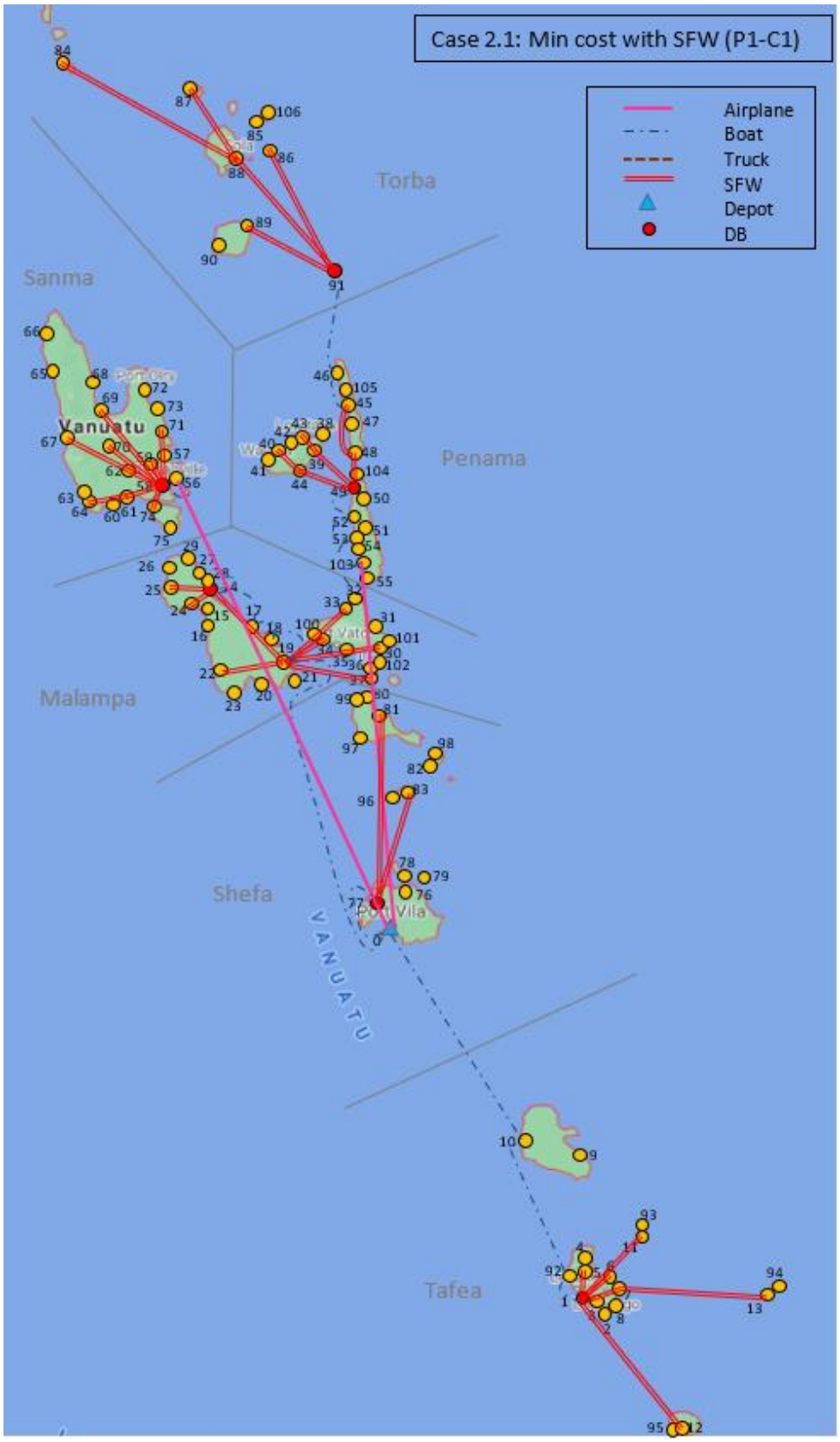

Figure 3.12 Solution map of Case 2.1 (SFW with P1-C1)

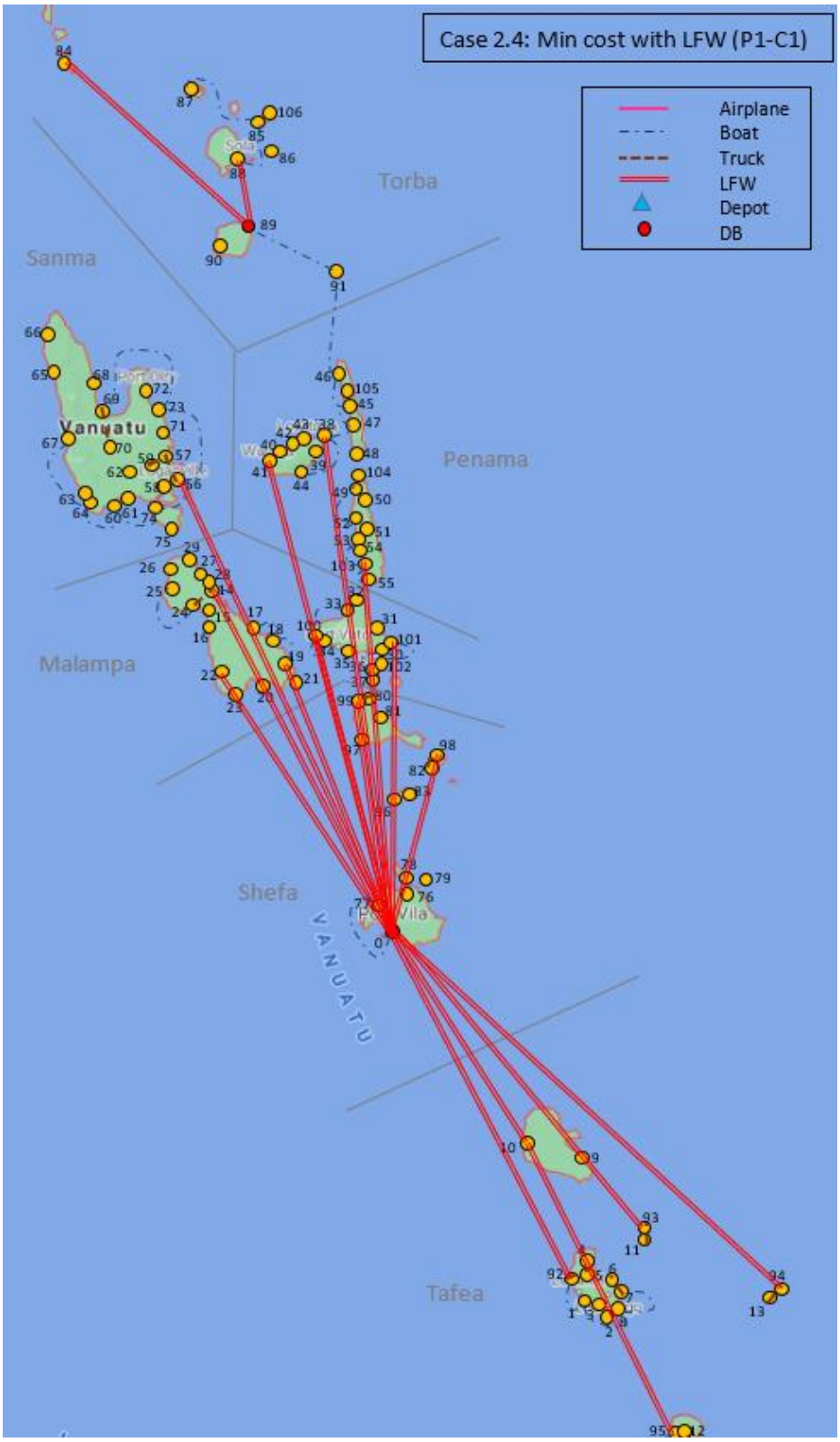

Figure 3.13 Solution map of Case 2.4 (LFW with P1-C1)

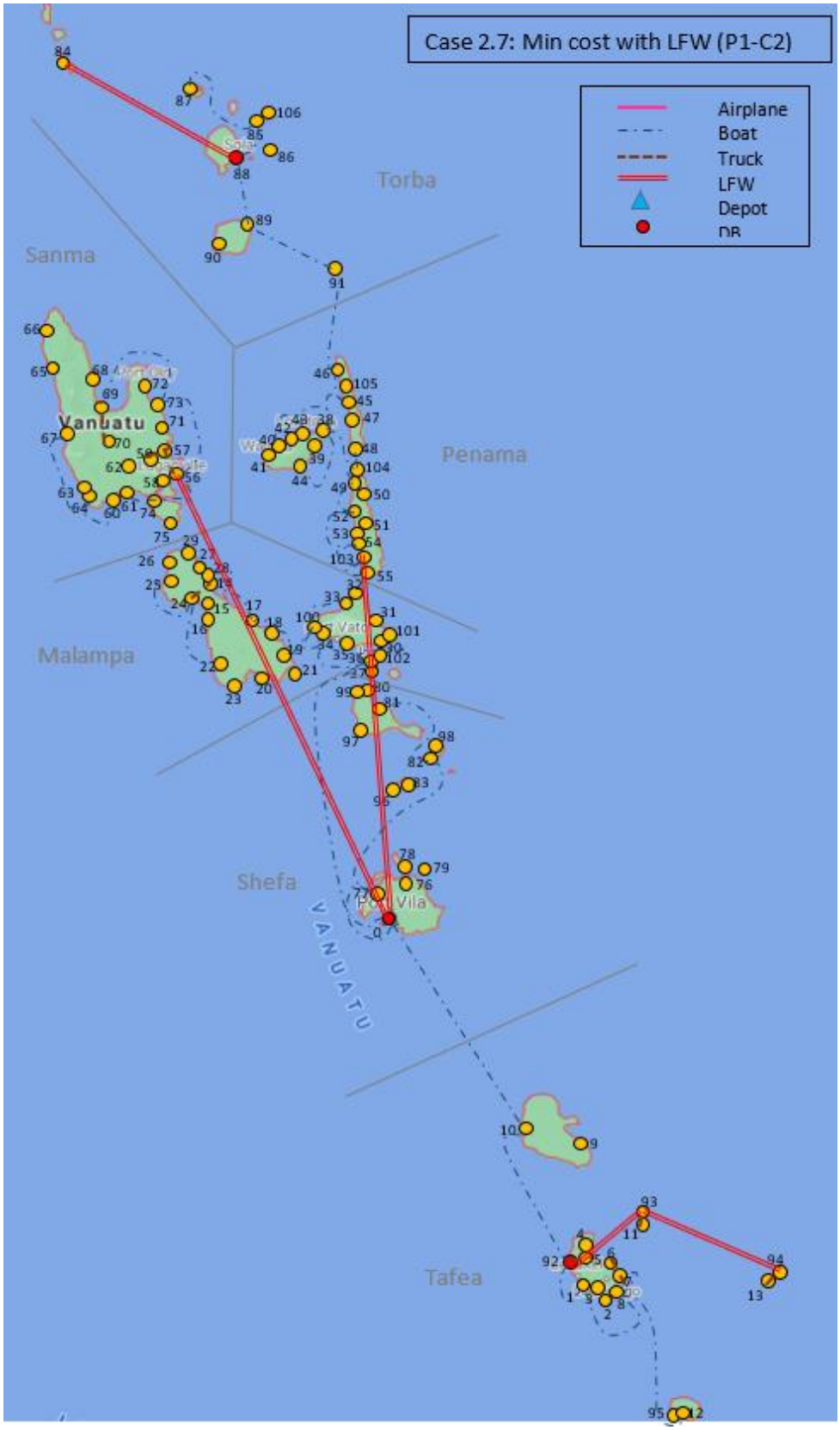

Figure 3.14 Solution map of Case 2.7 (LFW with P1-C2)

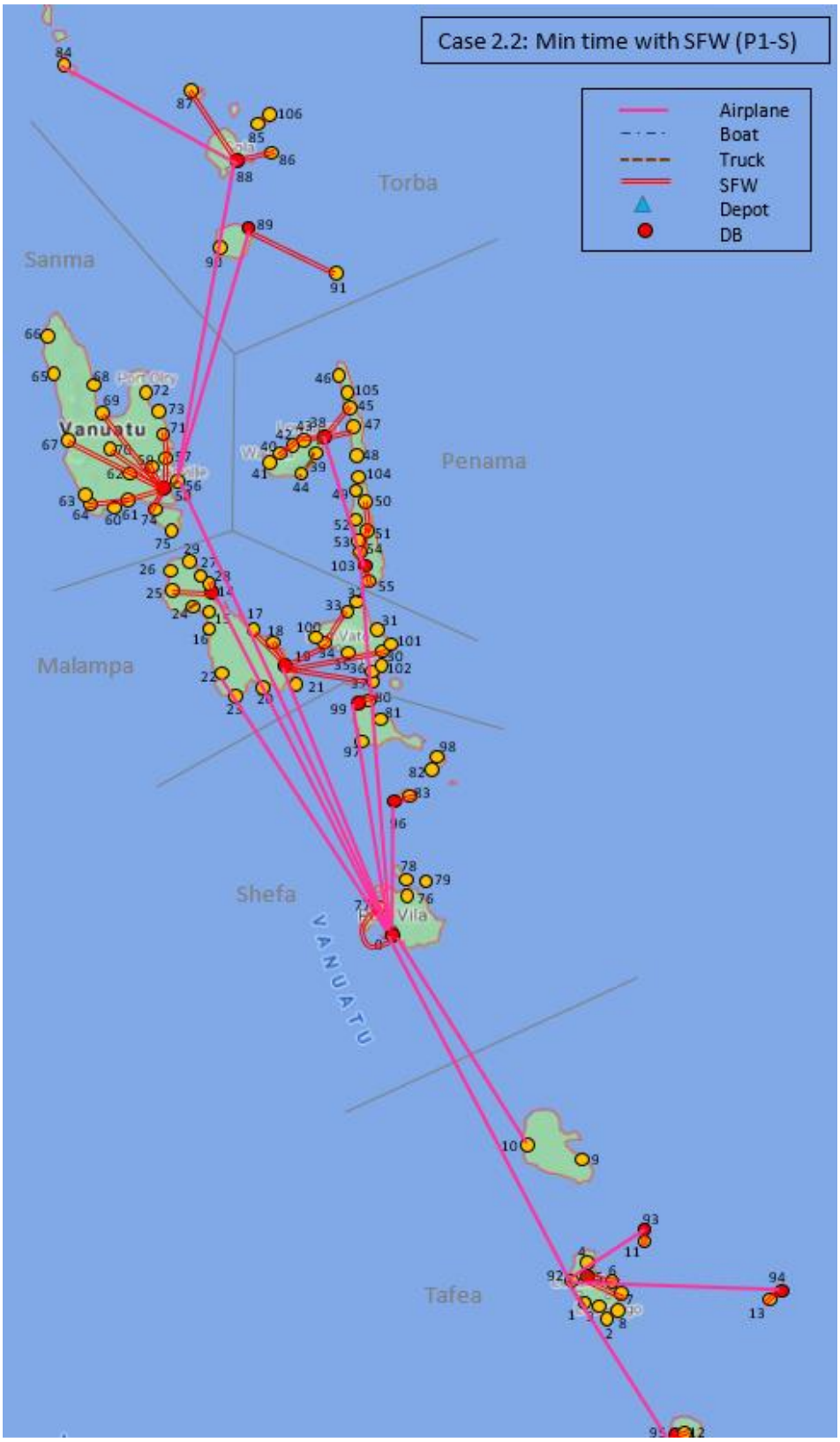

Figure 3.15 Solution map of Case 2.2 (SFW with P1-S)

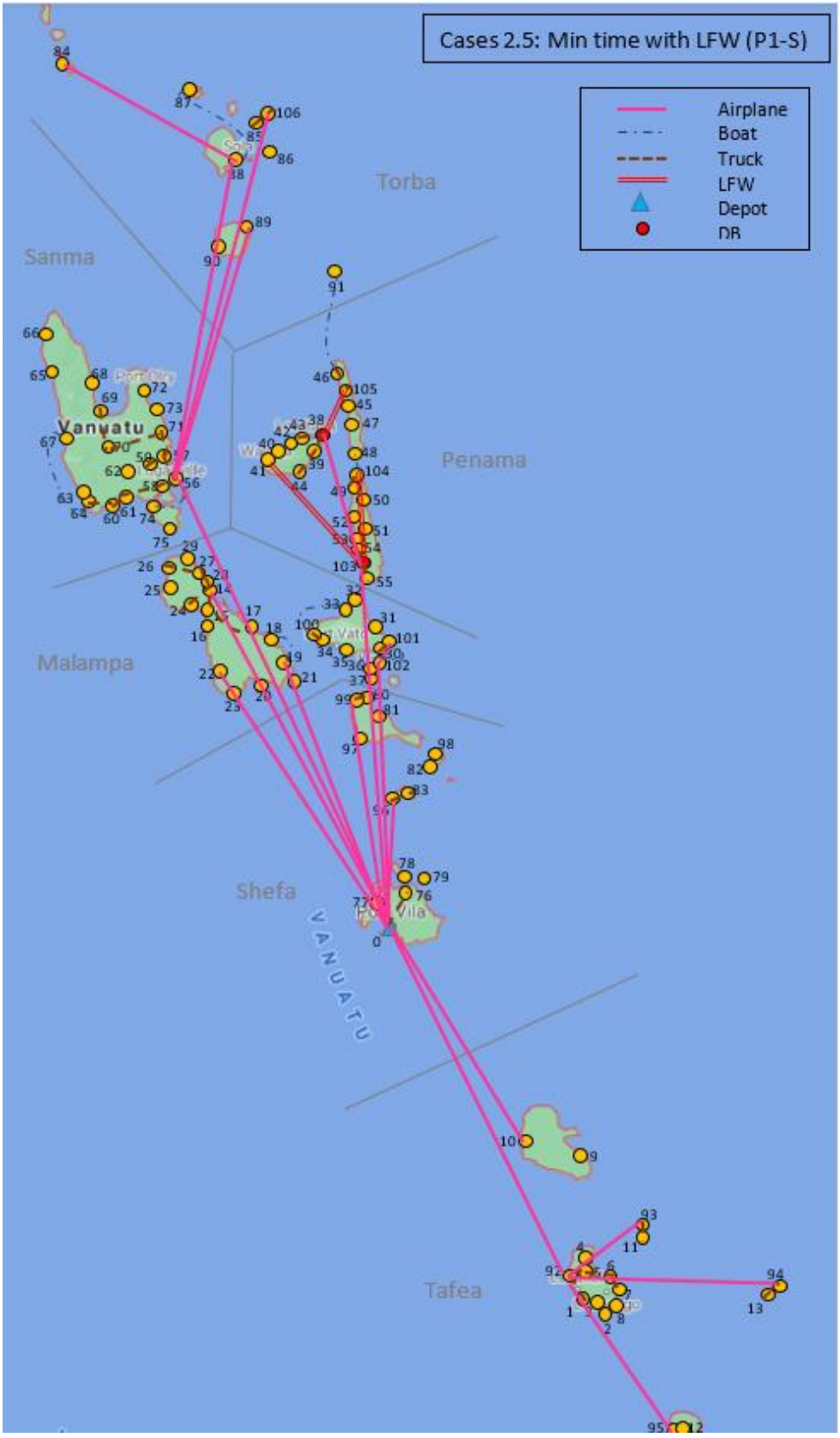

Figure 3.16 Solution map of Case 2.5 (LFW P1-S)

Cost and Service Decisions	Case	Drone: Model	Transportation Cost ($)/HZ	Weighted Hr/HZ	% Cost Savings
Min Cost	1.5	No drones: P1-ND	28.01	7h 49m	-
	2.1	SFW: P1-C1	17.22	5h 16m	38.5%
	2.4	LFW: P1-C1	14.08	2h 32m	49.7%
	2.7	LFW: P1-C2	16.32	6h 55m	41.7%
Min Time	1.6	No drones: P1-ND	65.81	1h 29m	-
	2.2	SFW: P1-S	53.45	1h 10m	18.8%
	2.5	LFW: P1-S	72.47	1h 22m	10.1%
Min Cost, <5h	1.8	No drones: P1-ND	35.43	3h 40m	-
	2.3	SFW: P1-C1	20.10	2h 50m	43.3%
	2.6	LFW: P1-C1	14.08	2h 17m	60.3%
	2.8	LFW: P1-C2	17.84	3h 51m	49.6%

Table 3.15 Comparison of solutions for Case Study I and II

Cost and Service Decisions	Case	Drone: Model	#Airplane Arcs	#Boat Arcs	#Truck Arcs	#Drone Arcs	Time of Longest Path (hr)
Min Cost	1.5	No drones: P1-ND	5	46	8	-	19
	2.1	SFW: P1-C1	2	16	0	35	10.8
	2.4	LFW: P1-C1	0	32	10	18	12.7
	2.7	LFW: P1-C2	0	44	8	5	17
Min Time	1.6	No drones: P1-ND	21	9	38	-	4.4
	2.2	SFW: P1-S	16	0	7	45	2.7
	2.5	LFW: P1-S	20	9	35	4	4.4
Min Cost, <5h	1.8	No drones: P1-ND	9	36	10	-	9.6
	2.3	SFW: P1-C1	4	13	0	36	6.6
	2.6	LFW: P1-C1	0	30	10	19	3.7
	2.8	LFW: P1-C2	1	39	8	7	5.8

Table 3.16 Comparison of arcs and longest path for Case Study I and II

Table 3.16 provides further information for the 11 solutions in Table 3.15 by showing the number of arcs of the four transportation modes and the time of the longest path to a health zone. When drones were allowed, the number of airplane arcs, boat arcs, and truck arcs decreased or stayed the same except in two cases, compared to the corresponding cases without drones. (In Case 2.4, the number of truck arcs increased by 2 compared to Case 1.5, and in Case 2.8, the number of boat arcs increased by 3 compared to Case 1.8.) In all three conditions (i.e., "Min Cost", "Min Time", and "Min Cost,<5 hours"), the cases with SFW drones always use the most drone arcs compared to the cases with LFW drones. We see the time of longest path decreased in all cases with drones compared to their corresponding no drone cases.

3.6.3. Cost and service tradeoff and mode usage analysis

Figure 3.17 shows the cost and service tradeoff among the cases in Table 3.15 and Figure 3.18 shows mode usage for the cases in Table 3.15. These two figures provide two complementary perspectives on the use of the two types of drones. In Figure 3.17, the three gray dots show the cost (average transportation cost per health zone) and the corresponding service (weighted average time to reach a health zone) without drones (these three points are Cases 1.5, 1.8 and 1.6 shown in Table 3.13 for Case Study I). The three cases with that minimize cost with no time limit when drones are allowed (Cases 2.1, 2.4 and 2.7) are plotted down and to the left compared to Case 1.5 (which minimizes cost without drones) in Figure 3.17, indicating that using drones improved both transportation cost and delivery time.

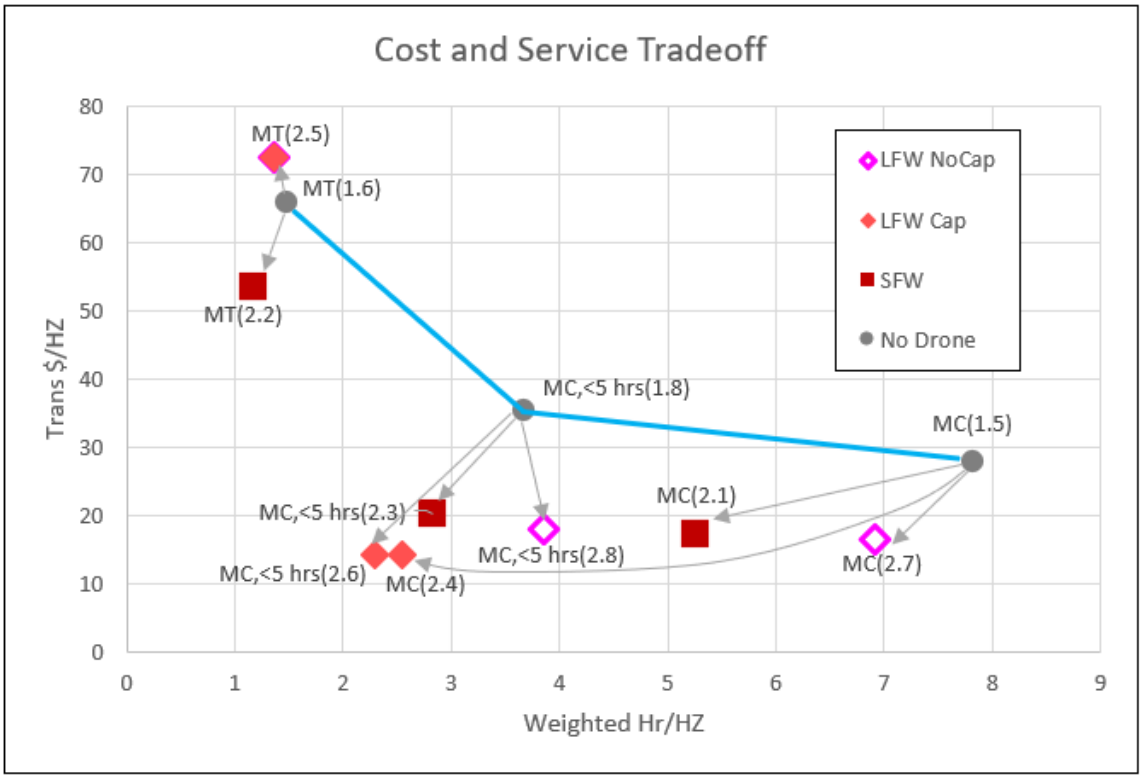

Figure 3.17 Cost and service tradeoff with drones in P1
(MC: min cost; MT: min time; ():case number)

Comparison of the solution maps of Case 1.5 (Figure 3.7) and Case 2.1 (Figure 3.12) shows that the SFW drones replaced all the expensive truck arcs, some of the expensive airplane arcs, and some slow boat arcs in Case 1.5 (see the first two bars in Figures 3.18(a) and 3.18(b)), and saved 39% in cost while improving service time 32% (see Figure 3.15). Comparison of the solution maps of Case 1.5 and Case 2.4 (Figure 3.7 and Figure 3.13), shows that the LFW drones in Case 2.4 replaced all the expensive airplane arcs and some slow boat arcs (see the first and third bar in Figures 3.18 (a) and 3.18(b)) and saved 50% of cost, while improving service time by 68%. Comparison of the solution maps of Case 1.5 and Case 2.7 (Figure 3.14), shows that the LFW drones in Case 2.7 replaced all the airplane arcs (see the first and third bar in Figures 3.18(a) and 3.18(b)), and saved 42% in cost, while improving service time 12%. Effectively, the

LFW drones functioned as small airplanes in Case 2.7. These findings on how drones replace other transportation modes are also apparent in examining relative mode use in the top two panels of Figure 3.18.

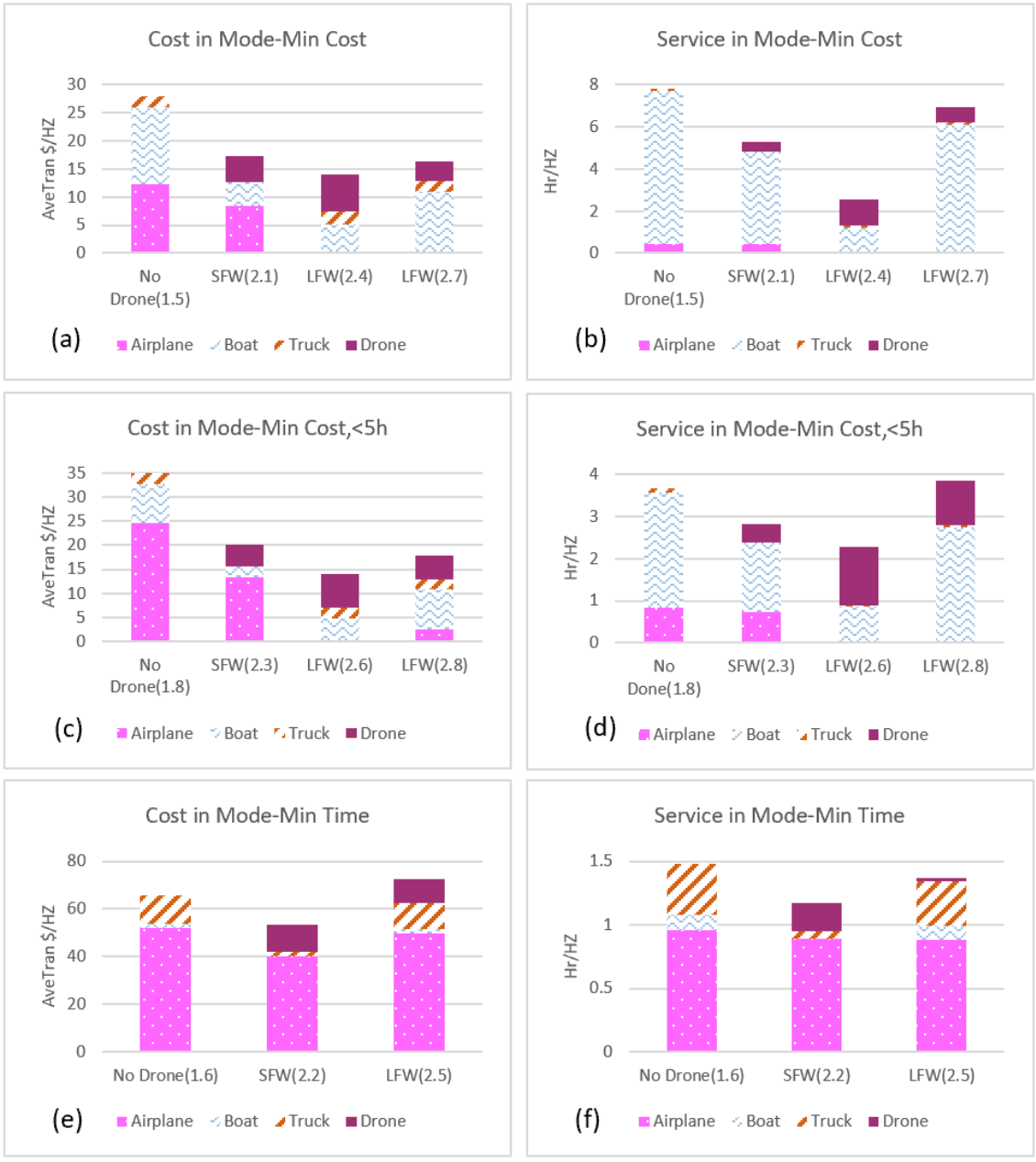

Figure 3.18 Mode usage comparison with and without drones for P1
((N.N) is the case number)

To compare the impact of different drone types, consider Cases 2.1, 2.4 and 2.7, shown towards the top of Table 3.15 and in Figure 3.18(a) and 3.18(b). Comparing the solution maps of Case 2.1 and Case 2.4, shows that Case 2.1 (SFW drones) used many shorter drone arcs and Case 2.4 (LFW: P1-C1) used many longer drone arcs; and this is due to the range difference of the SFW and LFW drones, and that LFW drones are allowed to fly only between airports, of which there are fewer that are widely separated. Comparing the cost for Case 2.1 and Case 2.4 shows that Case 2.4 has lower cost (see Table 3.15) because fewer RSs are used (see solution maps in Figure 3.12 and Figure 3.13), and because Case 2.4 used low cost boats instead of expensive airplanes (see the second and third bars in Figure 3.18(a)). Case 2.4 also provided much better service time (see Figure 3.17 and Table *3.15*) because the LFW drones are faster than SFW drones, and also there is a significant amount of slow boat travel in Case 2.l (see Figure 3.18(b)). So even though there are many SFW arcs in the solution map of Case 2.1, these are short arcs so that the total travel time savings for the SFW arcs is less than the savings with fewer, but longer LFW arcs as in Case 2.4. Comparing the solution maps of Case 2.4 and Case 2.7 shows very different usage of the LFW drones due to the different drone cost models (See also the third and fourth bars in Figure 3.18(b)). Case 2.4 with model P1-C1 charged the LFW drone cost based on the vaccine volumes carried (using the product of the rate ($0.38/km), the arc length and the flow on the arc divided by the LFW drone capacity), while Case 2.7 with model P1-C2 charged the LFW drone cost for essentially a full drone (using the product of the rate ($0.38/km) and the arc length). Because of this fundamental difference in cost modeling, Case 2.4 uses drones much more extensively

(See Figures 3.12 and 3.13, and the third and fourth bars in Figure 3.18(a) and Figure 3.18(b)) and has a 14% lower cost than Case 2.7, and saves 64% in service time.

When minimizing cost with a 5 hour delivery requirement (i.e., Cases 1.8, 2.3, 2.6 and 2.8), considering both drone types when using P1-C1 (when drone transportation cost on an arc is proportional to the vaccine carried) provided lower cost and faster delivery than Case 1.8 without drones (see Figure 3.17, Table 3.15, and the first three bars in Figures 3.18(c) and 3.18(d)). The SFW drones saved 43% in cost and 23% in service time, while the LFW drones (Case 2.6) saved 60% in cost and 38% in service time (see Table 3.15). The LFW drones with P1-C2 reduced cost by 50%, but increased the service time slightly (by 5%) (see the first and fourth bars in Figures 3.18(c) and 3.18(d)).

When minimizing the service time, Case 1.6 is for distribution without drones, while Cases 2.2 and 2.5 reflect the use of SFW and LFW drones, respectively. Results in Table 3.15 and Figure 3.17 show that both drone types allow the service to be improved relative to Case 1.6 (see the upper left of Figure 3.17, and Figure 3.18(f)), with the SFW and LFW drones saving 21% and 8% in average delivery time to a health zone, respectively. In Case 2.2, SFW drones replaced all boat arcs and most truck arcs compared to Case 1.6 (see the solution maps in Figure 3.8 and Figure 3.15, and the first two bars in Figures 3.18(e) and 3.18(f)), so the SFW drones provided better service. In addition, SFW drones replaced some expensive airplane arcs, so SFW also saved 19% in cost compared to Case 1.6. In Case 2.5, LFW drones replaced some truck arcs compared to Case 1.6, so LFW provided better service (See Figure 3.18(f)), but it actually increases cost relative to the situation with no drones (see the first and third bars in Figure 3.18(e)).

In this illustration, SFW drones are a better option than LFW drones to give the best service (lowest average delivery time) at lowest cost.

Case Study II can help answer three of our key research questions. First, comparing optimal results for Case Study I and Case Study II shows how useful drones can be in delivering vaccines for an LDC. Using either type of drone can achieve better performance than distribution without drones, so the results show that both types of drones are able to lower the cost and provide faster delivery when minimizing cost. A second set of research findings concern how the non-drone modes are affected by the use of drones. When minimizing cost, SFW drones are generally used to replace many (or all) truck arcs, some boat arcs, and a few airplane arcs. The LFW drones are used to replace expensive airplane arcs, some boat arcs and some truck arcs. The cost model used with LFW drones does have some impact on the usage of other modes. Use of LFW drones changed the delivery network configuration, and some health zones that used to be served by boat to a DC now can be served by the combination of LFW and truck to another DC in the same health zone. The new configuration combined LFW and truck travel to save more than the former configuration (e.g., using boat travel). The new configuration used truck arcs instead of boat arcs because the DC in the new configuration is only connected by a truck arc from the airport where the LFW drone comes from. Compared to P1-C2, LFW drones with the cost model in P1-C1 replace more boat arcs with LFW drone arcs.

The third set of research findings concern how the performance varies depending on the drone type. When minimizing cost, using LFW drones saves more in both cost and time than using SFW drones. Between the two cost models, LFW with P1-C1 saves more

both in time and cost than LFW with P1-C2. This is because LFW served as a small airplane, but with lower cost and faster delivery, that allows many direct deliveries to DCs. Because most LFW drone arcs are direct delivery from the national depot, many of the LFW drone arcs share the same DB at the depot, and thus there are fewer DBs needed in the entire network than when using SFW drones. Using SFW drones can lower the cost because SFW drones replace some truck arcs, which are more expensive than SFW drone arcs.

All parameters are fixed values in this case study, and I discuss the findings about how changes of key parameter values affect drone usage and performance in Section 3.7 which presents the sensitivity analysis.

3.7. Case Study III: drone path and step analysis

This case study is designed to examine how the number of drone paths (N) and number of drone arcs per path (Ω) that are allowed in the model affect the drone usage and model performance. This cases study uses \$3/month as the DB fixed cost, \$1.5/month as the RS fixed cost, the demand for each health zone discussed in section 3.4.1 for d_h and a cold chain limit of $\lambda_{max} = 4$. I designed 15 runs with various combinations of $N = 1, \dots, 5$, and $\Omega = 1, \dots, 3$ using the dataset for Tafea Province with the SFW drone and model P1-C1. All 15 runs generated optimal solutions with no gap in the same computational environment as in the previous two case studies.

Figure 3.19(a) plots the transportation cost per health zone with 1 to 5 drone paths, where the three lines represent different lengths allowed for the drone paths (i.e., values of Ω). This figure shows how allowing more drone paths reduces the cost for the same number of drone arcs per path (Ω), especially when Ω is small. When $\Omega = 1$, the

cost decreases for each value of N, but when $\Omega = 2$ and $\Omega = 3$, the cost decreases by only a very small amount when N reaches 3, which makes the two lines look flat. So when only one drone arc is allowed per drone path, having more drone paths reduces cost, but when multiple drone arcs per path are allowed then only a few drone paths are needed to achieve the best solution. When N is large enough (i.e., $N = 5$), notice that the cost is nearly the same no matter what Ω value is allowed in the model.

Figure 3.19(b) plots the average delivery time per health zone with 1 to 5 drone paths, where the three lines represent different lengths allowed for the drone paths. Figure 3.19(b) shows that multiple drone arcs per path can decrease the average delivery time compared to paths with a single drone arc when more than one drone path is allowed. The general trend is that increasing the number of drone paths allows a decrease in delivery time. But when $\Omega = 1$, the solution for $N = 2$ has a worse average delivery time than when $N = 1$. This is because the objective function is to minimize cost, so while $N = 2$ does generate a lower cost solution than $N = 1$, that solution has a slightly longer average delivery time. This figure shows that when allowing multiple drone steps ($\Omega \geq 2$), there is no need in Tafea to use many drone paths to achieve a good delivery time. (As Figure 3.19(a) indicates the minimum cost solution is essentially achieved with three drone paths.)

Figure 3.19(c) plots the cost and service tradeoff with 1 to 5 drone paths, where the three lines represent different lengths allowed for the drone paths (i.e., values of Ω). Thus, this figure integrates the results from Figure 3.19(a) and Figure 3.19(b). Each path for a particular color (value of Ω) shows the evolution of the tradeoff as the number of

drone paths increases. These paths are not strictly decreasing when moving to the left, reflecting the non-monotonic behavior of Figure 3.19(b).

Figure 3.19(d) plots the number of drone arcs used in the solution for Tafea with 1 to 5 drone paths, where the three lines represent different lengths allowed for the drone paths. This shows the number of drone arcs used increases as N and Ω increases. We see, as in the other charts, how the optimal solution does not use all available drone arcs. The results for $N = 5$ help explain why the cost of the three lines are about the same in Figure 3.19(a), but the delivery times are different (Figure 3.19(b)) for the three runs, as when $\Omega = 1$ fewer drone arcs are used. Note that even though 15 drones arc could be used when $N = 5$ and $\Omega = 3$, the optimal solution uses only 6 drone arcs.

Figure 3.19(e) plots the CPU time for the solutions for Tafea with 1 to 5 drone paths, where the three lines represent different values of Ω. This shows how the number of drone steps and drone paths affect the computation time. First we see that adding drone paths increased the CPU time, but with a slightly decreasing rate as the number of drone paths increases for larger drone steps (i.e., $\Omega = 2\ or\ 3$). It is interesting to see that using larger drone steps (i.e., $\Omega = 2\ or\ 3$) with few drones paths can be more time consuming to solve, but the rate of increase in cpu time is decreasing. So with five drone paths, the larger values of Ω require less cpu time than small values of Ω.

To sum up, this section analyzed the behavior of optimal solutions as the number of drone paths and number of drone arcs per path is varied. The optimal solution for Tafea Province often does not use the maximum allowed number of drone paths or drone arcs, which indicates that drones may not be used everywhere (or extensively), depending on the availability of other modes. In this section, the values of N and Ω used are

designed for the size of Tafea, which has 17 nodes, so the number of N and Ω in the analysis above may change if the model is applied in a larger area with more nodes. However, the general conclusions about combinations of drone paths and drone arcs per path may be similar to this analysis. One key finding from this analysis is that allowing a larger number of drone paths and more drone arcs per path will generally reduce the cost up to a certain point, beyond which further use of drones is not warranted. Thus, if the number of drone paths is restricted, longer drone paths should be considered to try to reduce costs. Likewise, if the drone path length (number of drone arcs per path) is limited, then more drone paths should be allowed to try to reduce costs. Finally, the results suggest that when allowing multiple drone arcs per path, it may not be necessary to use a large number of drone paths to achieve a good delivery time.

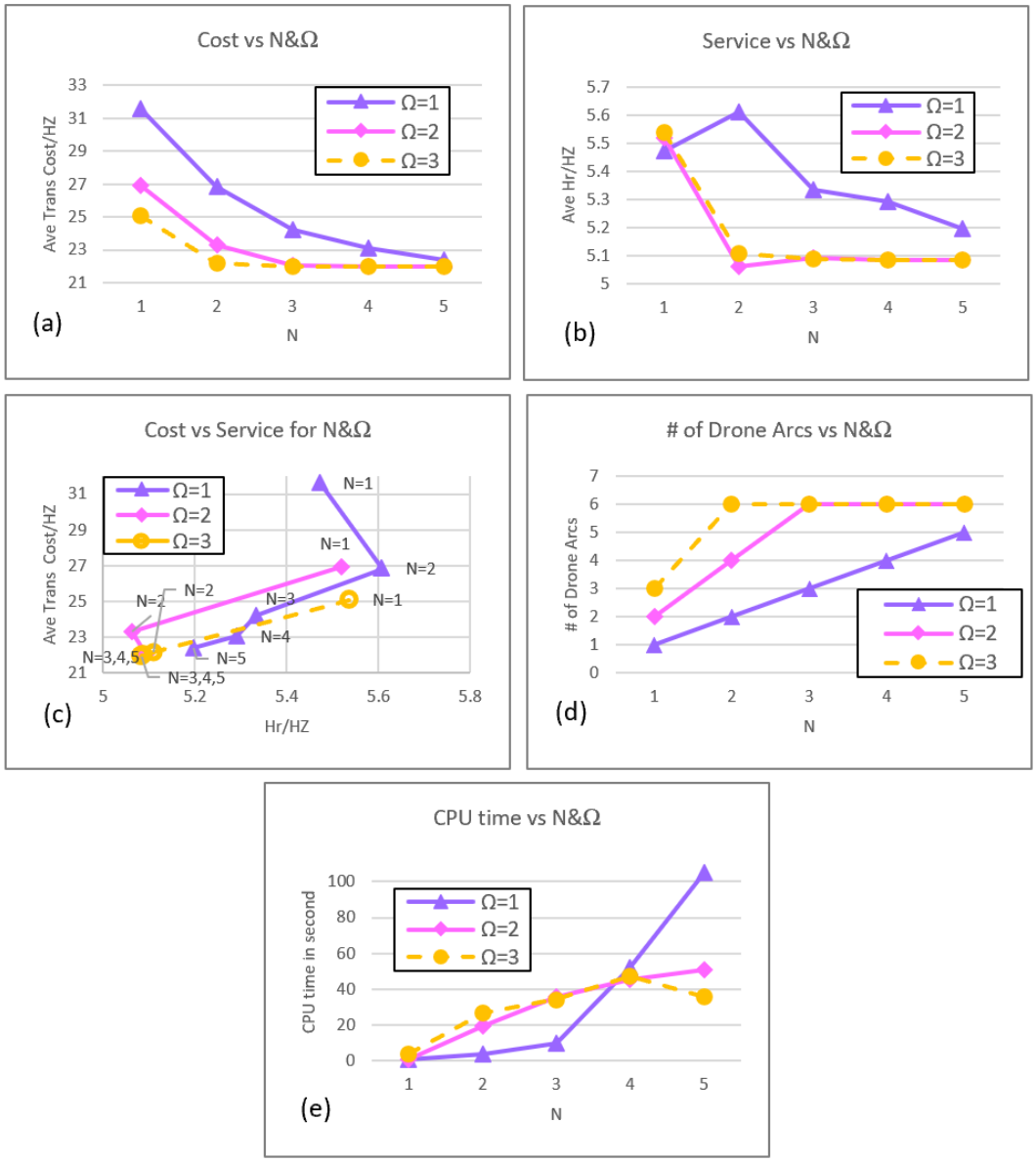

Figure 3.19 Drone step and path analysis charts

3.8. Sensitivity analysis on key parameters

In this section, sensitivity analysis is conducted to examine how some key parameters affect the drone usage and performance. Five parameters are selected to be examined, and they are the drone type, cold chain limitation λ_{max}, demand d_h, DB fixed cost m_i, and RS fixed cost h_i. The two drone types examined in the sensitivity analysis

are the SFW and LFW drones. I use model P1-C1 for SFW drones (where cost is the product of rate ($/km), arc distance, and flow divided by drone capacity) and model P1-C2 for LFW drones (where cost is the product of rate ($/km) and arc distance). Analyses for SFW and LFW drones are presented separately with the assessment on each of the key parameters.

Considering the computational challenges of the model, I conduct the sensitivity analysis on the Malampa Province of Vanuatu. Malampa is chosen because it is a medium sized province, relatively close to the depot, and also it has enough airports and nodes to provide representative and interesting solutions. Malampa consists of 12 health zones on three islands: Malekula, the second largest island in Vanuatu, with 8 health zones, Ambrym, with 3 health zones and Paama, which is one health zone. Malampa includes 27 nodes, including five airports. The center of Malampa is about 180 km north of the national depot in Port Vila. I first ran the P1-C1 model with all the 27 nodes in Malampa, but it was slow and often produced solution gaps of 10% or more after several hours of CPU time. To finish all the instances for the sensitivity analysis in a reasonable time, I developed a reduced version of Malampa with 20 nodes, that includes 19 nodes in Malampa and the national depot (in Shefa Province), denoted node 0. The reduction of nodes was based on test runs that showed eight nodes were never used in solutions. These 8 nodes were removed: node 20, 21, 29, 31, 32, 100, 101, and 102 (see Figure 3.20). See detailed information about the nodes in Malampa in Table 3.2 and Table 3.12. The reasons to remove these eight nodes, besides the observation that they are never used in any solution from the testing runs, are as follows:

1. Nodes 20 and 21 are in the same health zone as node 19, but on small islands off the coast of the large island. Node 19 is a large airport and is a good site to use as the first node in Malampa to be reached from the depot. Thus node 19 is often the entry point into Malampa, and thus the DC for that health zone, so nodes 20 and 21 are not selected DCs and can be removed.
2. Node 29 is at the periphery of the province (in the far north), with two other nodes in its health zone that seem more likely to be selected as DCs.
3. Node 31 and node 101 are in the same peripheral health zone (farthest east), with nearby node 30 that is closer to the entry node 19. Further node 101 is a remote airport that provides no locational advantage as it is peripheral to the other nodes.
4. Node 32 is the northernmost node on Ambrym Island and very close to node 33 in the same health zone, so removing node 32 has very little impact as node 33 can be used for essentially the same cost.
5. Nodes 100 and 102 are small airports that are not likely to be used as they are not DC candidates, so could only serve as transshipment points.

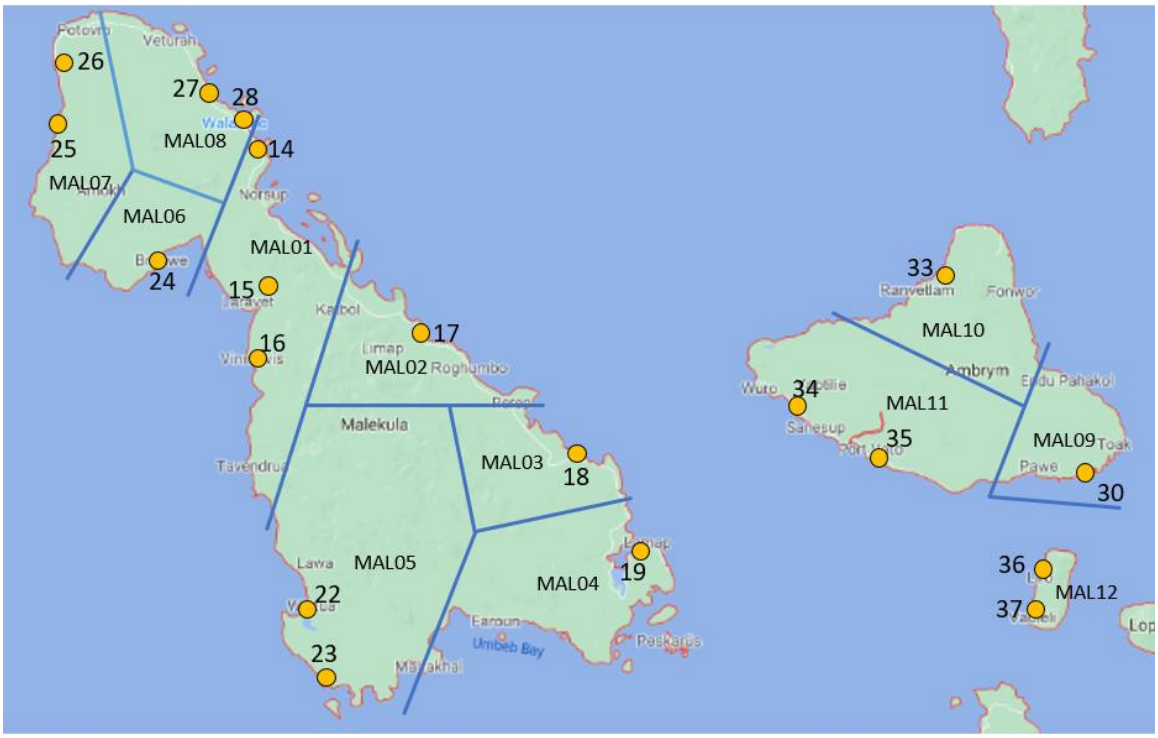

Figure 3.20 Malampa map with all nodes

3.8.1. Sensitivity analysis with SFW

For the SFW drone with model P1-C1, I designed a $3 \times 3 \times 3 \times 3$ experiment where each of the four key parameters have 3 levels, denoted low, medium, and high. The medium level is the baseline and the baseline values are as follows: (i) cold chain limit baseline = 2 hours, (ii) monthly demand baseline = values for Vanuatu (see Table 3.18); (iii) DB fixed cost baseline = \$6/month; (iv) RS fixed cost baseline = \$3/month. These values are designed to produce variation in the solutions across the low, medium (baseline) and high levels. Note that the baseline level of cold chain limit (2 hours) is smaller than typical values for vaccine cold chains, because vaccine distribution over a smaller geographic region is solved, and the shorter cold chain better allows the sensitivity of the model to be assessed. (In general, the vaccine cold chain may be 8 hours, as typical approved cold chain equipment is designed to that standard.) The low

and high levels for the cold chain limit are half of the baseline and twice the baseline, respectively. Thus, the low, medium, and high levels for the cold chain limit are chosen as 1 hour, 2 hours, and 4 hours.

For the level of demand, the baseline is the actual demand in each health zone in Malampa, which is shown in Table 3.17 (Ministry of Health Vanuatu, 2018). Table 3.17 lists the DC candidates, the island, the number of FIC (i.e., fully vaccinated children) and demand for each health zone on Malampa. Demand is calculated as the #FIC*0.05, which is discussed in detail in Section 3.4.1. The low and high demand levels are then selected as half of the baseline demand, and twice the baseline demand, respectively. The low, medium, and high levels of DB fixed cost are $0, $6, and $12 per month. The low, medium, and high levels of RS fixed cost are $0, $3, and $6 per month. The low level of $0 is selected as the extreme case with no cost to allow the model to use the largest number of DB and RS (given there is no cost penalty for adding a DB or RS). Recall though that any DB or RS are the endpoints of a drone arc, and drone arcs incur both a transportation cost and a fixed cost. The high levels for DB and RS costs are selected to be at a magnitude that will likely cause fewer of those facilities to be used.

Health zone	DC candidates	Island	#FIC	Demand in liter (d_h)
MAL01	14,15,16	Malekula	211	11
MAL02	17		100	5
MAL03	18		38	2
MAL04	19		118	6
MAL05	22,23		84	4
MAL06	24		85	4
MAL07	25,26		66	3
MAL08	27,28		152	8
MAL09	30	Ambrym	102	5
MAL10	33		110	6
MAL11	34,35		41	2
MAL12	36,37	Paama	29	1

Table 3.17 Health zone monthly demand in Malampa

Level	Cold Chain Limit	Demand	DB Cost	RS Cost
L: Low	1 hr	0.5*baseline	$0	$0
M: Medium (baseline)	2 hrs	baseline (in Table 3.20)	$6	$3
H: High	4 hrs	2*baseline	$12	$6

Table 3.18 Parameter values for sensitivity analysis with SFW drones

Because all transportation arcs in the model must obey the cold chain limitation, the number of arcs is different when the cold chain limitation is different. Table 3.19 lists the number of arcs by mode with the three levels of cold chain limit for the SFW drone. Because the arcs determine the number of variables and constraints in the MIP formulations, the size of the problem and the difficulty of solution are affected by the

cold chain limitation. Table 3.20 shows the number of decision variables and constraints in P1 based on the cold chain limitation.

Cold Chain	# Instances	#Airplane Arcs	#Boat Arcs	#Truck Arcs	#Drone Arcs	Sum
1 hr	27	6	28	22	188	244
2 hrs	27	7	74	24	330	435
4 hrs	27	7	186	24	336	553

Table 3.19 Number of arcs by mode in P1

Cold Chain	Number of Decision Variables	Number of Constraints
1 hr	5634	11130
2 hrs	9140	17997
4 hrs	9508	18397

Table 3.20 Number of decision variables and constraints in P1-C1 for Sensitivity Analysis with SFW drones

All 81 instances use $N = 11$ drone paths with $\Omega = 4$ drone arcs allowed per drone path. These values were selected because there are 12 health zones in Malampa, and all solutions use a plane from the national depot (node 0) to node 19, with node 19 always selected as the DC for health zone MAL04. This leaves 11 other health zones to be served in Malampa; thus there would be at most 11 drone paths from node 19 to serve the 11 health zones. The maximum number of drone arcs per path was selected as 4 to allow some complexity in the drone paths while maintaining computational tractability.

A solution overview is presented in Section 3.8.1.1, and detailed solutions of a few interesting instances are illustrated in Section 3.8.1.2. Sections 3.8.1.3 and 3.8.1.4 present an analysis on DC selection and an analysis on vaccine path to a node, respectively. The sensitivity analysis of how the variation of the four key parameters

affect the drone usage and performance is presented in Sections 3.8.1.5 to 3.8.1.8. In these four sections, I examine how the variation of the four key parameters affects both the transportation cost and delivery time performance metrics. Besides these two most important performance metrics, one or more other metrics in each section based on the character of the key parameter in that section are examined.

3.8.1.1. Solution overview of SFW instances

The 81 instances for the sensitivity analysis with SFW drones were run on Gurobi 9.1 with a 2 hour CPU time limit using an HP Intel Quard-Core i7 with 3.9 Ghz CPU and 64 GB RAM. Of the 81 instances, 52 found optimal solutions (completed with a 0% gap) and the other 29 instances had gaps ranging from 0.01% to 7.25% after 2 hours, with 24 of the 29 instances having a gap smaller than 5%. Table 3.21 shows the 5 instances with a gap that is larger than 5%. We see it includes a range of levels for the parameters, but not high demand and not low DB cost. Notice that row 2 and row 5 differ only in the level of RS cost, and row 2 and row 4 differ only in the level of demand. Any other row pairs have greater differences in the parameter settings. Note that a non-zero gap does not by itself mean that the optimal solution has not been found, just that it is not proven optimal.

Gap	Cold Chain	Demand	DB cost	RS cost
7.25%	H	M	M	H
6.54%	L	L	H	L
5.89%	M	L	H	H
5.75%	L	M	H	L
5.61%	L	L	H	M

Table 3.21 Instances with large gaps

There are 49 unique network configurations among the 81 solutions (including the solutions with non-zero gaps), which means some instances generate the same network configuration (i.e., the same set of arcs with the same modes that connect to the same nodes). Solutions with the same configuration do not necessarily have the same objective function value (i.e., the total transportation cost), because the vaccine flows on the arcs can differ with the different levels of demand, and the fixed costs for DBs and RSs may differ as well. Networks with the same configuration can have proportional flows on the arcs. For example, arcs 1-2 and 2-3 in solution A could have flows of 4 liters and 5 liters, respectively, while these same arcs in solution B could have flows of 2 liters and 2.5 liters, respectively. To distinguish the different solutions, each is represented with a unique identifier that includes the value of the four key parameters. For example, solution CC2_D2_DB0_RS0 has a 2 hour cold chain limit (CC2 = level M), 2 times the original demand in each health zone (D2 = level H), $0 for the DB fixed cost (DB0 = level L) and $0 for the RS fixed cost (RS0 = level L).

Figure 3.21 shows two solutions that have the same network configuration with different, but proportional, vaccine flows on arcs. Figure 3.21(a) shows the solution for CC1_D1_DB6_RS6, and Figure 3.21 (b) shows the solution for CC1_D0.5_DB12_RS6. Notice that both solutions are with a non-zero gap, which is denoted in parenthesis in the lower left corner. A non-zero gap of a solution in any of the following solution maps is denoted in the same manner. In each solution, the monthly flow in liters is shown in square brackets on each arc. Note that these solutions differ in both the demand level and the DB fixed cost. Because the demand of Figure 3.21(b) is half of the demand of Figure 3.21(a), all vaccine flows in Figure 3.21(b) are half of the vaccine flows in Figure

3.21(a). The two instances both have the same weighted average delivery time to a health zone of 2 hours and 54 minutes, but with a different transport cost to a health zone, due to the different levels of flow and the differing DB fixed costs. The average transport cost to a health zone in Figure 3.21(a) is $19.75/HZ, while Figure 3.21(b) has a cost of $19.67/HZ. Note that the drone cost model in P1-C1 calculating drone cost based on the vaccine flow volume on each drone arc, so the cost for drone travel is twice as large in CC1_D1_DB6_RS6 as in CC1_D0.5_DB12_RS6, since demand is twice as large. However, the travel costs for other modes (boat and plane) do not depend on the level of demand (those modes have a large capacity, so the travel cost is per arc traversal, and not based on flows). To give a general scale of the cost and service of the 81 solutions, the average transport cost is $16.91/HZ with a range of $12.62/HZ to $22.59/HZ, and the weighted average delivery time is 2 hour 31 minutes, with a range of 1 hour 32 minutes to 3 hours 39 minutes.

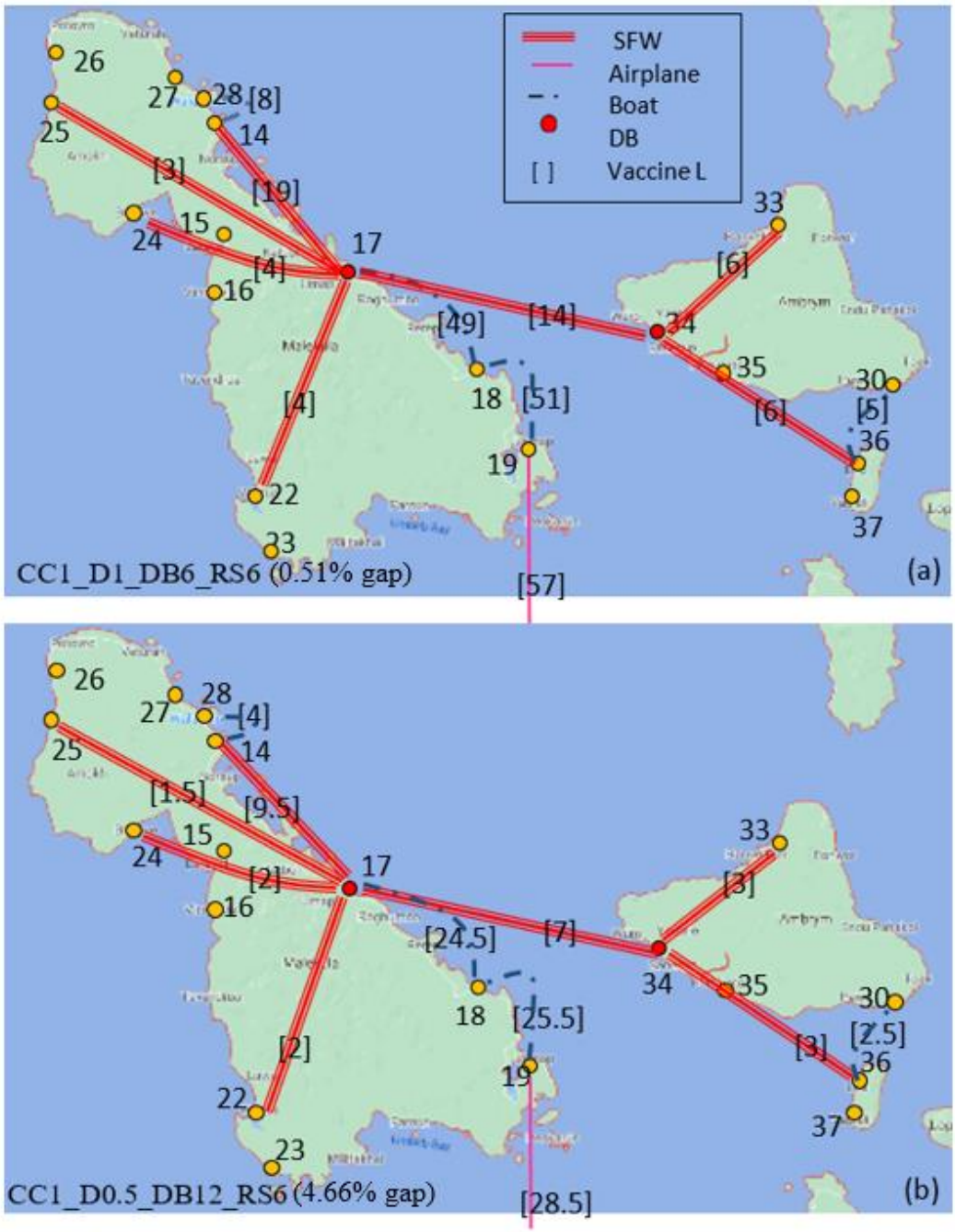

Figure 3.21 Example of solutions with the same network configuration

3.8.1.2. Solution illustration

Table 3.22 and Table 3.23 shows the summary of some important network features of the nodes and arcs in the 81 solutions. This section illustrates several of these solutions. Table 3.22 shows that all solutions use the same plane arc from the depot to

node 19 to bring all the vaccines for Malampa into the province. It also shows that truck arcs are used relatively rarely (in 6/81 solutions) and this is always for arc 14-24 to cross Malekula Island. In contrast, there is a wide range in the number of boat and drone arcs used in solutions, from none to 11.

Mode	Number of Arcs	Number of Solutions
Airplane	1	81
Boat	0	9
	2	21
	3	12
	4	15
	5	12
	7	4
	8	2
	10	3
	11	3
Truck	0	75
	1	6
Drone	0	6
	3	2
	4	4
	6	8
	7	15
	8	12
	9	17
	10	8
	11	9

Table 3.22 Summary of arc use in 81 SFW P1-C1 solutions

Characteristic	Number	Number of Solutions
Maximum number of drone arcs per path	0	6
	1	75
	2	37
	3	6
	4	3
Number of DB	0	6
	1	40
	2	32
	3	3
Number of RS	0	6
	4	2
	5	4
	7	6
	8	12
	9	9
	10	15
	11	217
	12	10

Table 3.23 Summary of drone paths in 81 SFW P1-C1 solutions

Figure 3.22 shows the percentage that each arc is used in the solutions of the 81 instances, for the 58 most frequently used arcs. There are in total 995 arcs used in the 81 solutions, so on average there are 12-13 arcs per solution. Among the 995 arcs, 603 arcs are drone arcs, 305 are boat arcs, 81 are airplane arcs, and 6 are truck arcs. Using Table 3.19 which shows the number of arcs in the input data for the 81 instances, 15% (81/540) of the available airplane arcs are used, 4% (305/7776) of the available boat arcs are used, 0.32% (6/1890) of the available truck arcs are used, and 3% (603/23,058) of the available SFW drone arcs are used. In total, 3% (995/33,264) of the available arcs are used in a

solution. Figure 3.22 shows that arc 0-19 is selected in all solutions, and is always traveled by plane. Arc 19-18 is also used in 100% of solutions, being traveled by boat in 86% of the solutions, and by drone in 14% of solutions. From Figure 3.22 we see that most arcs are dominated by one mode. For example, boat is the dominant mode for arcs 19-18, 18-17, 14-28, 17-14, 36-30, 24-25, 30-36, etc., while drone is the dominant mode for the majority of arcs. Interestingly, arc 36-30 is the 14^{th} most commonly used arc (in 22 solutions and always boat), while the opposite arc 30-36 is used in 5 solutions (always by boat). The model used a small set of arcs repetitively as the top 11 arcs in Figure 3.22 (i.e., from arc 0-19 to arc 17-22) take less than 5% of the available arcs in any input data set (see the "Sum" column in Table 3.19), but are each used in more than 45% of solutions.

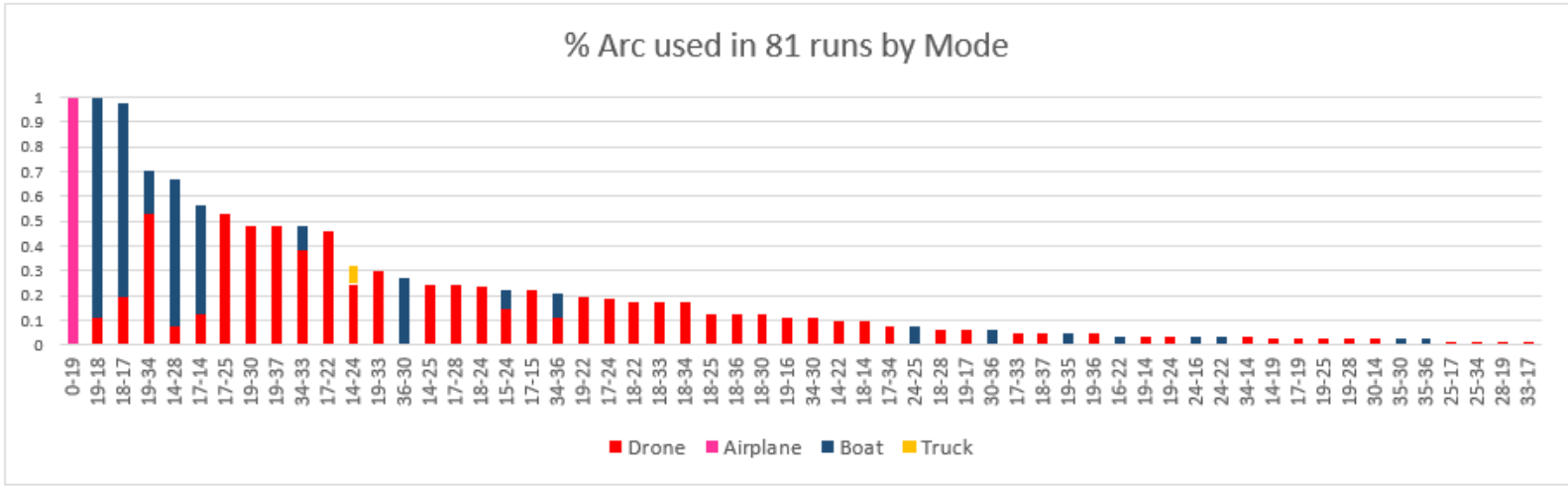

Figure 3.22 Percentage arc use by mode in the SFW study

Table 3.23 shows the maximum number of drone arcs per path, and the number of DBs and RSs in solutions. There are six solutions that do not use a DB or RS, which means these instances do not use drones, and Figure 3.23 shows the solution map of one of these solutions. (These six solutions share two network configurations; one uses 24-22 by boat, and the other uses 24-16-22 by boat as shown in Figure 3.23.) Table 3.24 shows the parameter levels for these six instances. We see that all six instances are with high RS cost and high or medium levels of the cold chain limit, demand, and DB cost. In these instances, the high fixed costs for DB and RS discourage the use of drones, as does the higher levels of demand (since SFW drones have a low payload). Also, the higher levels of the cold chain limit (longer time allowed) allow the use of boat transportation. For these six instances, the transportation costs are all on the expensive side compared to the average cost of the 81 instances (i.e., $16.91/HZ), and the service time is also on the slow side compared to the average time of the 81 instances (i.e., 2 hour and 31 minutes).

Cold Chain	Demand	DB cost	RS cost	$/HZ	Hr/HZ
M	H	M	H	$19.04	3h 28m
M	M	H	H	$19.04	3h 28m
M	H	H	H	$19.04	3h 39m
H	H	M	H	$18.99	3h 27m
H	M	H	H	$18.99	3h 27m
H	H	H	H	$18.99	3h 27m

Table 3.24 Instances that do not use drones in the 81 SFW solutions

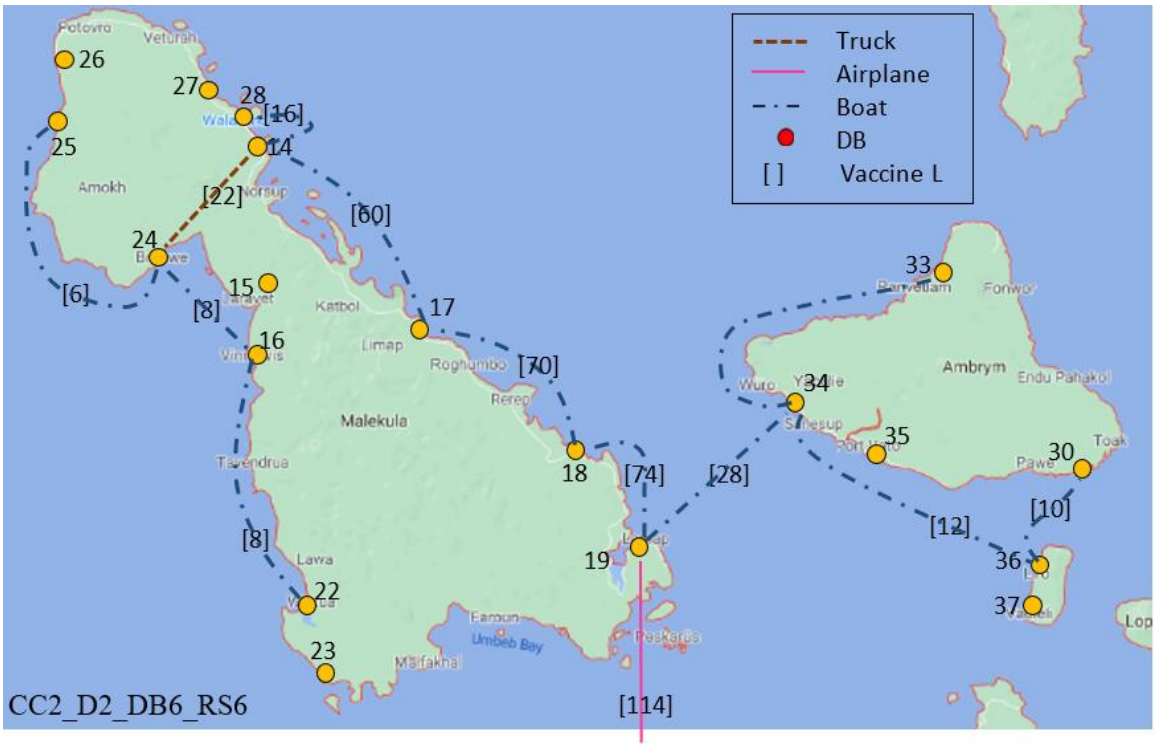

Figure 3.23 Solution map of an instance not using drones and with a truck arc

Figure 3.24 shows the map of a solution when the largest number of DBs are open. Here, there are three DBs open, because of the low level of DB cost. Notice that it took two SFW flights on the same arc to deliver the 16 liters of vaccine from node 14 to node 28 (since drone capacity is 10 liters). Similarly, drone arcs 19-34 and 19-33 require two flights. This solution has a cost of $15/HZ and the average weighted delivery time to a health zone is 2 hour and 40 minutes/HZ.

Figure 3.25 shows a solution that used the maximum of four drone arcs in a path and an empty drone arc. There is one DB at node 17, and all drone paths start from there. The longest drone path is 17-28-19-34-33 with 4 drone arcs and an empty drone arc on 28-19 to allow the drone to be repositioned to node 19, where it can pick up vaccine delivered there by the plane from node 0. The empty drone arc is created to avoid opening a second expensive DB. Also, note that with the P1-C1 model, using an empty

drone arc costs nothing, as the cost model is based on the flow carried. Thus, this solution uses an empty drone arc free of charge, with inexpensive relay stations (since the RS fixed cost = $0) to allow delivery by drone to more nodes. Also, note that the long drone path is allowed by the long cold chain limit in this solution (CC4 indicates a 4 hour cold chain). The average transportation cost to serve a health zone is $14.88, and the weighted average delivery time is 2 hour and 17 minutes for this solution.

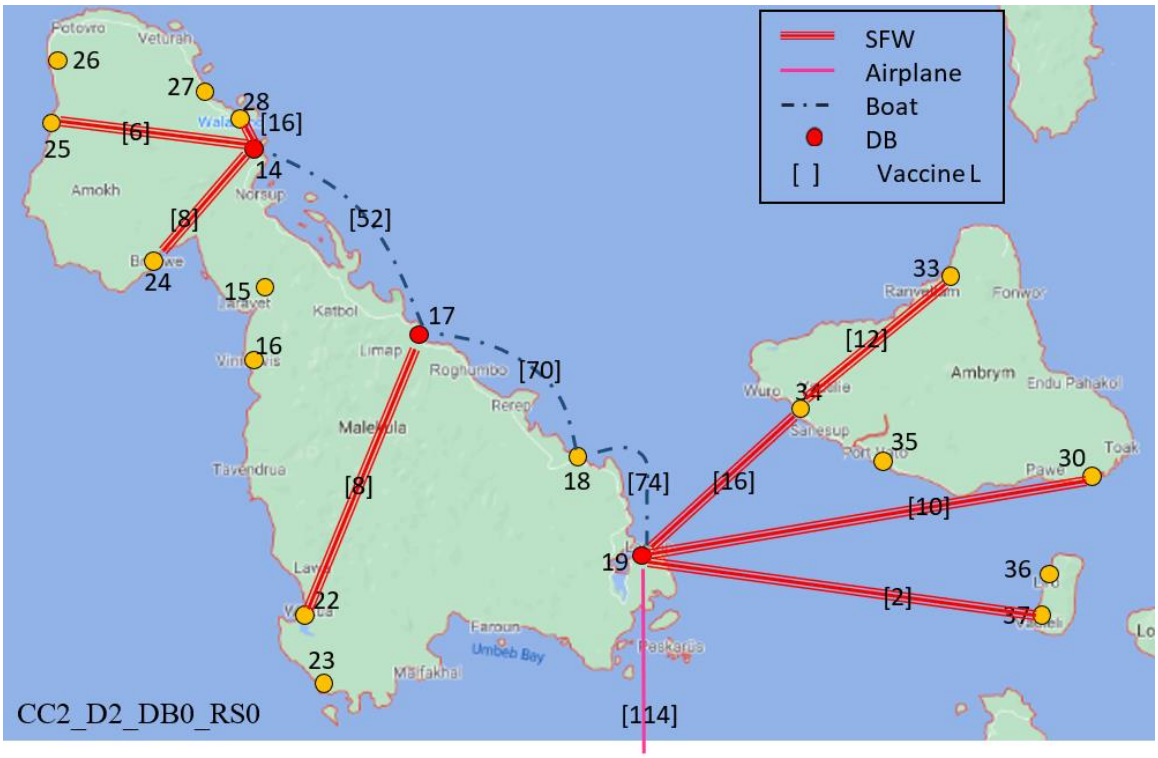

Figure 3.24 Solution map of an instance with three open DBs

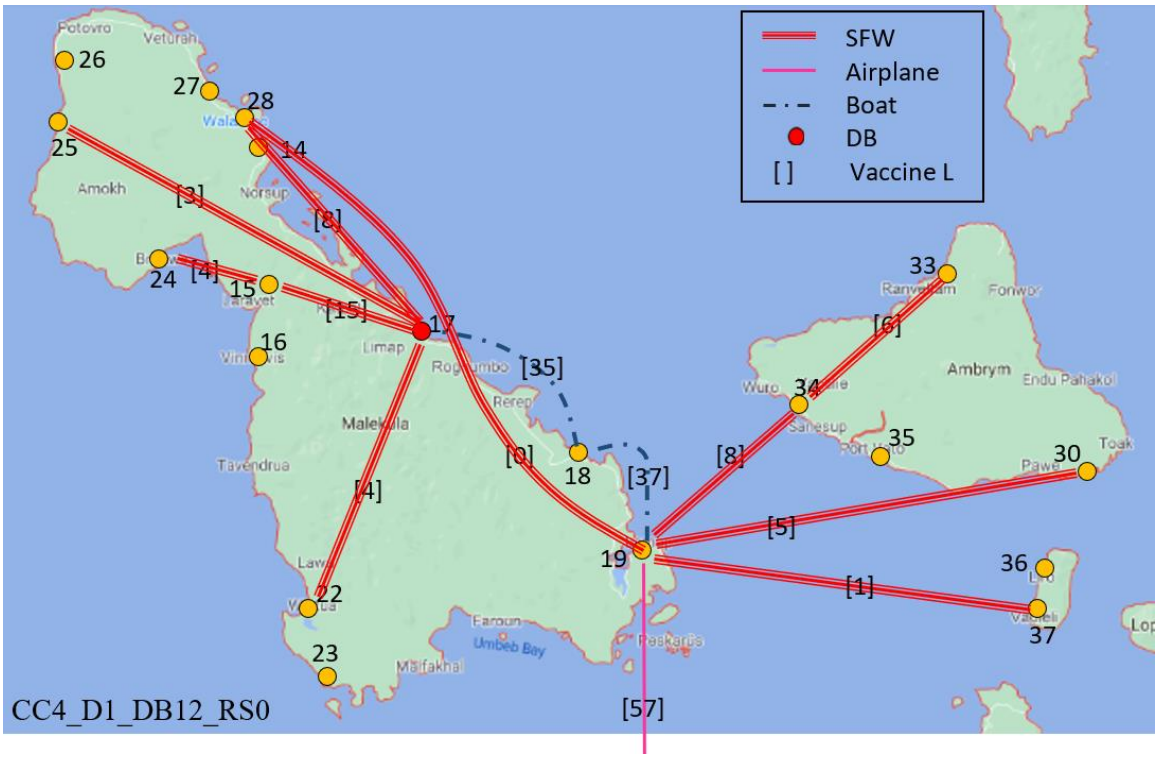

Figure 3.25 Solution of an instance with maximum 4 drone steps and an empty drone arc

Cold Chain	Demand	DB cost	RS cost	$/HZ	Hr/HZ
H	H	H	L	16.07	2h 40m
M	H	H	L	16.07	2h 40m
H	H	M	L	15.57	2h 40m
M	H	M	L	15.57	2h 40m

Table 3.25 Instances with 2 empty drone arcs

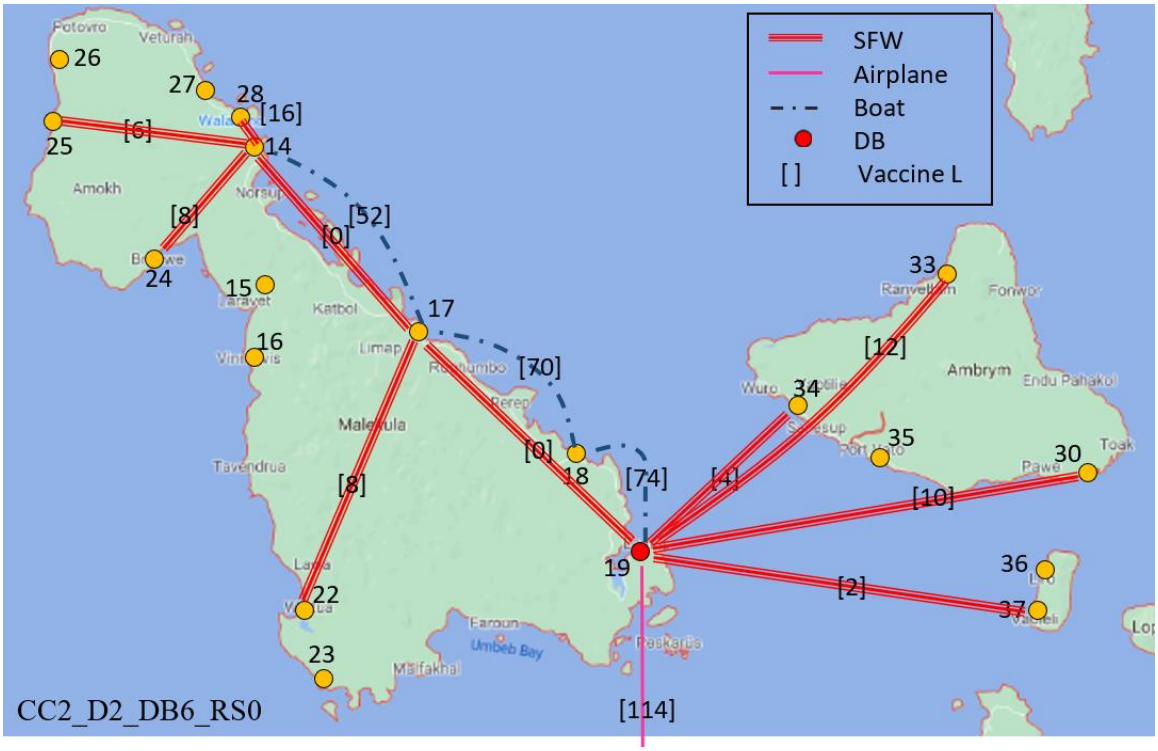

Figure 3.26 Solution map of an instance with 2 empty drone arcs that are connected

Table 3.25 shows the four solutions that used two empty drone arcs. All these solutions were with the high level of demand, low level of RS cost, high or medium level of DB cost and high or medium level for the cold chain limitation. Figure 3.26 shows the solution of an instance with two empty drone arcs (from 19 to 17, and from 17 to 14) that are consecutive. Comparing Figure 3.26 to Figure 3.24 shows the impact of the fixed costs for DB and RS, as both have the same levels of demand and the same cold chain limit. Both figures have the same or very similar drone use, except for the empty drone flights in Figure 3.26 that allow drones to be repositioned from a single DB, rather than needing to open new DBs. Thus, Figure 3.26 shows only one DB, versus three DBs in Figure 3.24 (where DB and RS costs are $0). Figure 3.27 shows another solution where there are two empty drone arcs (from 33 to 17, and from 30 to 14), but in this case they are not connected. In this solution, a drone carries 10 liters of vaccine from node 19 to

node 30, and then flies empty to node 14, where it loads vaccines that were delivered there by boat from node 17, and the drone then delivers from node 14 to nodes 24, 25, and 28. These examples described above indicate some of the complexity of the drone network configurations and show how those configurations depend on the parameter values.

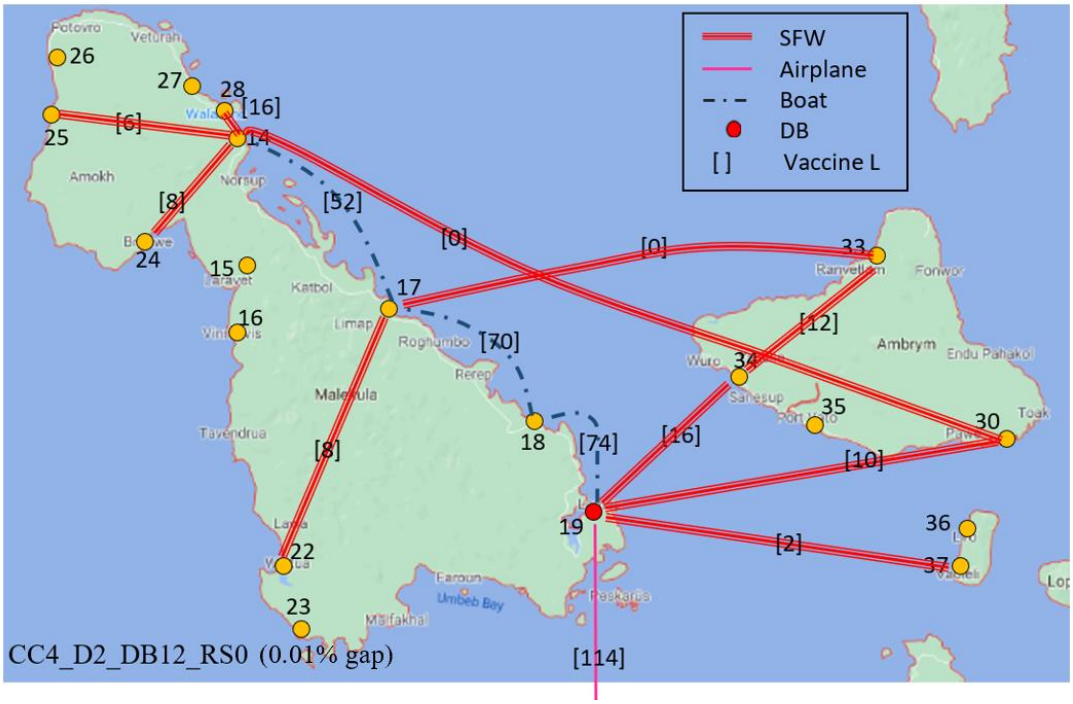

Figure 3.27 Solution map of an instance with 2 empty drone arcs not connected

3.8.1.3 DC selection analysis

Figure 3.28 show the percentage of times that each DC candidate is selected among the 81 solutions. Six health zones only have one DC candidate, so that DC candidate is always selected as the DC. In three health zones (MAL05, MAL07, and MAL08) there are two DC candidates, but the same one is selected in every solution (which are nodes 22, 25, and 28). Not surprisingly, these selected nodes are those in the health zone closest to node 19, where the vaccine arrives in the province. In three other

health zones (MAL1, MAL11, MAL12) there are two or three DC candidates, and two or more are selected as DCs in different solutions. In MAL01 and MAL11, two DC candidates, node 14 and node 34, are selected most of the time. MAL01 is an interesting health zone as it includes three DC candidates with node 14 on the east coast of Malekula and nodes 15 and 16 on the west coast. Because vaccines arrive in Malampa at node 19 (by plane) on the east coast, node 14 is often a DC that receives boat shipments of vaccines coming from node 19 (via nodes 18 and 17). However, in solutions where vaccines are delivered by drone to the northern part of Malekula (e.g., see Figure 3.25) node 14 is not a DC as vaccines can be sent by drone at lower cost (shorter flight) direct to node 15 or 16. In MAL11, node 34 is almost always selected as the DC as it is closer to nodes 17, 18, and 19, which are the nodes that vaccines have to pass through in all solutions to be distributed to the farther health zones. In MAL12, the DC is nearly evenly split between nodes 36 and 37 (in the southeast of Malampa) in the solutions because changing the drone base (e.g., from node 19 in Figure. 3.34 to node 18 in Figure 3.35) changes which of nodes 36 and 37 are closer to the drone base, and therefore selected.

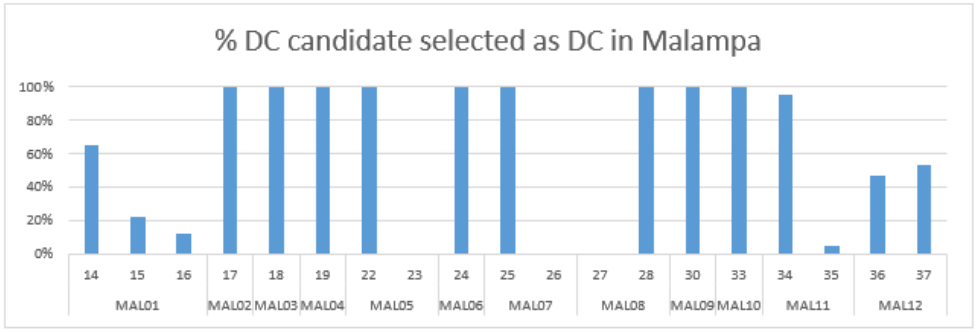

Figure 3.28 Percentages that each DC candidate is selected as a DC in Malampa

In the 81 instances, all DC candidates have the same fixed cost, so in these instances the location of a DC candidate (and the corresponding distances) determines

whether it is selected, as the model optimizes the cost based on arc distance to the DC. Thus, the results above about how often a DC candidate is selected may not represent solutions when DC candidates have different fixed costs, as the fixed costs could certainly influence the location of the DCs. More analysis would be needed to refine our initial assessment about reasons for DC locations.

3.8.1.4. Vaccine path analysis

In this section, the different ways that vaccines may be delivered to a DC in different solutions are illustrated. Note that some DCs may be reached by the same path in all 81 solutions, like 0-19 by plane for the DC at node 19. However, other DCs are reached by a wide variety of different paths. To illustrate this, I examine the vaccine paths in all 81 solutions to node 24. Table 3.26 shows there are 9 different vaccine paths to reach node 24 among the 81 solutions. The path can be traced by moving left to right across Table 3.26. Thus, all paths begin 0-19 by airplane, but then there are different arcs selected for the next step of the path (e.g., boat for 19-18, SFW drone for 19-18, or SFW drone for 19-24). The next-to-last column provides a path ID, and the last column "# Solutions" shows the count of solutions for each of the nine different vaccine paths.

<table>
<tr><th colspan="6">Vaccine path to node 24</th><th>Path ID</th><th># Solutions</th></tr>
<tr><td rowspan="10">From node 0</td><td rowspan="10">Airplane to 19</td><td rowspan="5">Boat to 18</td><td rowspan="5">Boat to 17</td><td rowspan="2">Boat to 14</td><td>SFW to 24</td><td>1</td><td>20</td></tr>
<tr><td>Truck to 24</td><td>2</td><td>6</td></tr>
<tr><td rowspan="2">SFW to 15</td><td>Boat to 24</td><td>3</td><td>6</td></tr>
<tr><td>SFW to 24</td><td>4</td><td>12</td></tr>
<tr><td rowspan="2">SFW to 24</td><td></td><td>5</td><td>13</td></tr>
<tr><td rowspan="2">SFW to 18</td><td rowspan="2">SFW to 17</td><td></td><td>6</td><td>2</td></tr>
<tr><td rowspan="3">SFW to 24</td><td></td><td>7</td><td>5</td></tr>
<tr><td>Boat to 18</td><td></td><td></td><td>8</td><td>14</td></tr>
<tr><td>SFW to 24</td><td></td><td></td><td></td><td>9</td><td>3</td></tr>
</table>

Table 3.26 Vaccine paths to node 24 in 81 SFW instances

Figure 3.29 illustrates the solution for path 1 in Table 3.26. There are 20 instances with this same vaccine path to node 24, including instances illustrated previously in Figure 3.24 (i.e., CC2_D2_DB0_RS0), Figure 3.26 (i.e., CC2_D2_DB6_RS0), and Figure 3.27 (i.e., CC4_D2_DB12_RS0). It is worth clarifying that the drone path to a node and the vaccine path to a node can be different. For example, in Figure 3.27 the drone path to node 24 is 19-30-14-24, while the vaccine path to node 24 is 0-19-18-17-14-24. Figure 3.29 illustrates vaccine path 2 (with boat and truck, but no drone arcs) to node 24. Figure 3.30 shows a solution with vaccine path 3 to node 24. There are six instances that used this same vaccine path, and all of these are with the low cold chain limitation and high demand. Note that this path uses boat arcs both before and after the drone arc from 17 to 15.

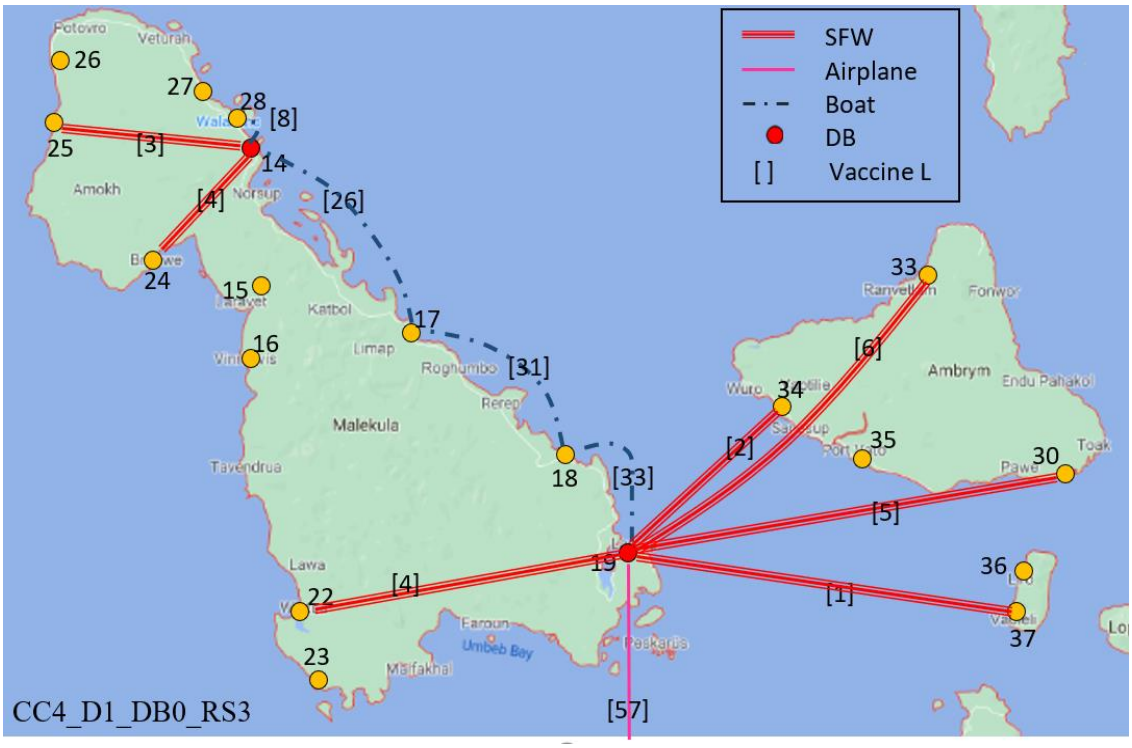

Figure 3.29 Solution map to illustrate path 1 to node 24

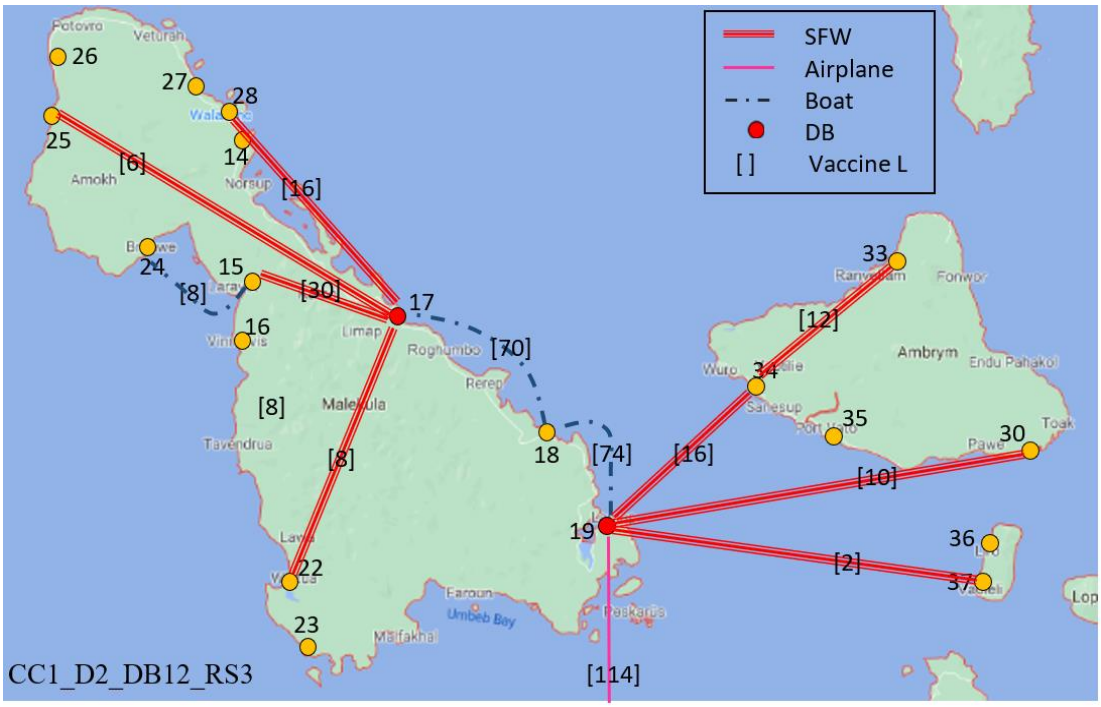

Figure 3.30 Solution map to illustrate path 3 to node 24

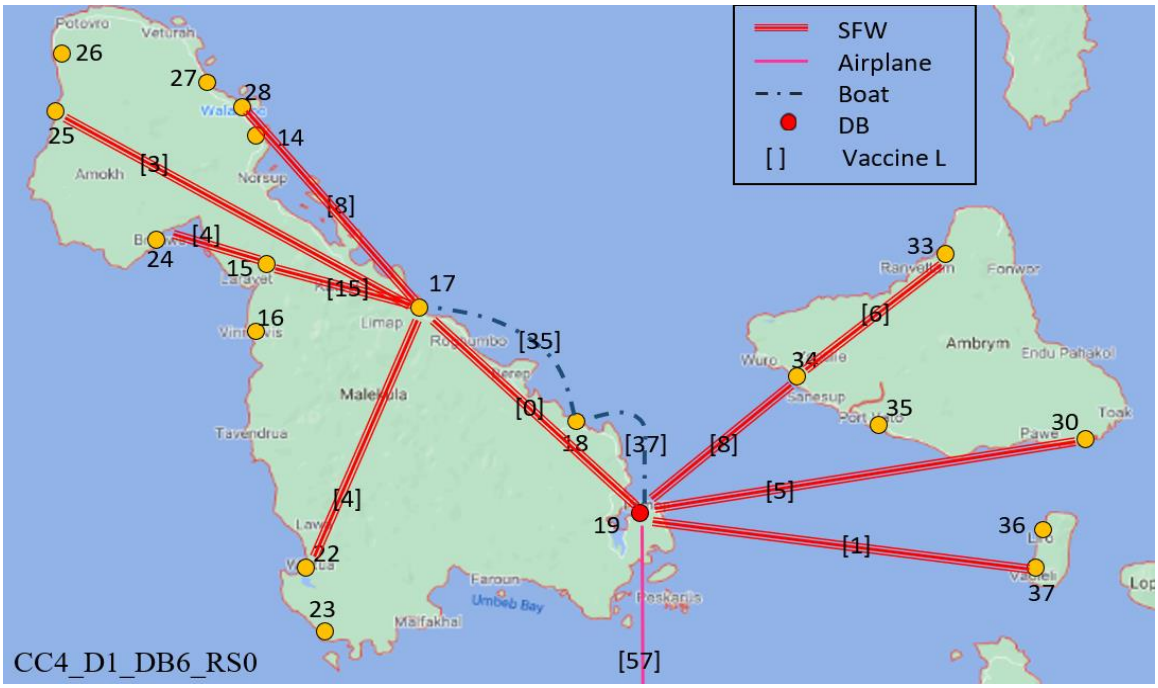

Figure 3.31 Solution map to illustrate path 4 to node 24

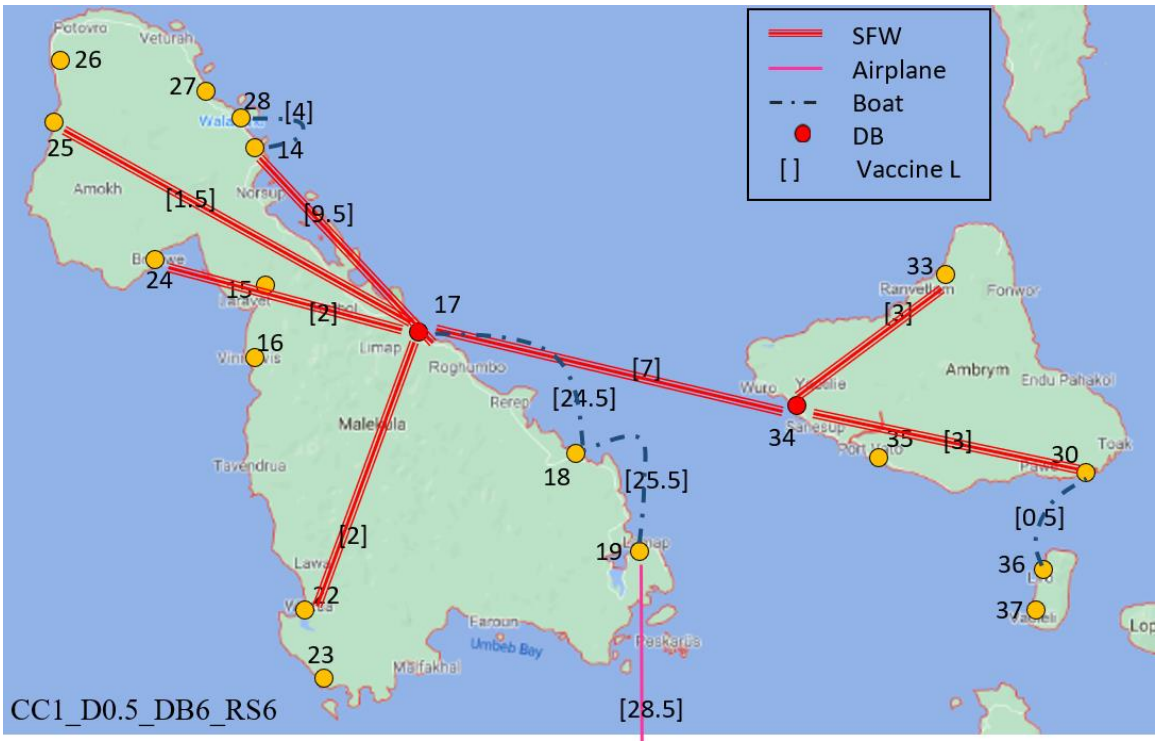

Figure 3.32 Solution map to illustrate path 5 to node 24

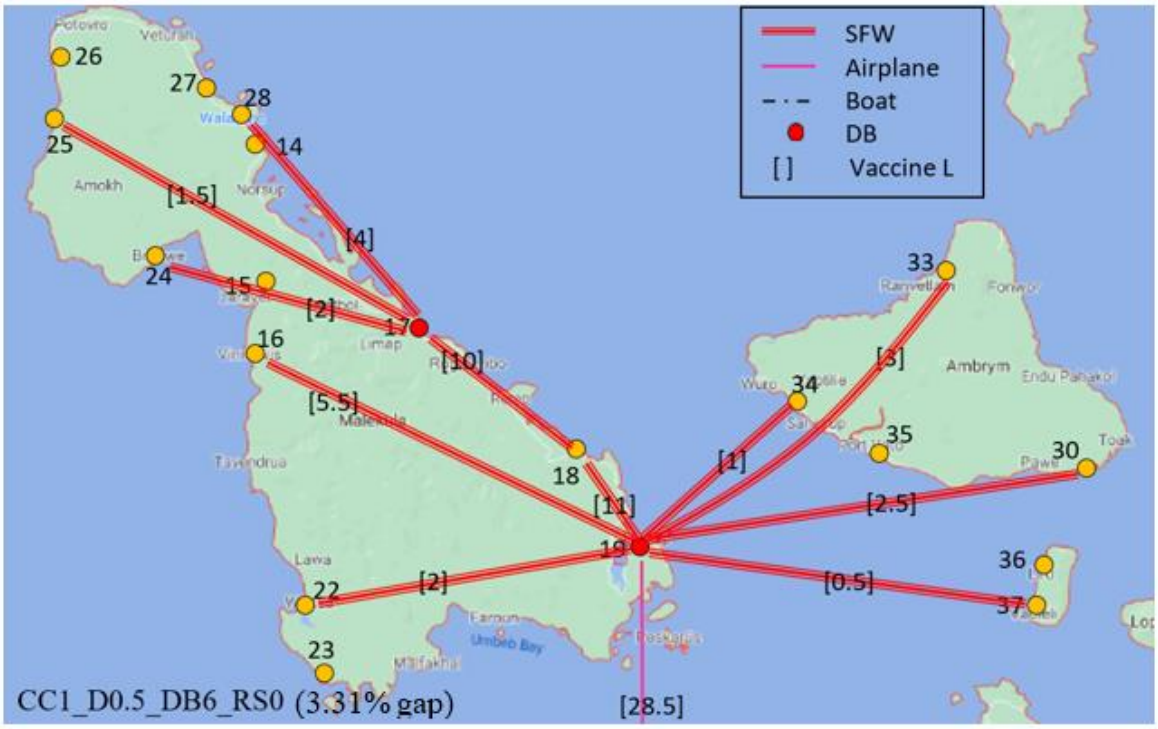

Figure 3.33 Solution map to illustrate path 6 to node 24

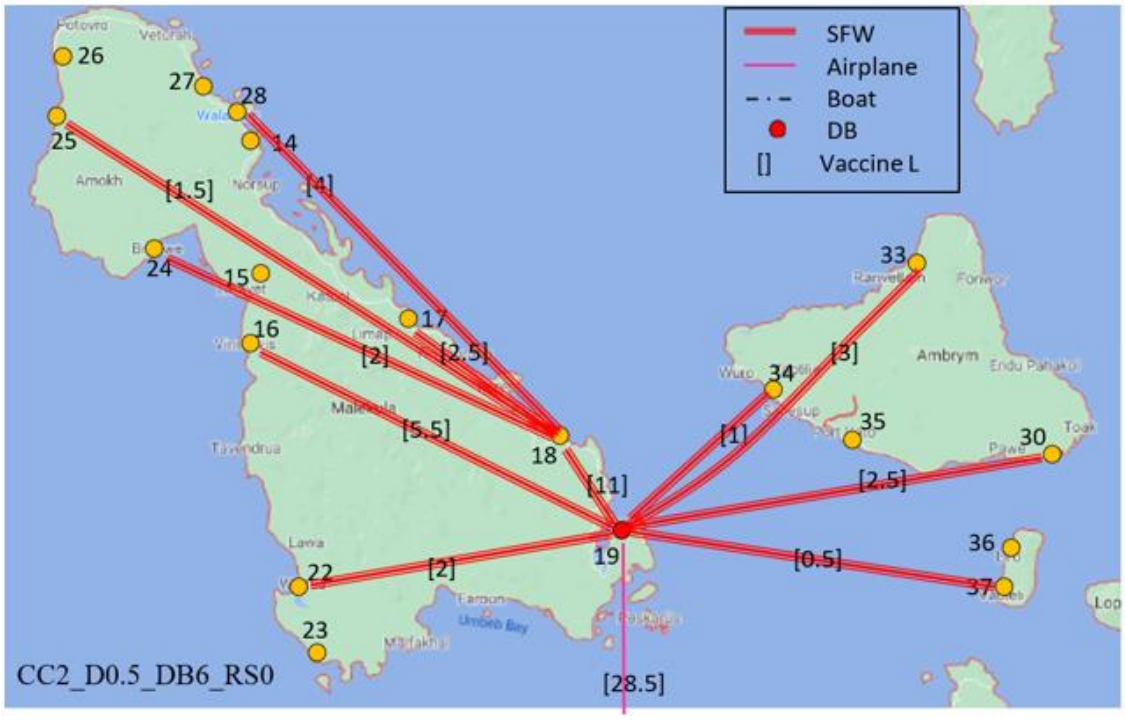

Figure 3.34 Solution map to illustrate path 7 to node 24

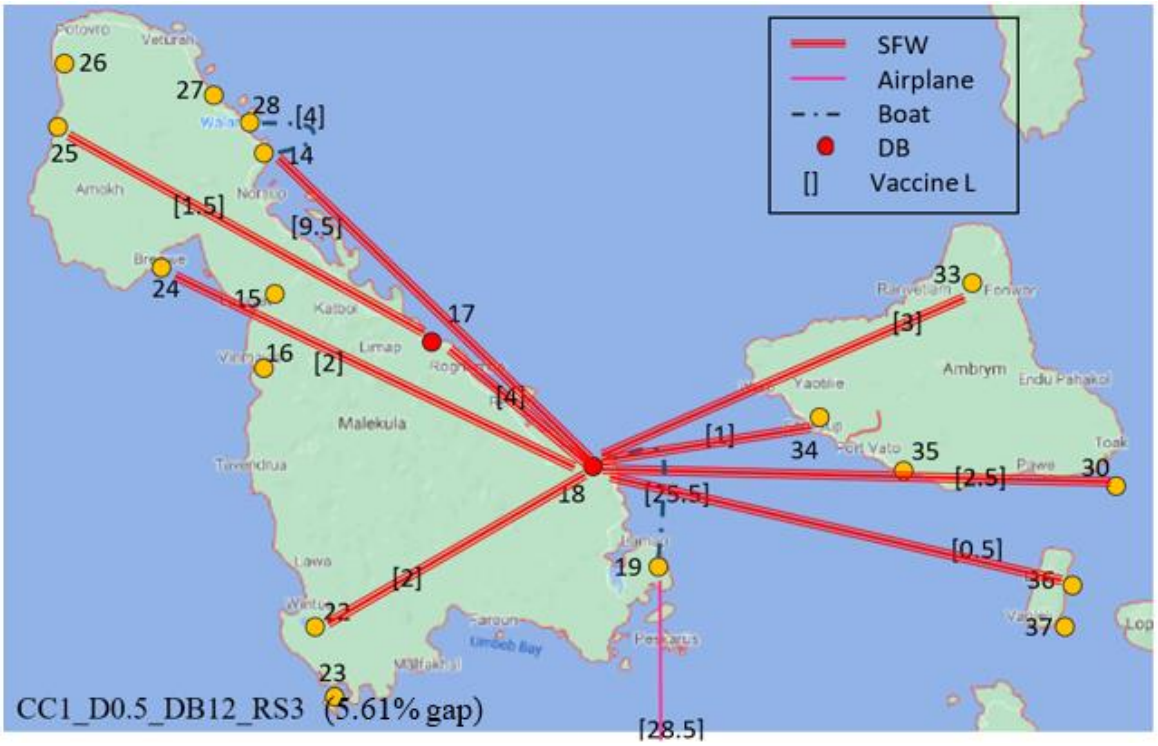

Figure 3.35 Solution map to illustrate path 8 to node 24

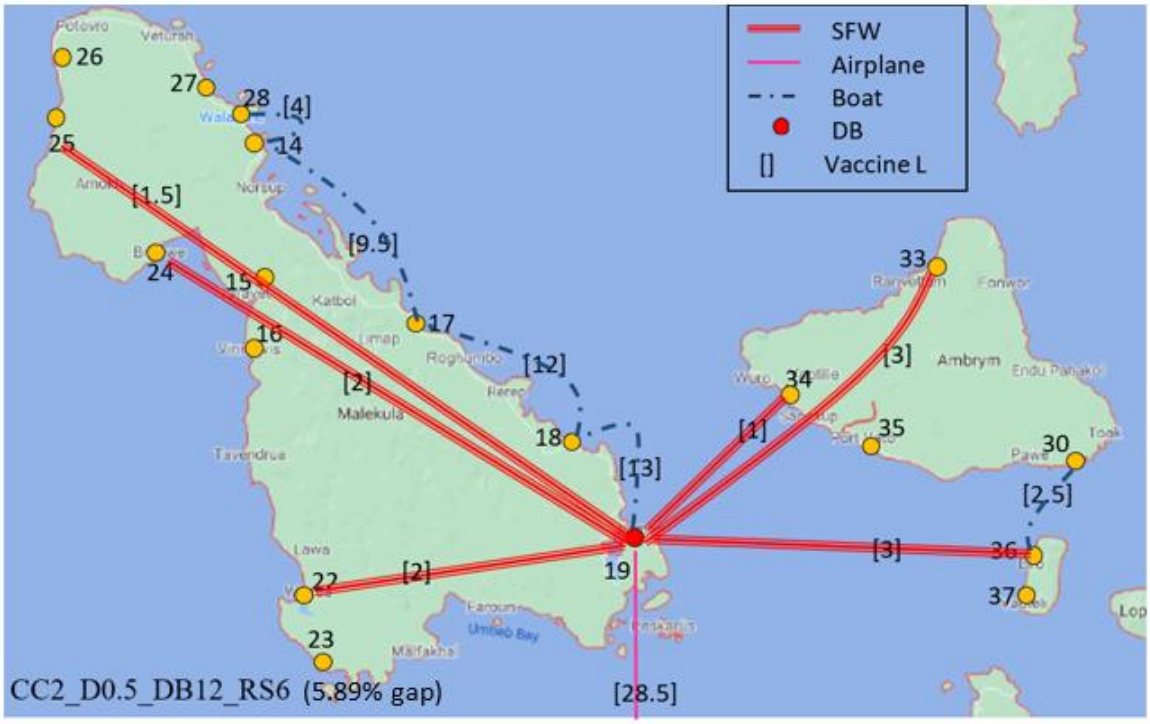

Figure 3.36 Solution map to illustrate path 9 to node 24

Figure 3.31 illustrates the solution of an instance with vaccine path 4 to node 24. There are 12 instances with this same vaccine path to node 24 and all these instances are with the low level of RS cost. Figure 3.25 (i.e., CC4_D1_DB12_RS0) also shows a instance with the same vaccine path to node 24. Note the different use of zero flow drone arcs in these solutions (Figure 3.25 and Figure 3.31) for the same path to node 24. Figure 3.32 illustrates the solution with vaccine path 5 to node 24, which uses airplane, then boat then drone. Figure 3.33 illustrates the solution for vaccine path 6 to node 24. This includes a three arc drone path, and both of the solutions that used vaccine path 6 have a low level for the RS cost, demand and cold chain limitation. Figure 3.34 illustrates the solution with vaccine path 7 to node 24. All 5 instances that used vaccine path 7 are with low levels of RS cost and demand. Figure 3.33 and Figure 3.34 are quite similar, but node 17 is a DB in Figure 3.33 due to the shorter cold chain limitation. Figure 3.35 illustrates the solution with vaccine path 8 to node 24. Here node 18 is the drone base rather than node 19, 17 or 14 in the other figures. All of the 14 solutions with vaccine path 8 are with the low level of demand. Figure 3.36 illustrates the solution with vaccine path 9 to node 24. This solution has a two-arc path 0-19-24. All 3 instances with vaccine path 9 are with the low level of demand.

There are similarities among the various vaccine paths to node 24. Except for 3 instances, all the other 78 solutions used arc 19-18; but 7 of these were by drone, and 71 were by boat. There are 59 solutions that used arc 18-17, but 2 of the 59 solutions were by drone, and the other 57 were by boat. There were 26 solutions that used 17-14 by boat, 18 solutions used 17-15 by drone, and 15 solutions used 17-24 by drone. Note also that node 24 is reached by several different nodes in the various paths. Node 24 is reached

from node 14 in 26 solutions, from node 15 in 18 solutions, from node 17 in 15 solutions, from node 18 in 19 solutions, and from node 19 in 3 solutions. The general trend is that solutions with low levels of demand, RS cost, DB cost and the cold chain limit tend to reach node 24 more frequently by drone.

3.8.1.5 Cold chain analysis

This section investigates how changing the cold chain time limit affects drone usage and performance. Figure 3.37 shows a histogram of the percentage changes of transportation cost resulting from changes of the cold chain limit.

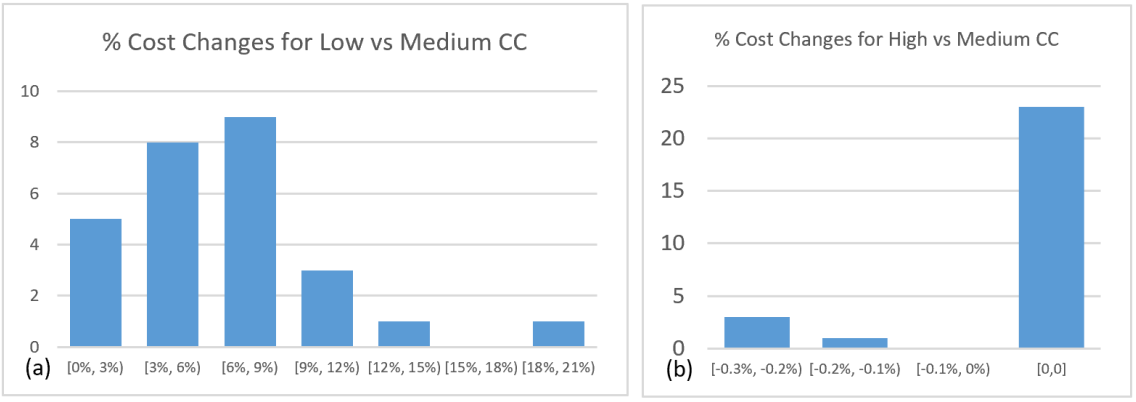

Figure 3.37 Percentage cost changes due to changes of the cold chain with SFW drones

Figure 3.37(a) shows the frequency that the percentage cost changes are in different ranges for the 27 solutions with a low cold chain limit (1 hour) compared to the 27 corresponding solutions with the baseline cold chain limit (2 hours). Figure 3.37(b) is a similar histogram but comparing the high cold chain limit (4 hours) to the corresponding solutions with the baseline cold chain limit (2 hours). For example, the first bar of Figure 3.37(a) shows that 5 of the 27 paired solutions with a low CC limit had a cost increase in the range of 0%-3%. The second bar of Figure 3.37(a) shows that 8 of the 27 paired solutions with a low CC limit had a cost increase in the range of 3%-6%.

Thus, the left histogram in Figure 3.37 shows the frequency of the percentage cost changes when the cold chain limit is decreased from the baseline medium level, while the right histogram shows the frequency of the percentage cost changes when the cold chain limit is increased from the baseline medium level. Figure 3.37(a) shows that the transportation cost increased in all cases when the cold chain limit decreased. The average percentage change among these solutions is 5.9% (the median is 6.0%) and the range is from 0% to 18.6%. Figure 3.37(b) shows that increasing the cold chain limit from 2 hours to 4 hours had little effect on the transportation cost, as in 23 of the 27 paired instances the cost did not change with the longer cold chain limit. In the other four paired instances, the transportation cost decreased slightly (less than 0.3%) with the longer cold chain limitation. The average percentage change of the transportation cost with the longer cold chain limit is -0.03% (median is 0), with a range from -0.26% to 0%.

Figure 3.38 uses a similar format to Figure 3.37 to examine the impact of changing the cold chain time limit on the average delivery time. Figure 3.38 (a) shows that the delivery time mostly decreased in the paired comparisons when the cold chain was reduced from 2 hours to 1 hour. The average delivery time decreased 14.48% (median of -12.7%), and the range is -42.36% to 5.38%. Figure 3.38 (b) shows that the delivery time mostly increased when the cold chain increased from 2 hours to 4 hours. The average delivery time increased 1.8% (median of 0%), and the range is -3.8% to 12.3%. Recall that the objective function is to minimize the total transportation cost, so the model does not guarantee to optimize any other performance metrics, such as the delivery time. Thus, the average delivery time may not always decrease (increase) when the cold chain limit is decreased (increased).

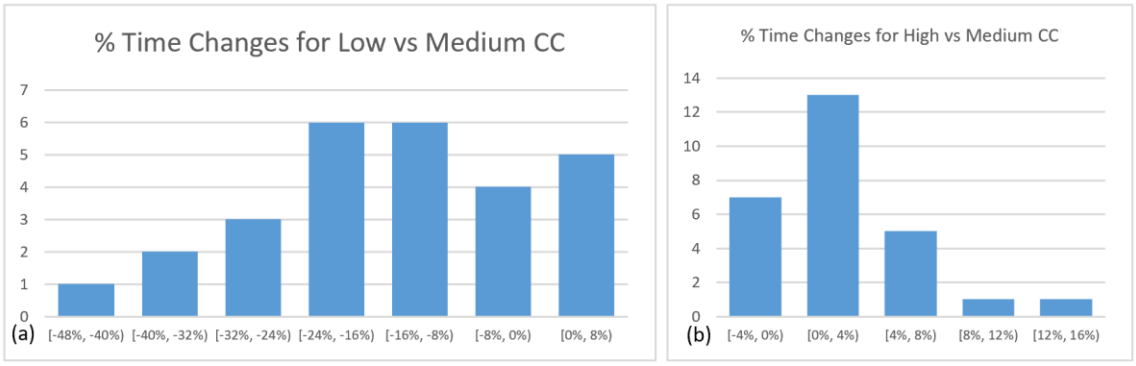

Figure 3.38 Percentage time changes due to changes of the cold chain with SFW drones

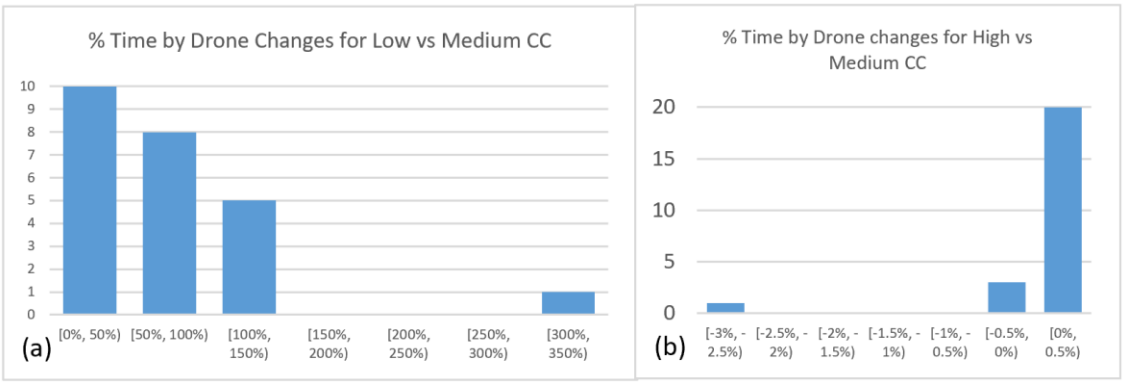

Figure 3.39 Percentage that drone travel time changes due to changes of the cold chain with SFW drones

Figure 3.39 uses a similar format to the earlier figures to examine the impact of changing the cold chain time limit on the use of drones, measured by the total travel time of drones in the solutions. There are three solutions that do not use drones for the baseline (medium) cold chain limitation (i.e., 2 hours), hence the paired comparisons (to calculate the percentage change) are for the 24 solutions that do use drones. Figure 3.39(a) shows that the drone use (flight time) increased substantially when the cold chain decreased from 2 hours to 1 hour. The average % change in drone use is +62.5% (median is 55.4%), and the range is from 0% to 338%. This increased drone use often comes with more DBs

and RSs, which leads to an increase in the transportation cost. The delivery time decreased when the cold chain limit decreased from the medium to the low level as shown in Figure 3.37(a) and Figure 3.38(a). Using more drones decreased the delivery time to meet the tighter cold chain, but usually increased the cost (often from more DBs and RSs). We see in Figure 3.39(a) that the drone usage increased significantly, by up to more than 300%, although note that a large percentage change could reflect a small absolute change if the baseline had very little usage of drones. Figure 3.39(b) shows that when the cold chain limitation relaxed from 2 hours to 4 hour, the usage of drones changed very little. The right-most bar in Figure 3.39 (b) included three counts that are small positive percentages, and 17 counts of 0 change. The other 2 bars in Figure 3.39(b) show that the percentage of drone delivery time decreased a small amount for 4 solutions when the cold chain limitation increased. As with Figure 3.39(a), Figure 3.39(b) can help explain why the transportation cost decreased and the delivery time mostly increased when the cold chain limit increased. This is because in most cases, drones could be used less when the cold chain limit was relaxed, and that can reduce the fixed DB and RS cost. Once again, the model is to minimize cost, not delivery time, so the drone usage (and delivery time) may not strictly increase (decrease) when the cold chain limit is tightened (relaxed).

3.8.1.6 Demand analysis

This section investigates how changes in the level of demand affect drone usage and performance. Similar to prior figures, Figure 3.40 shows the percentage changes of the transportation cost when the demand level changes.

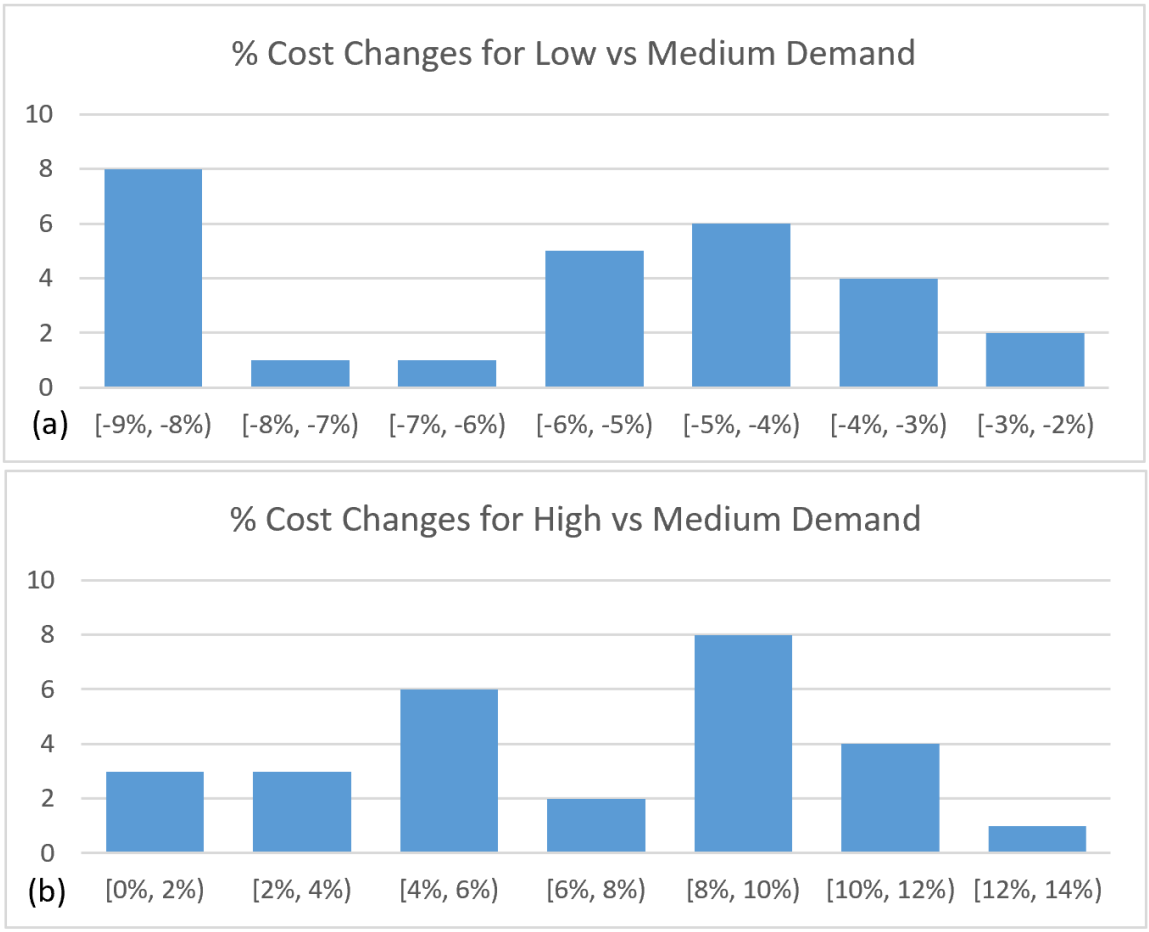

Figure 3.40 Percentage cost changes due to the changes of demand level with SFW drones

Figure 3.40(a) shows that the transportation cost decreased when the demand level decreased by half. The average change is -5.9% (median is -5.5%), and the range is -8.8% to -2.5%. Figure 3.40(b) shows that the transportation cost increased when the demand doubled. The average change is 6.8% (median is 8.0%), and the range is 0% to 12.6%. The direction of the cost changes are as expected, as transporting more vaccines should increase the transportation cost. But because only the drone mode is modeled with a capacity, and not all vaccines are carried on drones, the change in cost is less than proportional to the change in demand. The percentage of the vaccine liters carried by

drone decreased by 27.5% on average when the demand level decreased by half. On the other hand, the percentage of the vaccine liters carried by drone increased by 53.33% on average when the demand level doubled.

Figure 3.41 shows the percentage changes in the delivery time when the demand level changes. Figure 3.41(a) shows that the delivery time mostly decreased when the demand level decreased by half. The average change is -18.1% (median is -19.5%), and the range is -32.6% to 1.4%. Figure 3.41(b) shows that the delivery time mostly increased when the demand doubled. The average change is 6.9% (median is 13.1%), and the range is -18.9% to 16.8%. Note that in five of the paired instances with increased demand, the average delivery time decreased with the greater demand.

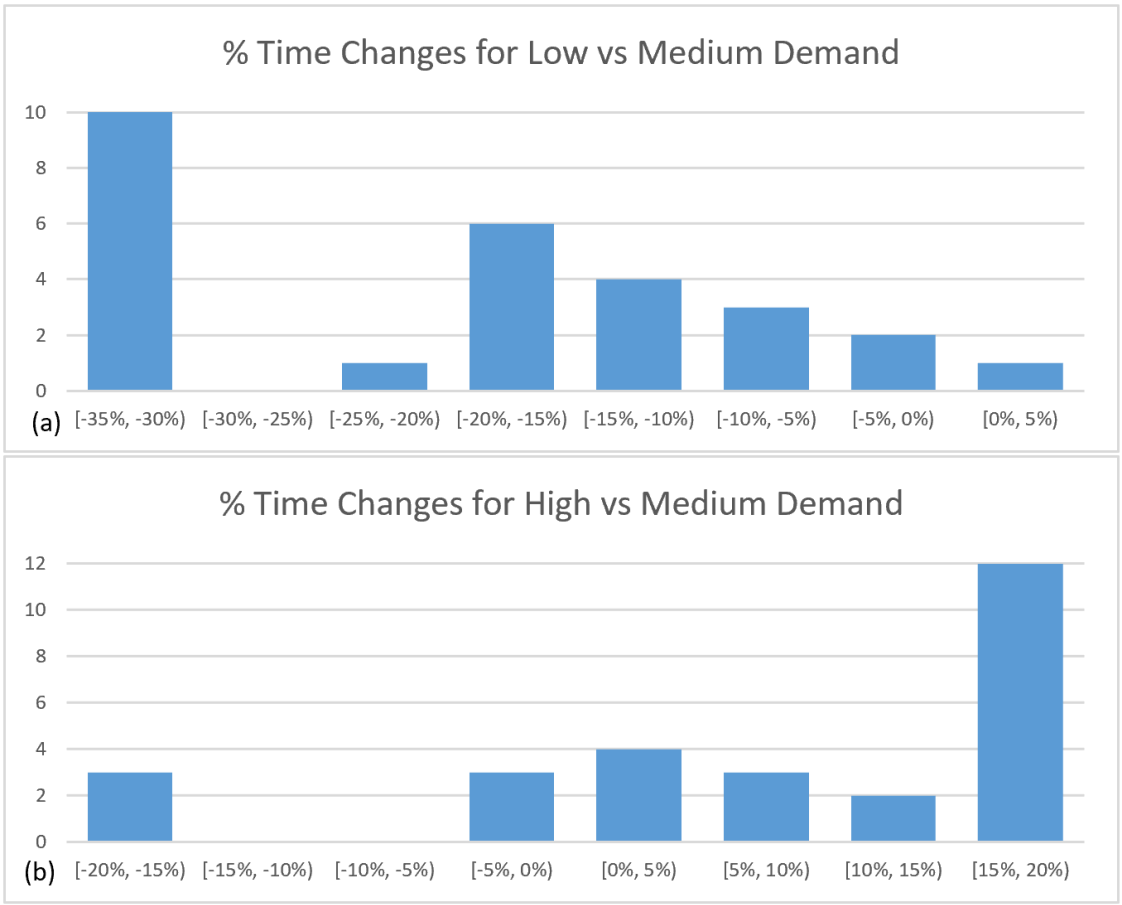

Figure 3.41 Percentage time changes due to the changes of demand with SFW drones

Figure 3.42 shows the percentage changes in the vaccine liters carried by drones when the demand level changes. There are 2 instances that did not use drones in the baseline (when the demand multiplier is 1; i.e., the original demand), so there are 25 paired comparisons in both histograms in Figure 3.42. Figure 3.42(a) shows that the percentage of vaccine liters carried by drone mostly increased when the demand level decreased by half. The average change is 71.6% (median is 85.7%), and the range is -1.8% to 122.9%. Figure 3.42(b) shows that the percentage of vaccine liters carried by drones mostly decreased when the demand doubled. The average change is -24.4% (median is -18.8%), and the range is -100% to 12.4%. The two histograms show that SFW drones are used more when the demand is less, and SFW drones are used less when the demand is large. This is because the drone cost model in P1-C1 charges drone travel based on the number of liters of vaccines carried on the drone arcs, so drones are more expensive when they carry more vaccine on an arc. For example, with the 10 liter capacity of the SFW drone, sending 16 liters requires two drone flights; but if demand was doubled, then carrying 32 liters requires 4 drone flights. That increase may make drone transport of 32 liters more expensive than boat transport of the same amount (as there is no capacity for the boat). This result also can help explain why the delivery time mostly decreased when the demand level decreased (as that encouraged more drone use), and the delivery time mostly increased when the demand level increased, as shown in Figure 3.41.

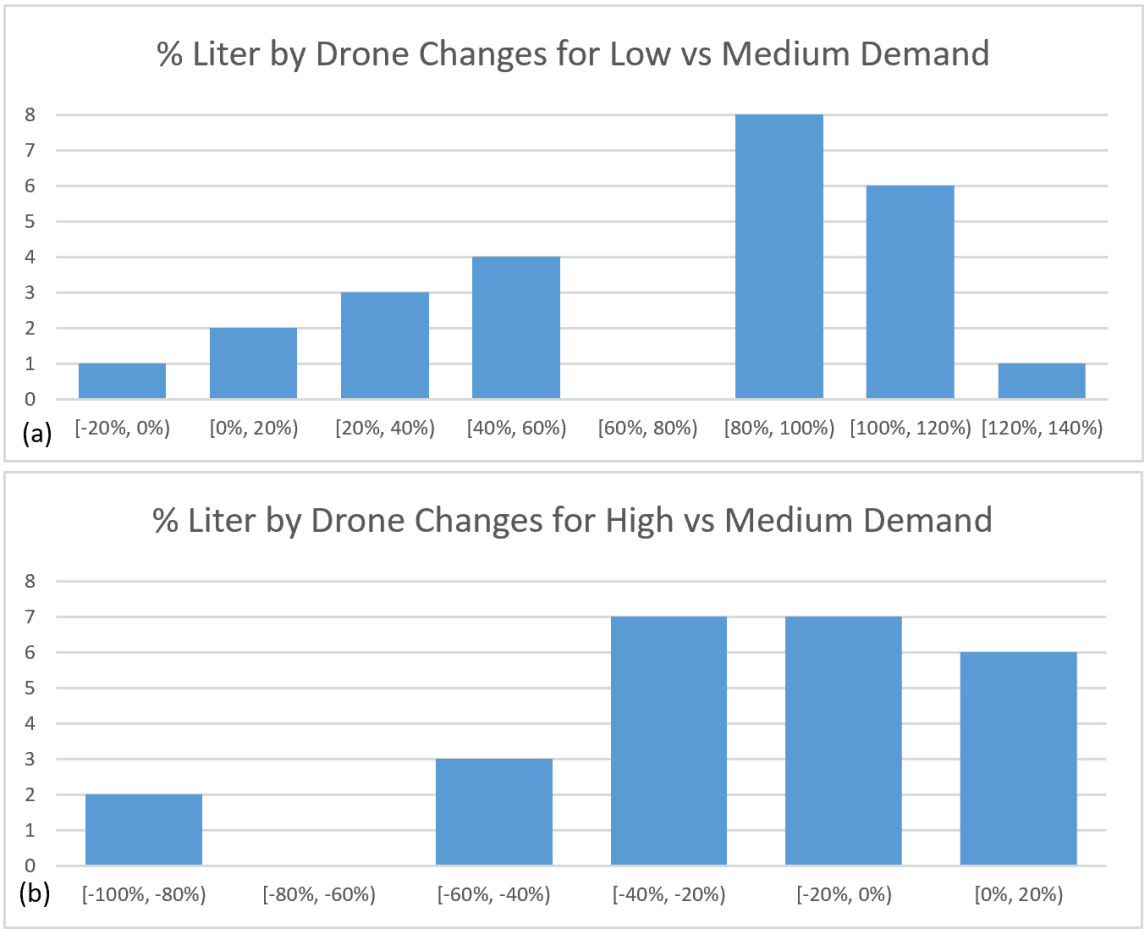

Figure 3.42 Percentage of liters delivered by drone changes due to the change of demand with SFW drones

3.8.1.7 DB cost analysis

Figure 3.43 shows the percentage changes in the transportation cost when the level of DB cost changes. Figure 3.43(a) shows that the transportation cost decreased when the DB cost decreased from \$6 to \$0, as expected. On average, the cost decreased by 4% when the DB cost decreased to \$0 (median is -3.6%), and the range of decrease is -7.4% to -1.8%. Figure 3.43(b) shows that the transportation cost increased when the DB cost doubled, as expected. On average, the cost increased by 3.7% when the DB cost

doubled (median is 3.2%), and the range is 0% to 7.3%. In general, the changes in cost were small for this range of change in the DB cost.

Figure 3.44 shows the percentage changes in the delivery time when the level of DB cost changes. Figure 3.44(a) shows that the delivery time mostly decreased when the DB cost decreased from $6 to $0. There are 24 changes of 0% in the right bin in Figure 3.44(a). On average, the delivery time decreased by 0.4% when the DB cost decreased to $0 (median is 0%), and the range is -5.2% to 0.2%. Figure 3.44(b) shows that the delivery time mostly increased when the DB cost doubled. On average, the delivery time increased by 0.8% (median is 0%), and the range is -11.3% to 14.9%. Compared to Figure 3.44, we see that DB cost changes affect the delivery time less than the transportation cost, as the two medians are 0%.

Figure 3.45 shows the percentage changes in the number of DB selected in solutions when the level of DB cost changes. There are 2 solutions that did not use drones when the DB cost is at the baseline (medium level), so there are 25 paired comparisons in both histograms in Figure 3.45. Figure 3.45(a) shows that the number of DBs increased in one-third of the solutions when the DB cost decreased from $6 to $0. On average, the number of DBs increased by 42% when the DB cost decreased to $0 (median is 0%), and the range is 0% to 200% (200% is an increase from 1 to 3 DBs). Figure 3.45(b) shows that the number of DBs decreased in only 2 cases when the DB cost doubled. So we see that the fixed cost of a DB affects the number of DBs that are selected to a rather small degree. As expected, we can see that the delivery time decreased when more DBs are open in most cases, and the delivery time increased when fewer DBs are open in most cases.

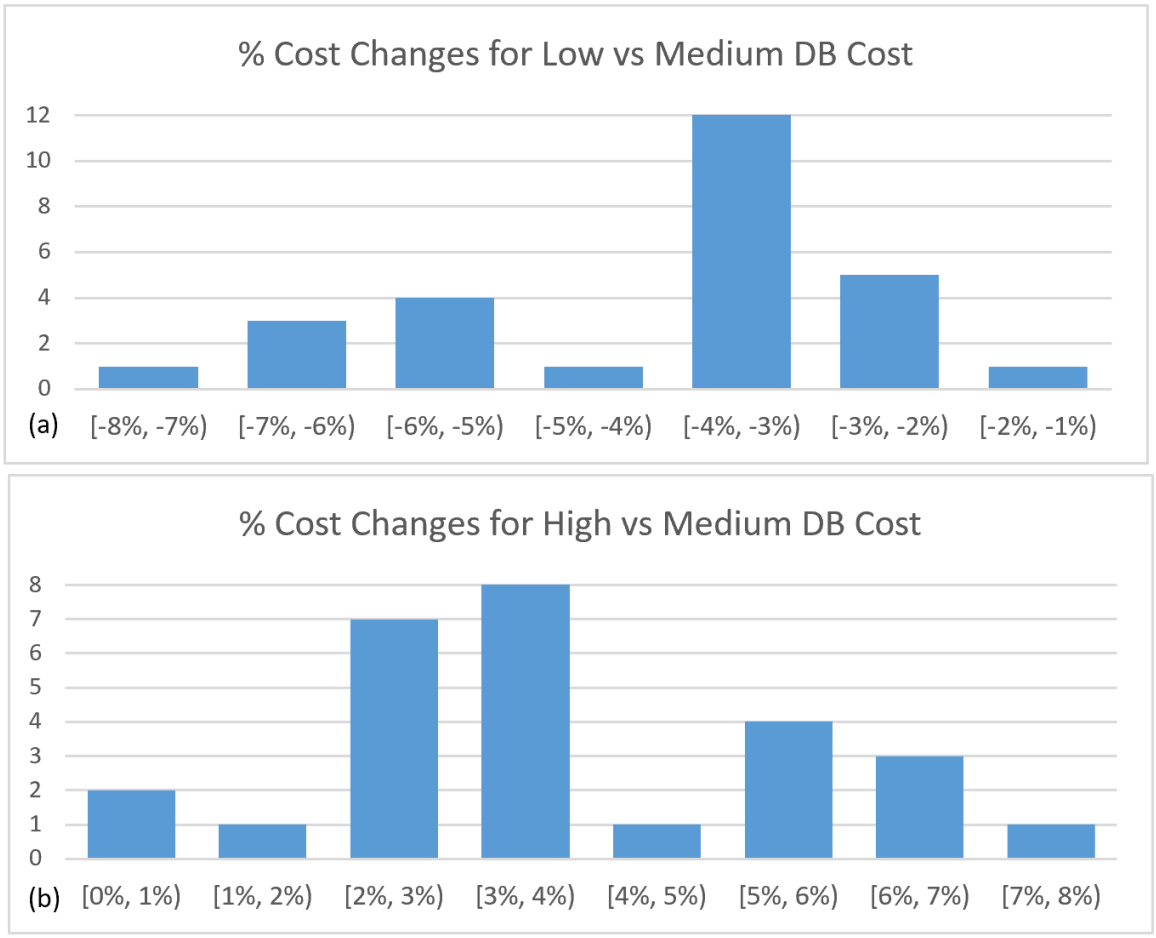

Figure 3.43 Percentage cost changes due to the DB cost changes with SFW drones

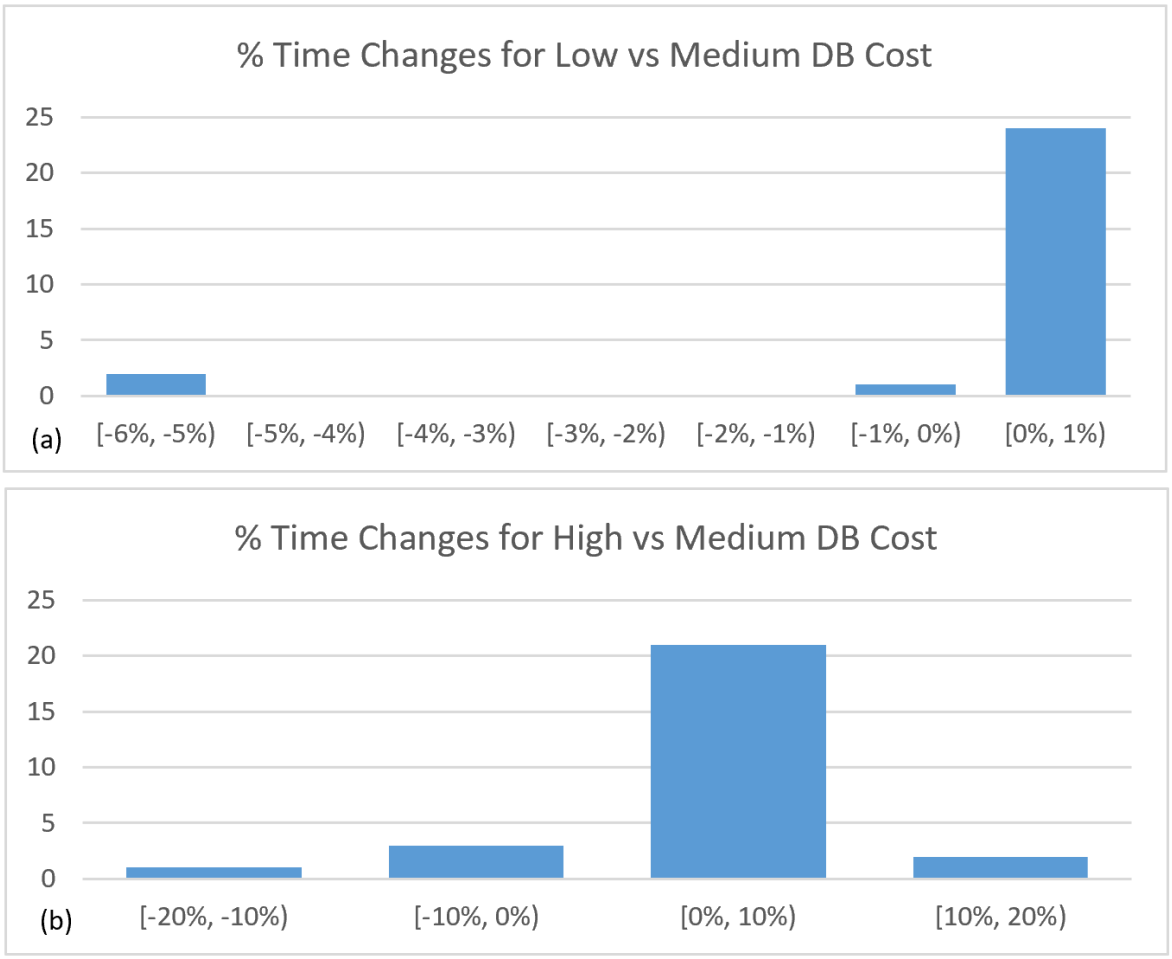

Figure 3.44 Percentage time changes due to the DB cost changes with SFW drones

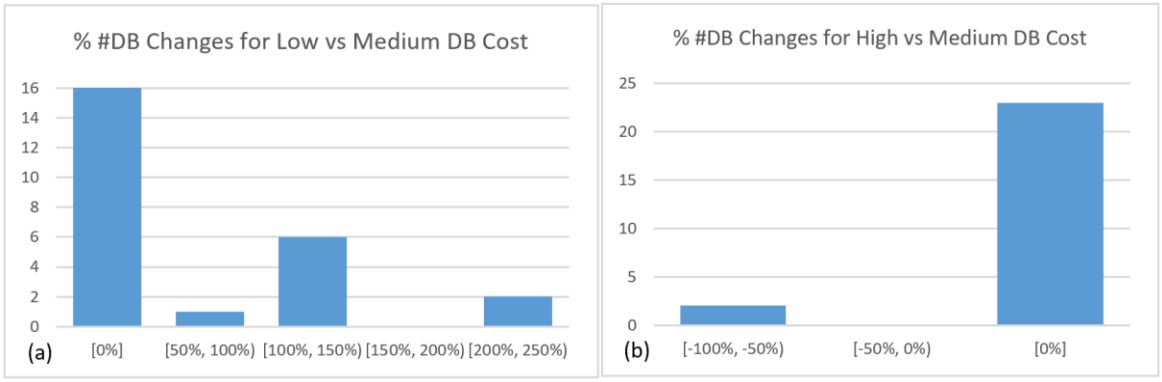

Figure 3.45 Percentage changes in the number of DB due to changes of DB cost with SFW drones

3.8.1.8 RS cost analysis

Figure 3.46 shows the percentage changes of the transportation cost when the level of RS cost changes. Figure 3.46(a) shows that the transportation cost decreased when the RS cost decreased from $6 to $0. On average, the cost decreased by 15.2% (median is -14.9%), and the range is -18.5% to -11.9%. Figure 3.46(b) shows that the transportation cost increased when the RS cost doubled. On average, the cost increased by 10.8% (median is 11.7%), and the range is 4.1% to 14%.

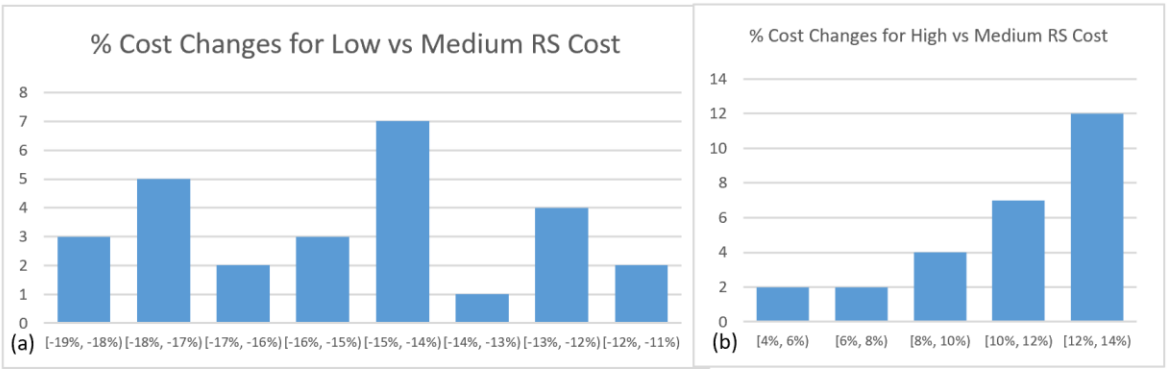

Figure 3.46 Percentage cost changes due to changes of RS cost with SFW drones

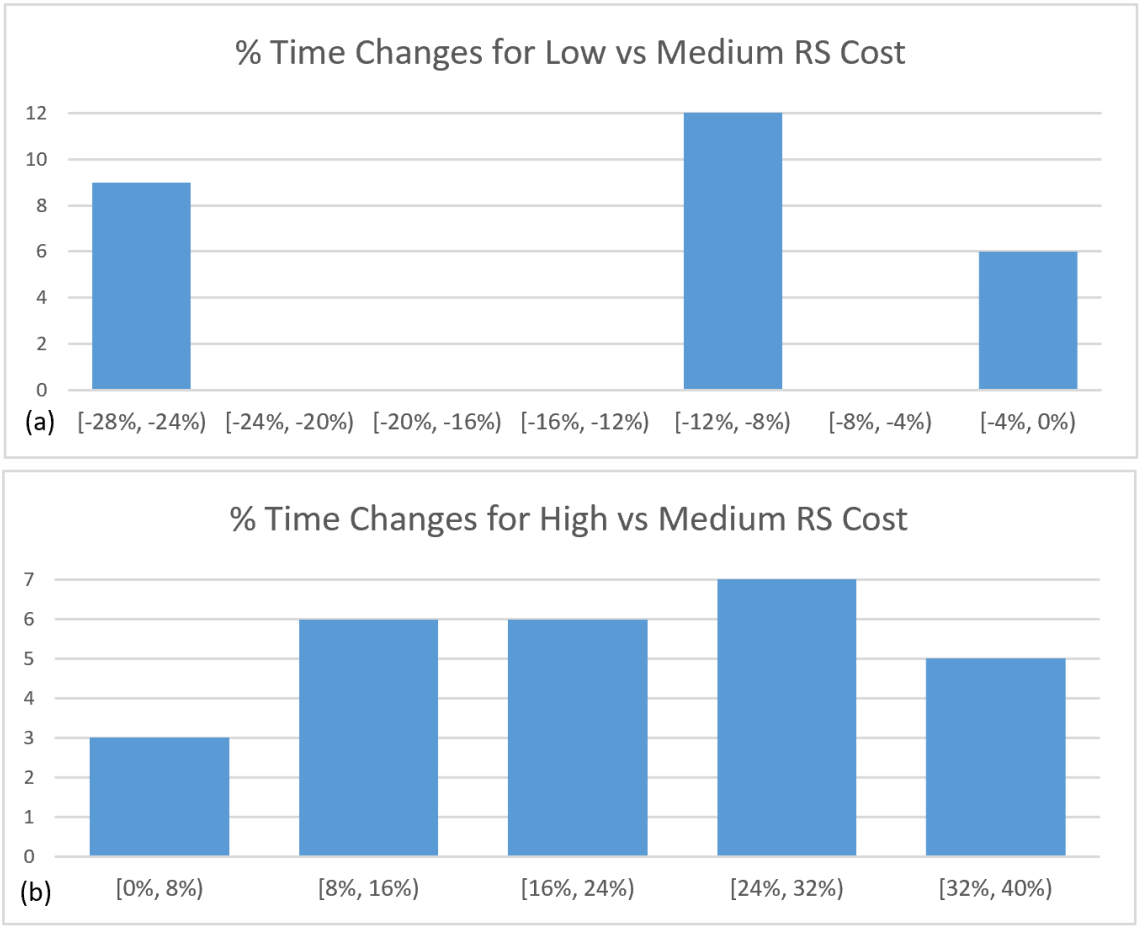

Figure 3.47 Percentage time changes due to the changes of RS cost with SFW drones

Figure 3.47 shows the percentage changes in the delivery time when the level of RS cost changes. Figure 3.47(a) shows that the delivery time decreased when the RS cost decreased from \$3 to \$0. On average, the delivery time decreased by 14.4% (median is a decrease of -11.7%), and the range is -27.3% to -1.2%. Figure 3.47(b) shows that the delivery time increased when the RS cost doubled. On average, the delivery time increased by 20.5% (median is 22.0%), and the range is 1.9% to 36.7%.

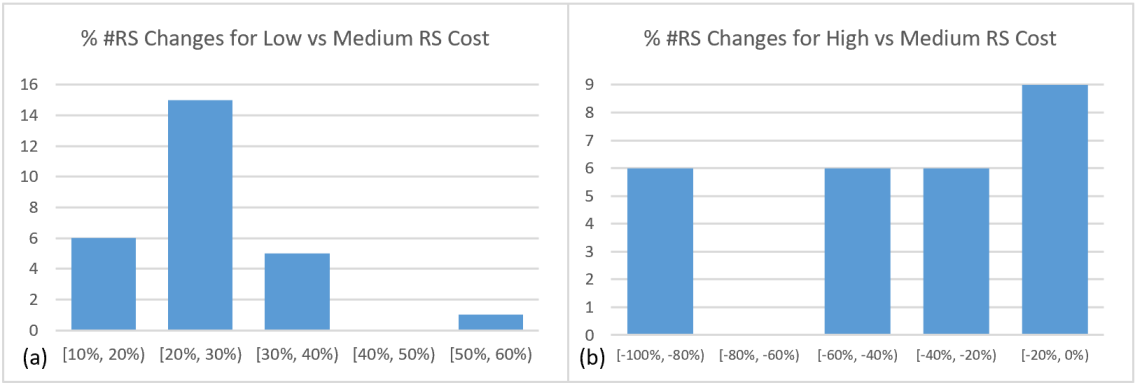

Figure 3.48 Percentage changes in the number of RS due to the changes of RS cost with SFW drones

Figure 3.48 shows the percentage change in the number of RSs that are selected in solutions when the level of RS cost changes. Figure 3.48(a) shows that the number of RSs increased when the RS cost decreased from $3 to $0. On average, the number of RSs increased by 22.6% (medium is 20%), and the range is 10% to 50%. Figure 3.48(b) shows that the number of RSs decreased when the RS cost doubled. On average, the number of RSs decreased by 44.7% (median is -30%), and the range is -100% (in cases when the number of RS decreased to 0) to -10%. We see that, as expected, the cost of a RS affects the number of RSs that are selected directly.

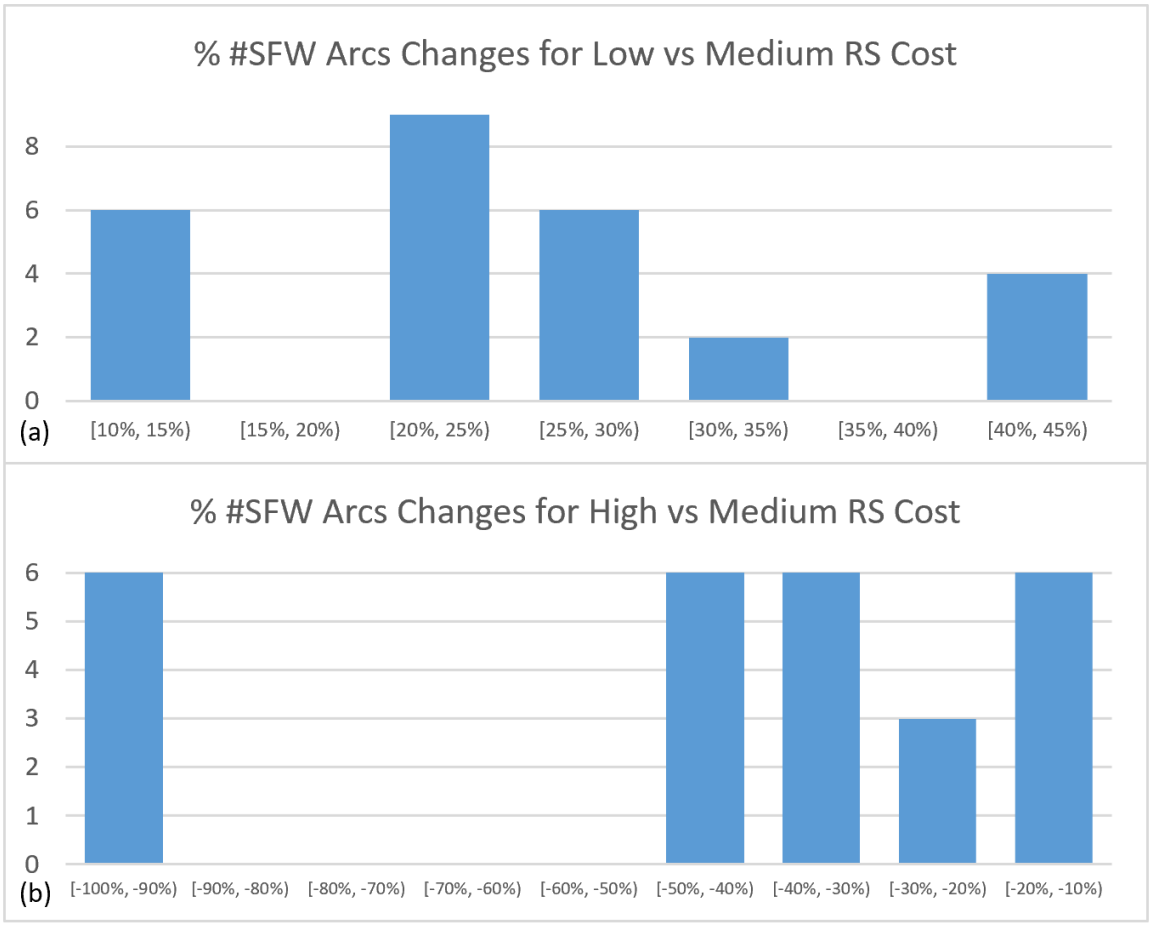

Figure 3.49 Percentage changes in the number of SFW arcs due to the changes of RS cost with SFW drones

Figure 3.49 shows the percentage changes in the number of SFW drone arcs used when the level of RS cost changes. Figure 3.49(a) shows that the number of SFW drone arcs increased when the RS cost decreased from \$3 to \$0. On average, the number of SFW drone arcs increased by 24.8% (median is 22.2%), and the range is 12.5% to 42.9%. Figure 3.49(b) shows that the number of SFW drone arcs decreased when the RS cost doubled. On average, the number of SFW drone arcs decreased by 45.5% (median change is -33.3%), and the range is -100% to -12.5%. The increasing percentage of SFW drone arcs means that drones are being used more, which helps explain why the delivery time

decreased when the RS cost decreased. This is due to the fast speed of the drones, which are used more when the RS cost decreased.

3.8.1.9 SFW sensitivity analysis summary

This section can help answer the last four of our key research questions. First, among the four key parameters, the change of the cold chain time limitation affects the transportation cost in different directions compared to the other three parameters. When the cold chain time level decreases, the transportation cost increases in most cases, and when the cold chain level increases, the cost decreases in a few cases (it does not change in the other cases). When the cold chain time is short, the fast and more expensive modes such as airplane will be used more, and the limited cold chain time also will lead to opening more expensive DBs and RSs when using drones to improve the delivery time. The results also show that the cold chain time limit affects the cost and time more significantly (i.e., with a larger percentage change) than the other three parameters, especially when the cold chain level decreases. Moreover, when the cold chain time is tight, drones are used more in delivering vaccines, thus the delivery time is shorter.

A second set of research findings concerns how the change of demand level affects the performance and drone usage. Unlike the cold chain time limitation, when the level of demand (or DB cost, or RS cost) decreases, then the transportation cost decreases. When the level of demand (or DB cost, or RS cost) increases, then the transportation cost increases. Increasing the level of demand impacts the cost more significantly (i.e., with a larger percentage change) than decreasing the level of demand in general (the increase of the demand level does not affect the cost in only two cases). When the demand decreases, delivery is faster, the cost decreases, and also SFW drones

are used more due to the drone cost being charged by the amount of vaccine liters carried. Thus, it is lower cost to use drones to carry small amounts of vaccines compared to when the demand is high.

A third set of research findings concern how the change of RS cost affects the performance and drone usage. Among the DB cost and RS cost, the change of RS cost impacts the total cost more compared to changing the DB cost in both directions, which is largely due to there being more RSs in a network than DBs. When the RS cost decreases, the total cost decreases and delivery is faster; moreover, more RSs are open and in use when the RS cost decreases.

Finally, the change of DB cost affects the performance and drone usage the least amount, compared to the other three key parameters. When DB cost decreases, the cost decreases, and more DBs are opened. The service time also improved when the DB cost decreases.

3.8.2. Sensitivity analysis with LFW

This section describes the sensitivity analysis to examine how some key parameters affect the LFW drone usage and performance. I designed a 3*3*3 experiment for LFW drones varying each of three key parameters, cold chain time limitation, DB cost, and RS cost, with 3 levels. I use model P1-C2 with the LFW drones as these drones have a large capacity and so drone travel cost based on one trip per drone arc is reasonable (these drones would not make multiple trips per drone arc unless demand is much, much larger than for our setting). The large capacity of LFW drones is also the reason for not performing a sensitivity analysis for the level of demand, as was done for the small SFW drones. Also, unlike the sensitivity analysis with SFW drones, the

analysis with LFW drones used all 27 nodes in Malampa as the computational times for all runs are short due to there being fewer LFW arcs than SFW arcs, since LFW drones are restricted to take off and land at airports.

The low, medium, and high levels of cold chain limitation in the sensitivity analysis for LFW drones are 2 hours, 4 hours, and 6 hours. Because the LFW drone arcs are only between airports, the distance of these arcs is generally longer than for the SFW drone arcs used earlier. In fact, the model becomes infeasible when the cold chain time limitation is 1 hour. The low, medium, and high levels of DB cost are $0, $15 and $29 per month, and the low, medium, and high levels of RS cost are $0, $7, and $14 per month. These values reflect higher costs for the larger, more expensive LFW drones compared to the SFW drones. The level of demand used is the baseline (current) demand shown in Table 3.17.

Table 3.27 lists the number of arcs by mode as inputs for model P1-C2 for the three levels of cold chain limit with LFW drones. Table 3.28 shows the number of decision variables and constraints in the models with LFW drones, based on the cold chain limits. Note that these numbers of variables and constraints for LFW drones are significantly smaller than those for SFW drones, as LFW drones require airports. Thus, the number of LFW drones arcs, as well as the number of drone bases and relay stations are significantly fewer than for SFW drones.

Cold Chain	# Run	#Airplane Arcs	#Boat Arcs	#Truck Arcs	#LFW Arcs	Sum
2	9	13	150	30	36	229
4	9	13	370	30	36	449
6	9	13	518	30	36	597

Table 3.27 Number of arcs by mode in P1 with LFW

Cold Chain	# DV	#Constraints
2	1060	1679
4	1500	1899
6	1796	2047

Table 3.28 Number of decision variables and constraints in P1 with LFW

All runs used $N = 6$ and $\Omega = 3$. This is because there are only 6 airports in Malampa, which are nodes 14, 19, 22, 100, 101, and 102, so there can be at most 5 LFW paths. Considering the distances between the 6 airports relative to the area of Malampa, three LFW steps seems reasonable and large enough to cover the province.

3.8.2.1. Solution analysis of LFW runs

Model P1-C2 was solved for the 27 instances (in the 3*3*3 experimental design) using Gurobi 9.1 with a 2 hour limit using HP Intel Quard-Core i7 with 3.9 Ghz CPU and 64 GB RAM. All runs solved to optimality quickly, with an average of 10.4 seconds of CPU time or 3 seconds of real time, and with a maximum CPU time of 23.4 seconds (or 6.4 seconds of real time).

There are only 2 unique solutions (see Figure 3.50) among the 27 optimal solutions: one solution for all 9 runs with the 2 hour cold chain time limitation, and one solution for all 18 runs with the 4 hour or 6 hour cold chain time limitation. Further, in

both solutions, the LFW drone was used only to carry vaccine from the national depot to node 19. From there, the vaccine was delivered by boat or truck to all health zones. Increasing the cold chain time limitation from 4 hours to 6 hours does not affect the optimal network design in this case. This is because the variable transportation cost of LFW drones, which is $0.38/km, is high compared to the variable cost of boats ($0.30/km), so the model prefers using boats to keep the total cost low. Thus, the cold chain time limit only affects the part of the solution where boat delivery is used. Figure 3.50 shows that with a 2 hour cold chain limit a boat needs to stop at node 16 first to restart the cold chain and then deliver the vaccines to node 22 for health zone MAL05. When the cold chain is relaxed to 4 hours or 6 hours, then a boat is able to deliver vaccines direct from node 24 to node 22 without restarting the cold chain in transit. Notice that airplanes are not used in the LFW drone solutions, as the LFW drone provides lower cost fast transit from the depot (node 0) to node 19. The solutions include two relay stations at nodes 0 and 19 and one drone base at node 0. All runs open the same DCs, which are nodes 14, 17, 18, 19, 22, 24, 25, 28, 30, 33, 34 and 36.

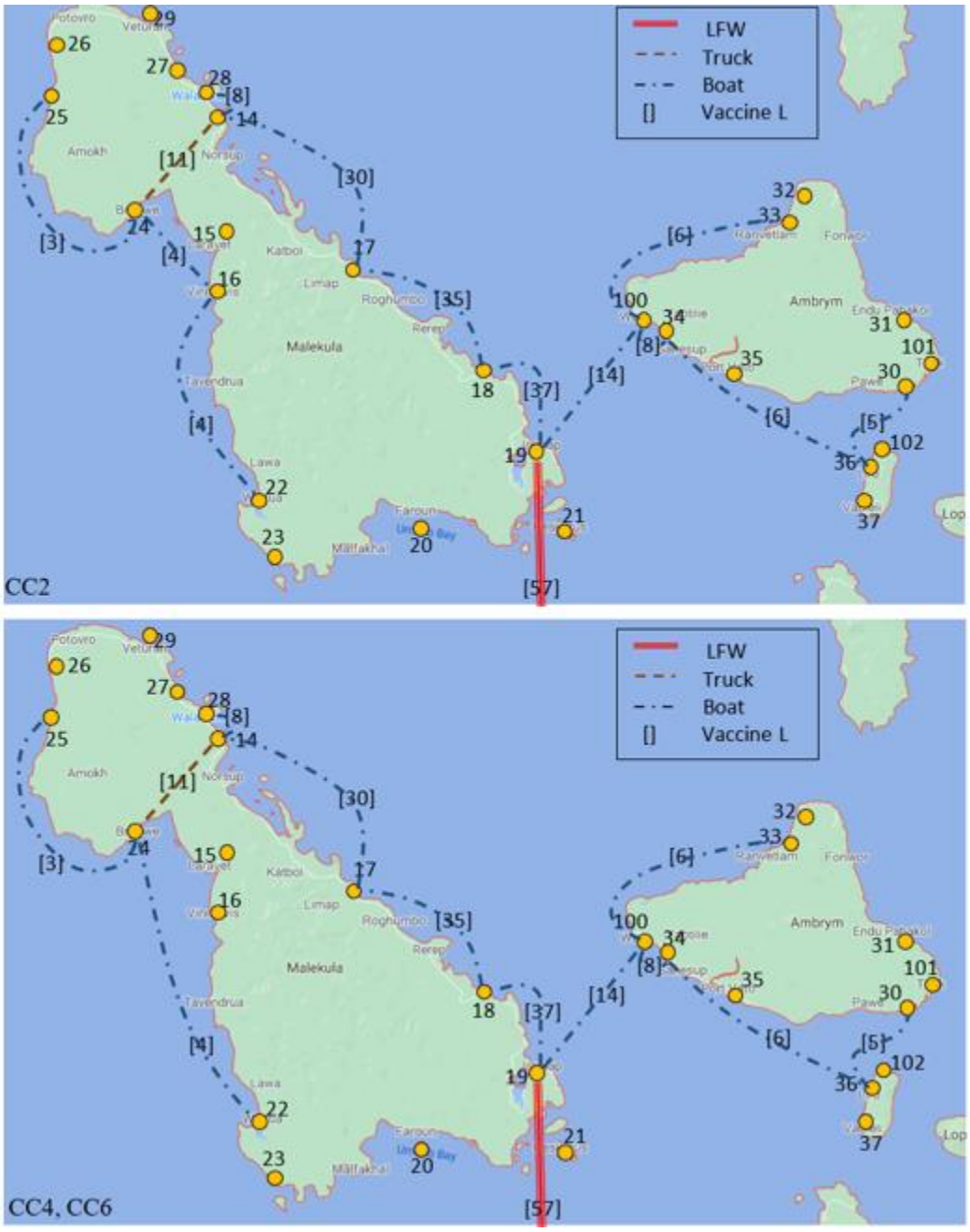

Figure 3.50 Solution maps of LFW

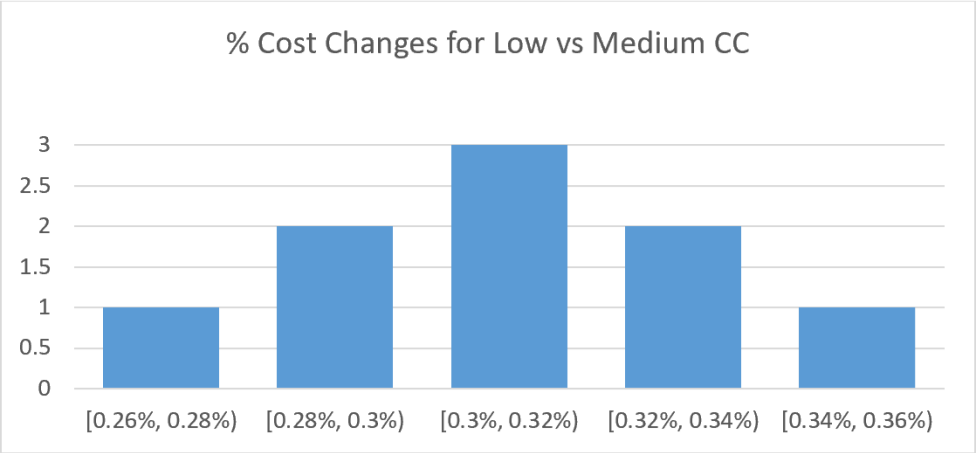

Figure 3.51 Percentage cost changes due to the changes of cold chain with LFW drones

Figure 3.51 shows the percentage changes in the transportation cost when the level of cold chain changes; specifically it shows that the transportation cost increased when the cold chain time decreased from 4 hours to 2 hours. On average, the cost increased by 0.3% (median is 0.3%), and the range is 0.26% to 0.36%. The transportation cost is $16.62/HZ on average when the cold chain time limitation is 2 hours, and it is $16.57/HZ on average when the cold chain time limitation is 4 or 6 hours. The transportation cost ranges from $14.23/HZ to $18.98/HZ when the cold chain time limitation is 2 hours, depending on the problem parameters in the nine runs. The transportation cost ranges from $14.18/HZ to $18.93/HZ when the cold chain time limitation is 4 or 6 hours. The different transportation costs are caused by the different combinations of DB and RS costs. The range of the cost for each cold chain time limitation is more than $4, which is about 25% of the cost. The large percentage change of the cost implies that the cost of DBs and RSs impact the transportation cost of the delivery network significantly. (Figure 3.52 and Figure 3.53 show the point and are

discussed below.) The percentage changes of the transportation cost are zero for all pairs of solutions when the cold chain time increased from 4 hours to 6 hours, so no histogram is shown for that. No histogram is shown for the percentage change of delivery time when the DB cost and RS cost changes for the same reason (i.e., changes are zero).

The percentage changes of the delivery time per health zone is 0.2% for all pairs of solutions when the cold chain time decreased from 4 hours to 2 hours. This is because there is one solution for all instances when the cold chain is 2 hours, and one solution for all instances when the cold chain is 4 or 6 hours. Thus, the average delivery time is essentially the same whether the cold chain limit is 2, 4, or 6 hours. (The average weighted delivery time per health zone is 3 hours 35 minutes when the cold chain limitation is 2 hours, and it is 3 hours 35.4 minutes when the cold chain time limitation is 4 or 6 hours.) As the top map in Figure 3.50 shows (with a 2 hour cold chain limit), a boat cannot reach node 22 directly from node 24 due to the tight cold chain time limitation; so it must stop at node 16 to restart the cold chain. With the longer cold chain in the lower map of Figure 3.50 the boat travels direct from node 24 to 22, which saves a small amount of time.

Recall that the range of transportation cost with SFW drones is from $12.62/HZ to $22.59/HZ, and the range of delivery time with SFW drones is from 1 hour 32 minutes to 3 hours 39 minutes. Thus, compared to SFW drones, the range of both transportation cost and delivery time with LFW drones is narrower, and the average delivery time is longer for the LFW drones, as the slower LFW drone replaces the faster (but more expensive) airplane. However, the LFW drones are limited to operate at airports, so they cannot be heavily used for deliveries as can the SFW drones.

Figure 3.52 and Figure 3.53 shows the percentage changes in the transportation cost when the level of DB cost and RS cost changes, respectively. Both figures show that the transportation cost decreased when the DB cost and RS cost decreased on the left, and the transportation cost increased when the DB cost and RS cost increased on the right. The cost percentage changes of plus or minus about 7% to 8% are larger than the very small percentage cost changes when the cold chain time changes (i.e., 0.26%-0.36%). This shows that the DB cost and RS cost have a moderate impact on the total transportation cost. Comparing Figure 3.52 with Figure 3.53, we see the level of the impact of DB cost and RS cost on transportation cost are similar.

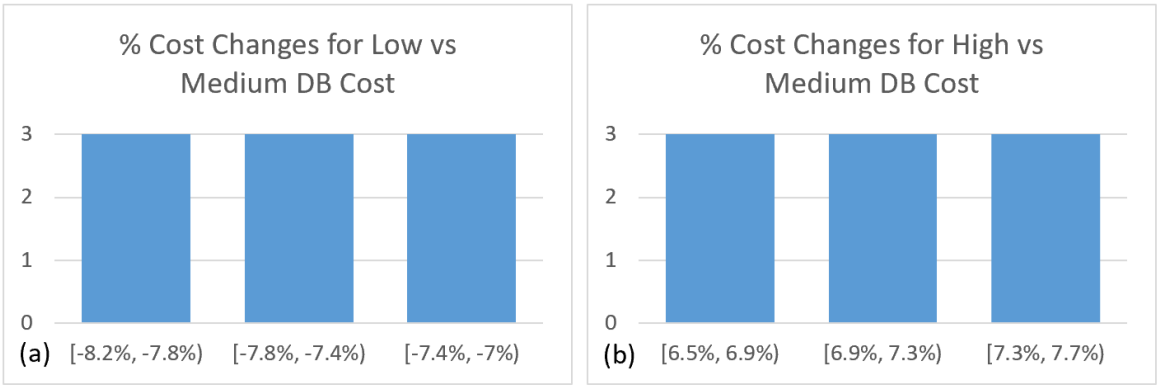

Figure 3.52 Percentage cost changes due to changes of DB cost with LFW drones

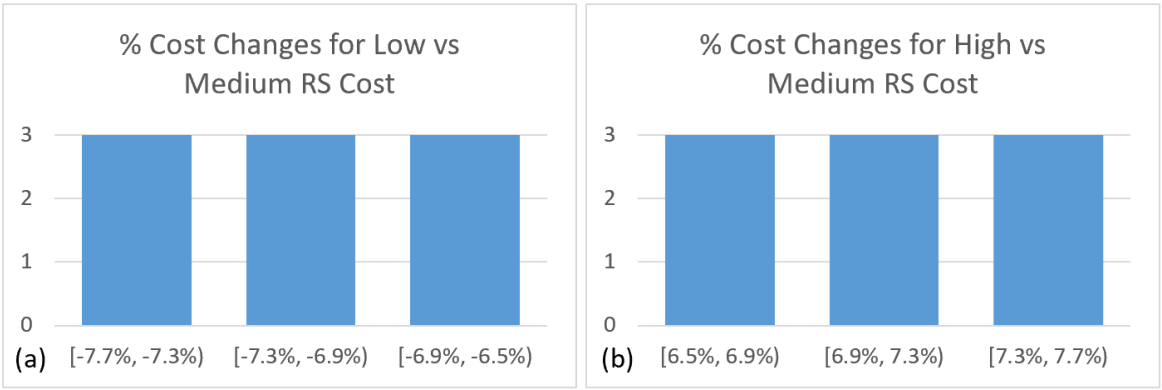

Figure 3.53 Percentage cost changes due to changes of RS cost with LFW drones

3.8.2.2. LFW sensitivity analysis summary

Compared to the SFW drones, LFW drones are used to a limited extent, mainly due to three reasons. First, LFW drones are limited to operate out of airports, so there are fewer LFW arcs (i.e., 6) in the network to begin with. Second, the cold chain time limitations, especially the high level (i.e., 6 hours), are not short enough to motivate the model to use more high speed LFW drones. Relatively long cold chain times allow many slow but low cost boat arcs to be used instead of LFW drone arcs. More LFW drone arcs might be used if there were fewer boat arcs available, although the LFW drones are still limited to the airport nodes. Third, the cost structure for the large capacity LFW drones discourages their use for small vaccine shipments, as the cost does not depend on the payload carried. If a different cost structure was employed, then more LFW drone arcs might be used.

This sensitivity analysis can help to answer several research questions. Results show that the transportation cost is essentially unchanged when the cold chain time limitation decreases from 4 or 6 hours to 2 hours. The fixed cost of DBs and RSs contribute to the transportation cost significantly. In contrast to results for SFW drones where the cold chain time limit strongly affects the average delivery time to a health zone, with LFW drones there is little impact in the settings I analyzed. Compared to SFW drones, LFW drones are used significantly less, mainly due to the LFW arcs being limited to airports, and the longer cold chain used in our experiments. This calls for future research that combines SFW and LFW drones in the same network to make the two types of drones complement each other. We might see solutions with LFW drones replacing airplanes for longer trips, while SFW drones replace shorter trips that were covered by

boat or truck. Such solutions might provide lower cost and faster service than using only one type of drone.

4. Vaccine Delivery in One Health Zone with Drones

The problem of vaccine delivery in one health zone with drones, called P2, is a novel multi-day multi-trip traveling salesman problem with time constraints on both vaccines and health workers' work time, and synchronization of the health workers and drones. Three models were developed in this dissertation, depending on the number of drone stops allowed in a drone trip. This problem is the second stage in the entire vaccine delivery problem (i.e., the dissertation), and it can be viewed as a continuation of the first problem (P1) for the distribution of vaccines from a national depot to a distribution center (DC) in each heath zone. Therefore, in the present problem P2, a single health zone is considered and vaccines originate from a given DC. They are sent from the DC to permanent clinics and then to temporary clinics in the health zone by available modes of transport every month. In the case of Vanuatu, it is by boat, truck, or walking. The problem description is given in section 4.1. The three optimization models are developed in Section 4.2. Section 4.3 provides the data used in the solution illustrations, which are presented in Section 4.4. Section 4.5 provides a summary.

4.1 Problem description

This problem optimizes vaccine delivery within a single health zone, which in Vanuatu might be part of a large island or a collection of several islands. The given information includes the location of the DC, locations of one or more permanent clinics, and locations of the temporary clinics served on outreach trips. Each health zone is divided into non-overlapping subzones, where each subzone includes one permanent clinic and a few nearby temporary clinics, that are served from the permanent clinic. Permanent clinics receive vaccines from the DC on a periodic (e.g., monthly) basis. Note

that the DC is also a permanent clinic, as all DCs are staffed with permanent health workers and cold chain equipment. Figure 4.1 shows a small illustration of a health zone with two subzones A and B on Erromango island in Vanuatu. There are two permanent clinics labeled 9 and 10, and eight temporary clinics labeled 1 to 8. Clinic 9 serves the three temporary clinics in subzone A (i.e., 1, 2, and 3), and clinic 10 serves the five temporary clinics in subzone B (i.e., 4 to 8). Permanent clinic 9 is also the DC for the health zone, so permanent clinic 10 receives vaccines from clinic 9. Unlike in problem P1, all locations (i.e., clinics and the DC) are given in P2, and all temporary clinics are preassigned to one permanent clinic in each subzone.

In each subzone, the permanent clinic is the base for permanent health workers in that subzone, and current practice is for a health worker to travel on periodic "outreach trips" from the permanent clinic to the temporary clinics carrying the vaccines using the available modes of transport. The outreach trips include administering vaccination and other healthcare services at each temporary clinic. Each outreach trip starts and ends at the permanent clinic in the subzone. Each temporary clinic has a demand for vaccinations based on the number of children that need vaccinations, referred to as fully immunized children or FIC. I assume in our model that the health worker will first administer vaccinations to all that need it and then provide various types of health care for other patients. I assume there is a fixed duration for each vaccination, so the total time for vaccinations is proportional to the number of FIC. I assume the time for other care at a temporary clinic is given, based on the population in the area. Currently, the outreach activities in Vanuatu are not scheduled analytically, and health workers generally visit only one temporary clinic per day on an outreach trip in order to keep the vaccines viable

(Ministry of Health Vanuatu, 2018). Thus, a health worker will carry vaccines in a cold box and visit one temporary clinic and then go back to the permanent clinic; and then visit another temporary clinic on another day with fresh vaccines. A health worker will continue to do this until all temporary clinics are served each month in a subzone.

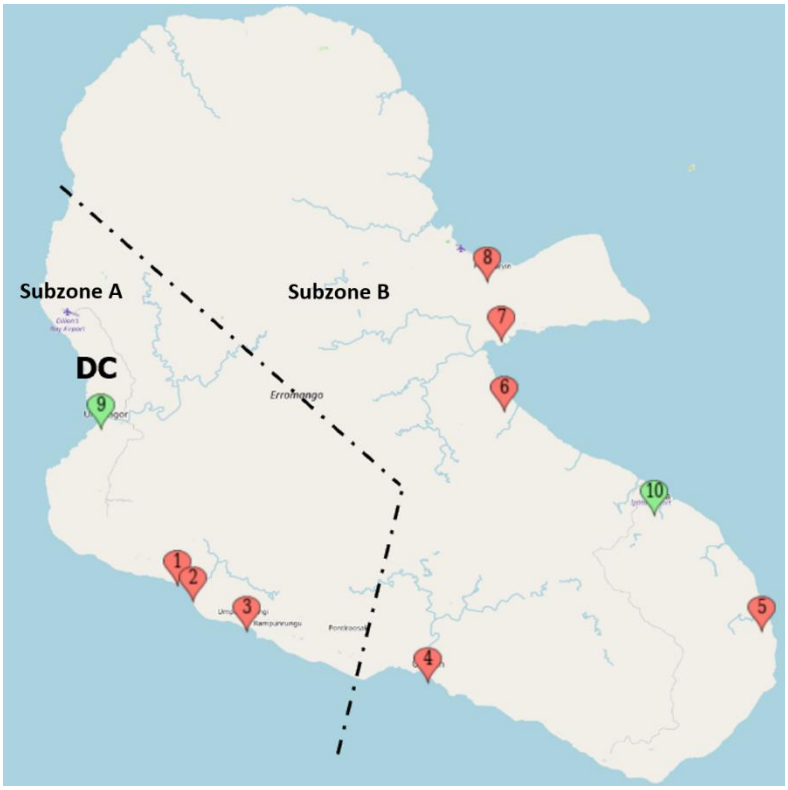

Figure 4.1 A health zone on Erromango island in Vanuatu.
(Green points 9 and 10 are permanent clinics; red points 1-8 are temporary clinics.)

Within a health zone, there are two levels in the vaccine delivery, where vaccines are first delivered from the DC to all permanent clinics, and then vaccines are delivered from the permanent clinics by health workers within each subzone. In P2, I focus on the second level, which means each permanent clinic has received vaccines from the DC in their health zone, and I do not model the vaccines being delivered from the DC to each

permanent clinic. The main reasons for this are that vaccines can only be delivered in the second level after the first level is finished, and that there are very few permanent clinics per health zone, at least in Vanuatu. This means that the delivery route in the first level from the DC to permanent clinics will be simple and does not require detailed modeling. For example, in the small illustration shown in Figure 4.1, there will be only one delivery from node 9 to node 10 in the first level. Because truck transport and walking are not available between node 9 and node 10, the mode of transport for that travel must be boat. Therefore, we know the best route in the first level without complex modeling in most cases. Integrating the first level deliveries with the second level deliveries to temporary clinics can be researched in future work.

An important feature of my models is to allow a health worker to visit multiple temporary clinics in an outreach trip while making sure the vaccines are viable before the vaccination activity is finished at the last clinic in a trip, all with a goal to minimize cost. Multiple day trips are modeled, as for example when the health worker finishes outreach activity at a clinic late in a day, and must stay overnight at that clinic and go back to his/her base (i.e., the permanent clinic) the next day. This will incur an overnight expense. Hence, the cost includes the transportation cost and the overnight cost to serve the health zone. In each outreach trip, a health worker will depart from his/her permanent clinic by a mode of transport and arrive at a temporary clinic. In this research, I assume the health worker will begin to administer vaccinations immediately upon arrival, and once the vaccination activity is finished then he/she will immediately begin to provide other health care. Hence the model tracks the departure time from the permanent clinic and the arrival time at the temporary clinic, which is the same as the vaccination start

time. A health worker has a daily work hour limit based on the work day (e.g., 9:00 am - 5:00 pm) and a vaccine payload limit per outreach trip based on how much vaccine (with ice packs) he/she can carry in a cold box. Each temporary clinic has a specified vaccine demand in liters, based on the number of FIC for that clinic. A health worker has to return to their permanent clinic to pick up new vaccines once the vaccines in the cold box run out, or the vaccines have been in the cold box for longer than the cold chain time limit. Thus, depending on the cold chain requirements, an outreach trip could take several days. The health worker will conduct enough outreach trips each period (e.g., month) so that all temporary clinics in the subzone are served.

This dissertation presents three optimization models developed for problem P2 of delivery of vaccines from a permanent clinic to temporary clinics. The three models differ by the number of drone stops allowed in a drone trip, and the model are built sequentially with added features. The first model, denoted P2-D0, is developed to optimize the existing vaccine delivery system for all subzones in one health zone with only the current available modes of transport (no drones). The model identifier "D0" indicates there are no drones (or drones make 0 stops). Because the cold box can keep the vaccines viable for a limited time (e.g., 8 hours), one of the limitations of P2-D0 (without drones) is that the number of clinics that can be served per outreach trip is restricted by the vaccine cold chain time limit (i.e., for vaccines in the cold box). With the help of drone delivery, a health worker can visit more clinics in an outreach trip and have a drone deliver fresh vaccines from the DC to these clinics. The second and third optimization models are developed for this setting. The second model, denoted P2-D1, allow drone deliveries of vaccines, but limits drone trips to visit only one temporary clinic (an out-

and-back trip from the DC to the temporary clinic). The third model, denoted P2-Dn, has no such limitation and allows multiple drone deliveries per trip. The DC in each health zone serves as the drone base for the health zone.

In this research, if a temporary clinic receives vaccines from a drone, then I require the health worker to arrive at the temporary clinic before the arrival of the drone to ensure the vaccines are safely collected. A drone has a payload limit for how much vaccine (with ice packs) it can carry. Thus, in models P2-D1 and P2-Dn drone delivery allows new flexibility to overcome the cold chain time limit for vaccines carried by the health worker, as well as the payload limit of the cold box carried by the health worker. For example, in Figure 4.1, suppose the capacity of a cold box carried by a health worker is 2 liters of vaccine, and the demands at clinics 1, 2, and 3 are 1 liter, 1 liter, and 0.5 liter of vaccine, respectively. Then without drones, the cold box capacity limit prevents the health worker in subzone A from serving all three clinics in one outreach trip, regardless of the cold chain time limit. When drone delivery is allowed, then the health worker may be able to serve all three clinics in one outreach trip by having a drone deliver vaccines to clinic 2 or 3, assuming the cold chain time limit is not violated. Notice that a clinic may receive vaccines that were delivered by both a health worker and a drone. In the above example, if the cold box capacity was 2.2 liters of vaccine, then clinic 3 could receive 0.2 liters of vaccine from the health worker and 0.3 liters of vaccine from a drone. The optimization model determines which clinic(s) will be served by drone to achieve the lowest total cost. In P2-D1 and P2-Dn, the total cost includes drone travel cost associated with each flight, in addition to the overnight cost and travel cost for non-drone modes.

The three models in this chapter are variants of the traveling salesman problem (TSP). Each subzone has a separate TSP, starting at the permanent clinic in the subzone. Thus there are two independent TSPs if there are two subzones in a health zone such as Figure 4.1 illustrated. The first optimization model P2-D0 is designed for a single subzone, as multiple subzones can be optimized independently. In the second and third optimization models, P2-D1 and P2-Dn, the independent TSP tours in a health zone may be connected by the drone delivery trips from the DC to temporary clinics, so for these models all subzones in a health zone are considered together.

4.2. Model formulations

This section provides the formulations for the three vaccine delivery models P2-D0, P2-D1, and P2-Dn. Model P2-D0 has no drones allowed, model P2-D1 has drones that can make one stop per trip, and model P2-Dn has drones that can make n>1 stops per drone trip. The three model formulations are presented in the following subsections, 4.2.1-4.2.3.

4.2.1. P2-D0

Let V denote the set of all nodes in a subzone which includes one permanent clinic and several temporary clinics. These are numbered sequentially with the permanent clinic being last, so $V = \{1,2, \ldots . |V-1|, |V|\}$, where node $\varphi = |V|$ is the permanent clinic. Let K be the set of transport modes, and P be the set of indices of the potential outreach trips by health workers to the temporary clinics, $P = \{1, 2, \ldots . |P|\}$, where $|P|$ is the number of potential outreach trips. However, there may be fewer than $|P|$ outreach trips used in a solution. Let binary variable λ^p track if there is a trip $p \in P$, so $\lambda^p = 1$ if

outreach trip p exists in a solution, and 0 otherwise. Let binary variable y_i^p track the nodes visited by a health worker in an outreach trip, so $y_i^p = 1$ if a health worker visits node $i \in V/\{\varphi\}$ in trip $p \in P$, and 0 otherwise. Let binary variable x_{ij}^{kp} track the arcs in an outreach trip, so $x_{ij}^{kp} = 1$ if a health worker travels from node $i \in V$ to node $j \in V$ by mode $k \in K$ in trip $p \in P$, and 0 otherwise. Health worker travel cost is represented by parameter c_{ij}^{kp}, which is the cost for travel from node $i \in V$ to node $j \in V$ by mode $k \in K$ in outreach trip $p \in P$. The corresponding health worker travel time from node $i \in V$ to node $j \in V$ by mode $k \in K$ is denoted by t_{ij}^k.

To handle scheduling of the multiple outreach trips in the model, time is measured in terms of the health worker work days starting from the departure of the first outreach trip. Thus the outreach trips are modeled as occurring sequentially (as if there was a single health worker at the permanent clinic to make all trips). Let b_i^p and s_i^p be continuous variables to track health worker departure time and vaccination start time at node $i \in V$ for outreach trip $p \in P$, respectively. The vaccination duration at node $i \in V\backslash\{\varphi\}$ and the duration of other health care at node $i \in V\backslash\{\varphi\}$ are denoted by v_i and o_i, respectively. The cumulative integer number of days (from the first day in the first outreach trip) to the completion of trip $p \in P$ is denoted by Θ^p. The cumulative integer number of days (from the first day in the first outreach trip) to the vaccination start time at node $i \in V$ in trip $p \in P$ is denoted by u_i^p. The cumulative integer number of days (from the first day in the first outreach trip) to the departure time at node $i \in V$ in trip $p \in P$ is denoted by π_i^p. The number of overnight stays by a health worker in outreach trip $p \in P$ is denoted by β^p. Each overnight stay will incur a cost ρ. D is the maximum

number of days allowed in an outreach trip. The daily working time limit of a health worker is Γ, so this is effectively the length of a day in problem P2. Time is tracked over each work day, where an overnight stay occurs after the end of a workday if the health worker has not returned to the permanent clinic that is their base (and the origin of their outreach trips). For example, suppose the health worker works from 9:00 am to 5:00 pm each day, and outreach trip 1 visits temporary clinic k at 3:00 pm on day 1 of the trip, and visits a second temporary clinic k' and 4:00 pm on day two of the trip, and then returns back to the origin permanent clinic on day three of the trip. For this trip, $s_k^1 = 6$ and $u_k^1 = 1$ (arrival at node k is 6 hours from the start of the trip on day 1), $s_{k'}^1 = 15$ and $u_{k'}^1 = 2$ (4:00 pm on day 2 is 15 work hours from the start of the trip on day 1), and $\Theta^1 = 3$. Thus, the models track the overnight stays and the total clock time the health worker is on an outreach trip.

The cold chain time limit is T, where T is measured in work hours. Thus if the cold chain time limit was 30 hours of wall clock time, and the health worker works eight hours a day from 9:00 am – 5:00 pm, then $T = 14$ hours, which is one day (8 hours of work and 24 hours of wall clock time) plus 6 hours of day 2. Models include the "cumulative integer number of days" from the start of the first trip (i.e., Θ^p, u_i^p, and π_i^p), along with the variables that track the start time of departure and vaccination at each node to ensure the start time of each day is correct. Finally, the demand (in liters of vaccine) at node $i \in V$ and the cold box capacity (or payload limit) of a health worker per trip are denoted by g_i and G'.

To illustrate how time is handled in the model, suppose the workday is 8 hours from 9:00 am to 5:00 pm, the vaccine cold chain limit is 26 hours, and there are two

outreach trips. Trip 1 is as follows: (i) 5 hours of travel to clinic 1, (ii) 1 hour for vaccination and other healthcare, (iii) 1 hour of travel to clinic 2, (iv) overnight at clinic 2, (v) 2 hours of vaccination and other health care at clinic 2, and (vi) 4 hours of travel back to the permanent clinic. For this trip, vaccination at clinic 1 starts at time $s_1^1 = 5$ hours, departure from clinic 1 is at $b_1^1 = 6$ hours, and arrival at clinic 2 is at 7 hours, which is too late in the work day to do the vaccination and other health care. On day 2, vaccination at clinic 2 starts at $s_2^1 = 8$ hours, departure from clinic 2 is at $b_2^1 = 10$ hours and the health worker arrives back at the permanent clinic after 14 hours of work time (at 3:00 pm on day 2). The integer variables for trip 1 are: $u_1^1 = \pi_1^1 = 1$ and $u_2^1 = \pi_2^1 = \Theta^1 = 2$. Suppose trip 2 is as follows: (i) 3 hours of travel to clinic 3, (ii) 1 hour for vaccination and other healthcare, (iii) 1 hour of travel to clinic 4, (iv) 1 hour for vaccination and other healthcare, and (v) 2 hours of travel back to the permanent clinic. For this trip, vaccination at clinic 3 starts at $s_3^2 = 19$ hours (3 hours into the third day), departure from clinic 3 is at $b_3^2 = 20$ hours, arrival at clinic 4 is at $s_4^2 = 21$ hours, departure from clinic 4 is at $b_4^2 = 22$ hours, with the health worker arriving back at the permanent clinic after 24 hours of work time (at 5:00 pm on day 3). The integer variable for trip 2 are: $u_3^2 = \pi_3^2 = u_4^2 = \pi_4^2 = \Theta^2 = 3$. Table 4.1 lists the sets, parameters, and decision variables in this model.

Sets	
V	Set of all nodes in a subzone including one permanent clinic and all temporary clinics. $V = \{1, 2, \ldots . \lvert V-1 \rvert, \lvert V \rvert\}$, where $\varphi = \lvert V \rvert$ is the permanent clinic, and the start and end node of all trips.
K	Set of transport modes
P	Set of outreach trips $P = \{1, 2, \ldots . \lvert P \rvert\}$
Parameters	

c_{ij}^{kp}	Cost for the travel from node $i \in V$ to node $j \in V$ by mode $k \in K$ in trip $p \in P$
t_{ij}^{k}	Health worker travel time from node $i \in V$ to node $j \in V$ by mode $k \in K$
v_i	Vaccination duration at node $i \in V \backslash \{\varphi\}$
o_i	Other treatment duration at node $i \in V \backslash \{\varphi\}$
T	Cold chain time limitation for vaccines measured in hours in terms of the work day length
Γ	Daily working time limit of a health worker, in hours (also day length in the model)
D	Maximum number of days allowed in each outreach trip
g_i	Vaccine demand at node $i \in V$ in liters
G'	Cold box capacity (payload limit) of a health worker per trip in liters
ρ	Cost for an overnight stay
M	A large number
ε	A small number
Decision Variables	
x_{ij}^{kp}	= 1 if a health worker travels from node $i \in V$ to node $j \in V$ by mode $k \in K$ in trip $p \in P$, and 0 otherwise
y_i^p	= 1 if a health worker visits node $i \in V$ in trip $p \in P$, 0 otherwise
s_i^p	Vaccination start time at node $i \in V$ in trip $p \in P$
b_i^p	Health worker departure time at node $i \in V$ in trip $p \in P$
Θ^p	Cumulative integer number of days (from the first day in the first trip) to the completion of trip $p \in P$, where $\Theta^0 = 0$
u_i^p	Cumulative integer number of days (from the first day in the first trip) to the vaccination start time at node $i \in V$ in trip $p \in P$
π_i^p	Cumulative integer number of days (from the first day in the first trip) to the departure time at node $i \in V$ in trip $p \in P$
λ^p	= 1 if there is a trip $p \in P$, 0 otherwise
β^p	Number of overnight stays in a trip $p \in P$

Table 4.1 Summary of notations in P2-D0

The goal is to determine the lowest total cost outreach trips (i.e., routes) for the health workers, which requires determining: (i) the outreach trips to serve a subzone in a

planning horizon (i.e., a month), (ii) the number of overnight stays of a health worker in a subzone in each trip, (iii) the departure time and vaccination start time at each node in each trip, and (iv) the set of travel arcs, so that the cold chain and daily work limit are never violated, and the cold box capacity (health worker payload limit) is respected. I present the MILP formulation for P2-D0 as follows:

P2-D0

Minimize:

$$\sum_{p\in P}\sum_{k\in K}\sum_{i\in V}\sum_{j\in V} x_{ij}^{kp} c_{ij}^{kp} + \rho \sum_{p\in P} \beta^{p} \quad 4.1$$

Subject to

$$\sum_{k\in K}\sum_{j\in V} x_{ij}^{kp} = y_i^p, \forall i \in V, \forall p \in P \quad 4.2$$

$$\sum_{k\in K}\sum_{i\in V} x_{ij}^{kp} = y_j^p, \forall j \in V, \forall p \in P \quad 4.3$$

$$\sum_{p\in P} y_i^p = 1, \forall i \in V\backslash\{\varphi\} \quad 4.4$$

$$s_j^p \geq b_i^p + \sum_{k\in K} t_{ij}^k x_{ij}^{kp} - M\left(1 - \sum_{k\in K} x_{ij}^{kp}\right), \forall i \in V, \forall j \in V\backslash\{\varphi\}, \forall p \in P \quad 4.5$$

$$b_i^p \geq s_i^p + v_i + o_i - M\left(1 - y_i^p\right), \forall i \in V, \forall p \in P \quad 4.6$$

$$u_i^p \geq \frac{s_i^p}{\Gamma}, \forall i \in V, \forall p \in P \quad 4.7$$

$$u_i^p \leq 1 - \varepsilon + \frac{s_i^p}{\Gamma}, \forall i \in V, \forall p \in P \quad 4.8$$

$$\pi_i^p \geq \frac{b_i^p}{\Gamma}, \forall i \in V, \forall p \in P \quad 4.9$$

$$\pi_i^p \leq 1 - \varepsilon + \frac{b_i^p}{\Gamma} \quad \forall i \in V, \forall p \in P \quad 4.10$$

$$\Theta^p \leq \pi_i^p + M\left(1 - \sum_{k\in K} x_{i\varphi}^{kp}\right), \varphi, i \in V, \forall p \in P \quad 4.11$$

$$\Theta^p \geq \pi_i^p, \varphi, i \in V, \forall p \in P \quad 4.12$$

$$s_i^p \leq \Gamma u_i^p, \forall i \in V, \forall p \in P \quad 4.13$$

$$s_i^p \geq \Gamma(u_i^p - 1), \forall i \in V, \forall p \in P \quad 4.14$$

$$s_i^p + v_i + o_i \le \Gamma u_i^p + M\left(1 - y_i^p\right), \forall i \in V, \forall p \in P \quad 4.15$$

$$s_i^p + v_i + o_i \ge \Gamma(u_i^p - 1), \forall i \in V, \forall p \in P \quad 4.16$$

$$b_i^p \le \Gamma \pi_i^p, \forall i \in V, \forall p \in P \quad 4.17$$

$$b_i^p \ge \Gamma(\pi_i^p - 1), \forall i \in V, \forall p \in P \quad 4.18$$

$$b_i^p + \sum_{k \in K} \sum_{j \in J} t_{ij}^k x_{ij}^{kp} \le \Gamma \pi_i^p, \forall i \in V \backslash \{\varphi\}, \forall p \in P \quad 4.19$$

$$b_i^p + \sum_{k \in K} \sum_{j \in J} t_{ij}^k x_{ij}^{kp} \ge \Gamma(\pi_i^p - 1), \forall i \in V \backslash \{\varphi\}, \forall p \in P \quad 4.20$$

$$s_j^p \le \Gamma \Theta^{p-1} + \sum_{k \in K} t_{\varphi j}^k x_{\varphi j}^{kp} + M\left(1 - \sum_{k \in K} x_{\varphi j}^{kp}\right), j \in V \backslash \{\varphi\}, \varphi, \forall p \in P \quad 4.21$$

$$s_j^p \ge \Gamma \Theta^{p-1} + \sum_{k \in K} t_{\varphi j}^k x_{\varphi j}^{kp} - M\left(1 - \sum_{k \in K} x_{\varphi j}^{kp}\right), j \in V \backslash \{\varphi\}, \varphi, \forall p \in P \quad 4.22$$

$$\beta^p \le \Theta^p - \Theta^{p-1} - \lambda^p + M(1 - \lambda^p), \forall p \in P \quad 4.23$$

$$\beta^p \ge \Theta^p - \Theta^{p-1} - \lambda^p, \forall p \in P \quad 4.24$$

$$s_i^p + v_i \le \Gamma \Theta^{p-1} + T + M\left(1 - \sum_{k \in K} x_{i\varphi}^{kp}\right), i \in V \backslash \{\varphi\}, \varphi, \forall p \in P \quad 4.25$$

$$b_i^p + \sum_{k \in K} t_{i\varphi}^k x_{i\varphi}^{kp} \le \Gamma \Theta^{p-1} + D\Gamma, i \in V \backslash \{\varphi\}, \varphi, \forall p \in P \quad 4.26$$

$$\sum_{i \in V} y_i^p g_i \le G' , \forall p \in P \quad 4.27$$

$$s_i^p \le D|P|\Gamma y_i^p , \forall i \in V, \forall p \in P \quad 4.28$$

$$b_i^p \le D|P|\Gamma y_i^p , \forall i \in V, \forall p \in P \quad 4.29$$

$$u_i^p \le D|P| y_i^p , \forall i \in V, \forall p \in P \quad 4.30$$

$$\pi_i^p \le D|P| y_i^p , \forall i \in V, \forall p \in P \quad 4.31$$

$$\Theta^p \le D|P| \sum_{i \in V} y_i^p , \forall p \in P \quad 4.32$$

$$\sum_{i \in V} y_i^p \le \left(|V| + 1\right)\lambda^p , \forall p \in P \quad 4.33$$

$$\lambda^p \le \lambda^{p-1} , \forall p \in P \backslash \{1\} \quad 4.34$$

$$x_{ij}^{kp} = \{0,1\}, i, j \in V, k \in K, p \in P \quad 4.35$$

$$y_i^p = \{0,1\}, i \in V, p \in P \quad 4.36$$

$$s_i^p \ge 0, i \in V, p \in P \quad 4.37$$

$$b_i^p \ge 0, i \in V, p \in P \quad 4.38$$

$$\Theta^p \in Z^* , p \in P \quad 4.39$$

$$u_i^p \in Z^*, i \in V, p \in P \quad 4.40$$

$$\pi_i^p \in Z^* , i \in V, \ p \in P \quad 4.41$$

$$\lambda^p = \{0,1\} , p \in P \quad 4.42$$

$\beta^p \in Z^*, p \in P$ 4.43

The objective function 4.1 minimizes the total cost, including the health worker travel cost in the first term and the overnight stay cost in the second term. Constraint 4.2 ensures that if node i is visited by a health worker in trip p, then there is only one arc out the node i in trip p. Constraint 4.3 ensures that if node j is visited by a health worker in trip p, then there is only one arc entering node j in trip p. Constraint 4.4 ensures that each node is visited exactly once on some trip in a planning horizon. Constraints 4.5 and 4.6 are precedence relationship constraints. Constraint 4.5 ensures a health worker can begin to administer vaccinations at a temporary clinic only after arrival at that clinic. Constraint 4.6 ensures a health worker can depart from a temporary clinic only after the vaccination and other care activities have finished. Constraints 4.7 and 4.8 calculate the cumulative integer number of days to the vaccination start time at a temporary clinic. For example, when the vaccination start time s_i^p at a temporary clinic i in trip p is less than Γ (the length of a work day), then the integer variable u_i^p will be 1 or greater from constraint 4.7, and it will be less than 2 from constraint 4.8; so in this case $u_i^p = 1$. In a similar fashion, constraint 4.9 and 4.10 determine the cumulative integer number of days for the departure time from a clinic at node $i \in V$ in trip $p \in P$. Constraint 4.11 and 4.12 determine the cumulative integer number of days for the completion of trip $p \in P$, based on the departure time from the last node visited on the trip. Constraints 4.13 and 4.14 ensure the vaccination start time s_i^p at node $i \in V$ in trip $p \in P$ is on the appropriate day (determined by u_i^p). For example, when $u_i^p = 2$, a health worker administers vaccinations at node $i \in V$ in the second day of trip $p \in P$, so if the work duration limit is 8 hours per

day ($\Gamma = 8$), then the vaccination start time s_i^p should be between 8 hours and 16 hours (counting the work time from the beginning of this trip). In a similar fashion, constraints 4.15 and 4.16 ensure the time of finishing all healthcare activities (i.e., vaccination and other care) at a node $i \in V$ in trip $p \in P$ is on the day that the vaccination at node i starts. Constraint 4.13-4.16 together ensure all healthcare activities at a temporary clinic are started and finished in the same day.

Constraints 4.17-4.20 are similar to constraints 4.13-4.16, but for the departure time from node i. Constraint 4.19-4.20 ensure the arrival time at a clinic is in the same day as the departure time from the preceding clinic (i.e., a health worker cannot arrive at a destination the day after they leave the previous clinic, because the travel time of health workers are part of their work time). Notice that there is no constraint to force the vaccination to start at a clinic the same day as a health worker departs from the same clinic (i.e., $u_i^p = \pi_i^p$), so there is the possibility for a health worker to depart from the clinic on the day after they finished the health care activities at the clinic (i.e. to spend overnight at the clinic after finishing all health care).

Constraints 4.21 and 4.22 ensure a health worker starts each trip at the beginning of a work day, where the term $\Gamma\theta^{p-1}$ accounts for the time (day) the previous trip finishes (where $\theta^0 = 0$). Constraints 4.23 and 4.24 calculate the number of overnights in a trip by a health worker, where the subtraction of the cumulative ending days of two sequential trips provides the number of days in the second trip. Constraint 4.25 ensures the cold chain requirement is satisfied for each clinic visit in each trip. Constraint 4.26 ensures the work hour limit is respected in each trip by ensuring the time to return to the permanent clinic is within the work limit of D days. Constraint 4.27 ensures the payload

(cold box) capacity is respected in each trip. Constraints 4.28-4.31 ensure s_i^p, b_i^p, u_i^p, π_i^p are 0 if y_i^p is 0 (i.e., if trip p does not visit node i). These are "big M" constraints where the coefficients of y_i^p provide tight constraints. Constraint 4.32 ensures θ^p is 0 if no clinic is visited in trip p (i.e. trip p does not exist in the solution). The coefficients to the left of $\sum_{i \in V} y_i^p$ are the smallest value to replace and tighten the value of M. Constraint 4.33 ensures no node is visited in trip p if there is no trip p. Constraint 4.34 ensures that the trips that exist in a solution are numbered sequentially starting with trip 1. Constraints 4.35 - 4.43 specify the domains for all the decision variables.

4.2.2. P2-D1

The first model P2-D0 is designed for a single subzone, while the second and third models are designed for a health zone containing multiple subzones. Thus, some of the sets in P2-D0 are modified in P2-D1 and P2-Dn. For problem P2-D1, drones can deliver vaccines to the health worker at a clinic on a direct trip from the drone distribution center (DC). For P2-D1 I assume all drone trips start and end at the same drone DC.

Let R denote the set of subzones, $R = \{1,2, \dots, |R|\}$. Let V^r denote the set of temporary clinics in subzone $r \in R$, such that $V^1 = \{1,2, \dots, |V^1|\}$, $V^2 = \{|V^1| + 1, \dots, |V^1| + |V^2|\}, \dots, V^{|R|} = \{\sum_{i=1}^{R-1}|V^i| + 1, \dots, \sum_{i=1}^{R-1}|V^i| + |V^{|R|}|\}$. (Notice that each V^r is like set V in P2-D0.) Let V^d denote the set of all temporary clinics that can be served by a drone, and I assume $V^d = \bigcup_{r=1}^{|R|} V^r$; hence all temporary clinics in the health zone can be served by drone. Let Δ denote the set of drone DC candidates for the health zone, such that $\Delta = \{|V^d| + 1, |V^d| + 2, \dots, |V^d| + |R|\}$, where node $\sigma = |V^d| + r$ represents

the drone DC candidate in subzone $r \in R$ for the health zone. A drone DC candidate is a permanent clinic, so I let Δ be the set of permanent clinics in a health zone. This model does not select the drone DC, which means the drone DC node σ in each run is a given location. For example, if there are two subzones in a health zone, then there will be two permanent clinics, and hence two drone DC candidates. Therefore, I can solve the P2-D1 model twice, to evaluate using each permanent clinic as the drone DC. (Note that the optimal cost from P2-D1 for a particular DC candidate location can be also used as part of the DC candidate cost in the national vaccine distribution problem P1.) Let V^a denote the set of all nodes for subzone a which includes all temporary clinics and the one permanent clinic for subzone a, $a \in R$. $V^a = V^r \cup \varphi$, where φ represents the permanent clinic in subzone a, which is also the drone DC candidate noted above. Let V denote the set of all nodes in the health zone, and $V = V^d \cup \Delta = \bigcup_{a=1}^{|R|} V^a$. As with model P2-D0, K is the set of transport modes for health workers, and P is the set of health worker trips in the planning horizon for each subzone, and $P = \{1,2, \ldots |P|\}$.

Nine decision variables for P2-D1are the same as in P2-D0: x_{ij}^{kp}, y_i^p, s_i^p, b_i^p, Θ^p, u_i^p, π_i^p, λ^p and β^p. Let binary variable $z_{\sigma i}$ be used to track whether the drone travels from DC σ to node $i \in V^d$, so when $z_{\sigma i} = 1$, then a drone serves clinic i from DC σ, and 0 otherwise. The landing (or delivery) time of the drone at node $i \in V^d$ is denoted by l_i. Let u_i be the cumulative integer number of days from the beginning of the time horizon to the takeoff time of a drone at node $i \in V^d$, and let π_i be the cumulative integer number of days from the beginning of the time horizon to the returning time of the drone to DC σ from node $i \in V^d$. Let g'^p_i denote the vaccine amount in liters delivered to node

$i \in V^r, r \in R$ in trip $p \in P$ by a health worker (carried in a cold box). Let g_i'' be the vaccine amount in liters delivered to node $i \in V^d$ by a drone. Let $\hat{T}_i^p$ be a binary variable to track if the arrival time of the health worker at node $i \in V^r, r \in R,$ in trip $p \in P$ is greater than the cold chain limitation. If $\hat{T}_i^p = 1$, then a drone instead of a health worker must serve that clinic (i.e. provide the needed vaccines).

Twelve parameters for P2-D1 are the same as in P2-D0: $t_{ij}^k, c_{ij}^{kp}, v_i, o_i, T, \Gamma, D, g_i$, G', ρ, M and ε. The drone travel time from DC σ to node $i \in V^d$ is denoted by $d_{\sigma i}$. The drone travel cost for the round trip from the DC σ to node $i \in V^d$ is denoted by $e_{\sigma i}$. The drone payload in liters is denoted by G. Table 4.2 lists sets, parameters, and decision variables in P2-D1.

Sets	
R	Set of subzones $R = \{1,2, \dots \lvert R \rvert\}$
V^r	Set of temporary clinics in subzone $r \in R$. $V^1 = \{1,2, \dots \lvert V^1 \rvert\}$, $V^2 = \{\lvert V^1 \rvert + 1, \dots \lvert V^2 \rvert\}, \dots, V^{\lvert R \rvert} = \{\sum_{i=1}^{R-1} \lvert V^i \rvert + 1, \dots, \sum_{i=1}^{R-1} \lvert V^i \rvert + \lvert V^{\lvert R \rvert} \rvert\}$
V^d	Set of all temporary clinics that can be served by drone, $V^d = \bigcup_{r=1}^{\lvert R \rvert} V^r$
Δ	Set of drone DC candidates for the health zone, such that $\Delta = \{\lvert V^d \rvert + 1, \lvert V^d \rvert + 2, \dots, \lvert V^d \rvert + \lvert R \rvert\}$, where $\sigma = \lvert V^d \rvert + r$ represents the drone DC in subzone $r \in R$ for the health zone. The drone DC σ is a given value in my research.
V^a	Set of all nodes for subzone a which includes all temporary clinics and the depot (a permanent clinic) for subzone a, $a \in R$. $V^a = V^r \cup \varphi$, where $\varphi = \lvert V^d \rvert + a$ represents the depot in subzone a
V	Set of all nodes in the health zone. $V = V^d \cup \Delta = \bigcup_{a=1}^{\lvert R \rvert} V^a$
K	Set of transport modes for health workers
P	Set of health worker outreach trips $P = \{1, 2, \dots . \lvert P \rvert\}$ for each subzone
Parameters	
c_{ij}^{kp}	Cost for the travel path from node $i \in V^a, a \in R$ to node $j \in V^a, a \in R$ by mode $k \in K$ in trip $p \in P$

t_{ij}^k	Health worker travel time from node $i \in V^a, a \in R$ to node $j \in V^a, a \in R$ by mode $k \in K$
σ	the given node number that is the DC and drone base
$d_{\sigma i}$	Drone travel time from the DC σ to node $i \in V^d$
$e_{\sigma i}$	Drone round trip travel cost from DC σ to node $i \in V^d$
v_i	Vaccination duration at node $i \in V^r, r \in R$
o_i	Other treatment duration at node $i \in V^r, r \in R$
T	Cold chain time limitation for vaccines
Γ	Daily working time limit of a health worker. Γ is also the length of a day.
D	Maximum number of days allowed in each trip
g_i	Vaccine demand at node $i \in V^r, r \in R$ in liters
G'	Payload (cold box) limit of a health worker per trip in liters
G	Drone payload in liters
ρ	Cost for an overnight stay of a health worker
M	A large number
ε	A small number

Decision Variables

x_{ij}^{kp}	= 1 if a health worker travels from node $i \in V^a, a \in R$ to node $j \in V^a, a \in R$ by mode $k \in K$ in trip $p \in P$, and 0 otherwise
y_i^p	= 1 if a health worker visits node $i \in V^r, r \in R$ in trip $p \in P$, 0 otherwise
s_i^p	Vaccination start time at node $i \in V^r, r \in R$ in trip $p \in P$
b_i^p	Health worker departure time at node $i \in V^r, r \in R$ in trip $p \in P$
Θ^p	Cumulative integer number of days (from the first day in the first trip) to the completion of trip $p \in P$
u_i^p	Cumulative integer number of days (from the first day in the first trip) to the vaccination start time at node $i \in V^r, r \in R$ in trip $p \in P$
π_i^p	Cumulative integer number of days (from the first day in the first trip) to the departure time at node $i \in V^r, r \in R$ in trip $p \in P$
λ^p	= 1 if there is an outreach trip $p \in P$ in the solution, 0 otherwise
β^p	Number of overnight stays in trip $p \in P$
$z_{\sigma i}$	= 1 if the drone travels from the DC σ to node $i \in V^d$, and 0 otherwise
l_i	The landing time of the drone at node $i \in V^d$

u_i	Cumulative integer number of days from the beginning of time horizon to the takeoff time of a drone at node $i \in V^d$
π_i	Cumulative integer number of days from the beginning of time horizon to the returning time of a drone at the drone DC σ from node $i \in V^d$
g'^p_i	Vaccine amount in liters delivered to node $i \in V^r, r \in R$ in trip $p \in P$ by health workers
g''_i	Vaccine amount in liters delivered to node $i \in V^d$ by a drone
$\hat{T}_i^p$	= 1 if the arrival time of the health worker at node $i \in V^r, r \in R$ in trip $p \in P$ is greater than the cold chain limitation, 0 otherwise.

Table 4.2 Summary of notations in P2-D1

In addition to the decisions required for P2-D0 (noted in Section 4.2.1 as (i) the outreach trips to serve a subzone in a planning horizon, (ii) the number of overnight stays of a health worker in each trip, (iii) the departure time and vaccination start time at each node in each trip, and (iv) the set of travel arcs), in problem P2-D1 one must also determine (v) the clinics to be (fully or partially) served by a drone, (vi) the landing time of a drone at a clinic to make sure the landing time of a drone and the vaccination start time at a clinic are synchronized, and (vii) the vaccine amount in liters delivered by a drone to a clinic if that clinic is served by drone. The MILP formulation for P2-D1 is as follows:

P2-D1

Minimize:

$$\sum_{p\in P}\sum_{k\in K}\sum_{i\in V^a}\sum_{j\in V^a}\sum_{a\in R} x_{ij}^{kp} c_{ij}^{kp} + 2\sum\nolimits_{i\in V^d} z_{\sigma i} e_{\sigma i} + \rho \sum\nolimits_{p\in P} \beta^p \qquad 4.44$$

Subject to

$$\textstyle\sum_{k\in K}\sum_{j\in V^a} x_{ij}^{kp} = y_i^p, \forall i \in V^a\backslash\{\varphi\}, \forall a \in R, \forall p \in P \qquad 4.45$$

$$\textstyle\sum_{k\in K}\sum_{i\in V^a} x_{ij}^{kp} = y_j^p, \forall j \in V^a\backslash\{\varphi\}, \forall a \in R, \forall p \in P \qquad 4.46$$

$$\sum_{p\in P} y_i^p = 1, \forall i \in V^r, \forall r \in R \quad 4.47$$

$$s_j^p \geq b_i^p + \sum_{k\in K} t_{ij}^k x_{ij}^{kp} - M\left(1 - \sum_{k\in K} x_{ij}^{kp}\right), \forall i,j \in V^a, \forall a \in R, , j \neq \varphi, \forall p \in P \quad 4.48$$

$$b_i^p \geq s_i^p + v_i + o_i - M\left(1 - y_i^p\right), \forall i \in V^a, \forall a \in R, \forall p \in P \quad 4.49$$

$$u_i^p \geq \frac{s_i^p}{\Gamma}, \forall i \in V^a, \forall a \in R, \forall p \in P \quad 4.50$$

$$u_i^p \leq 1 - \varepsilon + \frac{s_i^p}{\Gamma}, \forall i \in V^a, \forall a \in R, \forall p \in P \quad 4.51$$

$$\pi_i^p \geq \frac{b_i^p}{\Gamma}, \forall i \in V^a, \forall a \in R, \forall p \in P \quad 4.52$$

$$\pi_i^p \leq 1 - \varepsilon + \frac{b_i^p}{\Gamma}, \forall i \in V^a, \forall a \in R, \forall p \in P \quad 4.53$$

$$\Theta^p \leq \pi_i^p + M\left(1 - \sum_{k\in K} x_{i\varphi}^{kp}\right), \varphi, i \in V^a, \forall a \in R, \forall p \in P \quad 4.54$$

$$\Theta^p \geq \pi_i^p, \varphi, i \in V^a, \forall a \in R, \forall p \in P \quad 4.55$$

$$s_i^p \leq \Gamma u_i^p, \forall i \in V^a, \forall a \in R, \forall p \in P \quad 4.56$$

$$s_i^p \geq \Gamma(u_i^p - 1), \forall i \in V^a, \forall a \in R, \forall p \in P \quad 4.57$$

$$s_i^p + v_i + o_i \leq \Gamma u_i^p + M\left(1 - y_i^p\right), \forall i \in V^a, \forall a \in R, \forall p \in P \quad 4.58$$

$$s_i^p + v_i + o_i \geq \Gamma(u_i^p - 1), \forall i \in V^a, \forall a \in R, \forall p \in P \quad 4.59$$

$$b_i^p \leq \Gamma \pi_i^p, \forall i \in V^a, \forall a \in R, \forall p \in P \quad 4.60$$

$$b_i^p \geq \Gamma(\pi_i^p - 1), \forall i \in V^a, \forall a \in R, \forall p \in P \quad 4.61$$

$$b_i^p + \sum_{k\in K} \sum_{j\in J} t_{ij}^k x_{ij}^{kp} \leq \Gamma \pi_i^p, \forall i \in V^a \backslash \{\varphi\}, \forall a \in R, \forall p \in P \quad 4.62$$

$$b_i^p + \sum_{k\in K} \sum_{j\in J} t_{ij}^k x_{ij}^{kp} \geq \Gamma(\pi_i^p - 1), \ \forall i \in V^a \backslash \{\varphi\}, \forall a \in R, \forall p \in P \quad 4.63$$

$$s_j^p \leq \Gamma \Theta^{p-1} + \sum_{k\in K} t_{\varphi j}^k x_{\varphi j}^{kp} + M\left(1 - \sum_{k\in K} x_{\varphi j}^{kp}\right), \varphi, i \in V^a, \forall a \in R, \forall p \in P \quad 4.64$$

$$s_j^p \geq \Gamma \Theta^{p-1} + \sum_{k\in K} t_{\varphi j}^k x_{\varphi j}^{kp} - M\left(1 - \sum_{k\in K} x_{\varphi j}^{kp}\right), \varphi, i \in V^a, \forall a \in R, \forall p \in P \quad 4.65$$

$$s_i^p + v_i - (\Gamma \Theta^{p-1} + T) \geq M(\hat{T}_i^p - 1), i \in V^r, \forall r \in R, \forall p \in P \quad 4.66$$

$$s_i^p + v_i - (\Gamma \Theta^{p-1} + T) \leq M\hat{T}_i^p, i \in V^r, \forall r \in R, \forall p \in P \quad 4.67$$

$$b_i^p + \sum_{k\in K} t_{i\varphi}^k x_{i\varphi}^{kp} \leq \Gamma \Theta^{p-1} + D\Gamma, \varphi, i \in V^a, \forall a \in R, \forall p \in P \quad 4.68$$

$$\sum_{i\in V^r} g'^p_i \leq G', \forall i \in V^r, \forall r \in R, \forall p \in P \quad 4.69$$

$$g'^p_i \leq G' y_i^p, \forall i \in V^r, \forall r \in R, \forall p \in P \quad 4.70$$

$$g'^p_i \leq G'\left(1 - \hat{T}_i^p\right), \forall i \in V^r, \forall r \in R, \forall p \in P \quad 4.71$$

$$s_i^p \leq D \times |P| \Gamma y_i^p, \forall i \in V^r, \forall r \in R, \forall p \in P \quad 4.72$$

$b_i^p \leq D \times |P| \Gamma y_i^p \, , \forall i \in V^r, \forall r \in R, \forall p \in P$ 4.73

$u_i^p \leq D \times |P| y_i^p \, , \forall i \in V^r, \forall r \in R, \forall p \in P$ 4.74

$\pi_i^p \leq D \times |P| y_i^p \, , \forall i \in V^r, \forall r \in R, \forall p \in P$ 4.75

$\Theta^p \leq D \times |P| \sum_{i \in V^a} y_i^p \, , \forall a \in R, \forall p \in P$ 4.76

$\sum_{i \in V^a} y_i^p \leq |V^a| \lambda^p, \forall a \in R, \forall p \in P$ 4.77

$l_i \geq \sum_{p \in P} s_i^p - M(1 - z_{\sigma i}), \forall i \in V^d, \sigma \in \Delta$ 4.78

$l_i \leq \sum_{p \in P} s_i^p \, , \forall i \in V^d, \sigma \in \Delta$ 4.79

$u_i \geq \frac{l_i - z_{\sigma i} d_{\sigma i}}{\Gamma}, \forall i \in V^d, \sigma \in \Delta$ 4.80

$u_i \leq 1 - \varepsilon + \frac{l_i - z_{\sigma i} d_{\sigma i}}{\Gamma}, \forall i \in V^d, \sigma \in \Delta$ 4.81

$\pi_i \geq \frac{l_i + z_{\sigma i} d_{\sigma i}}{\Gamma}, \forall i \in V^d, \sigma \in \Delta$ 4.82

$\pi_i \leq 1 - \varepsilon + \frac{l_i + z_{\sigma i} d_{\sigma i}}{\Gamma}, \forall i \in V^d, \sigma \in \Delta$ 4.83

$u_i = \pi_i \, , \forall i \in V^d \, , \sigma \in \Delta$ 4.84

$z_{\sigma i} d_{\sigma i} + v_i \leq \Gamma \Theta^{p-1} + T, \forall i \in V^d, \sigma \in \Delta, \forall p \in P$ 4.85

$g_i'' \leq G z_{\sigma i} \, , \forall i \in V^d, \sigma \in \Delta$ 4.86

$g_i'' + \sum_{p \in P} g'^p_i = g_i, \forall i \in V^r, \forall r \in R$ 4.87

$l_i \leq D \times |P| \Gamma z_{\sigma i} \, , \forall i \in V^d, \sigma \in \Delta$ 4.88

$u_i \leq D \times |P| z_{\sigma i} \, , \forall i \in V^d, \sigma \in \Delta$ 4.89

$\pi_i \leq D \times |P| z_{\sigma i}, \forall i \in V^d, \sigma \in \Delta$ 4.90

$x_{ij}^{kp} = \{0,1\}, i, j \in V^a, a \in R, k \in K, p \in P$ 4.91

$y_i^p = \{0,1\}, i \in V^r, r \in R \, , p \in P$ 4.92

$s_i^p \geq 0, i \in V^r, r \in R, p \in P$ 4.93

$b_i^p \geq 0, i \in V^r, r \in R, p \in P$ 4.94

$u_i^p \in Z^*, i \in V^r, r \in R, p \in P$ 4.95

$\pi_i^p \in Z^*, i \in V^r, r \in R, p \in P$ 4.96

$z_{\sigma i} = \{0,1\} \, , i \in V^d, \sigma \in \Delta$ 4.97

$l_i \geq 0, i \in V^d$ 4.98

$u_i \in Z^*, i \in V^r, r \in R$ 4.99

$\pi_i \in Z^*, i \in V^r, r \in R$ 4.100

$g_i'' \geq 0, i \in V^d$ 4.101

$g'^{p}_{i} \geq 0, i \in V^{r}, \forall r \in R, p \in P$ 4.102

$\hat{T}^{p}_{i} = \{0,1\}, i \in V^{r}, r \in R, p \in P$ 4.103

Constraints 4.23, 4.24, 4.34, 4.39, 4.42 and 4.43 in P2-D0 are also used in P2-D1.

The objective function 4.44 minimizes the total cost including the total travel cost, total overnight cost, and the total drone trip cost. Constraints 4.45-4.65 have the same explanations as constraints 4.2-4.22, constraint 4.68 has the same explanation as constraint 4.26, and constraint 4.72-4.76 have the same explanation as constraints 4.28-4.32 (the only differences are the sets, since P2-D1 is modeled for a health zone and P2-D0 is modeled for a subzone). Constraints 4.66 and 4.67 set the value of $\hat{T}^{p}_{i}$. Constraint 4.67 forces $\hat{T}^{p}_{i} = 1$ when $s^{p}_{i} + v_{i} \geq \Gamma\Theta^{p-1} + T$, and constraint 4.66 forces $\hat{T}^{p}_{i} = 0$ when $s^{p}_{i} + v_{i} \leq \Gamma\Theta^{p-1} + T$. These two constraints also ensure that the cold chain limitation is respected when a health worker delivers vaccines to a clinic. Constraint 4.69 ensures the total vaccines delivered by a health worker in a trip is less than the health worker payload limit (i.e., the cold box capacity). Constraint 4.70 says a health worker cannot deliver vaccines to a clinic that they do not visit. Constraint 4.71 says when $\hat{T}^{p}_{i} = 0$, the vaccine delivered to clinic i by a health worker should be within the payload (cold box) capacity, and when $\hat{T}^{p}_{i} = 1$, a health worker cannot deliver vaccines to clinic i, as the vaccines would not be viable.

Constraint 4.77 is similar to constraint 4.33, and it ensures no node is visited in trip p if there is no trip p in the solution. Constraints 4.78 and 4.79 synchronize the landing time of a drone and the vaccination start time at a clinic. Constraints 4.80 and 4.81 calculate the cumulative integer number of days from the beginning of the time horizon to the takeoff time of the drone at node i. Constraints 4.82 and 4.83 calculate the

cumulative integer number of days from the beginning of the time horizon to the returning time of the drone from node i to the drone DC σ. Constraint 4.84 ensures a drone returns to the drone DC on the same day that the drone departs from the drone DC. Constraint 4.85 ensures the vaccines delivered by drone to a clinic are viable until the vaccination activity is finished. Constraint 4.86 ensures the vaccine liters delivered by drone to a clinic are within the drone payload limit. Constraint 4.87 ensures the demand at a clinic is satisfied by the combination of vaccines delivered by the drone and the health worker. Constraints 4.88-4.90 ensure l_i, u_i and π_i are 0 if $z_{\sigma i}$ is 0 (i.e., the drone does not deliver to node i). Again, $D \times |P|$ is the smallest value to replace and tighten the "big M" in these constraints. Constraints 4.91-4.103 specify the domains of the decision variables in P2-D1.

4.2.3. P2-Dn

Model P2-Dn extends the situation of model P2-D1 to allow drones to make multiple stops per trip. This requires some additional parameters and variables to track the drone routes. As in P2-D1, drones can deliver vaccines to the health worker at a clinic, but now that delivery may be part of a multi-stop drone route. As with P2-D1, I assume all drone trips (routes) start and end at the same drone DC.

Eight sets in P2-Dn are the same as in P2-D1 and they are: R, V^r, V^d, Δ, V^a, V, K and P. Among these sets, K and P are common sets in all three models for P2. There are two unique sets in P2-Dn. The set V^s is the set of nodes that a drone can stop at, such as $V^s = V^d \cup \sigma$, so this set includes all temporary clinics and the drone DC. The set H is the set of drone trips in the planning horizon, $H = \{1,2, \ldots |H|\}$. Note that a solution may not use all the allowed drone trips.

Eleven decision variables in P2-Dn are the same as in P2-D1, and they are: x_{ij}^{kp}, $y_i^p, s_i^p, b_i^p, u_i^p, \pi_i^p, g'^p_i, \hat{T}_i^p, \Theta^p, \lambda^p$ and β^p. These eleven decision variables are related to the activities of the health workers, so they are the same in the two models. There are seven new decision variables in P2-Dn. Let z_{ij}^h be a binary variable to track drone travel from node $i \in V^s$ to node $j \in V^s$ in drone trip $h \in H$. A drone travels from node i to node j as part of trip h if $z_{ij}^h = 1$, and 0 otherwise. Let binary variable w_i^h track if a drone visits node $i \in V^d$ in trip $h \in H$ in which case $w_i^h = 1$, and $w_i^h = 0$ otherwise. Let l_i^h denote the landing time of a drone at node $i \in V^s$ in trip $h \in H$. The cumulative integer number of days from the beginning of the time horizon to the takeoff time of a drone at node $i \in V^d$ in a drone trip $h \in H$ is denoted by u'^h_i. The cumulative integer number of days from the beginning of the time horizon to the landing time of a drone at the next node after node $i \in V^s$ in drone trip $h \in H$ is denoted by π'^h_i. The above two decision variables are used to ensure that a drone finishes its trip in the same day that it started. Let binary variable $\delta^h = 1$ if there is a drone trip $h \in H$ in the solution, and 0 otherwise. Let g''^h_i denote the vaccine in liters delivered by drone to node $i \in V^d$ in drone trip $h \in H$.

There are thirteen parameters in P2-Dn that are the same as in P2-D1, and they are: $t_{ij}^k, c_{ij}^{kp}, v_i, o_i, T, \Gamma, D, \rho, g_i, G', G, M$ and ε. There are three new parameters in P2-Dn. The maximum flight range of a drone in minutes is denoted by τ. The drone travel time from node $i \in V^s$ to node $j \in V^s$ is denoted by d_{ij}. The drone travel cost from node $i \in V^s$ to node $j \in V^s$ in drone trip $h \in H$ is denoted by e_{ij}^h. It is worth noting that any node visited in a drone trip (i.e., for a delivery of vaccines) is also on a trip of a health worker. Table 4.3 lists sets, parameters, and decision variables in P2-Dn.

Sets	
R	Set of subzones $R = \{1,2, \dots \lvert R \rvert\}$
V^r	Set of temporary clinics in subzone $r \in R$. $V^1 = \{1,2, \dots \lvert V^1 \rvert\}$, $V^2 = \{\lvert V^1 \rvert + 1, \dots \lvert V^2 \rvert\}, \dots, V^{\lvert R \rvert} = \{\lvert V^{\lvert R-1 \rvert} \rvert + 1, \dots, \lvert V^{\lvert R \rvert} \rvert\}$
V^d	Set of all temporary clinics that can be served by drone, $V^d = \bigcup_{r=1}^{\lvert R \rvert} V^r$
Δ	Set of drone DC candidates for the health zone, such that $\Delta = \{\lvert V^d \rvert + 1, \lvert V^d \rvert + 2, \dots, \lvert V^d \rvert + \lvert R \rvert\}$, where $\sigma = \lvert V^d \rvert + r$ represents the drone DC in subzone $r \in R$ for the health zone. The drone DC σ in each run is fixed.
V^a	Set of all nodes for subzone a which includes all temporary clinics and the depot (a permanent clinic) for subzone a, $a \in R$. $V^a = V^r \cup \varphi$, where φ represents the depot in subzone a
V^s	Set of nodes that a drone can stop at (i.e. deliver to), $V^s = V^d \cup \sigma$
H	Set of drone trips $H = \{1,2, \dots \lvert H \rvert\}$
V	Set of all nodes in the health zone, $V = V^d \cup \Delta = \bigcup_{a=1}^{\lvert R \rvert} V^a$
K	Set of transport modes for health workers
P	Set of health worker trips $P = \{1, 2, \dots . \lvert P \rvert\}$ for each subzone
Parameters	
c_{ij}^{kp}	Cost for the travel path from node $i \in V^a, a \in R$ to node $j \in V^a, a \in R$ by mode $k \in K$ in trip $p \in P$
t_{ij}^k	Health worker travel time from node $i \in V^a, a \in R$ to node $j \in V^a, a \in R$ by mode $k \in K$
σ	the given node number that is the DC and drone base
d_{ij}	Drone travel time from node $i \in V^s$ to node $j \in V^s$.
e_{ij}^h	Drone travel cost from node $i \in V^s$ to node $j \in V^s$ in drone trip $h \in H$
v_i	Vaccination duration at node $i \in V^r, r \in R$
o_i	Other treatment duration at node $i \in V^r, r \in R$
T	Cold chain time limitation for vaccines
Γ	Daily working time limit of a health worker. Γ is also the length of a day.
D	Maximum number of days allowed in each health worker outreach trip
g_i	Vaccine demand at node $i \in V^r, r \in R$ in liters
G'	Payload limit (cold box capacity) for a health worker per trip in liters
G	Drone payload in liters
ρ	Cost for an overnight stay of a health worker

τ	Maximum flight range of a drone in minutes
M	A large number
ε	A small number
	Decision Variables
x_{ij}^{kp}	= 1 if a health worker travels from node $i \in V^a, a \in R$ to node $j \in V^a, a \in R$ by mode $k \in K$ in trip $p \in P$, and 0 otherwise
y_i^p	= 1 if a health worker visits node $i \in V^r, r \in R$ in trip $p \in P$, 0 otherwise
s_i^p	Vaccination start time at node $i \in V^r, r \in R$ in trip $p \in P$
b_i^p	Health worker departure time at node $i \in V^r, r \in R$ in trip $p \in P$
Θ^p	Cumulative integer number of days (from the first day in the first trip) to the completion of trip $p \in P$
u_i^p	Cumulative integer number of days (from the first day in the first trip) to the vaccination start time at node $i \in V^r, r \in R$ in trip $p \in P$
π_i^p	Cumulative integer number of days (from the first day in the first trip) to the departure time at node $i \in V^r, r \in R$ in trip $p \in P$
λ^p	= 1 if there is a trip $p \in P$ in the solution, 0 otherwise
β^p	Number of overnight stays in trip $p \in P$
z_{ij}^h	= 1 if a drone travels from node $i \in V^s$ to node $j \in V^s$ in trip $h \in H$, and 0 otherwise
w_i^h	= 1 if a drone visits node $i \in V^d$ in trip $h \in H$, and 0 otherwise
l_i^h	The landing time of a drone at node $i \in V^s$ in drone trip $h \in H$
u'^h_i	Cumulative integer number of days from the beginning of time horizon to the takeoff time of drone at node $i \in V^d$ in drone trip $h \in H$
π'^h_i	Cumulative integer number of days from the beginning of time horizon to the landing time of a drone at the next node after node $i \in V^s$ in drone trip $h \in H$
g'^p_i	Vaccine amount in liters delivered to node $i \in V^r, r \in R$ in trip $p \in P$ by a health worker
g''^h_i	Vaccine amount in liters delivered to node $i \in V^d$ in drone trip $h \in H$
$\hat{T}_i^p$	= 1 if the arrival time of the health worker at node $i \in V^r, r \in R$ in trip $p \in P$ is greater than the cold chain limitation, 0 otherwise
δ^h	= 1 if there is a drone trip $h \in H$ in the solution, and 0 otherwise

Table 4.3 Summary of notations in P2-Dn

Besides the decisions (i)-(iv) in P2-D0, and (v)-(vii) in P2-D1 (noted above in Sections 4.2.1 and 4.2.2), model P2-Dn also determines (viii) the clinics that are served by drone in each drone trip and the precedence relationship among these clinics, (ix) the precedence relationship between the last node in a drone trip and the first node in the following drone trip (if it exists). The model also ensures the cold chain time limit and drone range limit are respected in drone trips. I present the MILP formulation for P2-Dn as follows:

P2-Dn

Minimize:

$$\sum_{p\in P}\sum_{k\in K}\sum_{i\in V^a}\sum_{j\in V^a}\sum_{a\in R} x_{ij}^{kp} c_{ij}^{kp} + \sum_{h\in H}\sum_{i\in V^s}\sum_{j\in V^s} z_{ij}^{h} e_{ij}^{h} + \rho \sum_{p\in P} \beta^{p} \quad 4.104$$

Subject to

Constraints 4.23, 4.24, 4.34, 4.39, 4.42 and 4.43 in P2-D0

Constraints 4.45-4.65, 4.67-4.77, 4.91-4.94, 4.95-4.96 and 4.102-4.103 in P2-D1

$s_i^p + v_i - \left(\Gamma\theta^{p-1} + T - M\left(1 - \sum_{h\in H} w_i^h\right)\right) \geq M\left(\hat{T}_i^p - 1\right), \forall i \in V^r, \forall r \in R, \forall p \in P$ 4.105

$\sum_{i\in V^s} z_{ij}^h \leq 1\ , \forall j \in V^d, \forall\ h \in H$ 4.106

$\sum_{j\in V^s} z_{ij}^h \leq 1, \forall i \in V^d, \forall\ h \in H$ 4.107

$\sum_{i\in V^s} z_{ij}^h = w_j^h\ , \forall j \in V^d, \forall\ h \in H$ 4.108

$\sum_{i\in V^s} z_{ji}^h = w_j^h\ , \forall j \in V^d, \forall\ h \in H$ 4.109

$\sum_{j\in V^d} z_{\sigma j}^h = \delta^h, \sigma \in \Delta, \forall\ h \in H$ 4.110

$\sum_{j\in V^d} z_{j\sigma}^h = \delta^h\ , \sigma \in \Delta, \forall\ h \in H$ 4.111

$l_j^h \geq l_i^h + z_{ij}^h d_{ij} - M(1 - z_{ij}^h), \forall i, j \in V^s, i \neq j, \forall\ h \in H$ 4.112

$l_j^h \geq l_i^{h-1} + z_{i\sigma}^{h-1} d_{i\sigma} + z_{\sigma j}^h d_{\sigma j} - M(1 - z_{\sigma j}^h) - M(1 - z_{i\sigma}^{h-1}), i, j \in V^d, \sigma \in \Delta, i \neq j, \forall\, h \in H \backslash \{1\}$ 4.113

$\sum_{h \in H} l_i^h \geq \sum_{p \in P} s_i^p - M(1 - \sum_{h \in H} w_i^h)\ , \forall i \in V^d, \forall\, h \in H$ 4.114

$\sum_{h \in H} l_i^h \leq \sum_{p \in P} s_i^p + M(1 - \sum_{h \in H} w_i^h), \forall i \in V^d, \forall\, h \in H$ 4.115

$l_j^h + v_j - l_i^h + z_{\sigma i}^h d_{\sigma i} \leq T + M(1 - z_{j\sigma}^h) + M(1 - z_{\sigma i}^h)\ \ i, j \in V^d, \sigma \in \Delta, i \neq j, \forall\, h \in H$ 4.116

$l_j^h + z_{j\sigma}^h d_{j\sigma} - l_i^h + z_{\sigma i}^h d_{\sigma i} \leq \tau + M\left(1 - z_{j\sigma}^h\right) + M\left(1 - z_{\sigma i}^h\right), i, j \in V^d, \sigma \in \Delta, i \neq j, \forall\, h \in H$ 4.117

$u'^h_i \geq \frac{l_i^h - \sum_{j \in V^s} z_{ji}^h d_{ji} - M\left(1 - \sum_{j \in V^s} z_{ji}^h\right)}{\Gamma}, \forall i \in V^d, \forall\, h \in H$ 4.118

$u'^h_i \leq 1 - \varepsilon + \frac{l_i^h - \sum_{j \in V^s} z_{ji}^h d_{ji} + M(1 - \sum_{j \in V^s} z_{ji}^h)}{\Gamma}, \forall i \in V^d, \forall\, h \in H$ 4.119

$\pi'^h_i \geq \frac{l_i^h + \sum_{j \in V^s} z_{ij}^h d_{ij} - M(1 - \sum_{j \in V^s} z_{ij}^h)}{\Gamma}, \forall i \in V^d, \forall\, h \in H$ 4.120

$\pi'^h_i \leq 1 - \varepsilon + \frac{l_i^h + \sum_{j \in V^s} z_{ji}^h d_{ji} + M(1 - \sum_{j \in V^s} z_{ij}^h)}{\Gamma}, \forall i \in V^d, \forall\, h \in H$ 4.121

$u'^h_i \geq \pi'^h_j - M\left(1 - w_i^h\right) - M\left(1 - w_j^h\right), \forall i, j \in V^d, \forall\, h \in H$ 4.122

$u'^h_i \leq \pi'^h_j + M\left(1 - w_i^h\right) + M\left(1 - w_j^h\right), \forall i, j \in V^d, \forall\, h \in H$ 4.123

$u'^h_i \leq D|P| w_i^h\ , \forall i \in V^d, \forall\, h \in H$ 4.124

$\pi'^p_i \leq D|P| w_i^h\ , \forall i \in V^d, \forall\, h \in H$ 4.125

$\sum_{i \in V^d} g''^h_i \leq\ G, \forall\, h \in H$ 4.126

$g''^h_i \leq G\, w_i^h\ , \forall i \in V^d, \forall h \in H$ 4.127

$\sum_{h \in H} g''^h_i + \sum_{p \in P} g'^p_i = g_i\ , i \in V^r, r \in R$ 4.128

$\delta^h \leq \delta^{h-1},\ \forall\, h \in H \backslash \{1\}$ 4.129

$\sum_{i \in V^d} w_i^h \leq |V^d| \delta^h, \forall\, h \in H$ 4.130

$l_j^h \leq D|P| \Gamma w_j^h, \forall j \in V^s, \forall\, h \in H$ 4.131

$z_{ij}^h = \{0,1\}, i, j \in V^s, \forall\, h \in H$ 4.132

$w_i^h = \{0,1\}, i \in V^d, h \in H$ 4.133

$l_i^h \geq 0\ , i \in V^d,\ h \in H$ 4.134

$\delta^h = \{0,1\}\ , h \in H$ 4.135

$g''^h_i \geq 0, i \in V^d, \forall\, h \in H$ 4.136

The objective function 4.104 minimizes the total cost including the total travel cost incurred by health workers, the total overnight stay cost, and the total drone travel cost. Constraint 4.105 ensures that a drone will deliver vaccines to a clinic if the vaccines would not be viable when delivered by a health worker. Constraint 4.106 ensures that there is at most one drone arc into a clinic visited by a drone in a drone trip. Constraint 4.107 ensures that there is at most one drone arc out of a clinic visited by a drone in a drone trip. These two constraints show that not all clinics have to be served by drone. Constraints 4.108 and 4.109 ensure that if a clinic is visited by a drone, then there is one drone arc into the clinic node and one drone arc out of that clinic node. Constraints 4.110 and 4.111 say if there is a drone trip used in the solution then there is a drone arc for that trip out of a drone DC and a drone arc for that trip into the drone DC.

Constraint 4.112 is the precedence relationship between two consecutive drone stops in a drone trip, and it ensures that the time the drone lands (or delivers) at the next stop is after the drone travels from the previous stop. Constraint 4.113 is a precedence relationship constraint for the last stop in a drone trip, and the first stop in the next drone trip (if it exist). It ensures if there are two drone trips, then a drone lands (delivers) at the first clinic in the next drone trip after the drone returns to the drone DC from the prior drone trip and travels to the first clinic in the next drone trip. Constraints 4.114 and 4.115 synchronize the landing time of a drone in a drone trip at a clinic with the vaccination start time at the clinic in a health worker trip. Constraint 4.116 ensures the vaccine is viable when the vaccination activity finishes at the last stop in a drone trip. Constraint 4.117 ensures the drone range in each drone trip is respected. Constraints 4.118 and 4.119 set the value of u'^{h}_{i} , the cumulative integer number of days from the beginning of the

planning horizon to the takeoff time of a drone at clinic i in a drone trip. Constraints 4.120 and 4.121 set the value of π'^{h}_{i} , the cumulative integer number of days from the beginning of the planning horizon to the landing of a drone at the next clinic after node i in a drone trip.

Constraints 4.122 and 4.123 ensure a drone finishes a drone trip in the same day from the takeoff to returning to the drone DC. Constraints 4.124, 4.125 and 4.131 ensure u'^{h}_{i}, π'^{h}_{i} and l^{h}_{i} are 0 if node i is not visited by a drone in trip h. Constraint 4.126 ensures the amount of vaccines delivered by a drone in a drone trip are within the drone payload limit. Constraint 4.127 ensures a clinic will not receive vaccines from a drone if a drone does not visit that clinic, and it also ensures the vaccine amount in liters delivered to a clinic is within the drone payload limit if a drone visits that clinic. Constraint 4.128 ensures the demand of vaccines at a clinic is satisfied by either a drone or a health worker or both. Constraint 4.129 ensures the drone trips in a solution are sequential beginning with drone trip 1. Constraint 4.130 ensures that no clinics are visited by a drone trip that is not part of the solution (i.e., when δ^{h}=0). Constraints 4.132-4.136 specify the domain of the decision variables.

4.3. Data

The three models presented above are used to solve illustrative examples for one health zone in Vanuatu. This section provides the data used in the solutions that are presented in the following section. These data are based on the health zone that comprises Erromongo Island and is shown in Figure 4.1. This includes two subzones, where subzone A has permanent clinic 9 and temporary clinics 1-3, and subzone B has permanent clinic 10 and temporary clinics 4-8. Health workers are based at permanent

clinics 9 and 10 and make outreach trips to serve the temporary clinics in their subzone. Table 4.4 lists the travel time and cost, t_{ij}^{k} and c_{ij}^{kp}, for both walking (i.e., t_{ij}^{w}, c_{ij}^{wp}) and boat (i.e., t_{ij}^{b}, c_{ij}^{bp}) for 21 undirected health worker arcs (i.e., 42 directed arcs) that are used in all the three P2 models for Erromango.

Subzone	**Node**	**Node**	$\boldsymbol{t_{ij}^{w}}$ **(minutes)**	$\boldsymbol{t_{ij}^{b}}$ **(minutes)**	$\boldsymbol{c_{ij}^{wp}}$ **(dollars)**	$\boldsymbol{c_{ij}^{bp}}$ **(dollars)**
A	9	1	188.72	37.74	78.63	110.09
	9	2	223.93	44.79	93.30	130.62
	9	3	252.96	50.59	105.4	147.56
	1	2	14.256	2.85	5.94	8.32
	1	3	57.31	11.46	23.88	33.43
	2	3	41.94	8.39	17.47	24.46
B	10	4	351.53	22.79	146.47	205.06
	10	5	118.53	23.71	49.39	69.14
	10	6	113.94	70.31	47.48	66.47
	10	7	146.76	65.69	61.15	85.61
	10	8	328.43	29.35	136.85	191.58
	4	5	331.55	66.31	138.14	193.40
	4	6	361.2	72.24	150.5	210.7
	4	7	514.96	102.99	214.58	300.39
	4	8	520.56	104.11	216.9	303.66
	5	6	232.58	46.52	96.91	135.67
	5	7	294.61	58.92	122.75	171.86
	5	8	421.15	84.23	175.48	245.67
	6	7	45.14	9.03	18.81	26.33
	6	8	252.47	50.49	105.20	147.27
	7	8	196.44	39.29	81.85	114.59

Table 4.4 Travel time and cost of health worker arcs in P2

The travel time t_{ij}^{k} is the product of haversine distance in kilometers and a circuity factor for each arc, divided by the speed of the modes. I assume the average walking and boat speeds are 5 km/h and 25 km/h, respectively. The travel cost c_{ij}^{kp} is the product of haversine distance in kilometers of each arc, a circuity factor for each arc, and the unit cost of each mode. I assume the unit cost of walking and boat are \$5/km and \$7/km, respectively. The circuity factors noted above are designed to account for the indirect travel by walking or boat due to the topography, trails, geography, etc.

Table 4.5 shows v_i, o_i and g_i, the demand, the vaccination duration, and other treatment duration at a clinic i. As in problem P1, the demand is the number of children in each clinic (FIC) multiplied by 0.05 liters. The historical total number of FICs for each subzone is provided by Ministry of Health Vanuatu (2018), where subzone A has 24 FIC and subzone B has 44 FIC. Details for each clinic are not provided, so the FIC of each clinic is assigned arbitrarily in Table 4.5. Since P2 does not include the vaccination and other treatment activities at permanent clinics, Table 4.5 does not show the FIC for nodes 9 and 10. I assume it takes 2.5 minutes to vaccinate a FIC on average, thus the vaccination duration is the number of FIC multiplied by 2.5. The other treatment duration for each clinic is assigned arbitrarily.

Subzone	Node	v_i (minutes)	o_i (minutes)	#FIC	g_i (liter)
A	1	10	35	4	0.2
	2	15	20	6	0.3
	3	12.5	30	5	0.25
B	4	17.5	20	7	0.35
	5	12.5	32	5	0.25
	6	10	30	4	0.2
	7	25	35	10	0.5
	8	27.5	33	11	0.55

Table 4.5 Vaccination duration v_i, other treatment duration o_i, and demand g_i for each clinic in P2

The cold chain limitation T used in P2 is 7.5 hours, and the daily work hour limitation for health workers Γ is 9 hours. The payload of a health worker G' is 1 liter. The overnight stay cost per night ρ is \$20.

Because the geographical area of a typical health zone in Vanuatu is small, I assume a small delivery drone would be used in problem P2. The drone range data, payload data, and the unit travel cost per kilometer in our illustration are from JSI and LLamasoft (2019) for a small hybrid drone. This drone has a range τ of 85 km and a unit travel cost of \$0.77/km. For these scenarios, I assume the payload capacity G is 1 liter, as it is more reasonable for a small drone. The unit travel cost is the total fixed and variable cost per kilometer that considers the cost of the drone, battery, energy, and maintenance. Table 4.6 shows $d_{\sigma i}$ and $e_{\sigma i}$, the drone travel time and travel cost for each drone arc in P2-D1. Node 9 is the DC and drone base for solution illustrations in section 4.4, so each drone arc starts from node 9 and goes to a temporary clinic in the health zone. The travel time is the haversine distance divided by the drone speed, which is assumed to be 70

km/h. The travel cost is the haversine distance multiplied by the drone unit travel cost (i.e., \$0.77/km). Similarly, Table 4.7 shows d_{ij} and e_{ij}^{h}, the drone travel time and travel cost for each drone arc in P2-D2.

Node	Node	$d_{\sigma i}$ (minutes)	$e_{\sigma i}$ (dollars)
9	1	7.93	7.12
9	2	8.89	7.98
9	3	11.29	10.14
9	4	18.41	16.54
9	5	30.35	27.26
9	6	17.69	15.89
9	7	17.96	16.13
9	8	18.20	16.35

Table 4.6 Travel time and travel cost of drone arcs in P2-D1

Node	Node	d_{ij} (minutes)	e_{ij}^{h} (dollars)
9	1	7.93	7.12
9	2	8.89	7.98
9	3	11.29	10.14
9	4	18.41	16.54
9	5	30.35	27.26
9	6	17.69	15.89
9	7	17.96	16.13
9	8	18.2	16.35
1	2	1.02	0.91
1	3	3.72	3.34
1	4	11.82	10.62
1	5	25.66	23.05
1	6	16.44	14.77
1	7	18.09	16.25

1	8	19.48	17.5
2	3	2.72	2.45
2	4	10.88	9.78
2	5	24.88	22.35
2	6	16.18	14.53
2	7	17.98	16.16
2	8	19.51	17.53
3	4	8.23	7.39
3	5	22.51	20.22
3	6	15.17	13.63
3	7	17.37	15.6
3	8	19.22	17.27
4	5	14.8	13.3
4	6	12.9	11.59
4	7	15.99	14.37
4	8	18.59	16.7
5	6	15.1	13.57
5	7	17.54	15.75
5	8	20.05	18.02
6	7	3.22	2.9
6	8	6.01	5.4
7	8	2.81	2.52

Table 4.7 Travel time d_{ij} and travel cost e_{ij}^{h} of drone arcs in P2-D2

4.4. Solution illustration

To demonstrate the capability of the P2 models, seven scenarios using the three vaccine delivery models are illustrated in this section. One scenario is the baseline with no drones, and 1-day 1-stop health worker trips. The other six scenarios consider either 1-day or multi-day health worker trips with each of the three models P2-D0, P2-D1, and P2-Dn. A 1-day trip means the health worker spends every night back at their depot

(permanent clinic), so each tour is limited to 9 hours. A multi-day trip allows the health worker to spend one or more overnights at a temporary clinic (for a cost) before returning back to their depot. Table 4.8 summarizes the seven scenarios. All scenarios except the baseline allow multiple stops in a health worker tour. For the computational analysis, a maximum of 3 days are allowed in the multi-day trips (i.e., D=3).

Scenarios	#Drone stops	Conditions on health worker tours
Baseline	0	1 –day, 1-stop
P2-D0-1day	0	1-day, multi-stop
P2-D0-nday	0	Multi-day, multi-stop
P2-D1-1day	1	1-day, multi-stop
P2-D1-nday	1	Multi-day, multi-stop
P2-Dn-1day	n	1-day, multi-stop
P2-Dn-nday	n	Multi-day, multi-stop

Table 4.8 Scenarios in P2

Optimal solutions were found for each of the seven scenarios in Table 4.8 using the appropriate model. All problems were solved on an HP Intel Quard-Core i7 with 3.9 Ghz CPU and 64 GB RAM using Gurobi 9.1. The wall clock times for solutions ranged from 0.37 to 416.37 seconds, and all problems solved to optimality. The scenarios that is the hardest to solve is P2-Dn-1day (i.e., 416.37 seconds), and it took 291 times more time than P2-D1-1day to solve, and 13 times more time than P2-Dn-nday to solve.

Figure 4.2 shows the health worker tours in the optimal solution for the Baseline scenario. The baseline is solved by limiting the number of days allowed in a trip to be 1 (i.e., D=1) and the number of health worker stops in a trip to be 1 in P2-D0 by changing constraints 4.2 and 4.3 to $\sum_{k\in K} x_{\varphi j}^{kp} = y_j^p$ and $\sum_{k\in K} x_{j\varphi}^{kp} = y_j^p$, where φ is the depot

(permanent clinic) for each subzone. This solution uses 8 trips to serve the 8 temporary clinics, and each trip is finished in one day. There are no precedence relationships among the 8 trips, so a health worker at subzone A can choose to serve the three temporary clinics in any order, as the health worker can do for the 5 trips in subzone B. This solution uses three boat arcs, which are more expensive but faster than walking arcs, to ensure the health worker can return to their depot within 9 hours for each trip (given the limit of one-day per trip). The total cost for baseline is $1593.

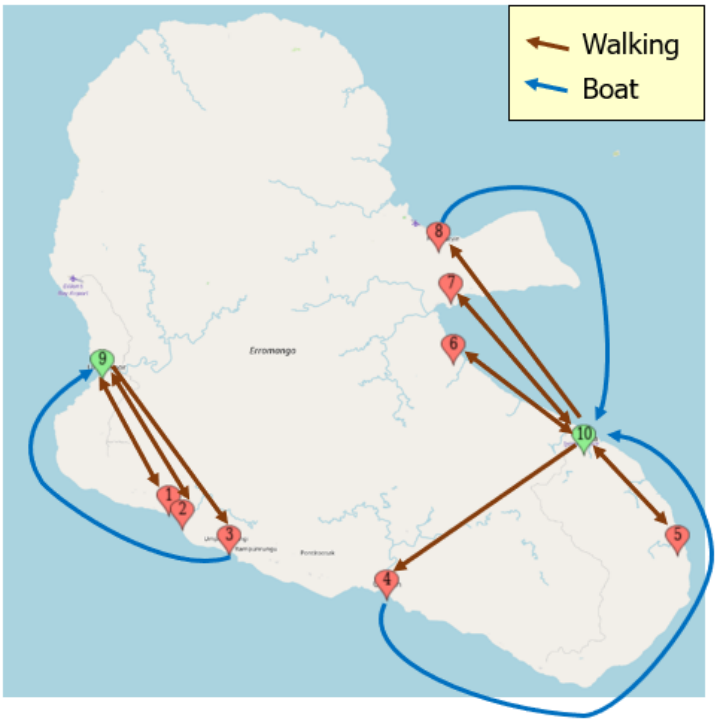

Figure 4.2 Solution for the Baseline scenario

P2-D0 Scenarios

Figure 4.3 shows the solution for the P2-D0-1day scenario. Subzone A is served on one trip visiting clinics 3, 2 and 1, with a boat used for the return to the depot (node 9) to ensure the trip is only one day long. Subzone B is served with three separate trips, each

taking one day, and shown with different line (dash) styles. One trip visits node 5 by boat, then node 4 by boat and then returns to the depot (node 10) by walking. The use of faster boat travel to visit nodes 5 and 4 ensures the cold chain is maintained for the vaccines; and lower cost, slower walking is used to return to the depot. The total cost is $1104, and it saves 31% compared to the baseline.

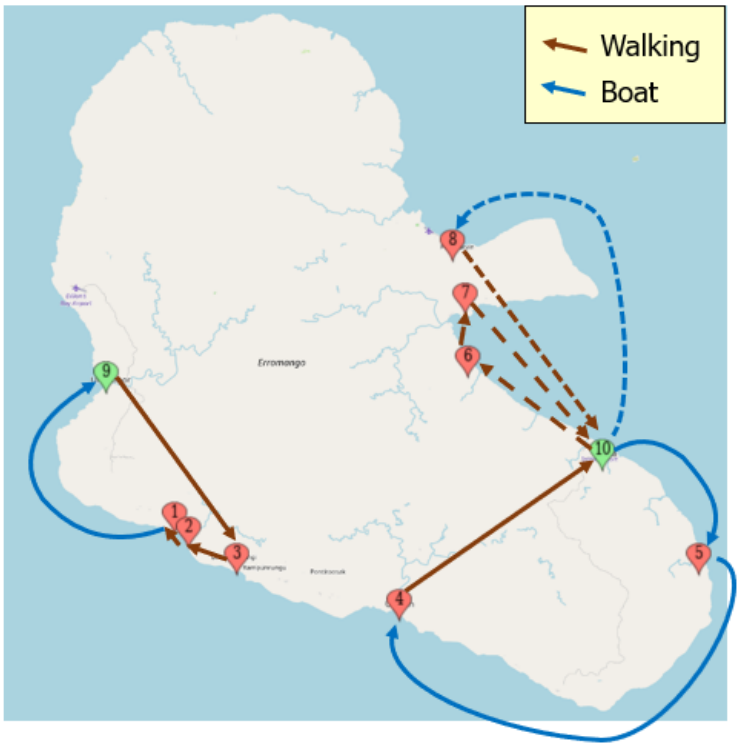

Figure 4.3 Solution for P2-D0-1day scenario in P2

Figure 4.4 shows the solution for the P2-D0-nday scenario. Here, subzone A is served by walking alone, as that is lower cost than using the boat; but it requires two days with an overnight spent in the field at node 3. In Figure 4.4, a change in the line style indicates an overnight stay (as at node 3 for subzone A). Subzone B is now served primarily by walking, with one boat trip from 10-5, but it requires a total of five days in three trips. The travel mode is shown as a single dash "-" to indicate walking and "=" to

indicate boat travel. Thus one trip in subzone B is 10=5-4-10, with an overnight at clinic 4. Another trip is the one day trip 10-6-7-10. The third trip is 10-8-10 with an overnight at node 8. This total cost of this scenario is $1022. It saves 36% compared to the Baseline, and 7.4% compared to the P2-D0-1day scenario. However, since this scenario allows multiple days in a trip, it takes 7 days and spends 3 nights in the field to serve the health zone. This shows the tradeoff between the cost and time spent away from the depot.

Figure 4.5 shows the timeline for the P2-D0-nday scenario for serving subzone A. The orange blocks show the vaccination time and the green blocks show the time for other treatment. The brackets above the timeline indicate travelling, with the mode, arc and time. Notice that the health worker completes the other treatment activities at node 3 at 14:08, but then does not have time that day to walk back to their depot (node 9), which takes 4:13. Therefore the health worker spends an overnight at node 3, and returns to their depot the next morning. This shows how allowing multi-days trips can replace expensive boat transportation (as for P2-D0-1day in Figure 4.3, where the health worker takes the boat to return to the base in one day) with an overnight stay in the field, to lower the total cost. The timeline shows the health worker departing from node 3 at 08:01on day two of the trip instead of at 08:00, which is the beginning of a day, because the model does not force a health worker to start their activity (i.e., vaccination, other treatment, or traveling) at 8:00 am on the second or subsequent days of a trip. Note that the cost in the model is the same for leaving at 8:00 am or any later time such that the health worker arrives back at their depot in the same day. However, in practice the health worker could leave at the beginning of the day to maximize their time back at the depot (i.e. the

permanent clinic). The Appendix shows the timelines for the trips for all the scenarios in this section.

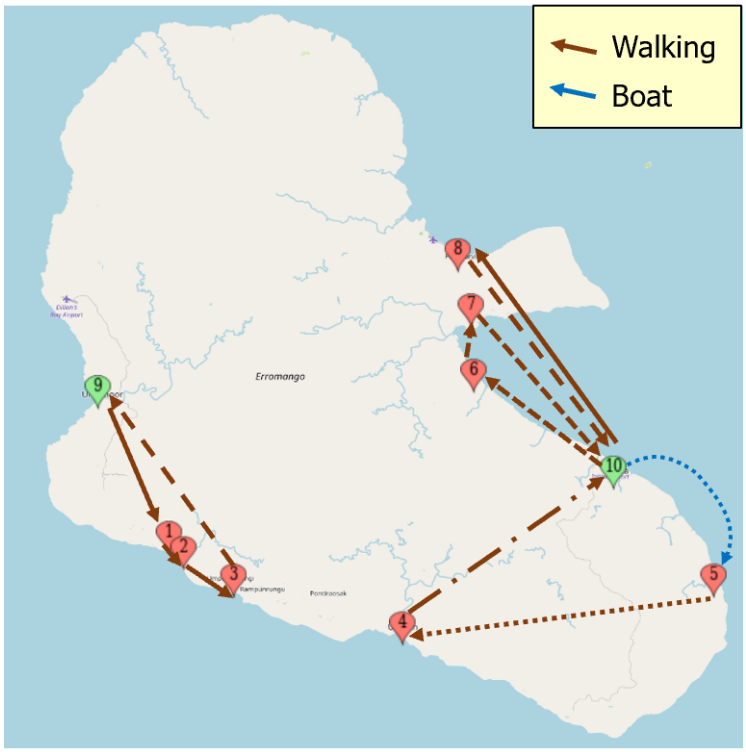

Figure 4.4 Solution for P2-D0-nday scenario in P2

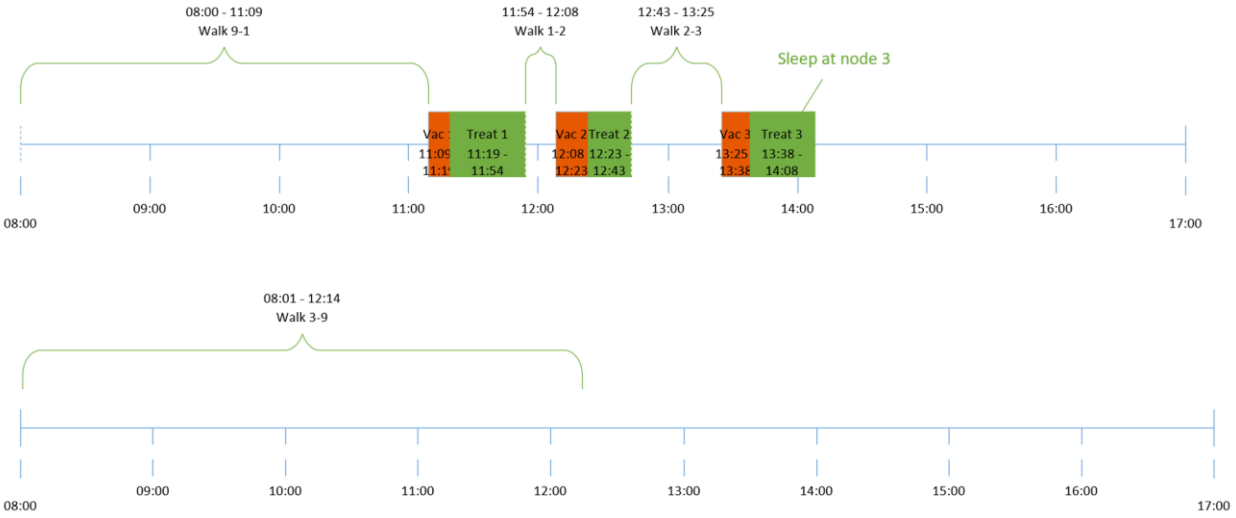

Figure 4.5 Timeline for serving subzone A in the P2-D0-nday scenario

P2-D1 Scenarios

In the P2-D0 scenarios, the health worker had to carry the vaccines, so the tour length and the tour direction was determined to maintain the cold chain. To acquire fresh vaccines, the health worker had to return to their depot (a permanent clinic). With the P2-D1 model, a drone can resupply the health worker with fresh vaccines at a temporary clinic while the health worker is on an outreach trip. Figure 4.6 shows the solution for the P2-D1-1day scenario. There are 3 health worker trips. Subzone A is served without a drone resupply on the trip 9=1-2-3-1 (the same trip in reverse from that for the P2-D0-1day solution in Figure 4.3). In Subzone B, there are two health worker trips with a drone resupply at node 7. One trip is 10=6-7-8=10, with the drone resupply at node 7. The other trip is 10=5=4-10 (the same trip in the P2-D0-1day solution in Figure 4.3). Figure 4.7 shows the timeline for the 10=6-7-8=10 trip. Interestingly, the drone resupply in this trip is due to the health worker's payload limit, not the cold chain limit. As indicated in the timeline, the health worker finished vaccination at the last clinic in the trip (at node 8) at 14:32, which is within the 7.5 hour cold chain time limit used in these scenarios. However, the total vaccine demand in this trip is 0.2+0.5+0.55=1.25 liters (see Table 4.5) which exceeds the payload limit of the health worker (i.e., 1 liter). Note that nodes 6 and 7 have a combined demand of 0.7 liters, which can be carried by the health worker. Thus 0.5 liters of vaccine delivered by the drone at node 7 is used later at node 8, but the delivery is to node 7 as that is closer to the drone DC at node 9 (and thus has lower transportation cost) than would be a delivery to node 8. The total cost of this scenario is $1039. It saves 35% compared to the Baseline, and 6% compared to the P2-D0-1day scenario. This scenario with the one drone delivery uses three trips on three days and

saves one day compared to the P2-D0-1day scenario as well. Therefore, we see how allowing drones to supply vaccines at clinics on outreach trips can save cost and time.

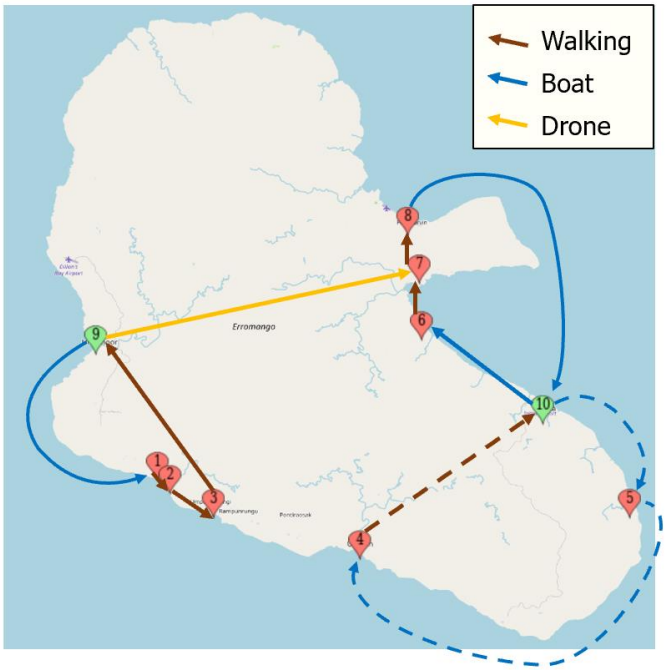

Figure 4.6 Solution for P2-D1-1day scenario

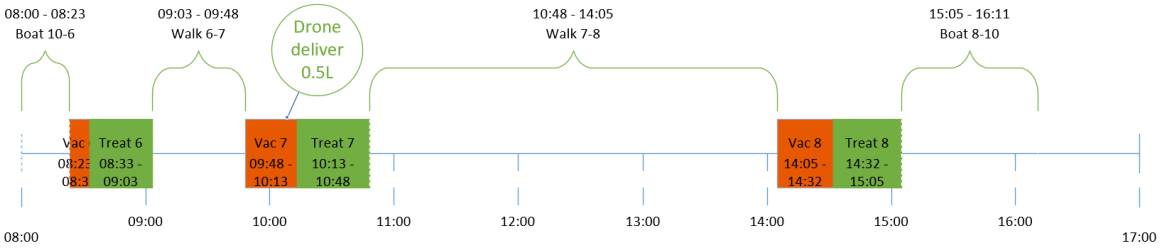

Figure 4.7 Timeline of one trip for serving nodes in subzone B in the P2-D1-1day scenario

Figure 4.8 shows the solution for the P2-D1-nday scenario. Subzone A is served by walking alone on a two-day trip, similar to the P2-D0-nday scenario in Figure 4.4 (the trip direction is reversed, but has the same cost), with an overnight spent at the clinic at node 1. Subzone B is served on a single three-day health worker trip (10=5-4-8-7-6-10),

with three 1-stop drone trips to resupply the health worker with fresh vaccines at nodes 8, 7 and 6. In this trip the health worker serves clinics 5 and 4 in day 1, spends the night at clinic 4, then spends almost all of day 2 (8:41) walking from node 4 to node 8 where they overnight. On day 3, the health worker begins vaccinations at clinic 8 using fresh vaccines supplied by a drone, then proceeds to clinics 7 and 6, with a drone providing fresh vaccines at each of those clinics. The total cost in this scenario is $937, and it saves 41% compared to the Baseline and 10% compared to the P2-D1-1day scenario. Compared to the P2-D0-nday scenario without drones, it saves 8.3% on cost and has health workers traveling on 3 fewer days.

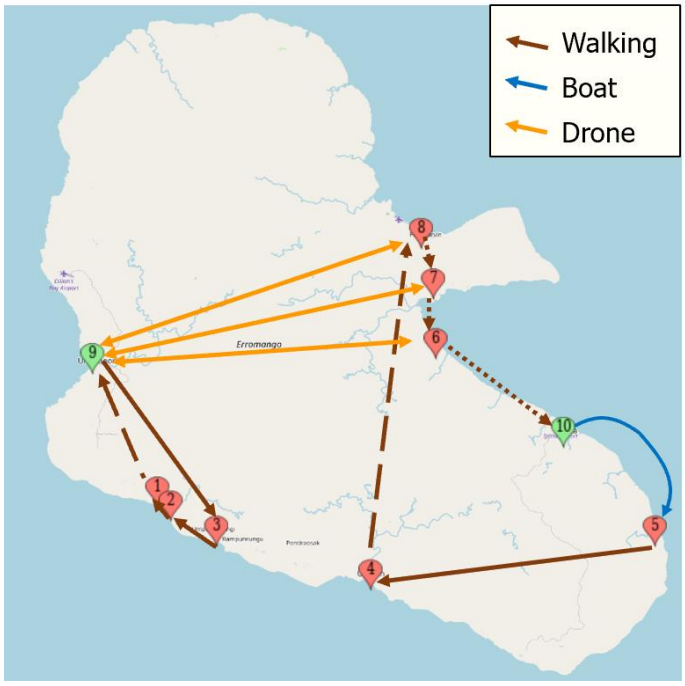

Figure 4.8 Solution for P2-D1-nday scenario

P2-Dn Scenarios

The P2-Dn scenarios allow the drone trips to make multiple stops, which may provide some economies over the P2-D1 scenarios. However, allowing multi-stop drone

trips raises coordination issues between the drone arrival and health worker arrival at a clinic, as the health worker is required to be present for any vaccine deliveries. Our models allow the drone to wait on the ground after a delivery to allow coordination with the health worker at a later delivery on the health worker and the drone trip.

The optimal solution of the P2-Dn-1day scenario is the same as the optimal solution of the P2-D1-1day scenario, because only one node needed drone resupply in the P2-D1-1day scenario, which was due to the health worker's payload limit and not the cold chain limit. Figure 4.9 shows the solution of the P2-Dn-nday scenario. The health worker trips for subzones A and B are the same as for the P2-D1-nday scenario, with a two-day trip for subzone A and a three-day trip for subzone B. However, rather than three separate drone resupply trips for the P2-D1-nday scenario in Figure 4.8, with the P2-Dn-nday scenario the three drone trips are combined into two drone trips: 9→8→9 and 9→7→6→9. Figure 4.10 shows the timeline of these drone trips. The brackets indicate the flight time of a drone from departing to landing. Figure 4.11 shows the timeline for the health worker serving subzone B in the P2-Dn-nday scenario. These two timelines show that the drone arrival times at clinic 8, 7, and 6 and the vaccination start times at the three clinics are synchronized. Also, note that because it takes a shorter time for the drone to travel between nodes than for the health worker, the drone waits after the delivery to node 7 at 12:41. It takes off at 14:23 for the short flight to node 6 (4 minutes) where it makes its second delivery. Notice that the drone waits at the location of the previous delivery (i.e., node 7) rather than flying to the next node (i.e., node 6), because the health worker has not yet arrived at node 6. Ideally, there should be a responsible individual to oversee the drone while it is waiting on the ground. With multiple drone stops, the cost

of the P2-Dn-nday scenario is $907, and it saves 43% compared to the Baseline. Comparing to the P2-D1-nday scenario, it saves 3.2% and reduces the number of days that health workers must travel by one.

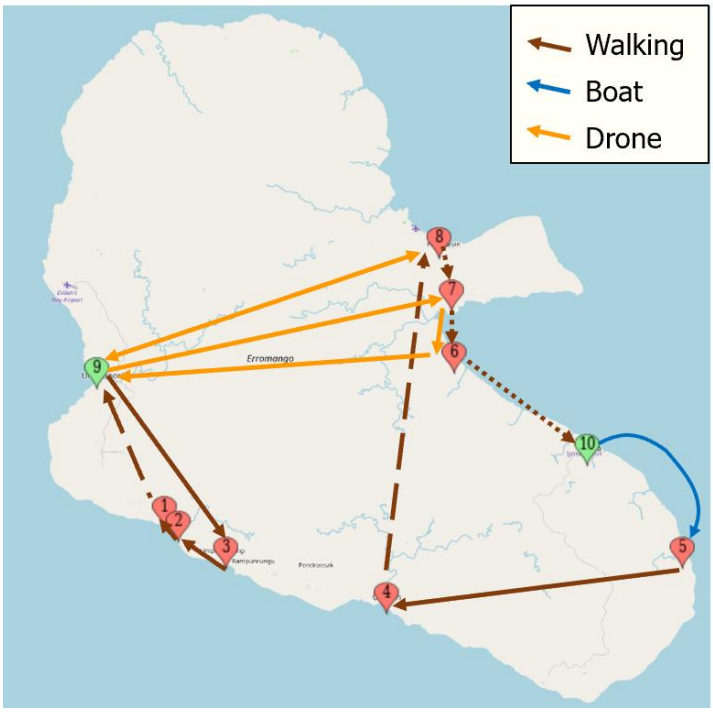

Figure 4.9 Solution for P2-Dn-nday scenario

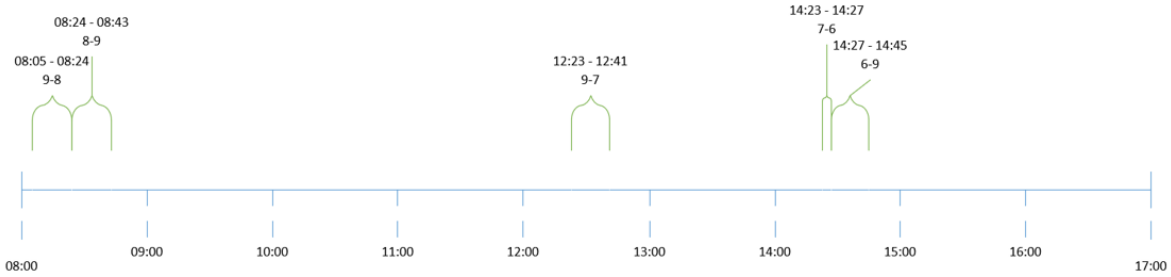

Figure 4.10 Timeline of a drone tour in the P2-Dn-nday scenario

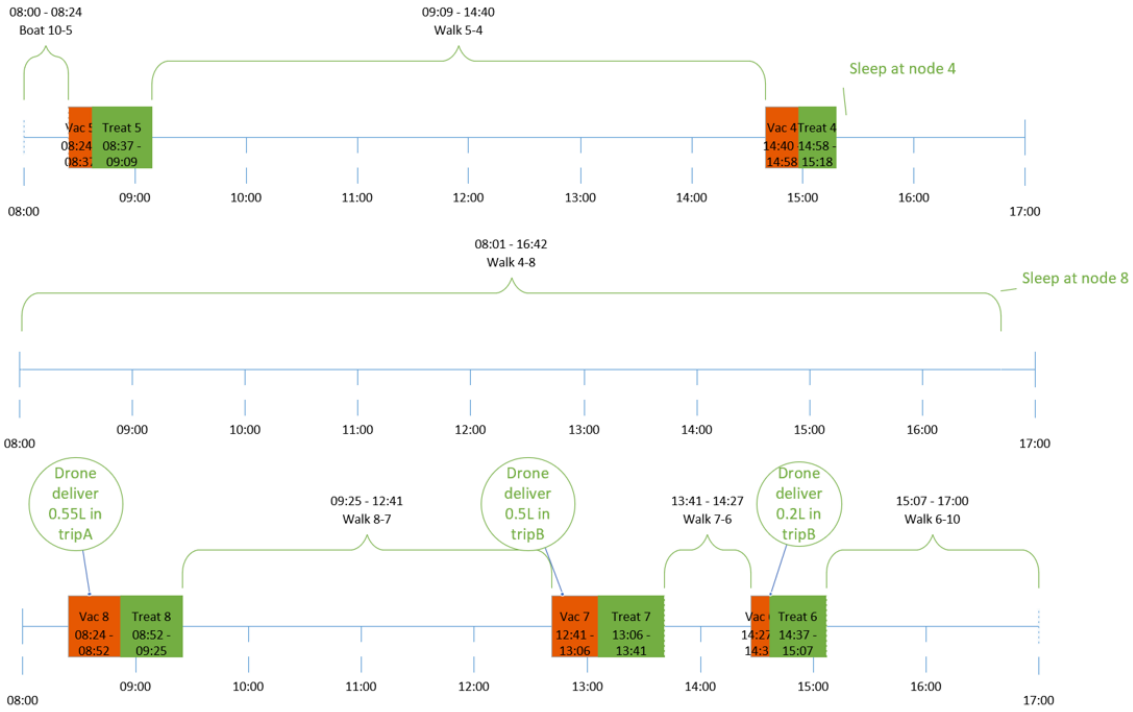

Figure 4.11 Timeline for serving subzone B in the P2-Dn-nday scenario

Analysis of all Scenarios

Table 4.9 provides key performance measures for the seven scenarios analyzed in this section. Column 2 (cost) reports the total cost for health worker and drone travel and overnight stays. Column 3 is the number of health worker trips in each scenario for subzones A and B together, and column 4 is the number of drone trips. Column 5 is the total time health workers are away from their depot on outreach trips to subzones A and B. This is measured in fractional work days, where each work day is nine hours, but all days except the last day in a trip count as whole days. For example, the two day trip shown in Figure 4.5, where the health worker finishes day 1 at 14:08 at node 3, and on day 2 has only a 4 hour 13 minute walk from node 3 back to their depot, counts as 1.47 days (1 day for day one of the trip and 253/540 = 0.47 days for the 253 minutes of walking on day 2 of the trip). As noted earlier, the optimization models do not provide

schedules that end as early as possible on the last day of a trip (there is nothing in the objective to force such a schedule); therefore, the times in column 5 of Table 4.9 reflect a manual shift of the schedule on the last day of the trip to end as early as possible. Column 6 of Table 4.9 shows the sum of the number of days with a health worker trip for sub zones A and B (if health workers for zone A and zone B are on an outreach trip on the same calendar day, that counts as 2 for this column). Column 7 of Table 4.9 shows the sum of overnight stays in each scenario. This table shows how allowing multi-day health worker trips ("nday" results vs. the corresponding "1-day" results) can reduce cost with fewer longer trips, and overnight stays.

Table 4.10 provides the percentage cost savings for the scenarios, compared to relevant benchmarks of 1-day health worker trips with no drones (i.e., P2-D0-1day) in columns 2 and 3, and the Baseline in column 4 and 5. First, we see that allowing multi-day health worker trips saves 5% to 12% more than having 1-day health worker trips (from comparing columns 3 and 2, and columns 5 and 4). Columns 4 and 5 show there is a substantial improvement over the baseline (over 31% cost savings) by allowing multi-stop health worker trips, with or without drones. Column 3 shows the savings from allowing multi-day health worker trips range from 7% to 18% over optimized 1-day trips. Column 2 shows smaller savings (only 6%) from limiting health worker trips to a single day. The use of drones (the last two rows vs. the "No Drone" row) shows savings of 6% to 11%. We also note that allowing multi-stop drone trips offers little benefit in these scenarios (0% - 3%). This is due to the simple setting in this case study where allowing multi-stop drone trips does not alter the optimal health worker trips, so the savings are

only in the drone costs, which are a small part of total costs. Other settings could produce different results when drone costs are higher or when solutions use more drone trips.

Scenario	Cost	Health worker trips	Drone trips	Days HW are away from their depot	Days with a health worker trip	Overnight stays
Baseline	1593	8	0	7.74	8	0
P2-D0-1day	1104	4	0	3.71	4	0
P2-D0-nday	1022	4	0	5.48	7	3
P2-D1-1day	1039	3	1	2.75	3	0
P2-D1-nday	937	2	3	4.34	5	3
P2-Dn-1day	1039	3	1	2.75	3	0
P2-Dn-nday	907	2	2	4.34	5	3

Table 4.9 Performance measures for P2 scenarios

	% Savings from P2-D0-1day		% Savings from Baseline	
	1-Day HW trip	Multi-Day HW trip	1-Day HW trip	Multi-Day HW trip
No Drones (P2-D0-*day)	-	7%	31%	36%
1-Stop Drones (P2-D1-*day)	6%	15%	35%	41%
Multi-Stop Drones (P2-Dn-*day)	6%	18%	35%	43%

Table 4.10 Cost savings versus P2-D0-1day and the Baseline

Figure 4.12 shows the cost and service tradeoff for the seven scenarios in problem P2. The horizontal axis shows fractional days health workers are away from their depot (reported in Table 4.9). The large difference from the baseline point in the chart shows that multi-day health worker trips provide large savings. The square blue symbols show

results without drones, while the triangles show results with drones. This clearly shows that using drones not only saves cost (moving down the chart), but also reduces the health worker time away from their depot (moving to the left in the chart). Comparing the "nday" and "1-day" results shows that allowing multi-day health worker trips saves cost (moving down in the chart), at the expense of more total time health workers are away from their depot (moving to the right in the chart).

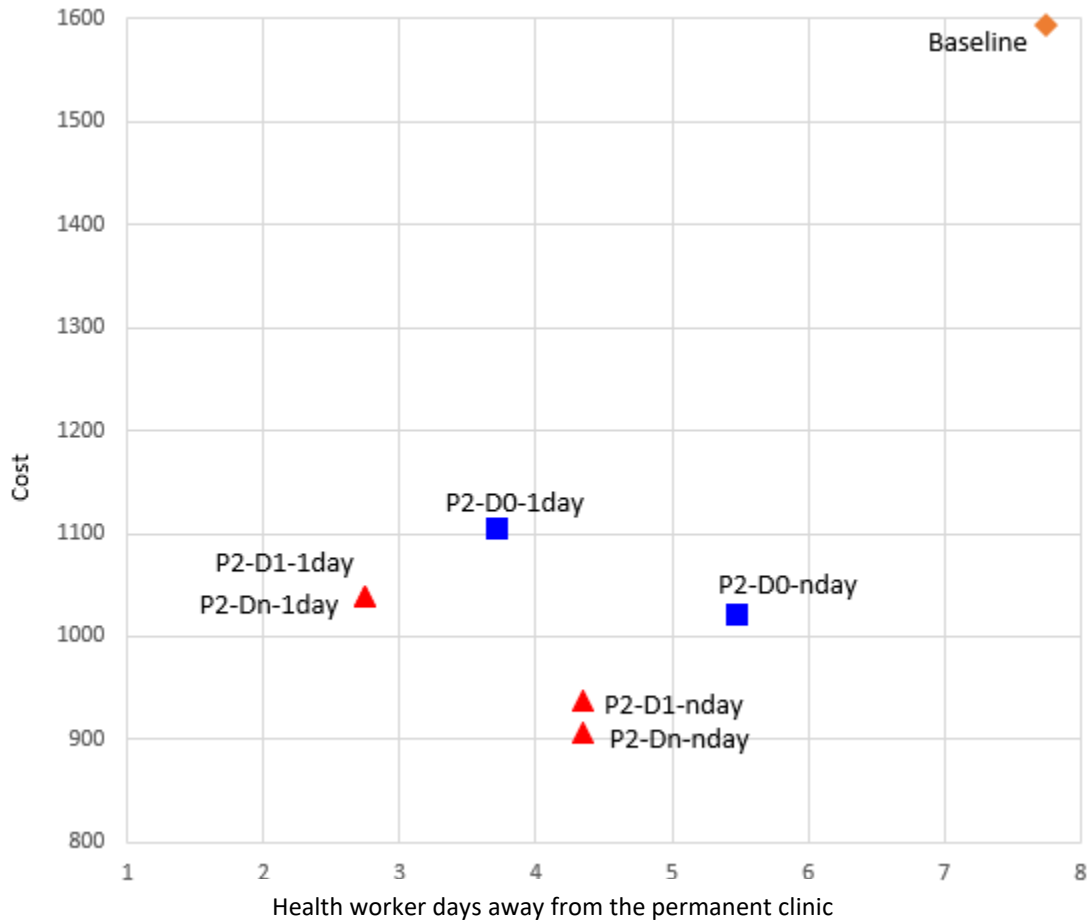

Figure 4.12 Cost and service tradeoff for the scenarios in problem P2

4.5. Summary

This chapter addresses the problem of vaccine delivery with drones in a single health zone in less developed regions by developing three MILP models to optimize the routes and delivery schedules of health workers in each subzone, and the routes and delivery schedules of drones in a health zone. The models with drones allow health worker trips to be one day or more than one day, and allow drone trips to make a single stop, or more than one stop. These models give local health officials (or relevant vaccine delivery schedulers) the flexibility to choose the right model according to the local needs and situations related to drone types. Comparing results from models with single day and multiple day health worker trips allow planners to assess the impact of allowing overnight stays on outreach trips. Comparing results from models with and without drones allows the impacts of a drone delivery option to be assessed.

The seven illustrations shown in this chapter demonstrate the flexible features of the three MILP models by varying the number of drone stops allowed and the number of days a health worker is allowed to be on an outreach tour. The illustrations show that using drones and multiday health worker trips can save up to 40% of the delivery cost versus a baseline of one-day health worker trips with no drones, while also improving the service performance. Compared to optimized one-day health worker trips with no drones, allowing drone delivery of vaccines can save up to 18% of the delivery cost. Using drones for vaccine delivery can not only resupply vaccines when a health worker's outreach trip violates the cold chain, but also when the payload for vaccines carried by a health worker (e.g., the cold box capacity carried by a health worker in an outreach trip) is smaller the total volume of vaccines required for clinics scheduled in an outreach trip.

With the help of drone deliveries, local health workers can have more time to focus on health care related duties, instead of wasting time on traveling in outreach activities. Outreach activities are the final step for children in remote regions receiving live saving vaccines, and in this chapter I demonstrated that adding drones to the delivery planning has considerable potential to make vaccine administration more efficient (saving health worker time) and economical.

5. Conclusions

This dissertation aims to design a comprehensive vaccine delivery network with drones for less developed regions that covers all delivery stages from the origin of the vaccines in the country to distribution centers (DCs) in local health zones, and on to local permanent clinics and then to the final vaccine outreach sites (i.e., temporary clinics). This complex problem is modeled in the dissertation by splitting the above-mentioned delivery stages into two parts, with P1 modeling the first part from the national vaccine origin to DCs in each health zone, and P2 modeling the second part from the DC in a health zone to the outreach sites within that health zone. Both problems incorporate multiple delivery modes and take the cold chain limitation into consideration.

Solving P1 includes the use of two cost models based on different cost structures for drones, and one service model to minimize delivery time. The models determine the optimal DCs, drone bases and drone relay stations that can extend the drone flight range, as well decide the vaccine flows on each selected arc with the corresponding transport mode. These models for P1 are strategic multi-modal network flow models with facility location decisions, that consider vaccine flows on a periodic basis (i.e., per month), rather than detailed delivery trips.

For problem P2 of vaccine delivery within one health zone, three MILP models based on the number of drone stops in a drone tour are developed. These three models take into consideration multi-day health worker tours, the health worker daily work limit, the health worker payload limit (i.e., cold box capacity), drone payload and overnight stay costs for health workers. These models in P2 are variants of the TSP with synchronized health worker and drone visits to clinics. The models for P2 are on an

operational level, and thus delivery details such as arrival and departure times for each trip on each day in the planning horizon are modeled.

The following three sections discuss the contributions and limitations of the research in this dissertation, as well as future research directions made possible by this work.

5.1. Contributions

This dissertation provides several contributions to the literatures on vaccine supply chain network design, delivery with drones and real-world synchronized delivery routing problems. There are:

1. Models for problem P1 provide an innovative method to model drone paths with relay stations that start with a drone base. Thus, multi-stop drone paths are a sequence of drone arcs connected via drone RSs. Models in P1 also allow remote relay stations that only serve drone paths; i.e., non-drone modes cannot transship at the locations of remote RS.

2. The second and third models in problem P2 (i.e., P2-D1 and P2-Dn) propose a complex variant of synchronized TSPs that can link multiple health worker outreach trips (TSPs) with deliveries on multi-stop drone trips.

3. Models for problem P2 optimize the delivery routes that include real-world features of multi-day health worker tours, multi-modal delivery, capacitated synchronized TSPs, and sequential health worker tours simultaneously.

4. Models for problem P2 include a unique method to calculate the time horizon in multi-day trips such that only the health worker work hours are included (e.g., a day is 8 hours long in the models if the work hours per day is 8).

5. The models are tested with a real-world case from Vanuatu which has a distinct geographic setting with many islands that is different than most cases in the literature of drone delivery or vaccine delivery.

The results of the analyses and case studies in this research also provide important contributions to show the potential savings that the use of drones offers for vaccine delivery in less developed countries. In the national level problem P1 with distribution from a national depot to the health zone DCs, using drones allows cost savings of up to 60.3% in the case study for Vanuatu. Further, the results for Vanuatu were used to identify the tradeoff between cost and service (average delivery time) to document how faster deliveries (as with tighter cold chain requirements) increase costs, but also alter the mix of modes for optimal distribution systems. The sensitivity analysis for problem P1 in Vanuatu shows that (i) for SFW, the transportation cost increased, and more drone bases and relay stations were open when the cold chain limitation decreased, and the transportation cost and delivery time both decreased and drones were used more when the demand level decreased; (ii) for LFW, the cost of drone bases and relay stations contribute to the transportation cost significantly. In the local health zone delivery problem P2 with delivery from the health zone DC to permanent and remote clinics via outreach trips, using drones allows cost savings of up to 43% in the case study for one heath zone in Vanuatu.

The results in this dissertation suggest there is a considerable potential for drones to reduce the costs to provide vaccinations in LDCs. By providing faster deliveries drones may also improve service levels (reduce delivery times). The results also suggest complimentary roles for large fixed wing drones that require runways to operate and small fixed wing drones that can deliver to sites with minimal (or no) infrastructure. The large drones appear most useful to replace expensive plane flights while carrying large amounts of vaccines long distances, as from the national depot to each province. The small drones appear most useful to replace trucks and boat trips that deliver small amounts of vaccines to serve a single clinic. However, the illustrations of the models with detailed data from Vanuatu does not guarantee there would be similar results in all health zones, or in settings for other LDCs.

5.2. Limitations

There are a number of limitations associated with the research in this dissertation.

1. The models developed are deterministic with constant parameter values (e.g., demand, cost, travel time, and payload, etc.), hence the models may not reflect the variation of the solution outputs based on stochastic parameters or probabilities of various scenarios with uncertainty that exist in the real world. For example, changing weather conditions may affect the distance a drone can fly.

2. Some data is very difficult to determine, especially for regular operations of drone deliveries in LDCs. As this is a new area, there have been relatively few pilot tests that provide limited data and may not reflect costs and performance from extended (routine) operations. Thus, while the data I used are the best I could obtain or develop, the lack of trustworthy drone delivery data in LDCs remains a challenge.

3. Models in P1 are strategic (with a monthly time frame) and are not able to capture individual drone trips with detailed scheduling, such as departure times, landing times, etc.

4. Models in problem P1 assume the starting node of all non-drone arcs can restart the cold chain for its corresponding transportation mode which might not be the case in reality.

5. The MILP models for problem P2 are rather large and might include some redundant constraints that may slow down the computation time. Further, the exact time of returning to his/her PC in the last day of a health worker tour in P2 is not controlled. Thus, the time should be manually adjusted to schedule the health worker in the last day of a trip.

5.3. Future research

This dissertation was originally envisioned as providing a holistic framework for vaccine delivery with drones in less developed countries. This challenging problem spans the time frames for periodic monthly resupply of the DCs (problem P1) and the detailed scheduling needed for synchronized health workers and drone tours for local health zone delivery from the DC (problem P2). Thus, the approach was to divide the research into a more strategic national-level model from vaccine origin to DCs, and a more detailed local delivery model from a designated DC to clinics.

This dissertation provides numerous contributions to the growing literature on drone applications to improve healthcare delivery and opens numerous avenues for future work. Ultimately, it is hoped that this work contributes to the improvement of health

outcomes and the wellbeing of individuals worldwide. This work opens many directions for future research, including the following.

1. Assess the efficiency of the models for improving the vaccine distribution in various scenarios with more performance measurements (besides transport cost, weighted average delivery time, and the number of days health workers are away from their base) such as the maximum or minimum delivery time to a health zone, the average, maximum or minimum number of drone steps to a health zone, and the average, maximum or minimum number of drone and vaccine paths in the delivery network.

2. The models developed are deterministic, but real-world conditions may lead to variation in the values of parameters used. Future work may consider models with uncertainty to ensure reliable delivery. Some factors to consider in future research might include uncertain travel times of transport modes in P1 (e.g., due to changing weather conditions and scheduling or maintenance issues), and variations in vaccine demand or vaccination and treatment durations (e.g., caused by an unexpected number of children and other patients showing up in remote clinics).

3. Future research could improve the quality of the MILP models to decrease the computational time. All models used “big-M” formulations in some constraints, which provide areas that may be addressed to improve the computational efficiency. With better MILP models, larger instances of problem P1 might then be solved (e.g., for an entire country rather than solving separately by province, as in the dissertation).

4. The models for problem P1 allow only one type of drone (i.e., either SFW drones or LFW drones), so it would be interesting to see how the performance of the vaccine delivery network would change when allowing more than one type of drones.

5. Even though the MILP models in problem P1 allow remote relay stations, I did not include remote RSs in the computational experiments due to the geographic situation in the study site Vanuatu. Hence, future research could analyze the use of remote RSs in computational experiments, including the use of mobile remote RSs such as boats that can be repositioned each day (over a monthly cycle) to provide drone recharging (e.g., via battery swaps) at key locations. Thus one mobile remote RS may be able to serve a large number of possible drone trips spread over many days.

6. The P1 model tracks monthly vaccine flows on arcs, but it might be enhanced by providing more details on the delivery trips for all modes and optimizing the number of vehicles of each mode for the delivery network. This could include tracking the return trips for modes, including drones.

7. Another future research area could be to test and modify the P1 models for geographical and vaccine supply chain settings with various population densities, demand levels, and the number of drone steps in a drone path. The current models and experiment studies for P1 were tested in Vanuatu which has a relatively low population density and low demand, and used a small number of drone steps in a drone path. These settings may not generate optimal solutions for regions with a high population density, high demand, or those that require more drone steps in a drone path.

8. Future research could incorporate in problem P2 the first level of delivery from a DC in the heath zone to the permanent clinics in each subzone. This could be especially beneficial in large health zones that include many subzones.

9. Future research could incorporate in problem P2 the value of creating more health worker time at their home clinic (depot) to provide health care and other related

activities. This might be accomplished by adding additional terms in the objective function or using constraints to control the return time of a health worker in the last day of a tour.

10. Future research could model inventory pooling for both problems, especially P2, to deal with uncertainty in vaccine inventory at various distribution levels. The permanent clinics in P2 are assumed to have uninterrupted power supplies (mainly solar panels in Vanuatu) and reliable cold chain facilities (e.g., refrigerators) that continuously maintain the vaccine cold chain, but this might not be the case in many LDCs. Using inventory pooling from a health care facility with highly reliable cold chain facilities, along with fast drone delivery, might reduce vaccine supply disruptions caused by unstable cold chain facilities in LDCs.

11. A large area of future research would be to address the allocation of a limited amount of vaccine. The P1 and P2 models are designed for routine vaccine distribution for all children under one year old assuming there are sufficient vaccine supplies. If vaccines were limited, then an optimal allocation of vaccines is important, which should consider limited resources and priority levels of vaccine necessity for equitable and efficient preventive health care (e.g., to achieve herd immunity with the lowest cost possible).

12. Integrating the two problems P1 and P2 into a single holistic model is an exciting and challenging area of future research. In this dissertation, models for P1 and P2 are tested separately, but the objective function value of P2 (the cost to serve a health zone from a particular DC) could be used as a part of the DC candidate cost in problem P1 to select the optimal DCs for each health zone. In the dissertation, the fixed DC costs

were the same for all DC candidates, so the total fixed DC cost was a constant value and could be removed from the models. Linking P1 and P2 would move the analysis one step closer to more comprehensive modeling that links national-level delivery with local delivery.

References

Ackerman, E. (2020). Zipline Launches Long-Distance Drone Delivery of COVID-19 Supplies in the U.S. Retrieved December 7, 2021, from https://spectrum.ieee.org/automaton/robotics/drones/zipline-long-distance-delivery-covid19-supplies

Agatz, N., Bouman, P., and Schmidt, M. (2018). Optimization Approaches for the Traveling Salesman Problem with Drone. *Transportation Science*, *52*(4), 965–981. https://doi.org/10.2139/ssrn.2639672

Aina, M., Igbokwe, U., Jegede, L., Fagge, R., Thompson, A., and Mahmoud, N. (2017). Preliminary results from direct-to-facility vaccine deliveries in Kano. *Vaccine*, *35*(17), 2175–2182. https://doi.org/10.1016/j.vaccine.2016.11.100

Amukele, T. K., Hernandez, J., Snozek, C. L., Wyatt, R. G., Douglas, M., Amini, R., and Street, J. (2017). Drone Transport of Chemistry and Hematology Samples over Long Distances. *American Journal of Clinical Pathology*, *148*(5), 427–435. https://doi.org/10.1093/ajcp/aqx090

Autry, C., Goldsby, T., Bell, J., Moon, M., Munson, C., Watson, M., … Jayaraman, J. (2013). The definitive guide to modern supply chain management (collection). *FT Press*.

Bard, J. F., Shao, Y., Qi, X., & Jarrah, A. I. (2014). The traveling therapist scheduling problem. *IIE Transactions*, *46*(7), 683–706.https://doi.org/10.1080/0740817X.2013.851434

Boutilier, J. J., Brooks, S. C., Janmohamed, A., Byers, A., Buick, J. E., Zhan, C., … Chan, T. C. Y. (2017). Optimizing a Drone Network to Deliver Automated External Defibrillators. *Circulation*. https://doi.org/10.1161/CIRCULATIONAHA.116.026318

Boysen, N., Schwerdfeger, S., and Weidinger, F. (2018). Scheduling last-mile deliveries with truck-based autonomous robots. *European Journal of Operational Research*, *271*(3), 1085–1099. https://doi.org/10.1016/j.ejor.2018.05.058

Bredstrom, D., and Ronnqvist, M. (2008). Combined vehicle routing and scheduling with temporal precedence and synchronization constraints. *European Journal of Operational Research*, *191*, 19–31. https://doi.org/10.1016/j.ejor.2007.07.033

Brown, A., and Gilbert, B. (2012). The Vanuatu medical supply system – documenting opportunities and challenges to meet the Millennium Development Goals. *Journal of Pharmaceutical Policy and Practice*, *7*(1). https://doi.org/10.1186/2052-3211-7-5

Brown, S. T., Schreiber, B., Cakouros, B. E., Wateska, A. R., Dicko, H. M., Connor, D. L., … Lee, B. Y. (2014). The benefits of redesigning Benin's vaccine supply chain. *Vaccine*, *32*(32), 4097–4103. https://doi.org/10.1016/j.vaccine.2014.04.090

Campbell, J. F., Sweeney, D., Zhang, J., and Pan, D. (2018). Strategic Design for Delivery with Linked Transportation Assets: Trucks and Drones.

CAPA. (2019). Air Vanuatu: new A220 fleet to support rapid inbound growth. Retrieved

from https://centreforaviation.com/analysis/reports/air-vanuatu-new-a220-fleet-to-support-rapid-inbound-growth-486447

Carlsson, J. G., and Song, S. (2018). Coordinated Logistics with a Truck and a Drone. *Management Science*, *64*(9), 4052–4069. https://doi.org/10.1287/mnsc.2017.2824

Chang, Y. S., and Lee, H. J. (2018). Optimal delivery routing with wider drone-delivery areas along a shorter truck-route. *Expert Systems with Applications*, *104*, 307–317. https://doi.org/10.1016/j.eswa.2018.03.032

Chapman, A. (2016). DRONE TYPES:MULTI-ROTOR VS FIXED-WING VS SINGLE ROTOR VS HYBRID VTOL. Retrieved from https://www.auav.com.au/articles/drone-types/

Chauhan, D., Unnikrishnan, A., and Figliozzi, M. (2019). Maximum coverage capacitated facility location problem with range constrained drones. *Transportation Research Part C: Emerging Technologies*, *99*, 1–18. https://doi.org/10.1016/j.trc.2018.12.001

Chen, S. I., Norman, B. A., Rajgopal, J., Assi, T. M., Lee, B. Y., and Brown, S. T. (2014). A planning model for the WHO-EPI vaccine distribution network in developing countries. *IIE Transactions (Institute of Industrial Engineers)*, *46*(8), 853–865. https://doi.org/10.1080/0740817X.2013.813094

Chiang, W. C., Li, Y., Shang, J., and Urban, T. L. (2019). Impact of drone delivery on sustainability and cost: Realizing the UAV potential through vehicle routing optimization. *Applied Energy*, *242*, 1164–1175. https://doi.org/10.1016/j.apenergy.2019.03.117

Choi, Y., & Schonfeld, P. M. (2017). Optimization of multi packages drone deliveries considering battery capacity. *Presentation at the 2017 TRB 96th Annual Meeting*.

Cissé, M., Yalçındağ, S., Kergosien, Y., Şahin, E., Lenté, C., and Matta, A. (2017). OR problems related to Home Health Care: A review of relevant routing and scheduling problems. *Operations Research for Health Care*, *13*, 1–22. https://doi.org/10.1016/j.orhc.2017.06.001

Claesson, A., Fredman, D., Svensson, L., Ringh, M., Hollenberg, J., Nordberg, P., … Ban, Y. (2016). Unmanned aerial vehicles (drones) in out-of-hospital-cardiac-arrest. *Scandinavian Journal of Trauma, Resuscitation and Emergency Medicine*, *24*(1), 1–9. https://doi.org/10.1186/s13049-016-0313-5

Coutinho, W. P., Battarra, M., and Fliege, J. (2018). The unmanned aerial vehicle routing and trajectory optimisation problem, a taxonomic review. *Computers and Industrial Engineering*, *120*, 116–128. https://doi.org/10.1016/j.cie.2018.04.037

Dorling, K., Heinrichs, J., Messier, G. G., and Magierowski, S. (2017). Vehicle Routing Problems for Drone Delivery. *IEEE Transactions on Systems, Man, and Cybernetics: Systems*. https://doi.org/10.1109/TSMC.2016.2582745

Drexl, M. (2012). Synchronization in Vehicle Routing—A Survey of VRPs with Multiple Synchronization Constraints. *Transportation Science*, *46*(3), 297–316. https://doi.org/10.1287/trsc.1110.0400

Duijzer, L. E. E., Jaarsveld, W. van, and Dekker, R. (2018). Literature review : The vaccine supply chain. *European Journal of Operational Research*, *268*(1), 174–192. https://doi.org/10.1016/j.ejor.2018.01.015

Ferrandez, S. M., Harbison, T., Weber, T., Sturges, R., and Rich, R. (2016). Optimization of a Truck-drone in Tandem Delivery Network Using K-means and Genetic Algorithm. *Journal of Industrial Engineering and Management*, *317*(22), 2332–2334. https://doi.org/10.1007/s10846-017-0548-z

Fikar, C., and Hirsch, P. (2017). Computers & Operations Research Home health care routing and scheduling : A review. *Computers and Operation Research*, *77*, 86–95. https://doi.org/10.1016/j.cor.2016.07.019

FlightConnections. (2021). Vanuatu flight connections. Retrieved January 3, 2021, from https://www.flightconnections.com/route-map-air-vanuatu-nf

Fredman, D. (2018). Placement of Automated External Defibrillators and Logistics to Facilitate Early Defibrillation in Sudden Cardiac Arrest. *Inst För Medicin, Solna/Dept of Medicine, Solna.*

Gavi. (2017). Vaccine progress in developing countries "in danger of stalling.

Gavi. (2019). Phase V (2021-2025) Gavi 5.0. Retrieved from https://www.gavi.org/our-alliance/strategy/phase-5-2021-2025

Ghelichi, Z., Gentili, M., and Mirchandani, P. B. (2021). Logistics for a fleet of drones for medical item delivery: A case study for Louisville, KY. *Computers and Operations Research*, *135*.

Graves, G. (2018). Remotely Piloted Aerial Services/ Unmanned Aerial Systems Vaccine and Health Supply Delivery in Vanuatu.

Gustiana, R. (2018). Vanuatu Immunisation Microplanning for 2018.

Ha, Q. M., Deville, Y., Pham, Q. D., and Hà, M. H. (2018). On the min-cost Traveling Salesman Problem with Drone. *Transportation Research Part C: Emerging Technologies*, *86*(November 2017), 597–621. https://doi.org/10.1016/j.trc.2017.11.015

Haidari, L. A., Brown, S. T., Ferguson, M., Bancroft, E., Spiker, M., Wilcox, A., … Lee, B. Y. (2016). The economic and operational value of using drones to transport vaccines. *Vaccine*, *34*(34), 4062–4067. https://doi.org/10.1016/j.vaccine.2016.06.022

Halper, R., Raghavan, S., and Halper, R. (2011). The Mobile Facility Routing Problem. *Transportation Science*, *45*(3), 413-434. https://doi.org/10.1287/trsc.1100.0335

Ham, A. M. (2018). Integrated scheduling of m-truck, m-drone, and m-depot constrained by time-window, drop-pickup, and m-visit using constraint programming. *Transportation Research Part C: Emerging Technologies*, 91, 1-14. https://doi.org/10.1016/j.trc.2018.03.025

Jeong, H. Y., Song, B. D., and Lee, S. (2019). Truck-drone hybrid delivery routing: Payload-energy dependency and No-Fly zones. *International Journal of Production*

Economics, *214*(January), 220–233. https://doi.org/10.1016/j.ijpe.2019.01.010

Karak, A., and Abdelghany, K. (2019). The hybrid vehicle-drone routing problem for pick-up and delivery services. *Transportation Research Part C: Emerging Technologies*, *102*(September 2018), 427–449. https://doi.org/10.1016/j.trc.2019.03.021

Karuri, K. (2019). Life-Saving Drones Fly Medicine to Tanzania's Remotest Spots. Retrieved from Bloomberg website: https://www.bloomberg.com/news/articles/2019-03-08/life-saving-drones-deliver-medicine-to-tanzania-s-remotest-spots

Kaufmann, B. J. R., Miller, R., and Cheyne, J. (2011). Vaccine Supply Chains Need To Be Better Funded And Strengthened, Or Lives Will Be At Risk. *Health Affairs*, (June), 1113–1121.

Khosiawan, Y., and Nielsen, I. (2016). A system of UAV application in indoor environment. *Production and Manufacturing Research*, *4*(1), 2–22. https://doi.org/10.1080/21693277.2016.1195304

Kim, S. J., Lim, G. J., Cho, J., and Côté, M. J. (2017). Drone-Aided Healthcare Services for Patients with Chronic Diseases in Rural Areas. *Journal of Intelligent and Robotic Systems: Theory and Applications*, *88*(1), 163–180. https://doi.org/10.1007/s10846-017-0548-z

Kim, S., and Moon, I. (2019). Traveling Salesman Problem With a Drone Station. *IEEE Transactions on Systems, Man, and Cybernetics: Systems*, *49*(1), 42–52. https://doi.org/10.1109/TSMC.2018.2867496

Kitjacharoenchai, P., Ventresca, M., Moshref-javadi, M., Lee, S., Tanchoco, J. M. A., Brunese, P. A., … States, U. (2019). Computers & Industrial Engineering Multiple traveling salesman problem with drones : Mathematical model and heuristic approach. *Computers & Industrial Engineering*, *129*(January), 14–30. https://doi.org/10.1016/j.cie.2019.01.020

Krarup, J., & Pruzan, P. (1983). The simple plant location problem: Survey and synthesis. *European Journal of Operational Research*, *12*, 36–81.

Labadie, N., Prins, C., and Yang, Y. (2014). Iterated local search for a vehicle routing problem with synchronization constraints. *In ICORES*.

Lee, B. Y., Cakouros, B. E., Assi, T. M., Connor, D. L., Welling, J., Kone, S., … Brown, S. T. (2012). The impact of making vaccines thermostable in Niger's vaccine supply chain. *Vaccine*, *30*(38), 5637–5643. https://doi.org/10.1016/j.vaccine.2012.06.087

Lee, B. Y., Connor, D. L., Wateska, A. R., Norman, B. A., Rajgopal, J., Cakouros, B. E., … Brown, S. T. (2015). Landscaping the structures of GAVI country vaccine supply chains and testing the effects of radical redesign. *Vaccine*, *33*(36), 4451–4458. https://doi.org/10.1016/j.vaccine.2015.07.033

Lemmens, S., Decouttere, C., Vandaele, N., and Bernuzzi, M. (2016). A review of integrated supply chain network design models : Key issues for vaccine supply chains. *Chemical Engineering Research and Design*, *109*, 366–384.

https://doi.org/10.1016/j.cherd.2016.02.015

Llamasoft. (2019). What Should You Deliver by Autonomous Aerial Systems? Tool for Determining Cost Effective Use Cases for AAVs. January 31, 2019, From https://www.updwg.org/resource-library/all-resources/page/11/, Accessed July 30, 2021.

Lin, Q., Zhao, Q., & Benjamin, L. (2020). Cold chain transportation decision in the vaccine supply chain. *European Journal of Operational Research*, 283(1) 182–195.

MacQueen, J. (1967). Some methods for classification and analysis of multivariate observations. *In Proceedings of the Fifth Symposium on Math, Statistics, and Probability. University of California Press*, *25*(8), 3439–3447. https://doi.org/10.1007/s11665-016-2173-6

Mathew, N., and Smith, S. (2015). Planning Paths for Package Delivery in Heterogeneous Multirobot Teams. *IEEE*, *31*(12), 5150–5158. https://doi.org/10.1007/s00464-017-5581-2

Matt, N. (2021). Vanuatu travel guide. Retrieved from https://www.nomadicmatt.com/travel-guides/vanuatu-travel-tips/#:~:text=How to Get Around Vanuatu,8%2C000 VUV (%2470 USD).

McNabb, M. (2019). How Zipline Became a $1.2 Billion Drone Company. Retrieved from dronelife website: https://dronelife.com/2019/05/21/how-zipline-became-a-1-2-billion-drone-company/%0D

Mehdi, R., Madjid, T., Afshin, M., and Hassan, M. (2021). An inventory-location optimization model for equitable influenza vaccine distribution in developing countries during the COVID-19 pandemic. *Vaccine*, *39*(3), 495–504.

Meier, P., and Soesilo, D. (2016). Using Drones for Medical Payload Delivery in Papua New Guinea. Retrieved from https://drones.fsd.ch/wp-content/uploads/2016/04/Case-Study-No2-PapuaNewGuinea.pdf

Ministry of Health Vanuatu, V. (2018). Request for Tender(RFT) Physical Services. Retrieved from https://www.unicef.org/innovation/reports/vanuatu-drone-trial-report

Ministry of public health and prevention, R. of S. (2012). *EPI comprehensive multiyear plan 2012-2016*.

Moshref-javadi, M., and Lee, S. (2017). Using Drones to Minimize Latency in Distribution Systems. *IIE Annual Conference. Proceedings. Institute of Industrial and Systems Engineers (IISE)*, 235–241.

Munoz, J. (2021). Drones Are Delivering Covid-19 Vaccines to Underserved Communities. Retrieved December 7, 2021, from https://www.smithsonianmag.com/innovation/drones-are-delivering-covid-19-vaccines-to-underserved-communities-180977407/

Murray, C. C., & Chu, A. G. (2015). The flying sidekick traveling salesman problem: Optimization of drone-assisted parcel delivery. *Transportation Research Part C: Emerging Technologies*, (54), 86-109. https://doi.org/10.1016/j.trc.2015.03.005

Murray, C. C., and Raj, R. (2019). The Multiple Flying Sidekicks Traveling Salesman Problem: Parcel Delivery with Multiple Drones. *Available at SSRN 3338436*. Retrieved from https://www.chasemurray.com/wp-content/uploads/2019/02/mFSTSP_02-20-19_POST_ONLINE.pdf

Nyaaba, A. A., and Ayamga, M. (2021). Intricacies of medical drones in healthcare delivery: Implications for Africa. *Technology in Society*, *66*(May), 101624. https://doi.org/10.1016/j.techsoc.2021.101624

Otto, A., Agatz, N., Campbell, J., Golden, B., and Pesch, E. (2018). Optimization approaches for civil applications of unmanned aerial vehicles (UAVs) or aerial drones: A survey. *Networks*, *72*(4), 411–458. https://doi.org/10.1002/net.21818

Otuto, A. C., and Chinenye, N. C. (2021). Surmounting inherent challenges in healthcare service delivery for effective procurement and distribution of COVID-19 vaccines; a developing country context. *Health Policy and Technology*, *10*(2).

Palermo, E. (2014). How drones are fighting infectious disease. Retrieved from https://www.livescience.com/48396-drones-track-infectious-disease.html

Peters, A. (2021). These drones will deliver the COVID-19 vaccine so it stays cold. Retrieved December 7, 2021, from https://www.fastcompany.com/90601106/these-drones-will-deliver-the-covid-19-vaccine-so-it-stays-cold

Phillips, N., Blauvelt, C., Ziba, M., Sherman, J., Saka, E., Bancroft, E., and Wilcox, A. (2016). Costs associated with the use of unmanned aerial vehicles for transportation of laboratory samples in Malawi. *VillageReach*. Retrieved from http://www.villagereach.org/wp-content/uploads/2017/06/Malawi-UAS-Report_MOH-Draft_-FINAL_14_07_16.pdf

Poikonen, S. (2017). The Vehicle Routing Problem with Drones: Extended Models and Connections. *Networks*, 70(1), 34-43.

Privett, N., and Gonsalvez, D. (2014). The top ten global health supply chain issues : Perspectives from the field. *Operations Research for Health Care*, *3*(4), 226–230. https://doi.org/10.1016/j.orhc.2014.09.002

Priye, A., Wong, S., Bi, Y., Carpio, M., Chang, J., Coen, M., … Ugaz, V. M. (2016). Lab-on-a-Drone: Toward Pinpoint Deployment of Smartphone- Enabled Nucleic Acid-Based Diagnostics for Mobile Health Care. *Analytical Chemistry*, *88*(9), 4651–4660. https://doi.org/10.1021/acs.analchem.5b04153

Pulver, A., and Wei, R. (2018). Optimizing the spatial location of medical drones. *Applied Geography*, *90*(November 2017), 9–16. https://doi.org/10.1016/j.apgeog.2017.11.009

Rabta, B., Wankmüller, C., & Reiner, G. (2018). A drone fleet model for last-mile distribution in disaster relief operations. *International Journal of Disaster Risk Reduction* 28, 107-112. https://doi.org/10.1016/j.ijdrr.2018.02.020

Rahman, S. U., and Smith, D. K. (2000). Use of location-allocation models in health service development planning in developing nations. *European Journal of Operational Research*, *123*(3), 437–452. https://doi.org/10.1016/S0377-

2217(99)00289-1

Rao, B., and Goutham, Ashwin Maione, G. R. (2016). The societal impact of commercial drones. *Technology in Society*, *45*(83), 90.

Rao, R., Schreiber, B., and Lee, B. Y. (2017). Immunization supply chains: Why they matter and how they are changing. *Vaccine*, *35*(17), 2103–2104. https://doi.org/10.1016/j.vaccine.2017.02.062

Rasmussen, M. S., Justesen, T., Dohn, A., and Larsen, J. (2012). The home care crew scheduling problem: Preference-based visit clustering and temporal dependencies. *European Journal of Operational Research*, *219*(3), 598–610.

Redjem, R., Kharraja, S., Xie, X., Routing, E. M., Of, S., Etienne, S., & Marcon, E. (2012). *Routing and scheduling of caregivers in home health care with synchronized visits*. 9th International Conference on Modeling, Optimization & SIMulation, Jun 2012, Bordeaux, France. 2012. <hal-00728631>

Rosser, J. C., Vignesh, V., and Terwilliger, B. (2018). Surgical and Medical Applications of Drones: A comprehensive Review. *JSLS*, *22*(3).

Sacramento, D., Pisinger, D., and Ropke, S. (2019). An adaptive large neighborhood search metaheuristic for the vehicle routing problem with drones. *Transportation Research Part C: Emerging Technologies*, *102*(March), 289–315. https://doi.org/10.1016/j.trc.2019.02.018

Sandvik, K. B., & Lohne, K. (2014). The Rise of the Humanitarian Drone: Giving Content to an Emerging Concept. *Millennium: Journal of International Studies*, (43(1), 145-164. https://doi.org/10.1177/0305829814529470

Scott, J. E., and Scott, C. H. (2019). Models for Drone Delivery of Medications and Other Healthcare Items. *In Unmanned Aerial Vehicles: Breakthroughs in Research and Practice. IGI Global*, *13*(3), 376–392. https://doi.org/10.4018/IJHISI.2018070102

Shadkam, E. (2021). Cuckoo optimization algorithm in reverse logistics: A network design for COVID-19 waste management. *Waste Management and Research*, (May). https://doi.org/10.1177/0734242X211003947

Shavarani, S. M., Mosallaeipour, S., Golabi, M., and İzbirak, G. (2019). A congested capacitated multi-level fuzzy facility location problem: An efficient drone delivery system. *Computers and Operations Research*, *108*, 57–68. https://doi.org/10.1016/j.cor.2019.04.001

Shavarani, S. M., Nejad, M. G., Rismanchian, F., and Izbirak, G. (2018). Application of hierarchical facility location problem for optimization of a drone delivery system: a case study of Amazon prime air in the city of San Francisco. *International Journal of Advanced Manufacturing Technology*, *95*(9–12), 3141–3153. https://doi.org/10.1007/s00170-017-1363-1

Shretta, R., Hupert, N., Osewe, P., and White, L. J. (2021). Vaccinating the world against COVID-19: Getting the delivery right is the greatest challenge. *BMJ Global Health*, *6*(3), 10–12. https://doi.org/10.1136/bmjgh-2021-005273

Smith, H. K., Harper, P. R., Potts, C. N., and Thyle, A. (2009). Planning sustainable community health schemes in rural areas of developing countries. *European Journal of Operational Research*, *193*(3), 768–777. https://doi.org/10.1016/j.ejor.2007.07.031

Spires, J. (2019). Zipline drone responds, saves a 9-day-old baby in hours. Retrieved from DroneDJ website: https://dronedj.com/2019/12/23/zipline-drone-save-9-day-old-baby/%0D

Stony Brook University News. (2016). Drones Used to Improve Healthcare Delivery in Madagascar. Retrieved from https://news.stonybrook.edu/homespotlight/drones-used-to-improve-healthcare-delivery-in-madagascar/

Tavana, M., Khalili-Damghani, K., Santos-Arteaga, F. J., & Zandi, M. H. (2017). Drone shipping versus truck delivery in a cross-docking system with multiple fleets and products. *Expert Systems with Applications*, 72, 93-107. https://doi.org/10.1016/j.eswa.2016.12.014

The United Nation. (2015). SDG3: Ensure healthy lives and promote wellbeing for all at all ages. Website: https://sdgs.un.org/goals/goal3

Thiels, C. A. DO, Aho, J. M. M., Zietlow, S. P. M., and Jenkins, D. H. M. (2015). Use of unmanned aerial vehicles for medical transport. *Air Medical Journal*, *34*(2), 104–108.

Troudi, A., Addouche, S. A., Dellagi, S., and El Mhamedi, A. (2018). Sizing of the drone delivery fleet considering energy autonomy. *Sustainability (Switzerland)*, *10*(9), 1–17. https://doi.org/10.3390/su10093344

UNICEF. (2018). Vanuatu Drone Trial Report. Retrieved from https://www.unicef.org/innovation/reports/vanuatu-drone-trial-report%0D

UNICEF. (2019). UNICEF pacific islands countries. Retrieved from https://www.unicef.org/pacificislands/about-us

Vanuatu Ministry of Health. (2011). *Vanuatu health facility catchment maps*.

Vanuatu Ministry of Health. (2016). Remoteness and vaccine supply cost. xlsx

VillageReach. (2017). Finding Efficiencies in Zambia's Immunisation Supply Chain. Retrieved from http://www.technet-21.org/iscstrengthening/index.php/en/

VillageReach. (2018). Increasing Access to Health Products in the DRC to the Next Generation Supply Chain Initiative.

VillageReach. (2019). Toolkit for Generating Evidence around the Use of Unmanned Aircraft Systems (UAS) for Medical Commodity Delivery. Retrieved from https://www.updwg.org/wp-content/uploads/2019/12/UAS-Evidence-Generation-Toolkit-V2-Nov-2019.pdf

VillageReach. (2021a). Drones for Health in the Democratic Republic of Congo. Retrieved from https://www.villagereach.org/work/drones-for-health/uav-drc/

VillageReach. (2021b). Medical Drone Delivery of COVID-19 and TB Samples – A Promising Solution for Mozambique. Retrieved from

https://www.villagereach.org/press-release-medical-drone-delivery-of-covid-19-and-tb-samples-a-promising-solution-for-mozambique/

Vincent, J. (2021). Self-flying drones are helping speed deliveries of COVID-19 vaccines in Ghana. Retrieved from https://www.theverge.com/2021/3/9/22320965/drone-delivery-vaccine-ghana-zipline-cold-chain-storage

Walia, S. S., Somarathna, K. U. S., Hendricks, R., Jackson, A., and Nagarur, N. (2018). Optimizing the Emergency Delivery of Medical Supplies with Unmanned Aircraft Vehicles. *IISE Annual Conference*. Retrieved from https://www.scopus.com/inward/record.uri?eid=2-s2.0-85054014297&partnerID=40&md5=9f6044bd6717a0e5c5a00d21f2a1e9a0

Wang, X., Poikonen, S., and Golden, B. (2017). The vehicle routing problem with drones: several worst-case results. *Optimization Letters*, *11*(4), 679–697. https://doi.org/10.1007/s11590-016-1035-3

Wang, Z., and Sheu, J. (2019). Vehicle routing problem with drones. *Transportation Research Part B*, *122*, 350–364. https://doi.org/10.1016/j.trb.2019.03.005

Wen, T., Zhang, Z., and Wong, K. K. L. (2016). Multi-objective algorithm for blood supply via unmanned aerial vehicles to the wounded in an emergency situation. *PLoS ONE*, *11*(5), 1–23. https://doi.org/10.1371/journal.pone.0155176

WeRobotics. (2019). WeRobotics Now Offers Cargo Drone Solutions. Retrieved from https://blog.werobotics.org/2019/09/11/werobotics-now-offers-cargo-drone-solutions/

WHO. (2011a). Child mortality Millenium Development Goal (MDG) 4. Retrieved February 12, 2019, from http://www.fao.org/sustainable-development-goals/mdg/goal-4/en/

WHO. (2011b). Global Vaccine action Plan 2011-2020. Retrieved from https://www.who.int/immunization/global_vaccine_action_plan/GVAP_doc_2011_2020/en/

WHO. (2012). Regional update: increasing and sustaining immunization coverage in SEAR. Retrieved from https://www.who.int/immunization/sage/SAGE_April_2011_SEARO.pdf

WHO. (2015). Immunization in practice: Module 2: The vaccine cold chain.

WHO. (2017). Global Health Observatory (GHO) data under-five mortality. Retrieved from https://www.who.int/gho/child_health/mortality/mortality_under_five_text/en/

Wingcopter. (2019). *Comprehensive Summary Vaccine Delivery Service in Vanuatu*. Retrieved from https://www.unicef.org/innovation/media/11956/file/Reference

WorldBank. (2018). Vanuatu Health System Assessment. Retrieved from http://documents.worldbank.org/curated/en/716131528786888780/text/Vanuatu-Health-Financing-Systems-Assessment.txt

Yang, Y., Bidkhori, H., & Rajgopal, J. (2021). Optimizing vaccine distribution networks in low and middle-income countries. *Omega*, *99*.

https://doi.org/10.1016/j.omega.2020.102197

Zaffran, M., Vandelaer, J., Kristensen, D., Melgaard, B., Yadav, P., Antwi-agyei, K. O., and Lasher, H. (2013). The imperative for stronger vaccine supply and logistics systems. *Vaccine*, *31*, B73–B80. https://doi.org/10.1016/j.vaccine.2012.11.036

Zhang, J. (2021). *Economic and Environmental Impacts of Drone Delivery*. PhD Thesis, University of Missouri - St. Louis.

Zipline. (2021). Zipline homepage. Retrieved September 12, 2019, from https://www.flyzipline.com/

Appendix

Subzone	Node	Node	Distance (km)	Circuity factor
A	9	1	9.25	1.7
	9	2	10.37	1.8
	9	3	13.18	1.6
	1	2	1.19	1
	1	3	4.34	1.1
	2	3	3.18	1.1
B	10	4	14.65	2
	10	5	8.23	1,2
	10	6	9.50	1
	10	7	12.23	1
	10	8	15.21	1.8
	4	5	17.27	1.6
	4	6	15.05	2
	4	7	18.66	2.3
	4	8	21.69	2
	5	6	17.62	1.1
	5	7	20.46	1.2
	5	8	23.40	1.5
	6	7	3.76	1
	6	8	7.01	3
	7	8	3.27	5

Table A. 1 Haversine distance and circuity factors in problem P2.
(Note: circuity factors are determined by analyzing maps, including Google Map. Boat and walking have the same circuity factor because the walking trails in Erromango are mostly along the coast.)

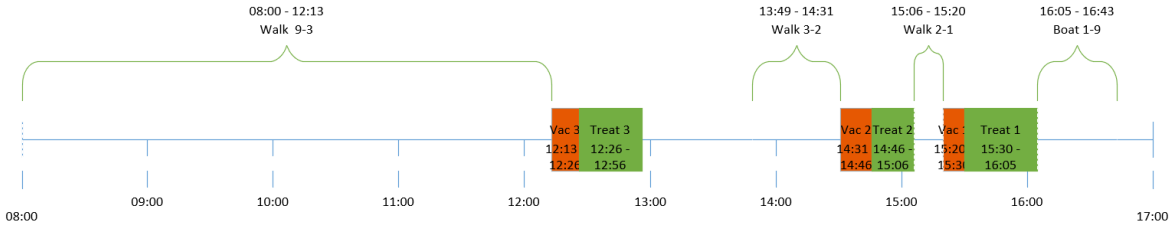

Figure A. 1 Timeline for serving subzone A in the P2-D0-1day scenario

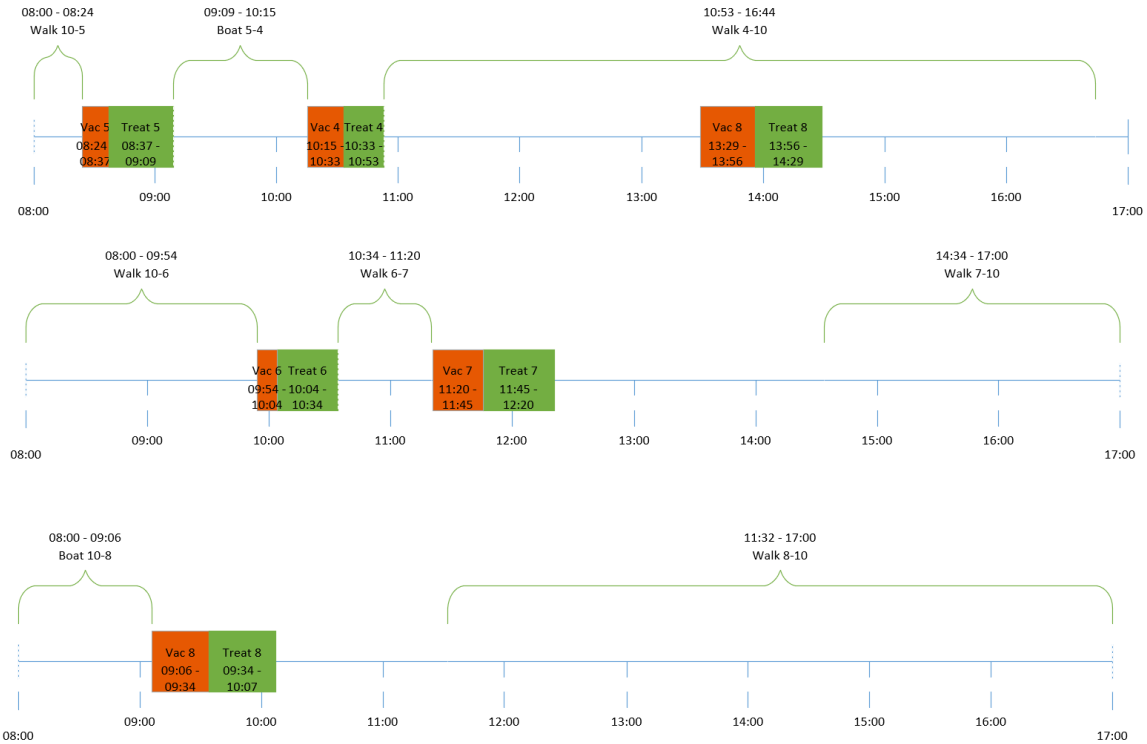

Figure A. 2 Timelines for serving subzone B in the P2-D0-1day scenario
(Note: The three timelines are for day 1, day 2, and day 3 are from top to bottom)

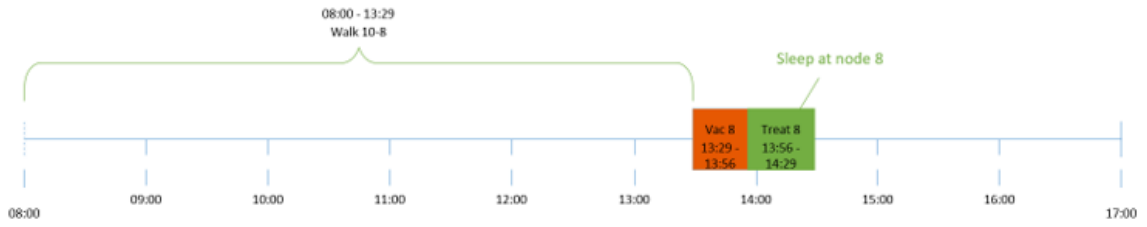

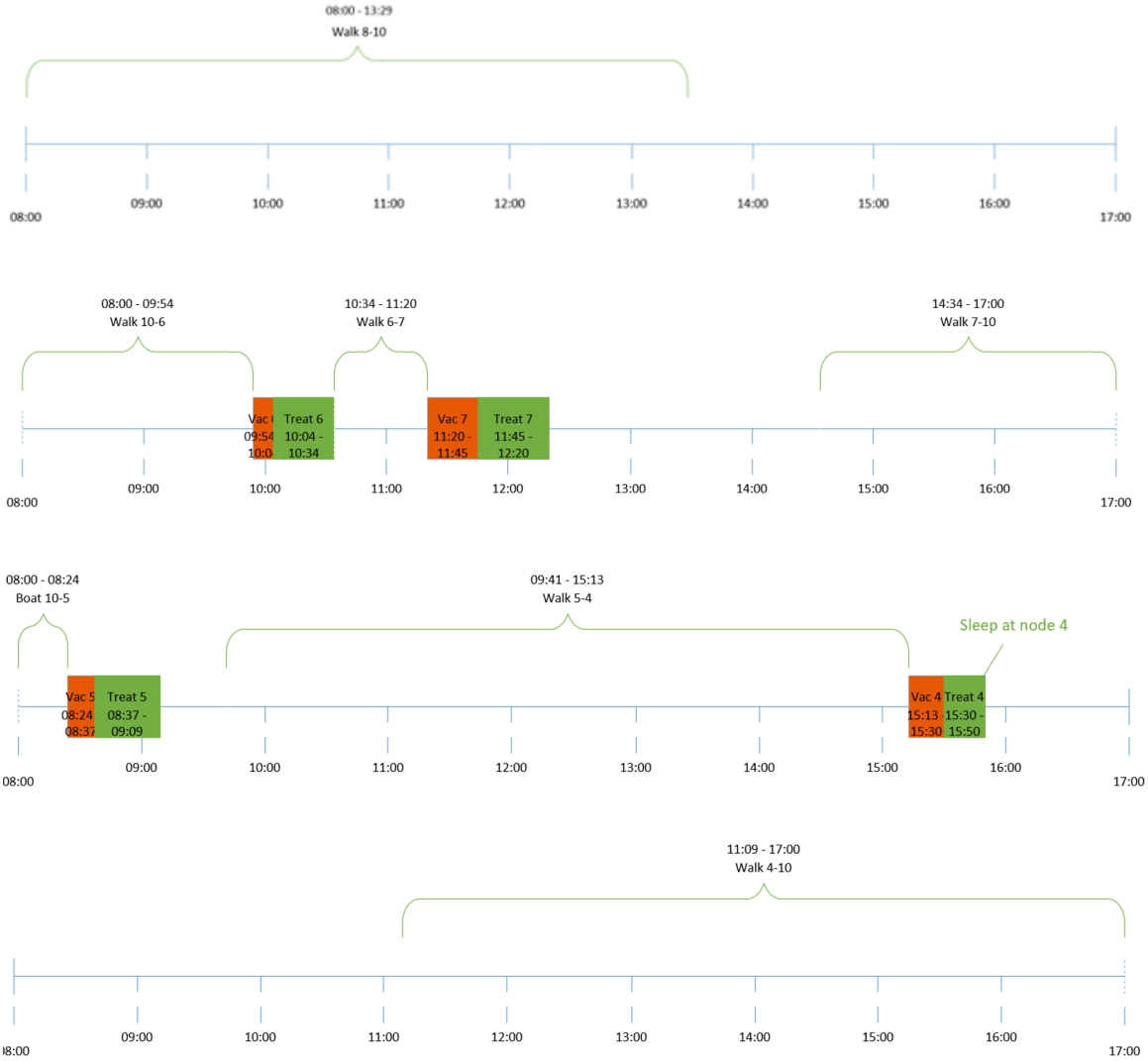

Figure A. 3 Timelines for serving subzone B in the P2-D0-nday scenario
(Note: The five timelines are for trip 1 (day 1 and day 2), trip 2 (day 3), trip 3 (day 4 and day 5) from top to bottom)

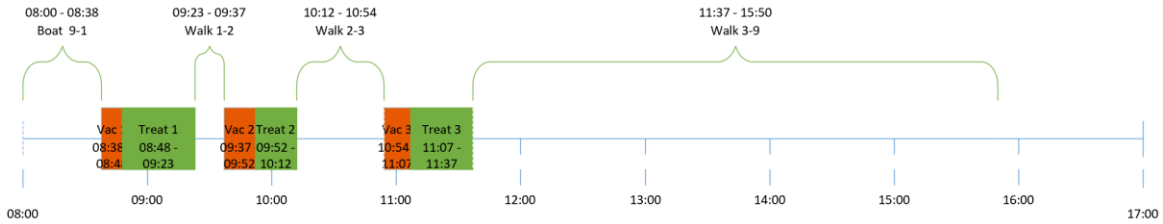

Figure A. 4 Timelines for serving subzone A in the P2-D1-1day scenario

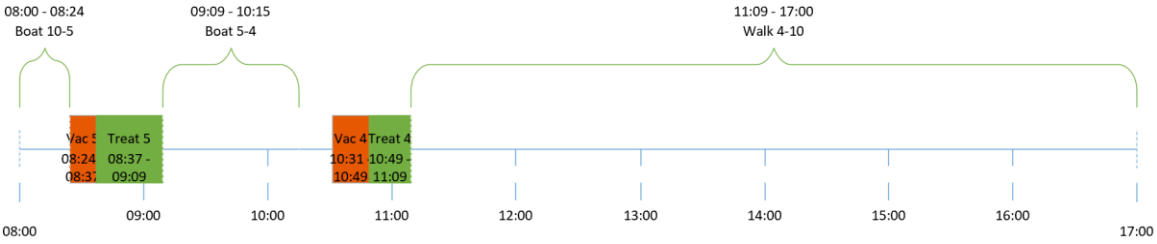

Figure A. 5 Timelines for serving nodes 4 and 5 in subzone B in the P2-D1-1day scenario

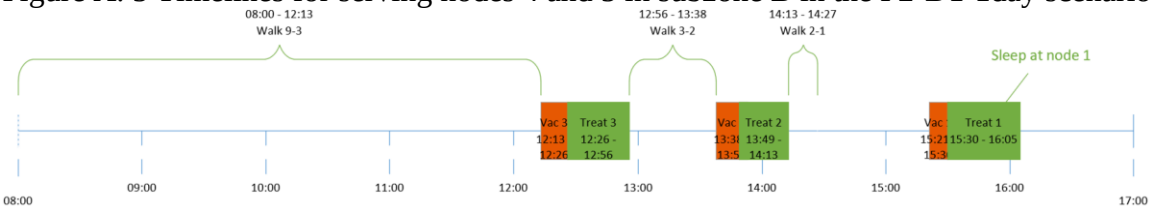

Figure A. 6 Timelines for serving subzone A in the P2-D1-nday scenario

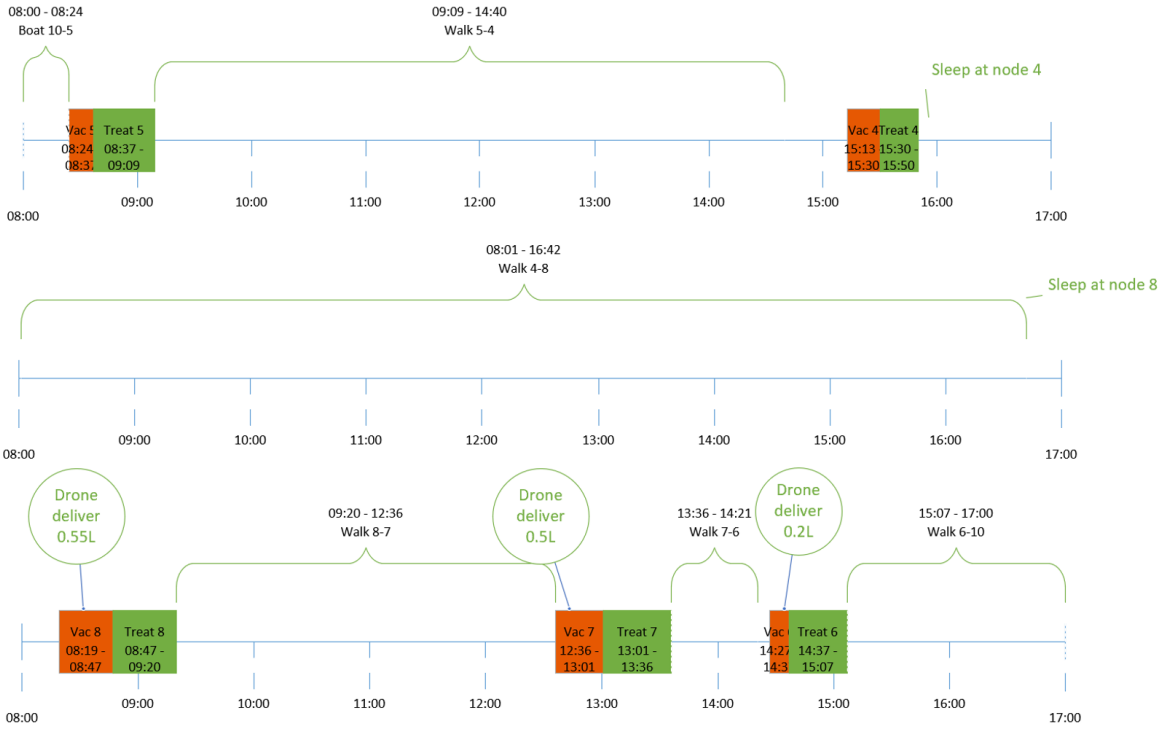

Figure A. 7 Timelines for serving subzone B in the P2-D1-nday scenario

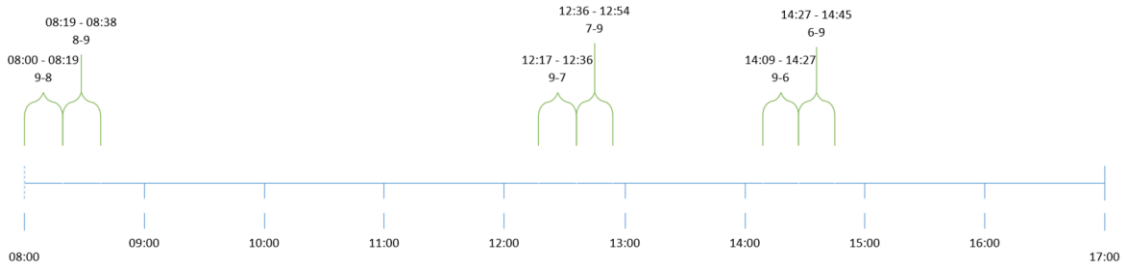

Figure A. 8 Timelines of drone trips in the P2-D1-nday scenario

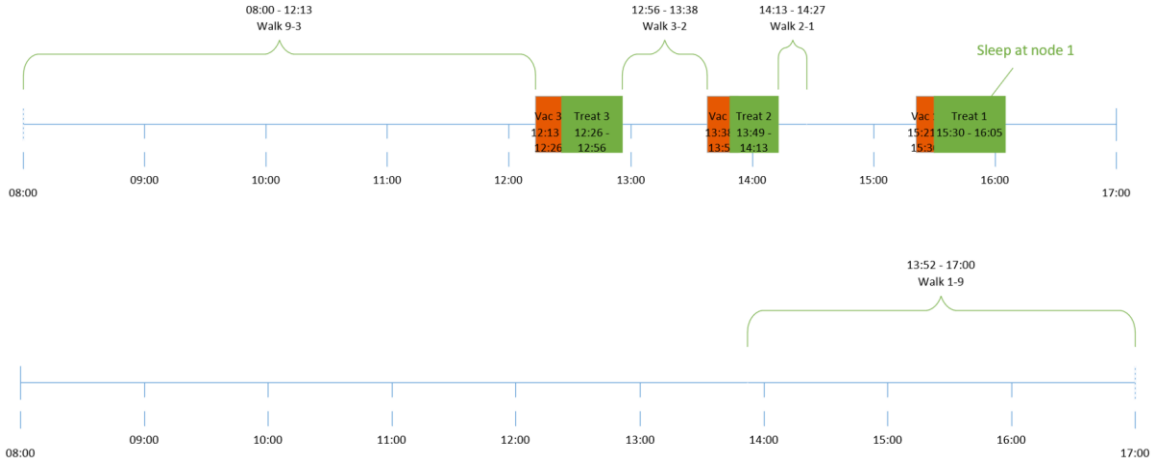

Figure A. 9 Timelines for serving subzone A in the P2-Dn-nday scenario